UNIVERSITÀ DEGLI STUDI DELLA TUSCIA DI VITERBO

DIPARTIMENTO DI ECOLOGIA E BIOLOGIA

Corso di Dottorato di Ricerca in

Ecologia e gestione sostenibile delle risorse ambientali - XXIX Ciclo

New Biocatalytic and biomimetic processes for the synthesis of
bioactive compounds: A green chemistry approach.
(Chim/08)

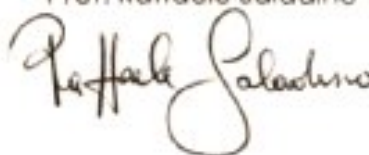**Tesi di dottorato di:**

Dott. Bruno Mattia Bizzarri

Coordinatore del corso

Prof. Daniele Canestrelli

Tutore

Prof. Raffaele Saladino

A.A. 2016/17

New Biocatalytic and biomimetic processes for the synthesis of bioactive compounds: A green chemistry approach.

CHAPTER I: SYNTHESIS OF NEW PEPTIDOMIMETICS BY BIOCATALYTIC AND BIOMIMETIC PROCESSES AGAINST PARKINSON'S DISEASE.

1.1 INTRODUCTION

    1.1.0 PARKINSON'S DISEASE

        1.1.0.1 The role of oxidative stress in PD

        1.1.0.2 L-DOPA therapy

    1.1.1 BIOMIMETIC CATALYSIS

        1.1.1.0 IBX

        1.1.1.1 Supported IBX

    1.1.2.0 ENZYMATIC CATALYSIS

    1.1.2.1 Hystorical background, general features, vantages and disadvantages of biocatalytic processes

    1.1.2.2 Immobilized Biocatalysts

    1.1.2.3 Choice of support

    1.1.2.4 Technique of enzyme immobilization

    1.1.2.5 Physical adsorption

    1.1.2.6 Entrapment

    1.1.2.7 Cross-Linking

    1.1.2.8 Covalent bonding

    1.1.2.9 *Tyrosinase from Agaricus Bisporus*: BIOTECHNOLOGIAL APPLICATIONS

    1.1.3.0. APPLICATION OF CNTs FOR IMMOBILIZED BIOCATALYSIS

    1.1.3.1. Structure and proprieties of CNTs

    1.1.3.2 Chemical reactivity

    1.1.4.0   DOPA DERIVATIVES: CHEMISTRY, APPLICATIONS AND CURRENT ADVANTAGES IN PD THERAPY

    1.1.4.1 DOPA PRODRUGS: Synthesis and biological activities

    1. 1.4.2 Dual acting forms

    1.1.4.3 Dimeric prodrug forms

    1.1.4.4 Dopamide derivatives

    1.1.5.0 PEPTIDOMIMETICS: Synthesis and biological activities

1.2. RESULTS AND DISCUSSIONS

    1.2.1 Oxidative functionalization IBX-Mediated

        1.2.1.0 Synthesis of O–C bonded L-DOPA peptidomimetics

        1.2.1.1Synthesis of N–C bonded L-DOPA peptidomimetics

    1.2.2 Oxidative functionalization by use of supported IBX

    1.2.3 Antioxidant activity

    1.2.4. Evaluation of the genotoxic potential

CHAPTER II: THE ROLE OF POLYPHENOLS IN ANTIVIRAL THERAPY

CHAPTER III: Prebiotic chemistry:First Compartmentalization Silica gardens mediated in presence of Formamide

1.1 Introduction

1.1.0. Parkinson's Disease

Parkinson's disease (PD) is a progressive neurodegenerative disorder characterized by the deplection of dopaminergic neurons[1]. Anxiety, depression Rigidity, tremor, and postural instability are the most important symptoms in PD, furthermore dementia involve lot of patients during the disease progression. The degeneration of Dopaminergic neurons in the SNpc (*Substantia Nigra Pars Compacta*) is considered the principal responsible of the pathology causing a consistent reduction of DA (Dopamine) levels in the striatum. It is well know that also other cathecolamines are involved in the disease in question and other focus of action in the brain, such as amygdala, autonomic nervous system, hippocampus and cerebral cortex were detected[2]. Actually, the therapy aim to increase the DA levels by replacing it, but the oral subministration of DA failed due to the impossibility to across the blood brain barrier (BBB)[3]. L-3,4-Dihydroxyphenylalanine [2-amino-3-(3,4-dihydroxyphenyl) propanoic acid (L-DOPA)], naturally presents in plants and animal, is actually the first choice in PD therapy[4,5,6,7]. Several derivatives of L-DOPA, such as prodrugs and peptides have been synthesized and studied with the aim of enhancing adsorption-distribution-metabolism-elimination (ADME) properties and decreasing enzymatic degradation[8]. L-DOPA containing-peptides show also important biological activities, for example, the L-DOPA analogues of the peptide alpha-factor interact with the G protein-coupled receptor of Ste2p (GPCR)[9]. L-DOPA peptides reduce the oxidation of low density lipoproteins (LDL) and represent the basic instruments for wet adhesives and coatings[10,11,12]. Multi-steps synthesis in solid or liquid phase, and classical or enzymatic reactions are used to prepare L-DOPA derivatives.[13,14]

1.1.0.0. The role of oxidative stress in PD

Oxidative stress is one of the main causes of the degeneration nigrale in patients with MP. It is caused by excessive production of reactive oxygen species (ROS) due to dopamine metabolism, mitochondrial dysfunction and neuroinflammation.[15]

Several data suggest that oxidative damage and mitochondrial dysfunction contribute to the cascade of events leading to degeneration of these dopaminergic neurons. [16,17]

This is supported by postmortem brain analyses showing increased levels of 4-hydroxyl-2-nonenal (HNE), that is a by-product of lipid peroxidation,[18,19] besides to carbonyl modifications of soluble

proteins,[20] and DNA and RNA oxidation products, such as 8-hydroxy-deoxyguanosine and 8-hydroxy-guanosine.[21,22] ROS can be generated through several pathways such as direct interactions between redox-active metals and oxygen species via Fenton and Haber-Weiss reactions, or by indirect pathways involving the activation of enzymes such as nitric oxide synthase (NOS) or NADPH oxidases.
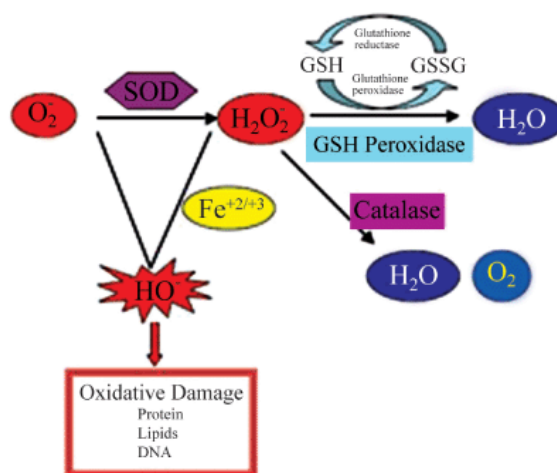
Figure 1. Balance between ROS generation and ROS elimination and the side effect of the ROS species in human cells[23]

Usually, the origin of free radicals requires the activation of molecular oxygen. [24] Examples of ROS include the superoxide anion radical (O_2^{2-}), and hydroxyl radical ($^{\bullet}OH$). Superoxide anion, which is produced mainly by mitochondrial complexes I and III of the electron transport chain, is highly reactive and can easily cross the inner mitochondrial membrane, where it can be reduced to H_2O_2. [25] As peroxisomes contain catalase, H_2O_2 is converted to water, preventing its accumulation. However, when peroxisomes are damaged, H_2O_2 is released to the cytosol where it contributes to oxidative stress. In the presence of reduced metals such as ferrous iron (Fe^{2+}), H_2O_2 is converted by the Fenton reaction into the highly reactive hydroxyl radical.[26] Besides ROS, evidence also exists for the involvement of reactive nitrogen species (RNS) in mediating nitrosative stress.[27] RNS are generated by the quick reaction of superoxide with nitric oxide (NO), which results in the production of large amounts of peroxynitrite ($ONOO.^{-}$). [28,29] NO is produced by NO synthase (NOS).[30] The extensive production of ROS in the brain provides an explanation for the role that these reactive molecules in PD. The brain consumes about 20% of the oxygen supply of the body, and a significant portion of that oxygen is converted to ROS.[31] ROS can be generated in the brain from several sources, both in neurons and ganglia, the electron transport chain being the major contributor at the mitochondrial level. [32,33.]

Other ROS sources include monoamine oxidase (MAO), NADPH oxidase (NOX) and flavo-enzymes along with NO.[34] Experimental evidences suggest that ROS play a significant role in dopaminergic neuronal damage in PD, which result from dopamine metabolism, low glutathione (GSH), and high levels of iron and calcium in the SNpc. Additionally, the brain contains high concentrations of polyunsaturated fatty acids, which under oxidative stress conditions result in lipid peroxidation and the generation of toxic products.[35] Normally, DA is sequestered in storage vesicles through an active transport process that requires vesicular monoamine transporter 2 (VMAT2). Thus, VMAT2 keeps cytoplasmic DA levels under control preventing ROS generation. In addition, the reuptake of synaptically released DA into nigrostriatal terminals requires DA transporters (DAT). Perturbations in this step modify the levels of cytoplasmic free DA that is susceptible to be oxidized.[36,37,38.]
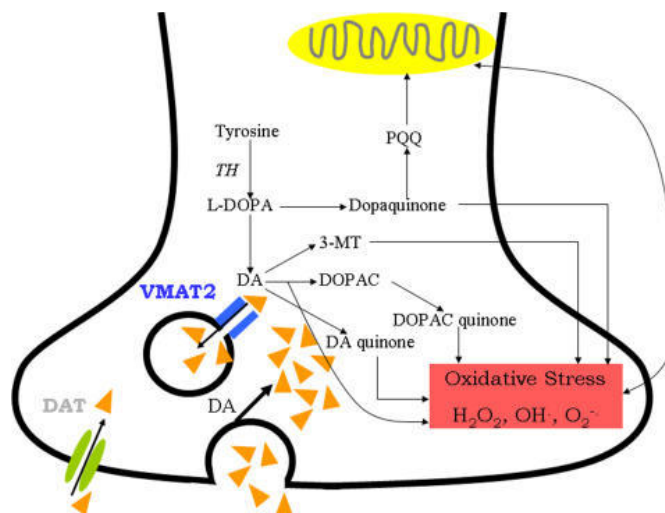
Figure 2. Dopamine metabolism and oxidative stress in neurons [39]

The discovery of genes linked to familial forms of PD, such as alpha-synuclein, parkin, DJ-1, PINK-1 and Leucine-rich repeat kinase 2 (LRRK2) has yielded important insights into the molecular pathways and highlighted novel mechanisms by which oxidative stress contributes to the disease.
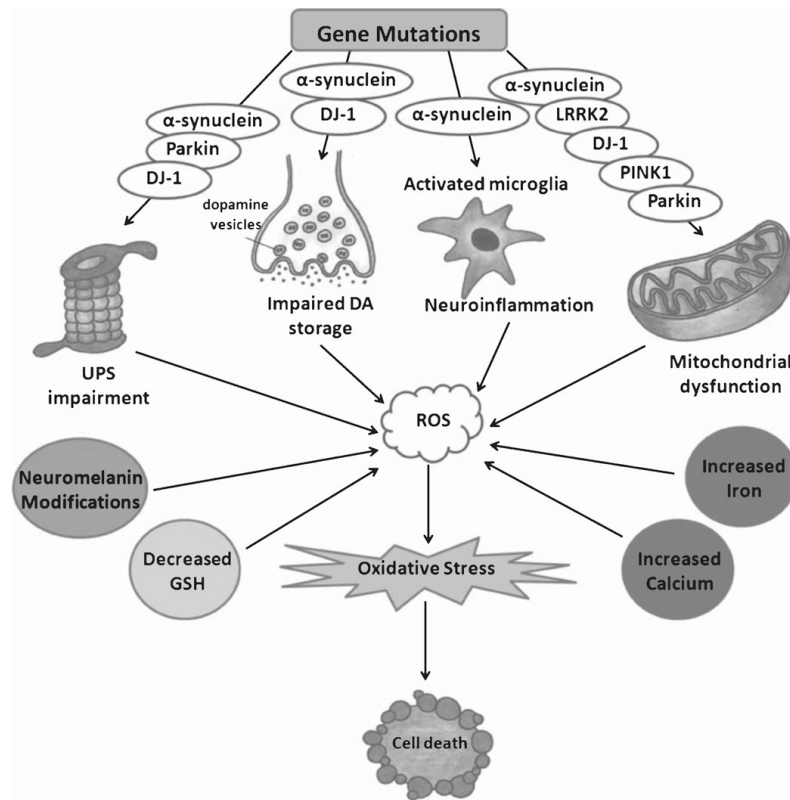
Figure 3. The role of oxidative stress in PD[40]

Some of these mechanisms are complex, involve various cell biologic processes, and are modulated by several proteins. Mutations and multiplication of the SNCA gene are linked to dominantly inherited PD and increase the propensity of the protein to aggregate and the formation of aggregates is associated with increased oxidative or nitrosative stress. Also Parkin and DJ-1 play a role in neuroprotection against several insults, including alpha-synuclein toxicity and oxidative stress, and it is crucial for dopamine neuron survival.[41]

Several reports have provided a link between parkinson and oxidative stress.[42] As for example, the over-expression of wild-type DJ-1 is protective against H_2O_2, 6-OHDA, rotenone or MPTP, while DJ-1 mutants lack this effect. Accordingly, over-expression of DJ-1 in dopaminergic cells inhibits protein aggregation and cytotoxicity caused by alpha-synuclein.[43] DJ-1 can also increase the expression of vesicular monoamine transporter-2 (VMAT2).[44]

Since VMAT2 keeps cytoplasmic dopamine levels in check by storing the transmitter in synaptic vesicles, DJ-1 decreases intracellular ROS levels and enhances the resistance of cells against dopamine toxicity. Reducing DJ-1 levels has the opposite effect.[45] Thus, DJ-1 can confer neuroprotection through up-regulating VMAT2 by enabling the rapid and efficient transport of

dopamine from the cytoplasm to vesicles. DJ-1 also contributes to mitochondrial quality control.[46] [47]

Finally, recent studies shown that the knock down of the endogenous orthology of LRRK2 in the worm reduces survival associated with mitochondrial impairment. LRRK2 mutations may also selectively exacerbate the vulnerability of dopaminergic neurons to oxidative stress[48] as these neurons are more influenced by the model than the survival of the whole worm.

1.1.0.2 L-DOPA therapy

L-DOPA still remains the most clinically useful drug for treatment of PD.[49] When administered orally, L-DOPA is adsorbed by a specific carrier mediate transport system and transported across the BBB, after which it undergoes decarboxylation to DA within the brain.
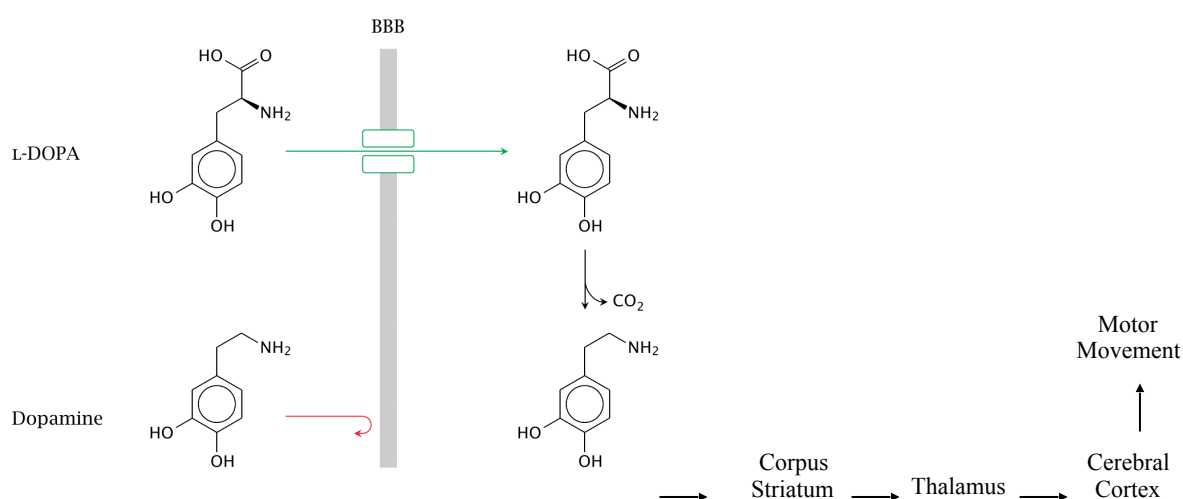
Figure 4. Different absorbiment between L-DOPA and dopamine through BBB

However, during chronic treatment with L-DOPA, a variety of problems may emerge: the patients experience a decrease in the duration of drug effect ('wearing-off' phenomenon) and they become more sensitive to L-DOPA plasma level fluctuations (on/off effects). L-DOPA is usually administered orally but the clinical response is variable because of its erratic oral absorption and metabolic transformations in the gastrointestinal tract. The oral bioavailability of L-DOPA alone is estimated to be about 10% and less than 1% of the administered oral dose reaches the brain.[50]

The major peripheral side effects such as cardiac arrhythmias, vomiting and hypotension are due to the formation of large amounts of DA during the first-pass metabolism in the gastrointestinal tract.The intravenous (i.v.) application of L-DOPA can increase the plasma levels improving the kinetic behavior. In particular, the duration of mobility is enhanced with contemporary reduction of the frequency of fluctuations.[51]

Furthermore, the i.v. co-administration of L-DOPA with carbidopa or benserazide, which are decarboxylase inhibitors (DDCIs), resulted in significant increases in the area under the curve (AUC) plasma concentration *versus* the time profile and of the plasma L-DOPA half-life.[52,53,54,55,56]

This association reduces the peripheral conversion to DA, thereby minimizing its predominant side effects.[57] Since the i.v. infusion is inconvenient for routine clinical use, several approaches have been attempted to enhance the bioavailability and minimize the side effects of L-DOPA.[58,59]

During 1980's, the controlled release (CR) of L-DOPA formulations has been developed with the aim of improving delivery to the brain, and CR tablets have been commercially available since 1991. CR compounds consist of L-DOPA in combination with DCCIs, inside a matrix designed to delay the release of the active ingredients. Thus, delayed absorption and more sustained plasma L-DOPA levels are obtained, as compared with native L-DOPA. [60,61]

The bioavailability of CR/L-DOPA formulations is, however, unpredictable, and generally requires a significant increase in the dose (30%).[62,63]A different way for improving the bioavailability of plasmatic L-DOPA is the inhibition of the catechol-*O*-methyltrasferase (COMT) metabolism. For example, entacapone, that is a specific COMT inhibitor, enhances the bioavailability of L-DOPA. [64,65] From a therapeutic point of view, simultaneous inhibition of both COMT and DDCI pathways results in a significant increase in daily ON time and a corresponding decrease in OFF time.[66,67] Usually, the administration of COMT inhibitors, is associated with an initial increase in dyskinesia that can generally be controlled with adjustments in the doses of L-DOPA. On the other hand, the addition in the early-stage of entacapone to L-DOPA/carbidopa therapy does not reduce the development of dyskinesia.[68]

1.1.1 BIOMIMETIC CATALYSIS

1.1.1.0. IBX

In 1893, the 2-iodoxybenzoic acid (1-hydroxy-1,2-benziodoxol-3(1*H*)-one 1-oxide, usually abbreviated as IBX, was discovered by Hartmann and Meyer[69], but due to its remarkable insolubility in most organic solvents and water and wasn't an election choice for long time. In 1983, Dess and Martin used it to prepare the 1,1,1- triacetoxy-1,1-dihydro-1,2-benziodoxol-3(1*H*)-one 1-oxide another hypervalent iodine reagent. This more soluble oxidative reagent known as Dess-Martin periodinane (DMP) became very popular in organic synthesis, as one of the most convenient reagents available for oxidation of alcohols and phenols.[70,71]
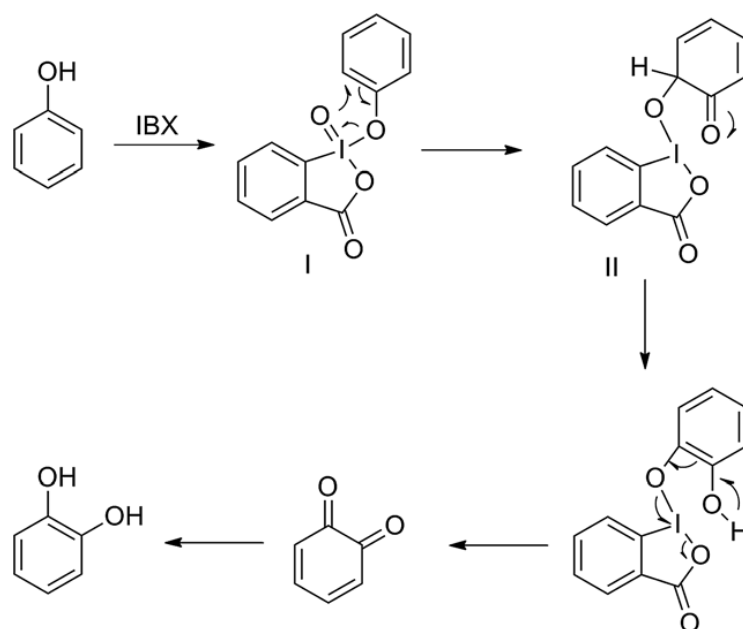
Figure 5. General mechanism of IBX on phenolic compounds

IBX is easily accessible, non-toxic and insensitive to the presence of air or moisture, moreover is commercially available but could also be prepared by oxidation of 2- iodoxybenzoic acid (IBA) with Oxone®. DMP and IBX decompose violently under impact and/or heating (>200°C), clearly limiting industrial applications, so SIMAFEX, a French company, developed and patented a non-explosive white-powder formulation of IBX composed of a mixture of IBX itself (49%), isophthalic acid (29%) and benzoic acid (22%)[72].

About reactivity many synthetically useful transformations, including *ortho*-oxidation reactions (Scheme1), cyclization reaction, hydroxylation were carried out with excellent results.[73,74,75,76,77]
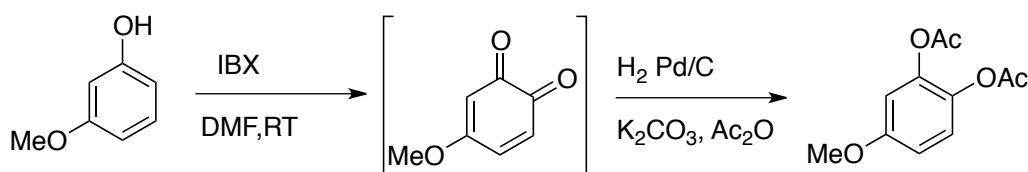
Scheme 1. O*rtho*-oxidation reactions of IBX

Oxidation of various phenolic compounds to *o*-quinone intermediates were reported with IBX. In DMF at RT, phenols containing at least one electron-donating group led regioselectively to *o*-quinones, which were reduced *in situ* to the corresponding catechols (Scheme 2).[78] In a $CHCl_3$/MeOH mixture at low temperature, the phenolic oxidation was found to be less regioselective but could be expanded to phenol itself (Scheme 2).
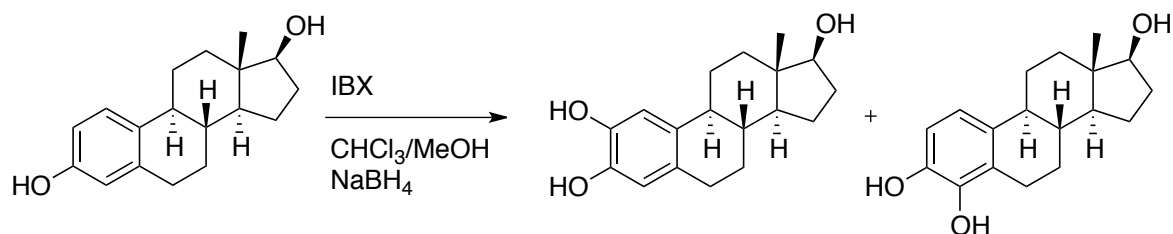
Scheme 2. Selective oxidation of estrogen compound via IBX

Wide applications as a highly efficient and mild oxidant for the conversion of alcohols to aldehydes, ketones and other versatile oxidative transformations[79,80,81,82] contribute to enhance theinterests in using IBX in organic chemistry, but poor solubility in most of organic solvents (except DMSO) and the low stability toward moisture have restricted the practical application of these oxidants. Several research groups have attempted to resolve this problem by raising a reaction temperature[83], adding a supermolecular catalyst to reaction mixture[84], using ionic liquid–water as a solvent[85], or employing

IBX derivatives that are soluble in oxidation reaction. Zhdankin et al. have reported on the synthesis of stable IBX derivatives, IBX amides and IBX esters , which are soluble reagents having oxidative properties similar to IBX.[86]

1.1.1.1 Supported IBX

The IBX and DMP have large range of substrates for their application under mild conditions and low range of organic solvents. The same group has recently synthesized N-(2-iodylphenyl) acylamides, which are soluble IBX analogus having pseudo benziodoxazine structure as well as their polymer-supported reagents. These reagents are found to be potent oxidants toward alcohols[87,88,89,90,91,92,93.]

The use of polymer-supported reagents have emerged as a leading strategy in organic synthesis as it combines the advantages of recycling, simple purification and reaction optimization.[94]

Current interest in developing mild, selective-supported oxidants has prompted numerous research groups to synthesize various supported IBX reagents. In general, the synthesis of IBX precursors occurs via many elaborate synthetic steps, starting from 2-amino-5-hydroxybenzoic acid, thereafter attaching them to appropriately-functionalized supports such as silica gel   and gel-type and macroporous polystyrene.[95,96,97,98,99]   Recents report on various IBX derivatives and the need for a facile synthetic method of preparing supported IBX have inspired us to develop polymer-supported IBX amides and IBX esters in two simple steps[100,101,102]. In brief, 2- iodobenzoic acid was attached to 2-(1-methyl)aminoethyl polystyrene or 2-(1-methyl)hydroxyethyl poly-styrene beads, and the resulting precursor bound resins were activated with tetra-n-butylammonium. Oxone in the presence of methanesulfonic acid to afford IBX amide and IBX ester resins. These polymer-supported reagents were mild and efficient oxidants in the successful conversion of a series of alcohols to the corresponding aldehydes or ketones. IBX amide resins showed similar oxidative properties compared to the previously reported IBX resin.[104] A three- step synthesis of a polymer-supported IBX amide by using 2- iodobenzoyl chloride and Merrifield resin and inserting spacers such as 5- aminopentanol and 3-aminopropanol was reported[105] and recently another way to furnish precursor resins for the polymer-supported oxidant was described. Briefly it consist into a coupling of 2-

iodobenzoyl chloride directly to amino-functionalized resins through an amide linkage, CMPS resin was converted first to azidomethyl polystyrene and then to amino polystyrene. On the prepared amino-functionalized resins, 2-iodobenzoyl chloride was coupled quantitatively to afford the resin bound precursors that was oxidized by TBA-Ox and MeSO3H in DCM solution.[106] (Scheme 3)
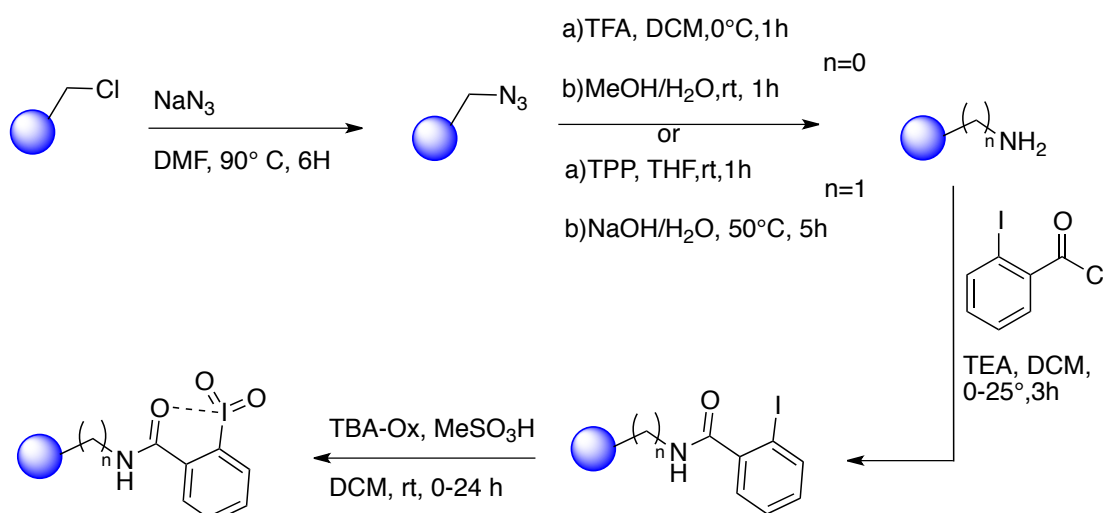
Scheme 3. Synthesis of IBX-polymer bond

1.1.2.0 ENZYMATIC CATALYSIS

1.1.2.1 Hystorical background, general features, vantages and disadvantages of biocatalytic processes

Biocatalysis is the use of natural catalysts, such as enzymes, to perform chemical transformations of organic compounds. Historically, the first applications of biocatalysis was related to foods and drinks processing. For example, the use in ancient China of proteases and amylases to produce foods derived from soybeans, or the use of fermentation to produce alcoholic beverages by Sumerians, Egyptians and Babylonians. [107]

The first company based on biocatalysis was founded in 1874 by Christian Hansen, which introduced on the market the "Rennet" standardized preparation, containing pepsin and rennin, and used in the production of cheese. [108] In 1897 Buchner demonstrated that a yeast extract was sufficient to convert glucose into ethyl alcohol and carbon anhydride, instead of the entire living

being. William Kunne called "enzyme" the agent responsible for the catalysis, from the greek "in yeast". In the subsequent 60 years, biocatalytic processes exhibited a dramatic diffusion in various industrial sectors, in which both whole cells and single enzymes were used to achieve a desired bio-conversion.

Today, biocatalysis has become an intensive scientific and technological discipline and it's improvement will probably continue, partly because relatively new biological and molecular tools as mutagenesis or recombinant technologies permit to influence virtually almost all the properties of biocatalysts. Many industrial realities are interested to biocatalysis, as demonstrated by the high number of sectors in which such processes are involved and by the growing number of university-industry spin-off centres. Almost all chemical reactions require a catalyst, that is in general a chemical species not involved in the stoichiometric balance, and capable to increase the rate at which the reaction reaches the equilibrium, without affecting the equilibrium constant. This is achieved by providing an alternative reaction pathway with an overall lower activation energy. In addition to the need of a catalyst, another important feature of chemical transformations, especially in organic synthesis, is the selectivity, in terms of molecular structure that is transformed (substrate selectivity), portion of the molecule which is transformed (chemo-selectivity), direction of bond making or breaking (regio-selectivity) and spatial way by which the transformation is achieved (stereoselectivity).

Enzymes respond to all of these criteria because are catalysts with high activity and selectivity. An impressive example of the catalytic efficiency is given by catalase, which is capable to decrease the activation energy for the decomposition of hydrogen peroxide of 67 KJ/mol, resulting in a rate accelerating factor of about 10^{15}, while other enzymes acceleration factors lie between 10^{10} and 10^{12}.[109]

Due to their biological functions, the enzymes are often substrate-specific and stereo-specific, and this results in a very limited formation of by-products. Several chemical processes are directing towards more sustainable methodologies (green chemistry), and enzymatic processes perfectly fit to this purpose because enzymes are biodegradable and require mild reaction conditions. [110]

Instead, the large employment of enzymes is limited by instability and inactivation by some reaction conditions e.g., high temperature and ionic strength, pH values, organic solvents and metal ions. Other disadvantages are related to the requirement of costly cofactors. [109]

1.1.2.2 Immobilized Biocatalysts

For the introduction of a biocatalytic transformation, the enzyme costs should amount only to a few percent of the entire production costs. [111]

Many problems related to enzymatic applications can be overcome by immobilization strategies, that consist in the attachment of the enzyme on an insoluble carrier or it's encapsulation into a matrix.

Historically, the first immobilized enzyme was realized by Nelson and Griffin in 1916, which demonstrated that the yeast invertase maintained the catalytic activity when bound to carbon and to aluminium hydroxide. The term 'immobilized enzymes' refers to 'enzymes physically confined or localized in a certain defined region of space with retention of their catalytic activities, and which can be used repeatedly and continuously.' The principal components of an immobilized enzyme system are the enzyme, the matrix and the mode of attachment. The enzymes can be immobilized by interactions ranging from reversible physical adsorption, ionic linkages and affinity binding, to irreversible covalent bonds. It is important to recognize that an enzyme would undergo changes in the chemical and physical properties upon immobilization, depending on the choice of the immobilization method. The surface on which the enzyme is immobilized shows several fundamental roles, such as the preservation of the catalytically active tertiary structure. The advantages of an immobilized enzyme are summarized as follows:

1) Easy recovery of the catalyst from the reaction medium e.g., with filtration or centrifugation, it permits to avoid protein contamination of the product.

2) Use of the same catalyst for more than a cycle; this imply the possible design of continuous and fixed-bed reactors.

3) Enhanced stability for both storage and operational conditions; the latter is particularly important for the achievement of the best enzyme performance into a non-aqueous media, where the immobilization generally provides a better accessibility and/or an extra stabilization towards a denaturing organic medium. [111]

4) Possibility to design multi-enzymatic or chemo-enzymatic cascade processes; a challenge in such context is represented by the possible unfavourable mutual interaction between the

catalysts, which could bring inhibition or deactivation, and an interesting solution is to achieve

compartmentalization *via* immobilization.[111]

1.1.2.3 Choice of support

The characteristics of the matrix are of paramount importance in determining the effectiveness of the immobilized enzyme.[112]

Ideal support properties are described to include hydrophilicity, inertness towards enzymes, biocompatibility, resistance to microbial attack, and resistance to compression.[113,114,115,116]

Various immobilization methods and supports have been developed in order to improve enzyme activity.[117,118] The selection of support depends on the type of enzyme, reaction media, safety policy in the field, and of specific hydrodynamic and reaction conditions.[117,118,119,120,121,122,123,124]

Supports are classified as organic and inorganic according to their chemical composition. The most commonly used supports are carboxymethyl-cellulose, starch, collagen, sepharose, ion exchange resins, active charcoal, silica, [125] clay, [126] aluminium oxide, titanium, diatomaceous earth, hydroxyapatite, ceramic, celite, [127,128,129] agarose,[130,131] porous glass [132] and certain polymers. [133]

Porous supports are generally preferred as the high surface area permits a higher enzyme loading and the immobilized enzyme receives better protection from the environment. These supports should also have a controlled pore distribution in order to optimize capacity and flow properties. [134]

For example, vesicular silica or vesicle-like mesoporous material with inter-lamellar, mesochannel and multimellar structure, enhances the affinity of interaction resulting in slower enzyme leaching during the recycle process.[135] Nanostructured forms such as nanoparticles, nanofibres, nanotubes and nanocomposites are among the most selected carrier for enzyme immobilization and stabilization.[136,137]

These robust nanoscaffolds are excellent supports for enzyme immobilization as they have large surface area and high mechanical properties, that allow effective enzyme amount with minimum diffusion limitation. [138,139,140,141]

1.1.2.4 Technique of enzyme immobilization

Selection of the appropriate immobilization method is a crucial step in the immobilization process, as it plays the biggest role in determining the enzyme activity. [142]

In general, the immobilization methods can be divided into two general classes: a) chemical, and b) physical methods (Figure 6). Physical methods are characterized by weaker, non-covalent interactions, such as hydrogen bonds, hydrophobic interactions, van der Waals forces, affinity binding, ionic binding, or mechanical containment of the enzyme within the support.[143,144]. In the chemical method, the formation of covalent bonds [144] through ether, thio-ether, amide or carbamate are involved. [145]
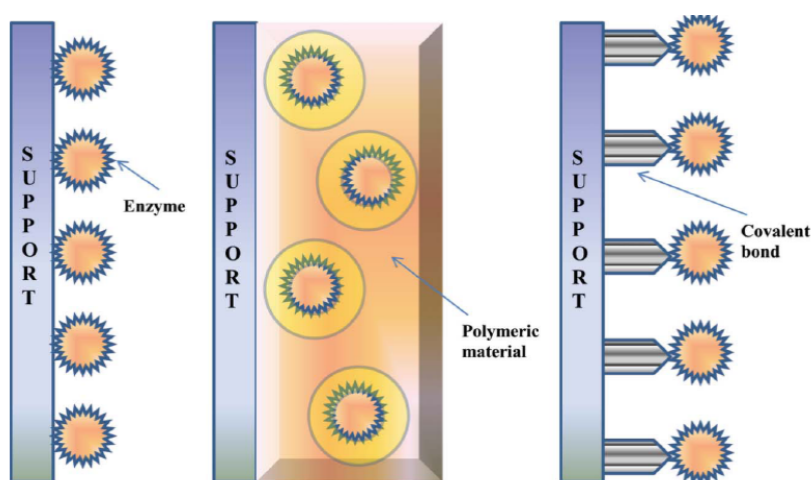
Figure 6. Schematics of the three most common enzyme immobilization techniques: (A) physical adsorption, (B) entrapment and (C) covalent attachment/cross-linking. [146]

1.1.2.5 Physical adsorption

The physical adsorption is one of the straightforward methods of reversible immobilization that involve the enzymes being physically adsorbed onto the support. Adsorption can occur through weak non-specific forces such as van der Waals, hydrophobic interactions and hydrogen bonds, [147,148,149] whereas, in ionic bonding, the enzymes are bound through salt linkages. [144,150,151]

These relatively weak non-specific forces suffer from some drawbacks, such as the enzyme leaching from the matrix.[152]

Depending on the pH of the solution and on the specific isoelectric point, the surface of the enzyme may be charged, [153] and the charge distribution can be calculated by modelling systems. [154]

Thus, the protein/matrix interactions can be (in principle) optimized by tuning the experimental conditions.[155]

However, highly charged support could present problems in the immobilization, such as distortion of kinetics due to partitioning or diffusion phenomena.[156] The remarkable selectivity of the interaction, control orientation of immobilized enzyme and minimal conformational changes are key advantages of the method [144,157,158,159]. The binding between enzyme and support may be achieved in two ways: a) the support is pre-coupled to an affinity ligand for target enzyme or the enzyme is conjugated to an entity that develops affinity towards the support.[160]

The strength of the interactions depends on the hydrophobicity of both the adsorbent and protein, that are regulated by the size of the hydrophobic ligand molecule and the degree of substitution of the support. Further modulation of the hydrophobic interactions between the enzyme and support is achieved through adjustment of the pH, temperature and concentration of salt during enzyme immobilization.
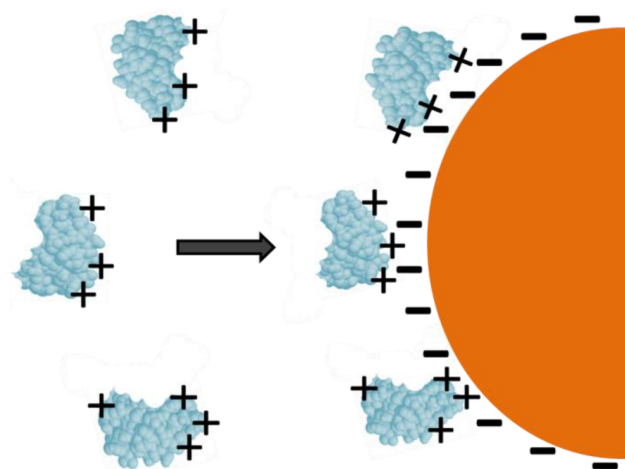
Figure 7. Electostatic adsorption of enzymes directly onto nanoparticles [161]

In general, enzyme immobilization through the technique of physical adsorption is quite simple and may have a higher commercial potential due to its simplicity, low cost and retaining high enzyme activity. [162,163]

1.1.2.6 Entrapment

Entrapment is defined as the enzyme immobilization within a confined space or network, such as fibres, membranes or cross-linked polymers.[164,165,166,167,168,169]

Typically, entrapment improves mechanical stability and minimize enzyme leaching,[170] and, since the enzyme does not chemically interact with the polymer, denaturation is usually avoided. This can be achieved with a variety of materials including polymers, sol-gels, polymer/sol-gel composites and other inorganic materials. [170,171,172,173,174,175]

entrapped in a matrix   entrapped in droplets
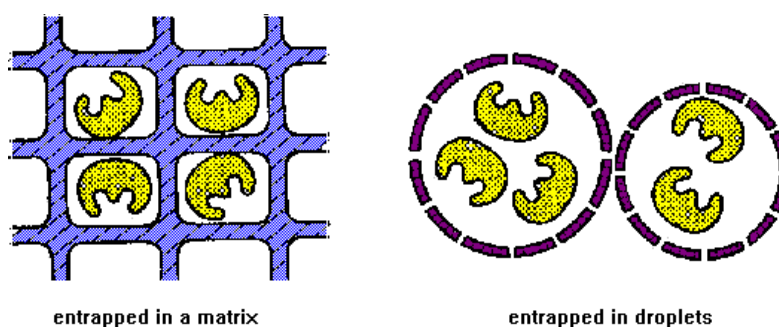
Figure 8. Entrapping Enzymes

Gelation of polyanionic or polycationic polymers (alginate, carrageenan, collagen, polyacrylamide, gelatin, silicon rubber, polyurethane and polyvinyl alcohol) by the addition of multivalent counter-ions is the simplest and common method for the enzyme entrapment.[176,177]

In particular, alginates, are one of the most frequently used polymers due to their mild gelling properties and non-toxicity.[178] Nonetheless, the use of this method is rather limited mainly due to mass transfer limitations to the enzyme active site. [179] Other disadvantages include possibility of enzyme leaching which can occur when the pores of the support are too large, deactivation during immobilization, low loading capacity and abrasion of support material.

1.1.2.7 Cross-Linking

Cross-linking is an irreversible method for the enzyme immobilization. [180,181,182] The method is also called "carrier-free immobilization" since the enzyme acts as its own carrier. Usually, the cross-linking is obtained by intermolecular cross-linkages between enzyme molecules by means of bi- or multifunctional reagents.
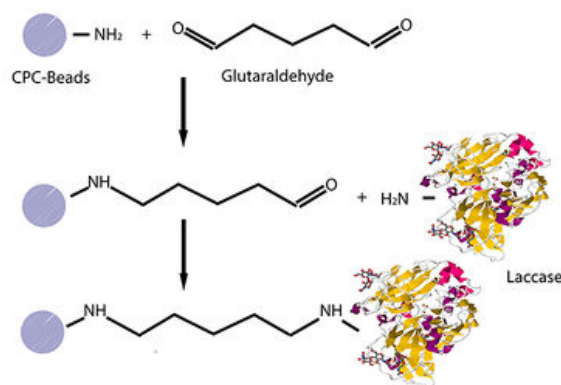
Figure 9. Glutaraldehyde cross-linking

The most commonly used cross-linking reagent is glutaraldehyde (Figure 9).[184] It has been used for decades for cross-linking of proteins *via* reaction of the free amino groups of lysine residues, on the surface of neighbouring enzyme molecules, with oligomers or polymers of glutaraldehyde resulting from inter- and intramolecular aldol condensations.

Cross-linking can involve both Schiff's base formation and Michael-type 1,4 addition to α,β-unsaturated aldehyde moieties.[183] Cross-linked enzyme aggregates (CLEAs) are first prepared by aggregating the enzymes in precipitants such as acetone, ammonium sulphate and ethanol followed by a cross-linker.[184] The reactions for enzyme immobilization can be executed in three different manners: a) mixing the polymers with a photosensitizer (e.g. benzoin ethyl ether); b) gelling by exposure to near ultraviolet (UV) radiation, or c) by polymerization initiated by gamma radiation.[185] Recently, nanodiametric supports have brought a decisive change in the field of biocatalyst immobilization.[186,187,188,189,190]
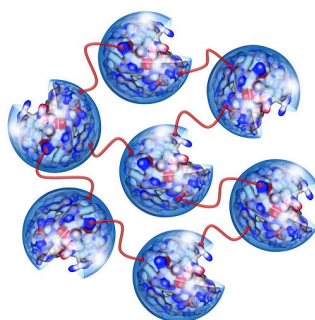
Figure 10. Schematic representation of a cross-linked enzyme aggregate; the enzymes are covalently X-linked to form a robust and recyclable biocatalyst. [275]

1.1.2.8 Covalent bonding

Covalent bonding is one of the most widely used methods for irreversible enzyme immobilization. The functional group that takes part in the binding of the enzyme usually involves binding via the side chains of lysine (ε-amino group), cysteine (thiol group), aspartic and glutamic acids, [191,192] imidazole and phenolic groups, which are not essential for the catalytic activity.[193] The activity of the covalent bonded enzyme depends on the size and shape of carrier material, nature of the coupling method, composition of the carrier material and specific conditions during coupling.[193] The direction of the enzyme binding is a crucial factor for the enzyme activity. The coupling with the support can be mainly obtained in two ways, depending on the active groups present in the molecule. The reactive functional groups can be added to the support without modifications, or the support matrix is modified to generate activated groups. In both cases, the electrophilic groups generated on the support will react with strong nucleophiles on the protein. Matrices of choice for such interactions usually include agarose, cellulose, poly(vinyl chloride), ion exchange resins and porous glass.[194] Dandavate and co-workers [195] covalently immobilized *Candida rugosa* lipase onto the surface of silica nanoparticles and glutaraldehyde-activated aminopropyl glass beads, which resulted in easy recovery and reuse of the enzyme.
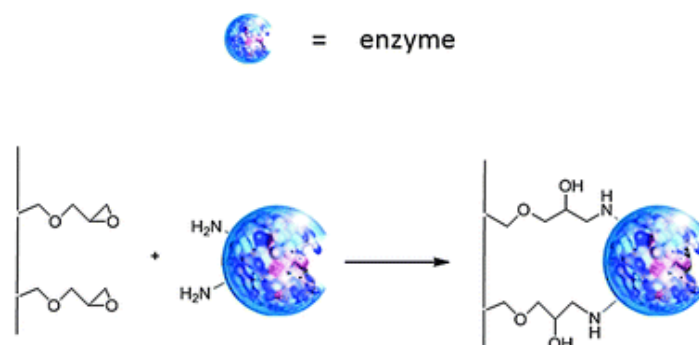
Figure 11. Covalent bonding of an enzyme to a functionalized support.

Similarly, Damnjanovic and co-workers reported that covalently bound *Candida rugosa* lipase was a robust and versatile biocatalyst for production of aroma ester in a fluidized bed reactor.[196,197] Covalent bonds provide powerful link between the enzyme and its carrier matrix, allow its reuse more often than with other available immobilization methods [112,197] and prevent enzyme release into the reaction environment. The method also increases half-life and thermal stability of enzymes.[198] The conferred stability comes from unlimited covalent binding between the enzyme and substrate

due to the lack of any barrier between them. Localization of the enzyme on the surface of the support further enhances enzyme attachment and enzyme loading binding method. [199]

1.1.4. *Tyrosinase* from *Agaricus Bisporus*: Biotechnologial Applications

Applications of *Ab*Tyro are reported in the design of biosensors and bioremediation. In the field of organic synthesis, great attention is given to production of L-DOPA, a drug used for the treatment of Parkinson's disease since 1967. The world market for L-DOPA is about 250 tons/year and most of it is produced by a chemical route which comprise eight reaction steps, including an optical resolution. [200] Mushroom tyrosinase represents a potential alternative to produce such interesting compound in a very clean way. Immobilisation of the enzyme is a fundamental requirement in order to obtain large-scale processes.[201] The productivities are still low due to two factors:

-The conversion of the added L-Tyrosine is incomplete

-Tyrosinase catalyzed reaction, the Dopaquinone brings the regeneration of one molecule of L-DOPA but also a molecule of Dopachrome, which spontaneously polymerize, yielding melanin (Figure 12). [202]
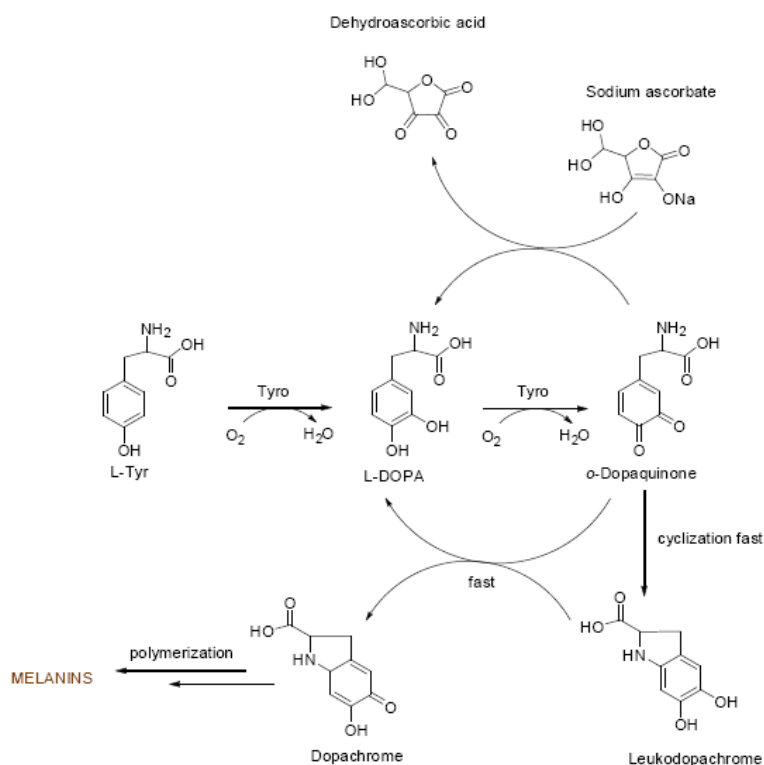
Figure 12. Scheme about biochemical mechanism of Tyrosinase's catalysis

An attempt to minimize the melanin production consists in putting L-ascorbate as a reducing agent in the reaction medium but, unfortunately, ascorbic acid inhibits the creolase activity, and irreversibly inactivates the enzyme. [203]

Creolase activity of Tyrosinase can also be used to produce catechols, which are important antioxidant molecules utilized in pharmaceutical, cosmetic and food industries.[204] Great attention is addressed to tyrosinase for such applications because catechols production by mean of chemical synthesis is difficult and requires not environmentally friendly conditions. This kind of biocatalytic synthesis has nevertheless some limits due to the production of the reactive quinones which tend to polymerize and consequently inactivate the enzyme.[205] Attempts to enhance catechols productivity were made by the involvement of immobilisation strategies, [206] by the use of ascorbic acid [207] or the use of an organic solvent as the reaction medium. [208] Such strategy shows numerous advantages: enhanced hydrophobic substrates solubility, enhanced oxygen solubility, and increased enzyme stability. The catalytic activity is guaranteed by a minimum water content in the medium, in order to give the enzyme the correct catalytic conformation. [209] Another important feature introduced by the organic solvent is the reduction of the quinones-driven polymerization, since inspections about the mechanism revealed water to be an essential component in that reaction. [210] Phenolic compounds are contained in many wastewaters produced by the textile, coal, chemical, petrolchemical, mining and paper industries and represent a significant health and environmental hazard. [211] In consequence of that is extremely important the design of convenient method for their removal from the environment. Regarding detection (and quantification) of phenols, traditional methods like chromatography or spectroscopy are time-consuming while among new techniques, such as biological sensors, are very attractive for this purpose, providing better specificity, lower costs and faster processing.[202] A key requirement is the immobilisation of tyrosinase, because it would assure an intimate contact between the enzyme and the detector and would prevent the enzyme to be washed out in aqueous solution. [211] Detection can be achieved following the oxygen consumption or the chemical reduction of the produced quinone.[212,213]

An important challenge that must be achieved is the improvement of the enzyme stability under operational and storage conditions, usually poor because of the generation of intermediate radicals in both enzymatic and electrochemical reactions, which can form enzyme-inactivating aromatic compounds. [214]

In the field of bioremediation, the removal of phenolic compounds is performed by traditional methods, like solvent extraction, chemical oxidations or absorption onto activated surfaces, which always present high costs. [215]

1.1.3.APPLICATION OF CNTs FOR IMMOBILIZED BIOCATALYSIS

1.1.3.1.Structure and proprieties of CNTs

Until the 1980's only two allotropic forms of Carbon were known: diamond and graphite. These two materials differ in physical and chemical properties due to the different ways by which carbon atoms are bonded to each other. Diamond contains sp^3 hybridized orbitals, where four valence electrons bond four carbon atoms in a tetrahedral structure. Bond electrons are strongly localized and this results in high hardness, electrical insulation, light colour and high thermal conductivity of the material. In contrast, graphite consists in planar carbon layers where three atoms are bonded to each other by sp^2 orbitals; the fourth electron is contained in the π orbital which has its lobes orthogonal to the graphite's plane. These π orbitals give rise to weak van-der-Waals forces between the planes, resulting in softness, dark colour and very good thermal and electrical conductivity. In 1985 Smalley, Curl and Kroto discovered the existence of another carbon allotrope after the vaporization of graphite with an intense pulse of laser light and the subsequent mass spectrometry analysis.
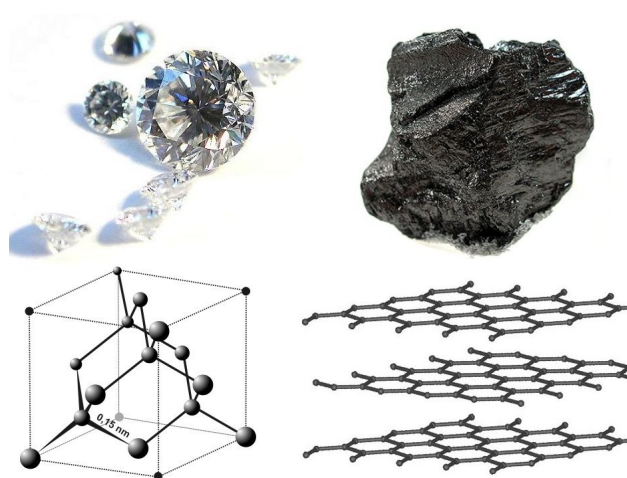
Figure 13. Allotropic form of carbon [274]

The mass spectrum showed a strong peak corresponding to C60 carbon atoms clusters of spherical shape, composed of 32 faces (12 pentagons and 20 hexagons, like a soccer ball) (Figure 13). This new allotrope was called "buckminsterfullerene", being Buckminster Fuller the architect designer of the first geodomes.
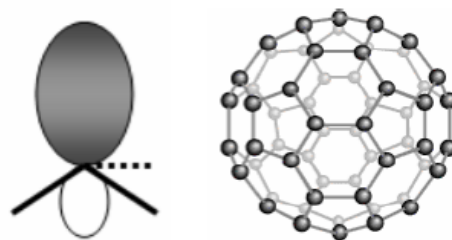
Figure 14. sp² orbital and structural representations of C60 fullerene

The graphite sp² orbital is deformed because of the structure's curvature. In 1991 another carbon allotropic form was fortuity discovered by Sumio Ijima and coworkers, which observed filamentous carbon residues of nanometric dimensions in the graphite vaporization process to obtain fullerenes. These structures were shaped like a tube, as a graphite sheet or a chicken wire rolled into a hollow cylinder (Figure 14).
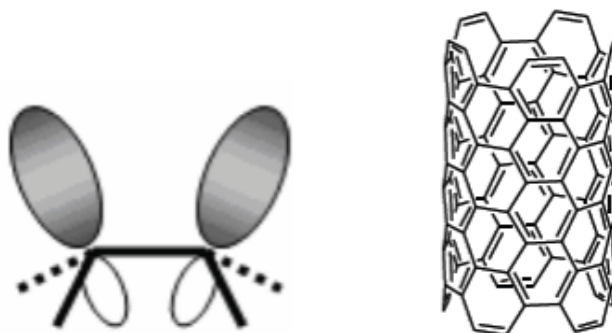
Figure 15. sp² orbital and structural representations of carbon nanotubes.

Because of the curvature, sp² orbitals are deformed and make π electrons more localized than the graphitic ones. This confers to these structures, called carbon nanotubes (CNTs), more mechanical resistance, electrical and thermal conductivity and higher chemical reactivity as well. Basically, two main kinds of CNTs exist: Single-Walled Carbon Nanotubes (SWCNTs) and Multi-Walled Carbon Nanotubes (MWCNTs). The former are rolled graphene sheets which normally have caps at the ends made by carbon pentagons and hexagons combinations. SWCNTs have average diameters of about 1.2 nm and the minimum theoretical diameter is around 0.4 nm [216] while the lengths of both types of nanotubes are generally in the micrometric scale, from 100 up to 10000 times greater than the diameter.

Every SWCNT is characterized by its chiral vector, of which I give here a little explanation. As to form a closed cylinder, it is possible to roll a graphene sheet in a diverse set of directions; if two

carbon atoms are chosen in the sheet, one of which serves as an origin, and the sheet itself is rolled to make the two atoms coincide, the vector pointing from one carbon atom to the other is called the chiral vector (Figure 16).
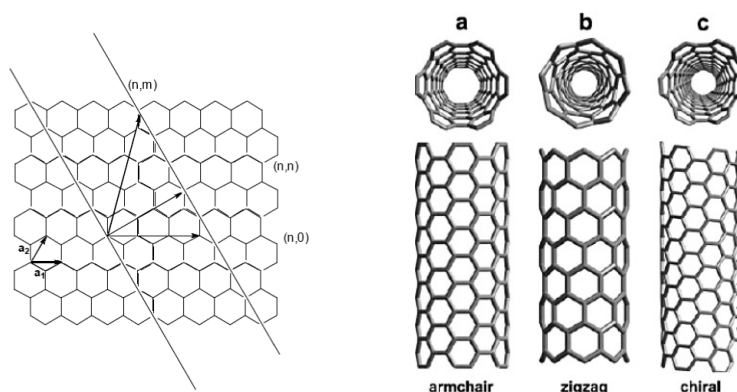
Figure 16. Representation of a graphene plane and configuration of CNTs [217]

Geometrically, the chiral vector is defined as $C = n\mathbf{a1} + m\mathbf{a2}$, where a1, a2 are the primitive vectors which define the hexagonal lattice, while (n,m) indicates the directions by which the graphitic sheet is rolled; n and m values define three "flavors" of nanotubes: armchair (n,0), zig-zag (n,n) and chiral (n,m). These different nanotubes geometries represent the major determinant for the electrical properties e.g., the zig-zag form behaves as a semiconductor. [216] MWCNTs are complex structures made of concentric cylindrical graphene tubes. Typically they have outer diameters in the tens up to 100 of nanometers, and lengths 100 times higher than the wideness. Since MWCNTs are easier to produce in large quantities at a reasonable price, they are involved in many applications. CNTs have peculiar properties which make them differ from the other carbon fibers that have been industrially used for a decade to construct batteries, reinforcement material in tennis rackets, etc. [218]

1.1.3.2 Chemical reactivity

because of the p-orbital mismatch caused by the high curvature, CNTs are more reactive if compared to a graphite sheet; such reactivity is proportional to the nanotube diameter and for the same reasons is also higher at the end caps with respect to the sidewalls. [219] Chemical modifications can be used to modify nanotube's behaviour, for example their solubility in aqueous solutions. (Figure 17)
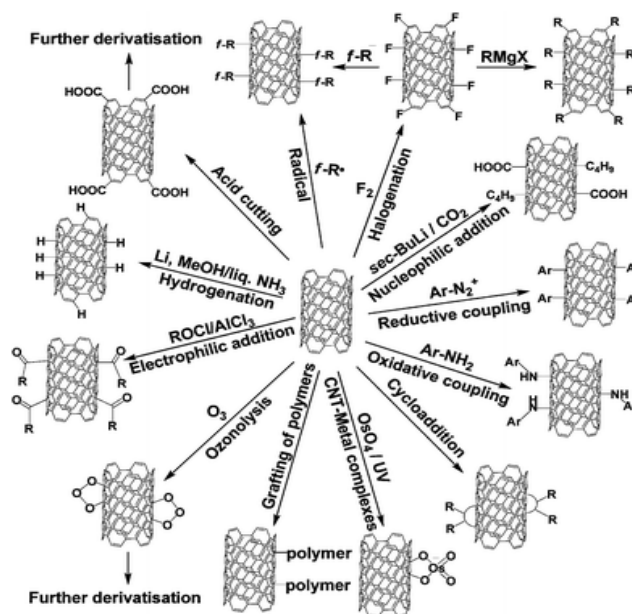
Figure 17. Surface functionalization of CNTs [220]

Mechanical strength: CNTs are very flexible because of the great length and have a very large Young's modulus (ratio of stress to strain) and tensile strength, higher than those of steel. [221] Thus, this material results potentially suitable to construct composites.

Eletrical conductivity: small diameter CNTs could behave as metallic or semi-metallic conductors on the basis of their chiral vector, which gives origin to different band gaps. Other useful properties of CNTs for applicative purposes are the optical, electromechanical and electrochemical ones.

1.1.5.2. CNTs as a support for immobilized biocatalysts

Many CNTs features render them potentially highly useful for proteins immobilization. The high surface area is one of the most important properties, because it permits high enzyme loadings and low mass transfer-resistance phenomena. Moreover, the highly curved surface may lead to decreased protein-protein interactions, thus leading to less deactivation processes.[222] Protein immobilization also require the employment of robust supports and this is well satisfied by the high thermal and mechanical CNTs stability. Biocompatibility of CNTs is also reported [223] and this focuses to the possibility to design completely environmental friendly catalysts. The immobilization can be achieved both by covalent and non covalent techniques.

A) non-covalent immobilization

As reported before, this type of immobilization has the main advantage to limit the structural alteration of the biomolecule, which could however be subjected to leaching. Some non covalent procedures are represented and include:

- **Direct adsorption** (Figure 24a). This technique can be directly performed on CNTs if the protein has an adequate hydrophobic region which can interact with the nanostructure e.g., soybean peroxidase can be well adsorbed on SWCNTs; [224] another driving force which is assessed to permit the direct physical adsorption is that of the π-π stacking interactions between the sidewalls of CNTs and the protein's aromatic rings. [225] Many factors contribute to determine the amount of the protein loaded: nature of the enzyme, surface chemistry of CNTs and operational variables.

- **Adsorption on functionalized CNTs** (Figure 24c). Positively or negatively charged CNT/polymer composites can be easily dispersed in aqueous solutions and proteins adsorption is highly facilitated thanks to the combination of various types of interactions: hydrophobic, hydrogen bonding and electrostatic forces. [226]For example, glucose oxidase is reported to be adsorbed on SWCNTs previously functionalized with Poly(4-vinylbenzenesulfonic acid) and ionic liquids.[227]Such a strategy can also be used to adsorb the protein by means of the "Layer by Layer" technique, which in general permits the repeated adsorption of oppositely charged polymers on a certain surface; this is also potentially useful to construct multi-enzymatic systems. [228] Alternatively, CNTs which have been previously functionalized with negatively charged hydrophilic groups *via* oxidation process (CNTs-COOH) can be used to adsorb proteins with a global positive charge at the operative pH, as glucose oxidase (Figure 24b).
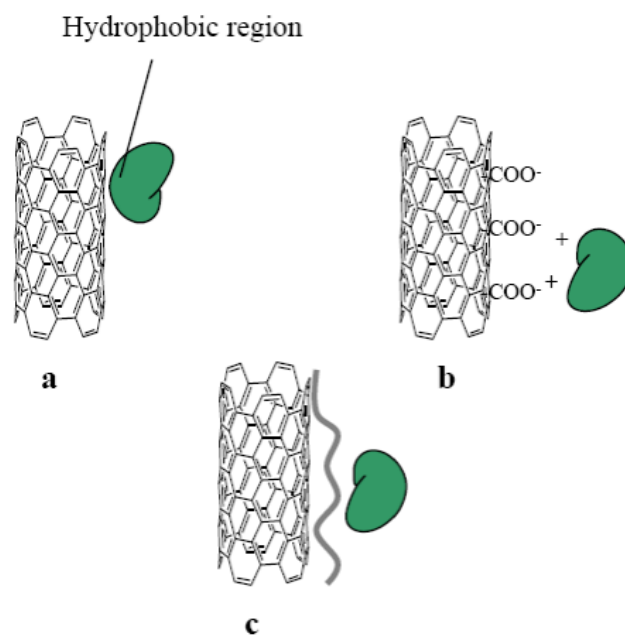
Figure 18. Representation of non-covalent immobilization techniques.

B) covalent immobilization

The use of a covalent bond permits to afford a stable linkage between the protein and the support, with the resulting vantages and disadvantages reported in the previous paragraph. Two main technique are largely diffused:

- **Direct covalent bond**

The carboxylic functionalized CNTs-COOH can be used to form an amidic bond between the enzyme and the support; for example the two step process of diimide-activated amidation represented in Figure 19a is widespread in the literature [229,230]

- **Covalent bond with the use of linking molecules**

Linking molecules can be bonded to CNTs through hydrophobic and π-π interactions and also to the enzyme by means of a covalent bond; alternatively, a spacer could be covalently bonded to both the nanotubes and the enzyme (Figure 19b), thus possibly limiting deactivation processes e.g., horseradish peroxidise was immobilized on CNTs with the use of pyrene butanoic acid succinimidyl ester as the spacer [231]
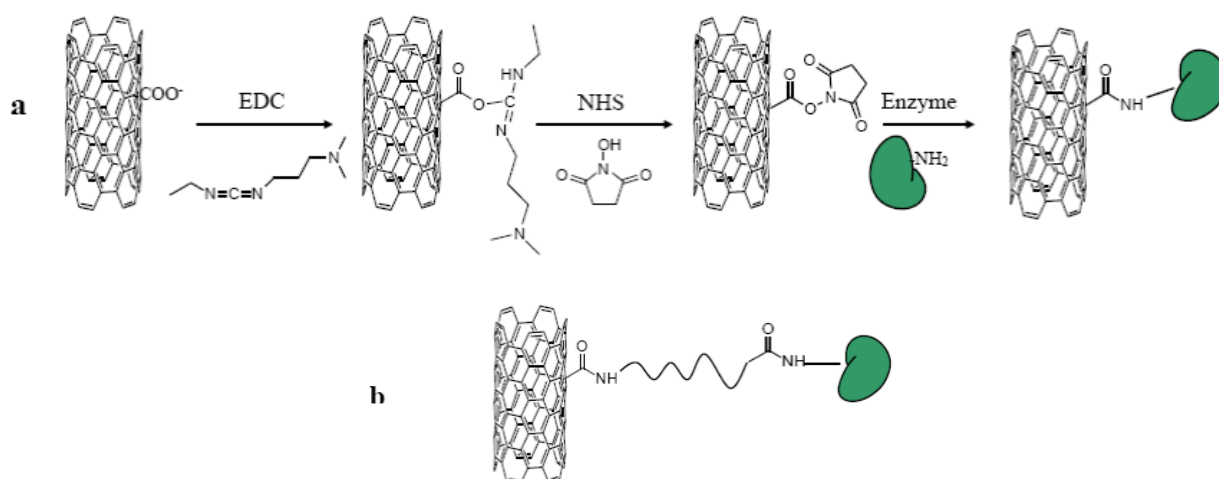
Figure 19. (a) Formation of an amide bond between an enzyme (green form) and CNTs *via* treatment of the oxidized carbon nanotubes with EDC (1-ethyl-3-3'-dimethyl amino propyl carbodiimide) and NHS (N-hydroxy succinimide). (b) curved line represents a spacer covalently bonded to both CNT and the enzyme.

1.1.4. DOPA DERIVATIVES: CHEMISTRY, APPLICATIONS AND CURRENT ADVANTAGES IN PD THERAPY

1.1.4.1 DOPA PRODRUGS: Synthesis and biological activities

The L-DOPA and DOPA-containing peptides, are active drugs for the control of degenerative diseases of the Central Nervous System (CNS), and in particular of Parkinson's disease. Peptides containing L-DOPA show important biological and pharmacological activities.

A prodrug is a medication or compound that, after administration, is metabolized (i.e., converted within the body) into a pharmacologically active drug.[232,233]Inactive prodrugs are pharmacologically inactive medications that are metabolized into an active form within the body. Instead of administering a drug directly, a prodrug might be used instead to improve how a medicine is absorbed, distributed, metabolized, and excreted (ADME).[234,235] Prodrugs are often designed to improve bioavailability when a drug itself is poorly absorbed from the gastrointestinal tract. A prodrug may be used to improve how selectively the drug interacts with cells or processes that are not its intended target. For example, DOPA analogues of the factor alpha receptor coupled to G protein,[236] inhibit the oxidation of low density lipoproteins in atherosclerotic plaques. [237]

DOPA peptides also provide the reactive tools for the preparation of adhesives and coatings of materials. [238] The high activity of L-DOPA is mainly due to the presence of the catechol moiety, characterized by strong antioxidant properties. This group can react with a radical species by

electron transfer to yield relatively stable semi-quinones, which in turn can trap a second radical to afford quinones (Scheme 4).
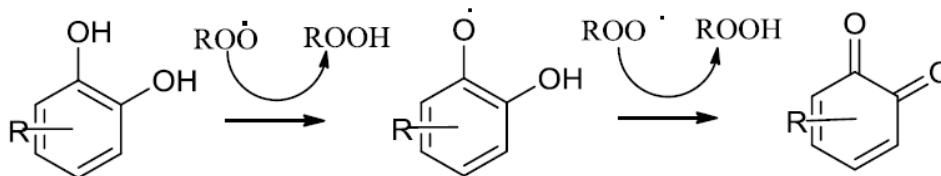
Scheme 4 . Mechanism of action of antioxidant systems catechol

1.1.4.2 Dual acting forms

Di Stefano et al. designed a novel prodrug based on the "dual-acting" concept, in which L-DOPA is covalently linked to a modified glutathione (GSH) residue by an amide bond. In this compound, the increasing of oral bioavailability due to the peptide transport mechanism [239,240,241] was synergistic with the known antioxidant activity of GSH. In GSH, the cysteine residue was replaced by methionine to optimize the antioxidant activity at pH 4 (rather than at pH 1, as in the case of native GSH), and   thus conferring resistance to degradation in the gastric fluid.[242] Furthermore, the presence of methionine increased stability against the γ-glutamyl transpeptidase (γ-GT) cleavage. [243]

The synthesis of DOPA-GSH is reported in Figure 28. The antioxidant activity of **2** [evaluated by the 1,1-diphenyl-2-picrylhydrazyl (DPPH) method] was higher than **3**, suggesting that L-DOPA moiety in **3** exerted a pro-oxidant effect prevailing on the antioxidant activity of the native molecule.
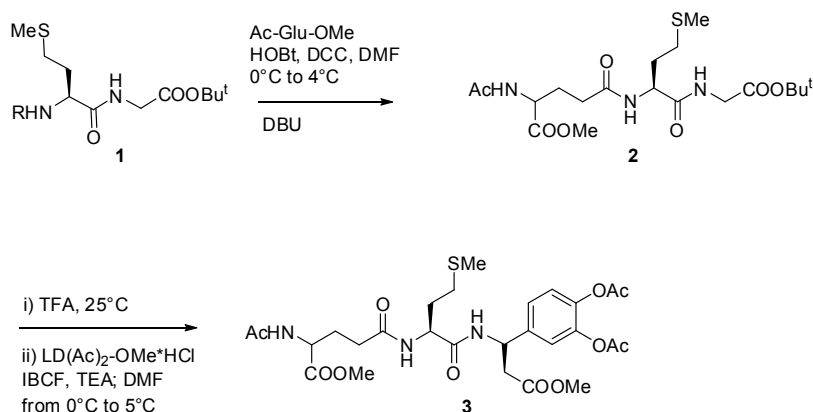
Scheme 5. DOPA-GSH compounds

Denora et al., designed a family of pro-drugs based on the link between L-DOPA and appropriately substituted 2-phenyl-imidazopyridine-3-acetic acids.[244] Phenyl-imidazopyridine derivatives show high affinity and selectivity for GABA-benzodiazepine receptor (GABA-BZR) complexes ,[245,246] which are involved in the modulation of activity of mesocortical and mesolimbic dopaminergic neurons. [247] Moreover, the phenyl-imidazolepyridine moiety was enough lipophilic to function as a carrier for L-DOPA leading to increase of brain levels, in accordance with the high BBB crossing ability (e.g log Cbrain/Cblood 0.4).[247]
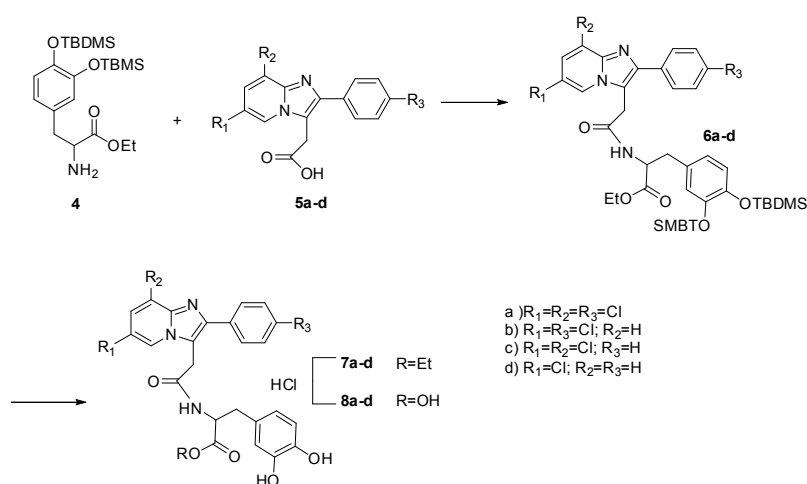
Scheme 6. DOPA-GSH compounds

The novel compounds showed a significant penetration across bovine brain microvessel endothelial cells (BBMECs) monolayers [248,249] suggesting the ability to cross the BBB. Moreover, brain micro-dialysis experiments in rat [250] showed that intraperitoneal acute administration of compounds **7a** and **7b** induced dose-dependent increase in cortical DA output, confirming their role as L-DOPA prodrugs.

1.1.4.3 Dimeric prodrug forms

A further class of DOPA prodrugs is based on the "dimeric prodrug forms" concept, in which two identical molecules are linked together through a spacer. These compounds are hydrolized after administration into their identical active agents.[251] Di Stefano et al. reported the synthesis of dimeric DOPA derivatives containing an amide moiety as spacer group and characterized by protection of all three sensitive centers of the molecule: the carboxyl function, the amino group and the catechol

system.[252] The novel compounds showed values of the lipophilicity parameter (logP) high enough for a good oral absorption. Moreover, the logP increased as the acyl spacer lengthened. A considerable chemical stability in aqueous buffer solution (pH 1.3, 37°C) was observed, accompanied by relatively slow release of L-DOPA in human plasma and rat plasma models. While in the human plasma the release of L-DOPA occurred by two steps mechanism, with formation of catechols as key intermediates, in the case of the rat plasma the hydrolysis required only one step.
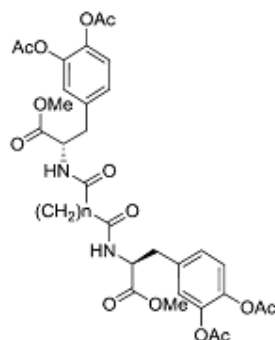
Figure 20. Example of dimeric prodrug form

1.1.4.4 Dopamide derivatives

In an effort to investigate the structure-activity relationships of L-DOPA amides, Hobbs et al. described the preparation of novel derivatives with different substituents on the amide and catechol moiety.[253] As reported in Scheme 7, the first series of derivatives was prepared starting from L-DOPA methyl ester hydrochloride
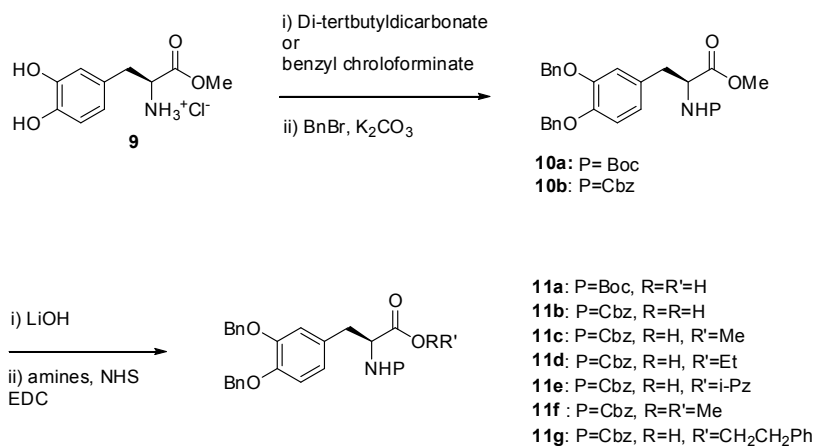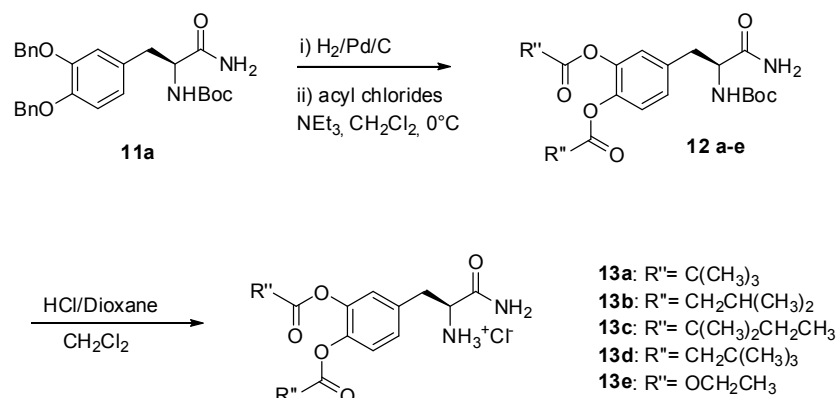
Scheme 7. First series of dopamide derivatives

13a: R''= C(CH$_3$)$_3$
13b: R''= CH$_2$CH(CH$_3$)$_2$
13c: R''= C(CH$_3$)$_2$CH$_2$CH$_3$
13d: R''= CH$_2$C(CH$_3$)$_3$
13e: R''= OCH$_2$CH$_3$

11a

i) H$_2$/Pd/C
ii) acyl chlorides
NEt$_3$, CH$_2$Cl$_2$, 0°C

12 a-e

HCl/Dioxane
CH$_2$Cl$_2$
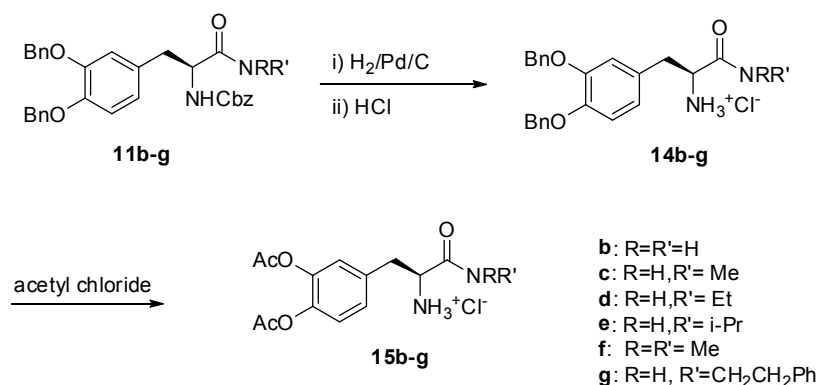
Scheme 8. Acetyl-Dopa derivatives

11b-g

i) H$_2$/Pd/C
ii) HCl

14b-g

acetyl chloride

15b-g

b: R=R'=H
c: R=H,R'= Me
d: R=H,R'= Et
e: R=H,R'= i-Pr
f: R=R'= Me
g: R=H, R'=CH$_2$CH$_2$Ph

The anti-parkinsonian activity of novel pro-drugs was evaluated by 6-OHDA lesioned rat test, the compounds **14b** and **15b** were the most active. In particular, compound **15b** showed high activity after oral administration resulting in prolonged plasma levels of released L-DOPA compared to equivalent dose of native L-DOPA. At contrary, due to the inability of *N*-alkylated prodrugs to be cleaved in the plasma,[254] only low levels of L-DOPA resulted after administration of **14c-g**.

1.1.5.0 PEPTIDOMIMETICS: Synthesis and biological activities

Peptidomimetics are small molecules which are designed to mimic a naturally occurring peptide. They are typically obtained by modification of parent peptides or by total synthesis [255] in order to optimize pharmacological properties, such as bioavailability and biological activity. [256] The modifications can involve N-alkylation, Cα-substitution, cyclization, N-replacement, carbonyl replacement, heterocyclic generation, Cα-replacement, and backbone or side-chain transformations, as well as the incorporation of unnatural amino acids. [257] Among peptidomimetics, DOPA

derivatives play a crucial role in the therapy of Parkinson disease (PD). PD is one of the most important neurodegenerative disorder, characterized by dopamine (DA) depletion in dopaminergic neurons of the striatum of the brain, inducing rigidity, tremor, and postural instability as some of the most important symptoms. [258] DOPA peptides are able to increase the capacity of DOPA in penetration of the blood brain barrier (BBB) [259] by specific peptide-mediated carrier transport systems (PMCTS), thus restoring adequate DA concentration and inhibiting oxidative cell damage. [260] They also act as pro-drugs, preserving DOPA from fast metabolic decarboxylation and avoiding the peripheral DA-related side effects.[261] L-DOPA-L-Phe is absorbed more efficiently than L-DOPA *via* the peptide transporter in Caco-2 cells, which are considered to be a good model for in vivo intestinal absorption in humans. [262]

In a similar way, D-Phe-L-DOPA showed 31-fold higher oral bioavailability and anti-Parkinson activity than L-DOPA in rats. [263] DOPA peptides and peptidomimetics are usually synthesized by solution or solid phase procedures, which show a different degree of complexity depending on the method used for the activation/protection of amino acids. [264] Irrespective to experimental conditions, these syntheses requires tedious and long time protecting/deprotecting steps and have, in principle, an intrinsic low selectivity. This study is focused on the design of a novel synthetic procedure for the preparation of DOPA peptidomimetics by oxidative side chain modification of amino acid residues. [265,266,267,268,269,270] In this context, DOPA-peptides have been previously synthesized with complete stereochemical integrity by oxidation of Tyr residues with tyrosinase from *Agaricus bisporus* in organic solvent.[271]

In the last few times, our group of research is involved in the utilization of tyrosinase for the synthesis of bioactive catechol derivatives and DOPA peptides oxidated from L-tyrosine and L-tyrosine derivatives. The oxidation is carried out with freshly purified tyrosinase from A.bisporus in CH_2Cl_2/Buffer at room temperature under O_2 atmosphere for 4 hour. DOPA is obtained after an situ reduction of the corresponding ortho-quinone with sodium dithionite. Oxidation reactions proceeded in good yields.

The oxidation of Boc-Tyr-OMe **16** afforded Boc-DOPA-OMe derivative **17** as the only reaction product in 82% yield and 88% conversion of substrate (Scheme 9).
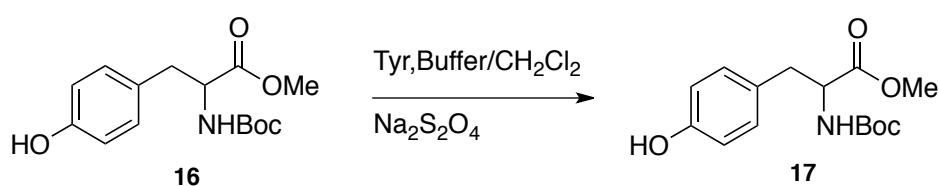
Scheme 9. Oxidation of Boc-Tyr-OMe **16** to Boc-DOPA-OMe **17**

On the basis of the efficiency observed in the oxidation **16**, the biocatalyst procedure was extended to a panel of selected Tyr-containing dipeptides and tripeptides bearing amino acids with aliphatic or aromatic side-chain residues

The oxidation of Boc-Gly-Tyr-OMe **18** with Tyr afforded Boc-Gly-DOPA-OMe **19** in good conversion and yields after 4 h. In a similar way, treatment of Boc-Tyr-Phe-OMe **20** gave the corresponding Boc-DOPA-Phe-OMe **21** in satisfactory conversion and yields.

Also compounds Boc-Ala-Tyr-OMe **22**, Boc-Tyr-Leu-OMe **24**, Boc-Leu-Tyr-OMe **26** and Boc-Val-Tyr-OMe **28** were treated with Tyr to give the corresponding oxidized products, **23** ,**25** ,**27** ,**29** , in good conversion and yields.
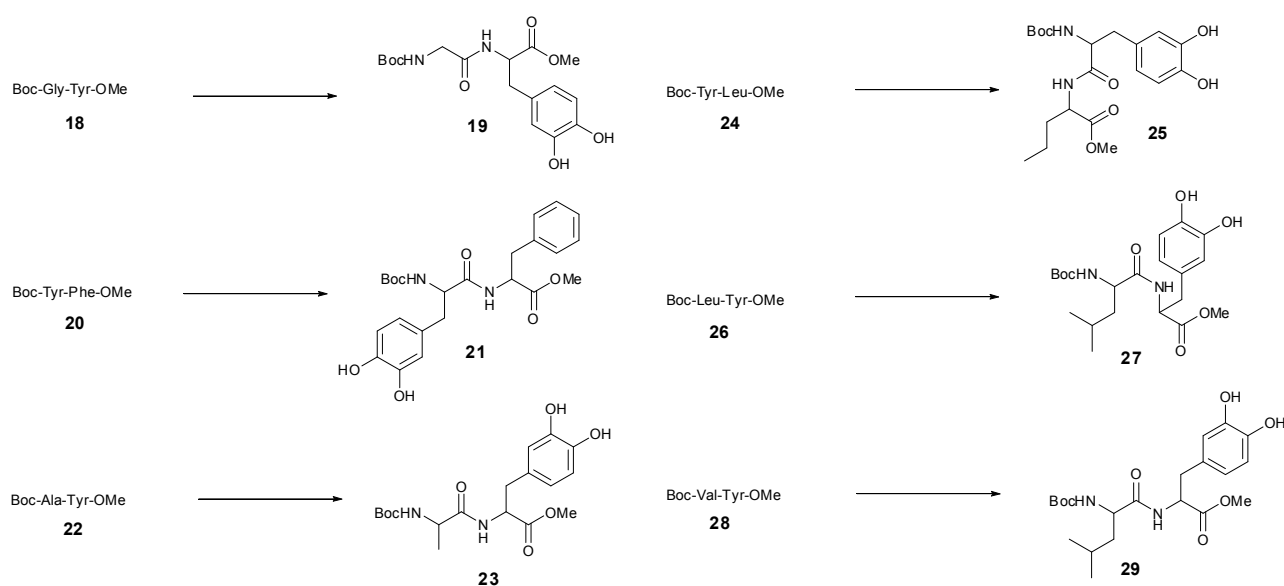
Scheme 10. Oxidative modification of dipeptides 18,20,22,24,26,28 with tyrosinase and CH_2Cl_2/buffer system

The oxidation of tripeptides Boc-Gly-Leu-Tyr-OMe **30** bearing one reactive Tyr residues, as well as, Boc-Val-Tyr-Val-OMe **32** and Boc-Tyr-Tyr-Tyr-OMe **34** bearing three reactive Tyr residues, was studied. In the case of tripeptides **30** and **32** the Tyr residue was selectively oxidized to give Boc-Gly-Leu-DOPA-OMe **31** and Boc-Val-DOPA-Val-OMe **33** in good conversion and yields. The treatment of **34** with an excess of tyrosinase gave the tripeptide **35** in which all Tyr residues are functionalized.
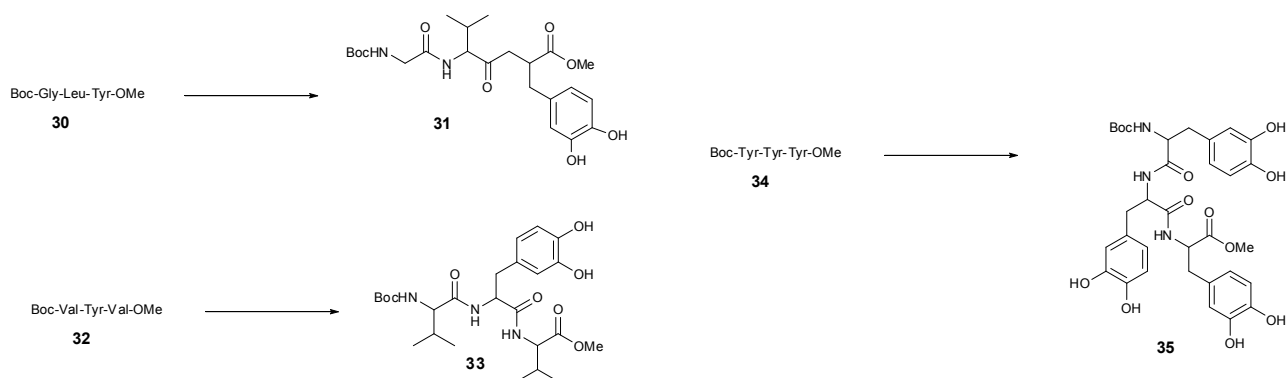
Scheme 11. Oxidative modification of tripeptides 30,32,34 with Tyr/Buffer/CH₂Cl₂ system

With the aim to further improve the procedure, the oxidation of Boc-Tyr-OMe **16** and the selected dipeptide Boc-Gly-Tyr-OMe **18,** was repeated by using immobilized tyrosinase on Eupergit C250L (Tyro/E) and the latter catalyst after coating by the layer-by-layer (LbL) technique (Tyro/E-LbL).[272]
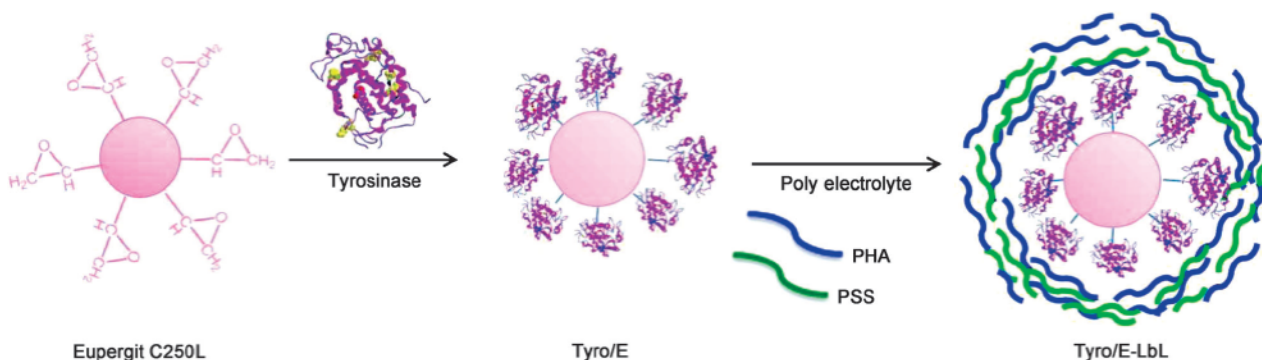
Figure 21. Preparation of Tyro/E and Tyro/E-LbL[272]

Briefly, tyrosinase was suspended in Na phosphate buffer (0.1m, pH 7) in the presence of Eupergit _C250L for 24 h at room temperature, followed by treatment with glycine to block residual epoxy groups, to yield Tyro/E. Under these experimental conditions Tyro/E retained about 37% of the native activity Then the LbL technique was applied by coating the particles through sequential deposition of alternately charged polyelectrolytes. The immobilized LbL enzymes retained approximately 87% of the Tyro/E activity. The structure and morphology of particles of Tyro/E and Tyro/E-LbL in CH2Cl2 was similar to that in Na phosphate buffer.[272]

The oxidation of **16** with Tyro/E in CH2Cl2/buffer afforded **17** in 53% yield and 91% conversion of substrate as the only product while the oxidation compound **18** in the same conditions afforded **19**

in 46% yield and 90% conversion of substrate. About the effect of LbL coating, compound **17** was again obtained as the only reaction product by treatment of **16** with Tyro/E/LbL, in 67% yield and 98% conversion of substrate. Compound **18** was oxidated with Tyr/E-LbL to give **19** in 70% yield and 98% conversion of substrate. Thus, the reactivity and selectivity of tyrosinase was found to be decreased after the immobilization, suggesting that the free enzyme is more reactive than that supported.

1.2.0 RESULTS AND DISCUSSIONS

1.2.1 Biomimetic oxidative functionalization with IBX

This study is focused on the design of a novel synthetic procedure for the preparation of DOPA peptidomimetics by oxidative side chain modification of amino acid residues.[273-278] L-DOPA-peptides have been previously synthesized with complete stereochemical integrity by oxidation of Tyr residues with tyrosinase from *Agaricus bisporus* in organic solvent.[279] IBX was also used in similar transformations[280,281] performing for the *ortho*-hydroxylation of phenol to catechols, with a selectivity similar to natural polyphenol oxidases.[282-286] The regioselectivity of the oxidation is a consequence of the concerted intramolecular oxygen transfer, from iodine (V) in l^5-iodanyl intermediate (I), to *ortho*-position of the phenol moiety, with concomitant reduction to l^3-iodanyl *ortho*-quinol monoketal (II) (Scheme 12).[287] In the reaction described below, the chirality of L-DOPA residues is not affected, the L-enantiomer being the only stereoisomer obtained.[288] The idea to replace the natural amide bond with more stable covalent linkages in DOPA peptides could significantly improve the bioavailability and activity of Dopa derivatives.[289-297] Although few informations are available for the structure of these products, it is expected that the reaction proceeds through nucleophilic addition on reactive DOPA ortho-quinone intermediate following the Michael-like 1-4-regiochemistry.[298] With the aim to synthesize new L-DOPA-peptidomimetics characterized by stable O–C and N–C bonds we deep investigated the IBX mediated aromatic oxidative functionalization of Tyr with different oxygen and nitrogen protected α-amino acids. The chemical rationale of this new approach is related to the oxidation of the phenol moiety to catechol group with concomitant introduction of the α-amino acid residues on the aromatic ring, exploiting the reactivity of the DOPA-quinone intermediate.[299] The general synthetic pathway is described in Scheme 12.
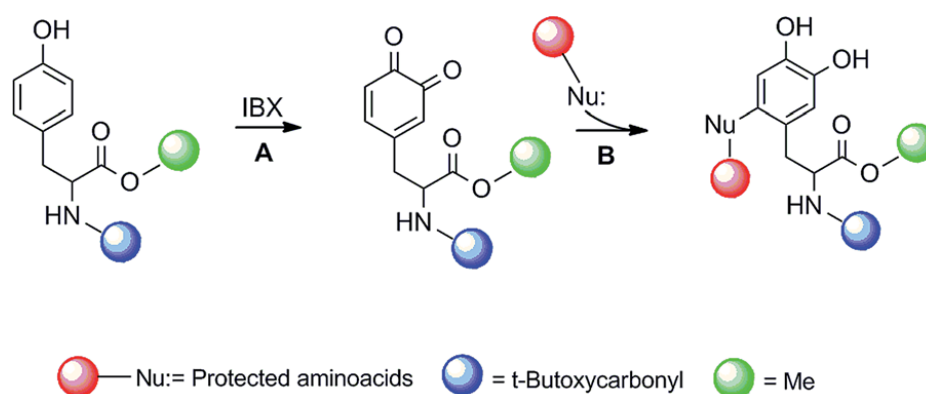
Scheme 12. General reactivity scheme of Tyr with IBX in the presence of protected α-amino acids. Step A: oxidation of Tyr to DOPA-quinone. Step B: In situ Michael-like 1-4-addition of protected α-amino acids on DOPA-quinone intermediate, followed by a reduction step.

1.2.1.0 Synthesis of O–C bonded L-DOPA peptidomimetics

Following the general procedure in Scheme 12, we analyzed the reactivity of N-Boc-Tyr-OMe (**36**) with a panel of N-Boc protected a-amino acids, including glycine (N-Boc-Gly, **37**), alanine (N-Boc-Ala, **38**), valine (N-Boc-Val, **39**), leucine (N-Boc-Leu, **40**), phenylalanine (N-Boc-Phe, **41**), proline (N-Boc-Pro, **42**), tryptophan (N-Boc-Trp, **43**) and methionine (N-Boc-Met, **44**).Briefly the oxidation of Boc-Tyrosine-OMe (BTO **36**) [280] (0.1 mmol), was dissolved in THF (1.5 mL) with a large excess of (**37**) (1.0 mmol, as selected nucleophile) and treated with IBX (0.3 mmol) at 45 °C for 3.0 h. The color turned into brown-orange, that is characteristic for the formation of quinone species. After work- up and purification procedures, the desired N-Boc-Gly-N-Boc- DOPA-OMe (**46**) was obtained in low yield, besides to unreacted substrate and N-Boc-DOPA-OMe (**45**) (Scheme 13, Table 1, entry 1). The ^{1}H-NMR confirmed the mono-substitution pattern of BTO **36**. Better results were obtained increasing the temperature (45° C) and the reaction time (72 h) to afford **46** in higher conversion and product yield (Table 1, entry 2). On the basis of these data, the reaction was extended to a-amino acids **38–44** to obtain the corresponding L- DOPA peptidomimetics N-Boc-Ala-N-Boc-DOPA-OMe (**47**), N- Boc-Val-N-Boc-DOPA-OMe (**48**), N-Boc-Leu-N-Boc-DOPA-OMe (**49**), N-Boc-Phe-OMe (**50**) N-Boc-Pro-N-Boc-DOPA-OMe(**51**), N-Boc-Trp-N-Boc-DOPA-OMe, (**52**) and N-Boc-Met-N-Boc-DOPA-OMe, (**53**) with N-protected *a*-amino acids. In the case of aliphatic *a*-amino acids, the yield increased by decreasing of the steric

hindrance of the side chain (Table 1, entries 2 and 3 versus entries 4 and 5). Possible side-products due to IBX side-chain oxidation of others low redox potential residues (e.g. tryptophan), were not detected in the reaction mixture. This result is in accordance with the high selectivity of IBX towards the oxidation of phenolic aromatic moieties.[300]

R = H (37), (46)
  CH$_3$ (38), (47)
  -CH(CH$_3$)-CH$_3$ (39), (48)
  -CH$_2$-CH(CH$_3$)-CH$_3$ (40), (49)
  -CH$_2$-C$_6$H$_5$ (41), (50)
  -CH$_2$-CH$_2$-CH$_2$- (42), (51)
  -CH$_2$-C(CH)-NH-C$_6$H$_4$ (43), (52)
  -CH$_2$-CH$_2$-S-CH$_3$ (44), (53)
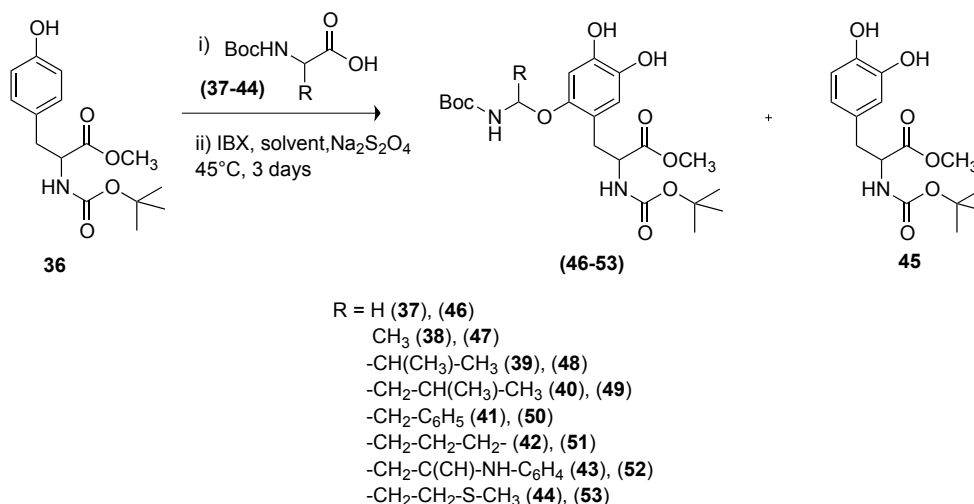
Scheme 13. IBX mediated oxidative functionalization of N-Boc-Tyr OMe (36) with N-protected α-amino acids.

Table 1. Synthesis of O-C bonded L-Dopa peptidomimetic

Entry	Aminoacids	R	Products	Conversion(%)	Yields(%)[a]
2	37	N-Boc-Gly-	46 (45)	≥98	70(10)
3	38	N-Boc- Ala-	47 (45)	≥98	65(15)
4	39	N-Boc-Val-	48 (45)	≥98	58(8)
5	40	N-Boc-Leu-	49 (45)	≥98	56(10)
6	41	N-Boc-Phe-	50 (45)	≥98	50(16)
7	42	N-Boc-Pro-	51 (45)	≥98	52(12)
8	43	N-Boc-Trp-	52 (45)	≥98	51(12)
9	44	N-Boc-Met-	53 (45)	≥98	57(3)
1	37	N-Boc-Gly-	46 (45)	70	21(19)[b]

[a] Reaction conditions: compound 1 (0.1 mmol) was dissolved in THF (1.5 mL) in the presence of the appropriate protected a-amino acids 2–9 (1.0 mmol) and treated with IBX (0.3 mmol) at 45 C for 72 h. [b] Reaction performed at 25 C for 3 h.

1.2.1.1. Synthesis of N–C bonded L-DOPA peptidomimetics

The procedure was than extended to the case of α-amino acid methyl ester derivatives Gly-OMe (**54**), Ala-OMe (**55**), Val-OMe (**56**), Leu-OMe (**57**), Phe-OMe (**58**), Pro-OMe (**59**), Trp-OMe (**60**), Met-OMe (**61**) to synthesize N–C bonded L-DOPA peptido- mimetics. The oxidation of compound **36** (0.1 mmol) with IBX (0.3 mmol) in THF (1.5 mL) in the presence of **54** (1.0 mmol) afforded Gly-N-Boc-DOPA-OMe (**62**) in low yield, besides to traces of N-Boc-DOPA-OMe (**45**) (Scheme 14). The reactivity of IBX can be tuned by the use of organic solvents with different polarities, the efficacy of the oxidation depending on the nature of the substrate.[301] For this reason, we repeated the reaction in the presence of MeOH (1.5 mL) as an alternative solvent, under previously described experimental conditions. As reported in Table 2 (entry 2 versus entry 1), the reaction in MeOH afforded compound **62** in highest yield and conversion of substrate. Further oxidations were then performed with both THF and MeOH solvents. Better results were obtained for aliphatic α-amino acids **55-56-57** in MeOH, to afford Ala-N-Boc- DOPA-OMe (**63**), Val-N-Boc-DOPA-OMe (**64**), and Leu-N-Boc-DOPA-OMe (**65**) in appreciable yield and quantitative conversion of substrate (Table 2, entries 2, 4, 6 and 8 versus entries 1, 3, 5 and 7). In this latter case, we were not able to recognize any specific relationship between the steric hindrance of the side-chain and the yield of desired product. A different reaction pathway was observed with a-amino acids **59-61** in which case THF was the best reaction solvent (Table 2, entries 9–16). In some cases (e.g. Table 2, entries 3, 5, 14 and 16), the low value of the mass balance was probably due to formation of undesired oligomeric side-products difficult to be detected and recovered from the reaction mixture. Note that a dimeric. Note that in some case, a dimeric DOPA derivative (compound **70**, Scheme 3) was detected in low amount as a side-product (7% and 9%, respectively). This compound is< probably obtained by oxidative coupling of radical intermediates in accor- dance with previously reported results during IBX oxidation of 2-methoxy and 2-methyl-substituted phenols in THF.[302] The C(6)–C(6) regiochemistry in **70** was assigned by comparison of the ^{1}H NMR multiplicity of aromatic protons with similar dimeric species produced during the polymerization of 3-(3,4-dihydroxyphenyl) propionic acid (DHPA) with Fe^{3+} ions.[303].
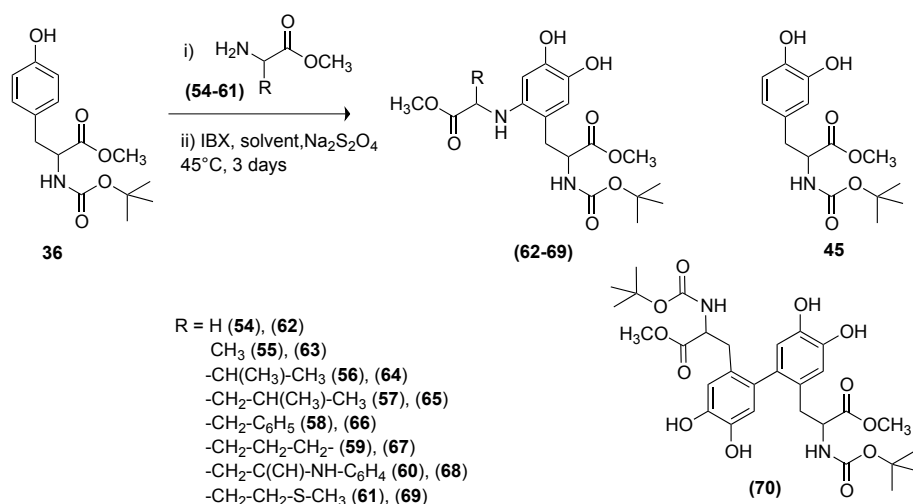
Scheme 14. IBX mediated oxidative functionalization of N-Boc-Tyr-OMe (**36**) with O-protected α-amino acids.

Table 2. Synthesis of N-C bonded L-Dopa peptidomimetics[a]

Entry	Amino acid	Solvent	R	Product	Conversion (%)	Yields (%)
1	**54**	THF	H	**62(45)**	85	27(5)
2	**54**	MeOH	H	**62(45)**	≥ 98	65(10)
3	**55**	THF	CH$_3$	**63(45)**	≥ 98	48(10)
4	**55**	MeOH	CH$_3$	**63(45)**	≥ 98	80(5)
5	**56**	THF	CH(CH$_3$)$_2$	**64(45)**	70	40(16)
6	**56**	MeOH	CH(CH$_3$)$_2$	**64(45)**	95	60(13)
7	**57**	THF	CH$_2$CH(CH$_3$)$_2$	**65(45)**	87	43(21)
8	**57**	MeOH	CH$_2$CH(CH$_3$)$_2$	**65(45)**	96	65(11)
9	**58**	THF	CH$_2$C$_6$H$_5$	**66(45)**	≥ 98	90(8)
10	**58**	MeOH	CH$_2$C$_6$H$_5$	**66(45)**	81	45(25)
11	**59**	THF	CH$_2$CH$_2$CH$_2$	**67(45)**	87	53(13)
12	**59**	MeOH	CH$_2$CH$_2$CH$_2$	**67(45)**	85	11(36)
13	**60**	THF		**68(45)(70)**	≥ 98	80(4)(7)
14	**60**	MeOH		**68(45)**	≥ 98	32(20)
15	**61**	THF	CH$_2$CH$_2$SCH$_3$	**69(45)(70)**	≥98	72(5)(9)
16	**61**	MeOH	CH$_2$CH$_2$SCH$_3$	**69(45)**	96	40(20)

[a]Reaction conditions: compound **1** (0.1 mmol) was dissolved in the appropriate solvent (1.5 mL) in the presence of protected α-amino acids **54-61** (1.0 mmol) and treated with IBX (0.3 mmol) at 45°C for 72 hrs

1.2.2 Oxidative functionalization of L-Dopa by use of supported IBX

Since the role played by the heterogeneous catalysis in green chemistry, we evaluated the use of heterogeneous conditions for the synthesis of DOPA peptidomimetics by applying the polymer supported IBX-amide, that is an easily recoverable and reusable oxidant.[304] The oxidation of **36** in the presence of Gly-OMe **54** in MeOH was performed under previously optimized experimental conditions. Comparable results in terms of conversion of substrate and yield of **62** were obtained with respect to IBX. Recycling experiments proceeded with success (Table 3). After the disappearance of compound **36**, the IBX-amide was recovered by filtration, regenerated with Oxone® and used [305] in further oxidations. IBX-amide was active for at least five cycles to give **62** without appreciable loss of efficiency (Table 3, runs 1–5).
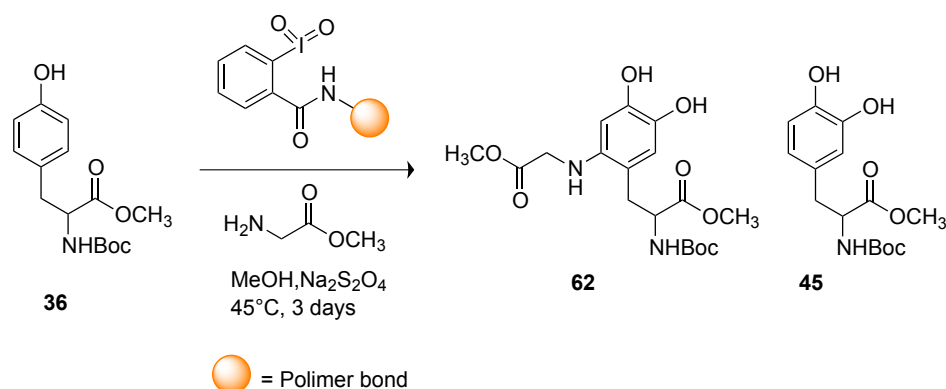
Scheme 15. Supported IBX-amide mediated oxidative functionalization of N-Boc-Tyr-OMe (**36**) with Gly-OMe (**54**).

Table 3. Reusability of heterogeneous IBX-amide in oxidative functionalization of N-Boc-Tyr-OMe (**36**) with Gly-OMe (**54**)[a].

Run	Aminoacid	Product	Conversion (%)	Yield (%)
1	**54**	**62(45)**	≥ 98	65(8)
2	**54**	**62(45)**	≥ 98	67(9)
3	**54**	**62(45)**	≥ 98	63(10)
4	**54**	**62(45)**	≥ 98	65(11)
5	**54**	**62(45)**	≥ 98	66(7)

[a]Reaction conditions: compound **1** (0.1 mmol) was dissolved in MeOH (1.5 mL) in the presence of protected -amino acids **19** (1.0 mmol) and treated with sIBX amide at 45°C for 72 hrs.

1.2.3 Antioxidant activity

Radical oxygen centered species (ROS) are formed in the cell under normal metabolic and physiologic processes.[306] In PD, hydroxyl and superoxide radicals, which are produced by oxidative phosphorylation,[307] can damage mitochondrial DNA (mtDNA), causing modulation in the electron transport chain (ETC).[308] The catechol pharmacophore in DOPA plays a key role in scavenging ROS by formation of stable phenoxyl radical species,[309] as evaluated by standard and modified comet assays in mammalian cells.[310]

Furthermore, the administration of L-DOPA reduces hypoxia conditions and induces the over-expression of ORP150 (oxygen regulated protein 150-kDa) with concomitant cytoprotective effects, and possible activation of endogenous antioxidant mechanisms.[311] On the basis of these data, we started to evaluate the antioxidant activity of novel synthesized DOPA peptidomimetic derivatives. The in vitro antioxidant activity of cathecol compounds is usually determined by spectrophotometric analyses. We evaluated the 2,2-diphenyil picrylhydrazyl (DPPH) radical scavenging properties of compounds 46-52 and 62-69 using Dopa as reference. Briefly, the appropriate compound was added to freshly prepared DPPH solution (6×10^{-5} M in EtOH) and the decrease in absorbance (475 nm) was determined at different times until the reaction reached a
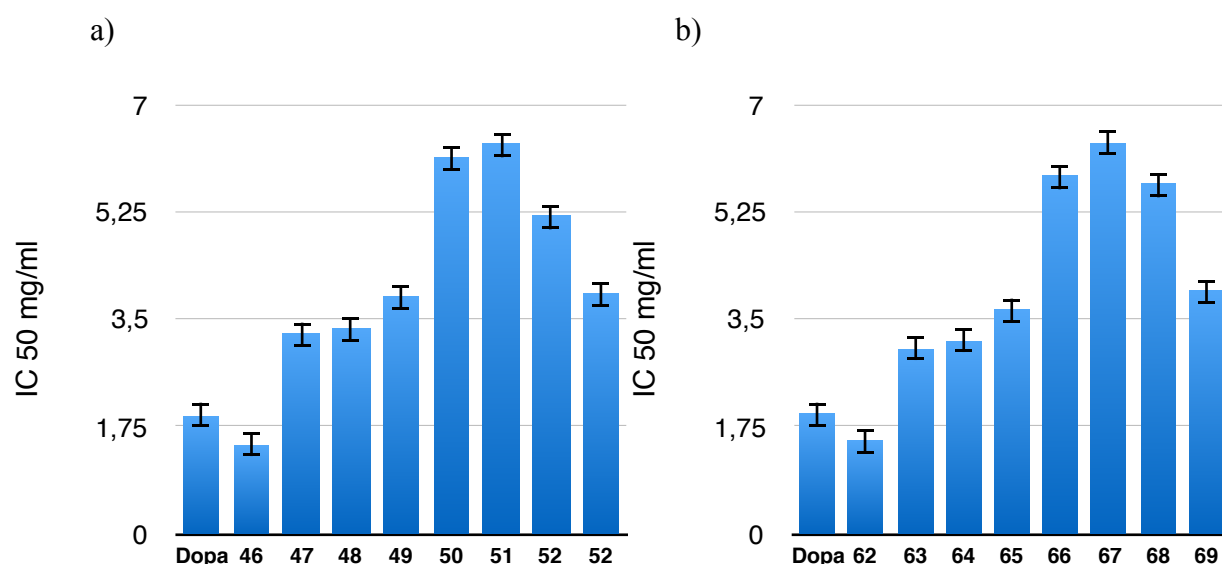
Figure 22. a) IC50 value of O-C bonded L-Dopa peptidomimetics 46-52 b) IC50 value of N-C bonded L-Dopa peptidomimetics 62-69. IC50 is the drug concentration causing 50% inhibition of the desired activity.

plateau. The kinetic of the process was analyzed for each concentration tested, and the rate of DPPH remaining at the steady state was estimated. This value was used to calculate the IC50 (defined as

the concentration of substrate that causes 50% loss of DPPH activity). Results for news O-C and N-C bonded L-Dopa peptidomimetics are reported in Figure 41 a), b) respectively. All compounds showed appreciable an antioxidant activity compared to DOPA. Note that glycine derivatives **46** and **62** showed the highest antioxidant activity higher than Dopa. As a general trend, the IC50 decreased by increasing the steric hindrance of the side-chain substituents in the aliphatic amino acid type.

1.2.4 Evaluation of the genotoxic activity

The genotoxic activity of N-Boc-Gly-N-Boc-DOPA-OMe (**46**), N-Boc-Val-N-Boc-DOPA-OMe (**48**), Gly-N-Boc-DOPA-OMe (**62**) and Val-N-Boc-DOPA-OMe (**64**), selected as representative examples of couples of O-C and N-C bonded L-Dopa peptidomimetics, was evaluated in Chinese hamster ovary (CHO) cells, by analyzing the induction of chromosomal aberrations, which are highly predictive of long term genetic effects and cancer risk.[312] Compounds like Dopa, and the natural L-Dopa peptides Boc-Gly-DOPA (**71**) and Boc-Val-DOPA (**72**) (Figure 2), were also evaluated as reference compounds. The peptides **71** and **72** have been synthesized by selective oxidation of corresponding tyrosine containing substrates with native tyrosinase, as previously reported.[313]Following dose-range finding experiments, toxic dose-levels causing a complete suppression of mitotic activity and/or cell lethality were identified.
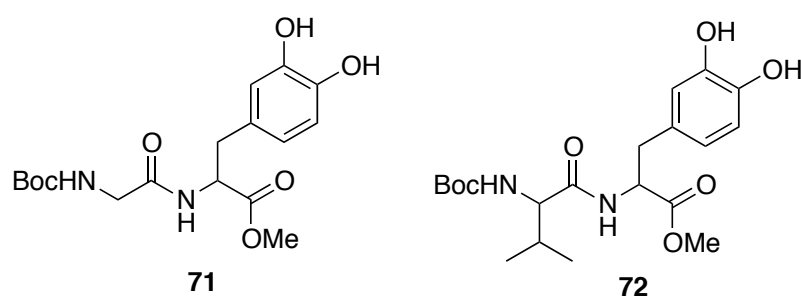
Figure 23. Stucture of L-Dopa peptides Boc-Gly-DOPA (71) and Boc-Val-DOPA (72).

Table 4. Analysis of mitotic index and chromosomal aberrations of reference compounds Dopa, 71 and 72, in CHO cells.

Entry	Compound	Dose-levels (µg/ml)	MI (%)[a]	Relative MI[b]	Aberrant cells (%)[c]	Stat. Sig.
1	Control	-	6.9	100	4	-
2		1.76	7.9	114	3	NS
3		3.17	6.9	100	2	NS
4	**Dopa**	5.72	7.9	114	3	NS
5		10.3	6.9	100	2	NS
6		18.5	4.6	67	7	NS
7	Control	-	9.3	100	3	-
8		9.91	8.8	95	2	NS
9		17.8	7.7	83	3	NS
10	**71**	32.1	4.5	48	2	NS
11		57.8	3.7	40	2	NS
12		104	3.2	34	3	NS
13	Control	-	9.3	100	3	-
14		22.9	8.8	95	2	NS
15		41.2	7.1	76	5	NS
16	**72**	74.1	5.6	60	2	NS
17		133	3.8	41	1	NS
18		240	3.2	34	3	NS

[a]Mitotic indices (MI) corresponding to the ratio between the number of cells in a population undergoing mitosis to the number of cells not undergoing mitosis (interphase cells) out of a total of 1000 cells scored and expressed as percentage. [b]) Value of MI relative to solvent control. The solvent control value is considered to be equal to 100. [c]) Percentage of cells bearing aberrations (excluding gaps).

Table 5. Analysis of mitotic index and chromosomal aberrations of peptidomimetics 46,48, 62 and 64, in CHO cells

Entry	Compound	Dose-levels (µg/ml)	MI (%)[a]	Relative MI[b]	Aberrant cells (%)[c]	Stat. Sig.
1	Control	-	9.2	100	4	-
2		6.10	68.2	89	3	NS
3		11.0	7.4	80	5	NS
4	**46**	19.8	6.4	70	5	NS
5		35.6	5.8	63	3	NS
6		64.0	3.9	42	2	NS
7	Control	-	9.2	100	4	-
8		1.33	8.4	91	2	NS
9		2.40	7.7	84	2	NS
10	**48**	4.32	6.2	67	3	NS
11		7.78	4.2	46	4	NS
12		14.0	3.7	40	4	NS
13	Control	-	9.2	100	4	-
14		4.57	9.7	105	2	NS
15		8.23	8.0	87	2	NS
16	**62**	14.8	7.3	79	5	NS
17		26.7	4.5	49	4	NS
18		48.0	4.1	45	3	NS
19	Control	-	6.9	100	4	-
20		6.29	6.9	100	5	NS
21		11.3	6.1	88	3	NS
22	**64**	20.4	5.7	83	2	NS
23		36.7	4.8	70	1	NS
24		66.0	3.1	45	3	NS

[a])Mitotic indices corresponding to the ratio between the number of cells in a population undergoing mitosis to the number of cells not undergoing mitosis (interphase cells) out of a total of 1000 cells scored and expressed as percentage. [b]) Value of MI relative to solvent control considered equal to 100. [c]) Percentage of cells bearing aberrations (excluding gaps).

The assay was then performed using a set of five dose-levels spaced by a factor of 1.8, starting from a maximum concentration expected to induce moderate toxicity, as evaluated by mitotic index (MI). [314]All tested compounds, following a treatment of 24 hours, induced at the highest dose-levels selected, moderate reduction of mitotic indices up to 32-67% of the concurrent solvent controls (Tables 4-5). Notably, compound **48** proved to be the most active compound in terms of reduction of MI compared to references **Dopa**, and compounds **71, 72** since active at lower concentrations (Table 5, entry 8 versus Table 4, entries 2, 8 and 14). Alternatively, compounds **46, 62** and **64**, (although slightly less active than reference compound **Dopa)** (Table 5, entries 2, 14 and 20 versus Table 4, entry 2), showed a greater capability to reduce MI with respect to **71** and **72** (Table 5, entries 2, 14 and 20 versus Table 4, entries 8 and 14). No statistically significant increases in the incidence of chromosomal aberrations were observed at any dose-level employed with any compound (Tables 4-5) indicating the absence of genotoxic potential.

1.2.5 Antioxidant activity in cultured mammalian cells

The antioxidant activity of peptidomimetics **46, 48, 62** and **64**, and reference compounds **Dopa**, **71** and **72,** was further evaluated against mouse lymphoma L5178Y (TK$^{+/-}$) cells. The antioxidant activity was assessed by their ability to reduce the extent of DNA breakage induced by hydrogen peroxide (H_2O_2) at 0.25 µM for 5 min., using a slightly modified version of the alkaline comet assay.[315] The L5178Y mouse lymphoma cells were treated with the appropriate compound at the highest non cytotoxic concentration. For the reference compounds **Dopa**, **71** and **72,** the selected dose-levels were 18.5, 104 and 240 µg/ml, respectively, as shown in Table 4 (entries 6, 12 and 18), while for peptidomimetics (**46, 48, 62** and **64**) the selected dose-levels were 64, 14, 48 and 66 µg/ml, respectively (Table 5, entries 6, 12, 18, 24, respectively). No increase in DNA migration was noted with any of tested compounds, while a marked and statistically significant increases in the tail moment values (TM), reflecting an increased DNA breakage, was observed in the H_2O_2 treated cells. The TM is defined as the product of the tail length and the fraction of total DNA in the tail. This data incorporates a measure of both the smallest detectable size of migrating DNA (reflected in the comet tail length) and the number of relaxed/broken DNA fragments (represented by the intensity of DNA in the tail)
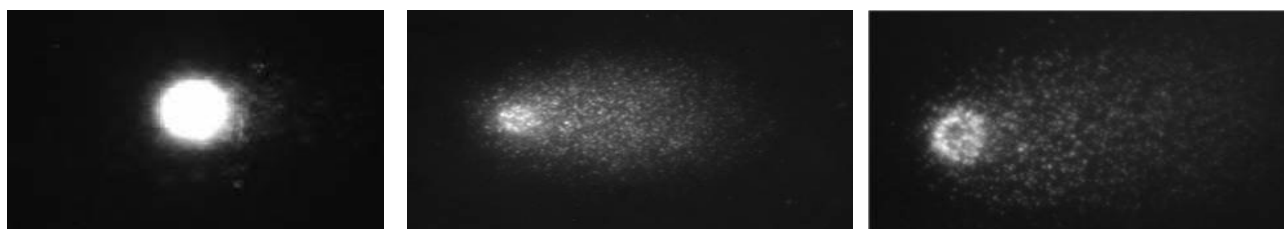
Figure 24 a) Comet assay performed on untreated cells (control PBS). **b)**Comet assay performed in presence of an aliquot of 50 µl of H_2O_2 (0.25 µM). **c)** Comet assay showing the efficacy of compound N-Boc-Gly-N-Boc-DOPA-OMe (**46**), against the extent of DNA breakage induced by H_2O.

Dopa peptides Boc-Gly-DOPA **71** and Boc-Val-DOPA **72** were able to reduce the tail moment values (TM) in the range of 94-96% (Table 7, entries 2-4). The TM is defined as the product of the tail length and the fraction of total DNA in the tail. This data incorporates a measure of both the smallest detectable size of migrating DNA (reflected in the comet tail length) and the number of relaxed/broken DNA fragments (represented by the intensity of DNA in the tail). A lower but still significant protection was also observed for O-C and N-C bonded L-Dopa peptidomimetics, N-Boc-Val-N-Boc-DOPA-OMe (**48**), Val-N-Boc-DOPA-OMe (**64**) and N-Boc-Gly-N-Boc-DOPA-

Table 6. Tail moment values (TM) of compounds **46, 48, 62, 64 36 aDopa**, **71** and **72** by the comet assay.

Entry	Compound	TM[b]	TM[c]	Reduction of TM (%)[a]
1	DMSO	0.1	17.14	-
2	71	0.25	0.76	96
3	72	0.22	0.84	95
4	Dopa	0.8	1.02	94
5	46	0.62	4.2	75
6	48	0.22	5.57	68
7	62	0.38	9.3	46
8	64	0.42	10.85	36

[a] Reduction of the extent of DNA breakage induced by hydrogen peroxide (H_2O_2) at 0.25 µM for 5 min. in L5178Y (TK^{+/-}) mouse lymphoma cells. [b]Experiment performed without H_2O_2. [c] Experiment performed with H_2O

OMe (**46**) (Table 6, entries 5-7). The Gly-N-Boc-DOPA-OMe (**62**) proved to be the less active compound (Table 6, entry 8). On the basis of these data, it is possible to suggest that the modification of the presence of unnatural bonds between amino acid residues (that is, natural peptide bond linkage versus modified O-C and N-C bonds) does not alter the antioxidant activity of the compounds in L5178Y (TK+/) mouse lymphoma cells. However, L-DOPA peptides are still the most active. Note that the stereo-electronic properties of the catechol moiety in peptidomimetic derivatives can be modified, following the functionalization of the aromatic ring.[316] Moreover, in the family of peptidomimetic derivatives, the valine derivatives (compounds **48** and **64**) showed the highest antioxidant activity.

1.2.6. Towards a completely green chemistry approach: Synthesis of peptidomimetics by Tyrosinase mediated oxidative functionalization

With the aim to better develop procedures based on the oxidative side chain modification of amino acids in a green chemistry approach we focus our work to the use of Tyrosinase from *Agaricus bisporus*.[317] both in homogeneous and heterogeneous conditions. In recent studies use of this enzyme was largely discussed including the preparation of DOPA peptides with complete stereochemical integrity by selective oxidation of tyrosine in organic solvents[318]. Tyrosinase (monophenol, o-diphenol: oxidoreductase, E.C. 1.14.18.1)[319] is a metalloprotein able to activate di-oxygen for the conversion of tyrosine to DOPA (creolase or monophenolase activity) and DOPA quinone (catecholase or diphenolase activity) [320]. It shows high substrate affinity towards phenolic monomers, oligomers and polymers, the efficacy of the catalytic process depending on the substitution pattern in the aromatic ring, both in terms of position and chemical structure [321,322, 323]. We investigated the Tyrosinase mediated synthesis of DOPA peptidomimetics containing glycine (N-Boc-Gly-N-Boc-DOPA-OMe **46** and Gly-N-Boc-DOPA-OMe **62**), that showed the highest antioxidant effect in the 2,2-diphenyl picrylhydrazyl (DPPH) test, and the valine derivatives (N-Boc-Val-N-Boc-DOPA-OMe **48** and Val-N-Boc-DOPA-OMe **64**), that were found to be the most active compounds in the comet assay [325] in L5178Y (TK+/-) mouse lymphoma cells.

1.2.6.1. Synthesis of Dopa Peptidomimetics in homogeneous conditions

Boc-Tyr-OMe (BTO) **36** was used as starting material. Reactions were designed according to the procedure previously applied with IBX and are generalized in Scheme 16.
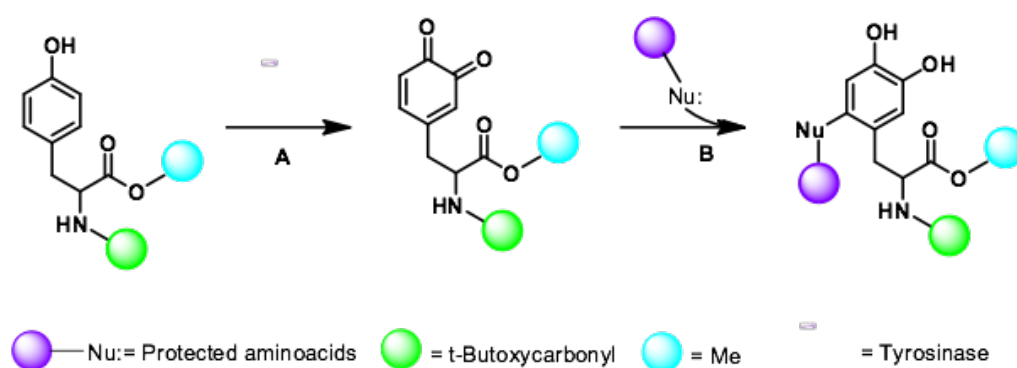
Scheme 16 . General reactivity scheme of protected tyrosine with α-amino acids in the presence of tyrosinase. Step A: oxidation of tyrosine to DOPA-quinone. Step B: Michael-like 1-4-addition of protected α-amino acids on the DOPA-quinone intermediate, followed by a reduction step.

The oxidation of BTO **36** (20 mg, 0.068 mmol) with tyrosinase from *Agaricus bisporus* (600 UA) was performed in phosphate buffer solution (PBS; pH 7) at 25 °C for 48 h, in the presence of different amount of EtOH (from 9:1 v/v to 1:9 v/v PBS/EtOH ratio, respectively) to increase the solubility of the reagents, followed by a reduction step ($Na_2S_2O_4$). EtOH shows a complete miscibility and high compatibility with PBS in various enzymatic reaction[327]. Initially, glycine methyl ester (NH_2-Gly-OMe **37**, 0.68 mmol) was used as a selected nitrogen centered nucleophile for the addition on the reactive DOPA quinone intermediate. The highest yield of OMe-Gly-N-Boc-DOPA-OMe **62** was observed in the presence of PBS/EtOH 3:7 v/v after 24h (87%) (Figure 25)
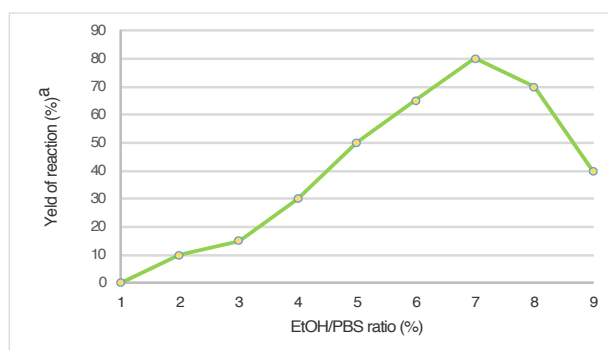
Figure 25. Yield of OMe-Gly-N-Boc-DOPA-OMe during the oxidation of BTO and NH$_2$-Gly-OMe with tyrosinase at different EtOH/ PBS ratio values.

The oxidative functionalization of BTO **36** was then repeated using *N*-Boc-Gly **37** as oxygen centered nucleophile under optimal conditions, to yield *N*-Boc-Gly-*N*-Boc-DOPA-OMe **46** in 80% yield (Table 7, entry 3), besides to residual BTO **36** (Scheme 6, pathway B). To evaluate the generality of the transformation, we used the more hindered amino acids NH$_2$-Val-OMe **56** and N-Boc-Val **39** as nucleophiles.
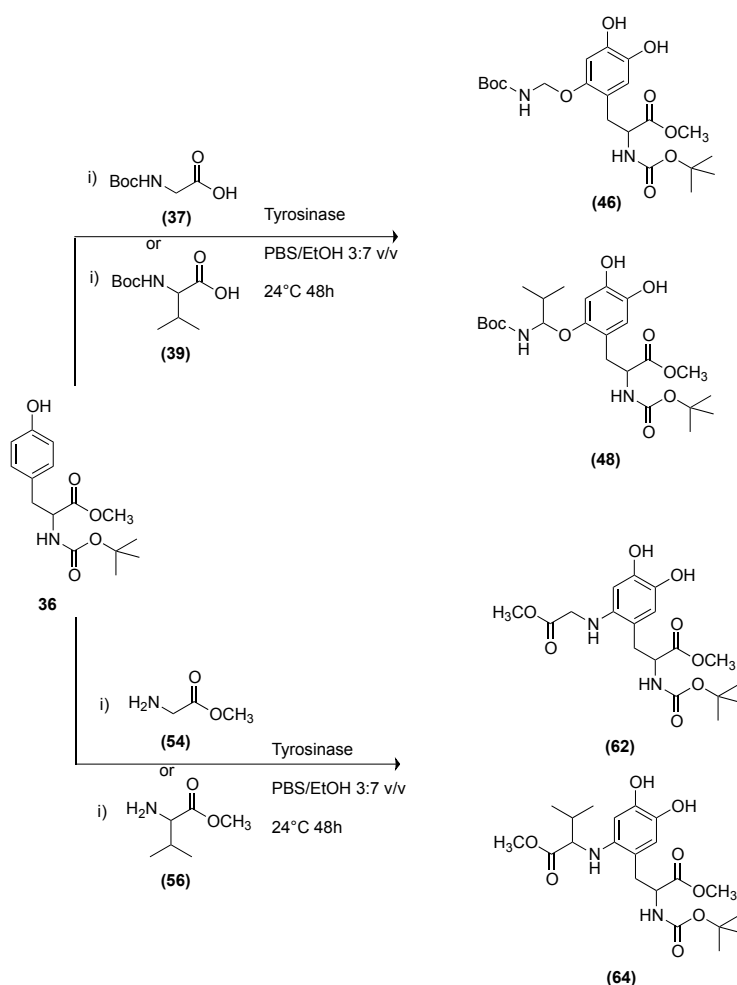
Scheme 17. Synthesis of DOPA peptidomimetics **46,48,62** and **64** by oxidative functionalization of BTO **36** with tyrosinase from *Agaricus bisporus* in the presence of glycine and valine nucleophiles.

The corresponding DOPA peptidomimetics OMe-Val-*N*-Boc-DOPA-OMe **48** and *N*-Boc-Val-*N*-Boc-DOPA-OMe **64** were obtained in 77% and 74% yield, respectively (Table 7, entries 2 and 4), besides to residual BTO (6% and 13%, respectively) (Scheme 17, pathways A and B). Amino acids with *N*- and *O*-centered nuclephile sites showed a similar reactivity, *N*-centered nucleophiles being slightly more efficient than the *O*-centered counterpart. Moreover, Gly nucleophiles were more reactive than Val, probably due to side-chain steric hindrance effects.

1.2.6.2 Synthesis of DOPA peptidomimetics in heterogeneous condition

The oxidative functionalization of BTO **36** was performed using tyrosinase supported on multi-walled carbon nanotubes (MWCNTs) by the Layer by Layer (LbL) approach, by applying a procedure previously developed by us.[329] Oxidized MWCNTs were treated with a positively charged poly(diallyldimethylammonium) chloride PDDA to facilitate the loading of tyrosinase, that is negatively charged at the operative pH 7. Bovine Serum Albumin (BSA) was used to reduce undesired conformational changes due to enzyme strive for the greatest surface coverage[330] ,Glutaraldehyde (GA) increased the reticulation grade and the stability of the system (Figure 26)[331]. The structural characterization and the activity parameters of the novel catalyst Tyro/MWCNT, as well as its application in the synthesis of bioactive catechol derivatives are detailed in material and methods.
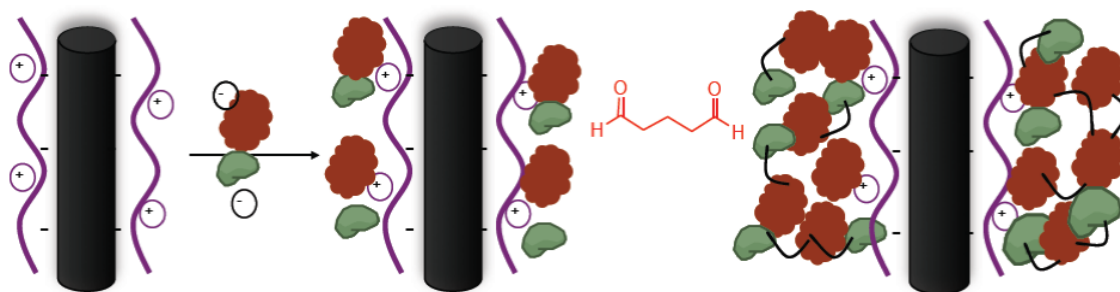
Figure 26. Loading of Tyrosinase (green) on oxidized MWCNTs (black) coated with positively charged poly(diallyldimethylammonium) chloride PDDA (ink rubber). Bovine Serum Albumin (BSA; red) was used to reduce undesired tyrosinase conformational changes and glutaraldehyde (GA) to increase the reticulation grade and the stability of the system.

The oxidative functionalization of BTO **36** (20 mg, 0.068 mmol) with NH$_2$-Gly-OMe **54** and N-Boc-Gly-COOH **37** (0.68 mmol), catalysed by Tyro/MWCNT (600 UA) in PBS/EtOH (7:3 v/v, 12 mL) at 25 °C for 24 h, afforded compounds **62** and **46** in 85% and 79% yield, respectively (Table 1, entries 5 and 6). In a similar way the oxidative functionalization of BTO **36** (20 mg, 0.068 mmol) with NH$_2$-Val-OMe **56** and Boc-Val-COOH **39** (0.68 mmol) afforded DOPA compounds **64** and **48** in 75% and 70% yield, respectively (Table 7, entries 7 and 8).Recycling experiments proceeded with success in the oxidation of compound BTO **1** with NH$_2$-Gly-OMe as selected nucleophile. As shown in Table 7 (entries 9-13), MWCNT/Tyr was used for at least five cycles with only a slight decrease of efficiency to give **2**. The oxidative functionalization of BTO **1** (20 mg, 0.068 mmol) with NH$_2$-Gly-OMe and N-Boc-Gly-COOH (0.68 mmol), catalysed by Tyro/MWCNT (600 UA) in PBS/EtOH (3:7 v/v, 12 mL) at 25 °C for 24 h, afforded compounds **62** and **46** in 85% and 79% yield, respectively (Table 7, entries 5 and 6).

Table 7: Synthesis of O-C and N-C bonded DOPA peptidomimetics under homogeneous and heterogeneous conditions and recycling experiment

Entry	Nucleophile	Catalyst	product	Yield (%)
1	NH$_2$-Gly-OMe	tyrosinase[a]	OMe-Gly-N-Boc-DOPA-OMe **62**	87
2	N-Boc-Gly-COOH	tyrosinase	N-Boc-Gly-N-Boc-Dopa-OMe **46**	80
3	NH$_2$-Val-OMe	tyrosinase[a]	OMe-Val-N-Boc-Dopa-OMe **64**	77
4	N-Boc-Val-COOH	tyrosinase	N-Boc-Val-N-Boc-Dopa-OMe **48**	74
5	NH$_2$-Gly-OMe	Tyr/MWCNT[b]	**62**	85
6	N-Boc-Gly-COOH	Tyr/MWCNT	**46**	79
7	NH$_2$-Val-OMe	Tyr/MWCNT[b]	**64**	75
8	N-Boc-Val-COOH	Tyr/MWCNT	**48**	70
9	NH$_2$-Gly-OMe	Tyr/MWCNT[c]	**62**	88
10	NH$_2$-Gly-OMe	Tyr/MWCNT	**62**	85
11	NH$_2$-Gly-OMe	Tyr/MWCNT	**62**	85
12	NH$_2$-Gly-OMe	Tyr/MWCNT	**62**	83
13	NH$_2$-Gly-OMe	Tyr/MWCNT	**62**	81

[a]BTO **1** (20 mg, 0.068 mmol) was treated with tyrosinase from Agaricus bisporus (600 UA) and different amino acid residues (0.68 mmol) in PBS/EtOH (7:3 v/v; mL) at 25 °C for 48 h, followed by a reduction step (Na$_2$S$_2$O$_4$). [b]BTO **1** (20 mg, 0.068 mmol) was treated with Tyro/MWCNT (600 UA) and different amino acids residues in PBS/EtOH (3:7 v/v; 12mL) at 25 °C for 24 h, followed by a reduction step (Na$_2$S$_2$O$_4$). [c]Reusability is expressed as the yield in % of DOPA peptidomimetic **2** obtained by oxidation of BTO **1** with MWCTN/Tyr under optimal conditions.

1.2.7 Evaluation of the dopamine-like activity of DOPA peptidomimetics

Because PD is mainly characterized by low content of DA in the basal ganglia nuclei, potential anti-Parkinson drugs should mimic DA effects. Thus, the activity of the novel L-DOPA peptidomimetics was evaluated by measuring their effects on neuronal firing/membrane currents in comparison to those evoked by exogenous mediator. Briefly, DA was applied to individual dopaminergic neurons of the rat substantia nigra pars compacta (SNpc), in which the effects of DA and dopaminergic drugs have been extensively characterized.[333] Simultaneous neuronal firing of a large population of neurons located in the SNpc was recorded by MEA. Spontaneously active neurons were firstly challenged with DA (30 uM, 2 min, Figure 27 A) and only neurons that were inhibited by DA (>15% spontaneous firing inhibition; Berretta et al., 2010) were considered in the present study. Similarly, the effect of the L-DOPA peptidomimetics was evaluated in those DA sensitive neurons which responded to drug perfusion with at least a 15% change in firing rate. DOPA peptidomimetics were analyzed both in the protected and de-protected form, the latter obtained by treatment of parent compounds with a dilute solution of HCl (0.05N for 3 days at rt). Compound **64** and the deprotected L-Dopa Gly-**73** and L-Dopa-Val **74** (Showed in figure 27) showed a significant activity.

(73)   **(74)**
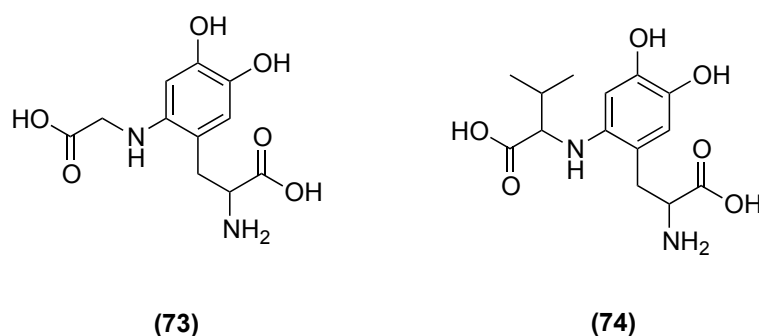
Figure 27.Dopa Gly-**73** and L-Dopa-Val **74**

We recorded 39 neurons inhibited by DA, and in 33 of these neurons the application of L-DOPA Gly **73** (200 μM) caused a slow onset firing inhibition that was completely reversed by the D2 receptor antagonist Sulpiride (10 μM; Figure 28 A, B). The extent of firing inhibition by L-DOPA Gly paralleled that of DA. Indeed, the effect of L-DOPA Gly **73** was more pronounced (P= 0.00014; Figure 27 B) in those DA-sensitive neurons that were strongly inhibited by DA (74.66 ± 7.07%, N=17), compared to those (P = 0.041; Figure 28 C) inhibited by DA by a lesser extent (35.96 ± 9.03%, N=16). In 6 out of the 39 SNpc DA neurons, L-DOPA Gly **73** (200 μM) did not

cause firing inhibition (< 15%), although they responded to DA with 26.73 ± 10.88% firing inhibition.
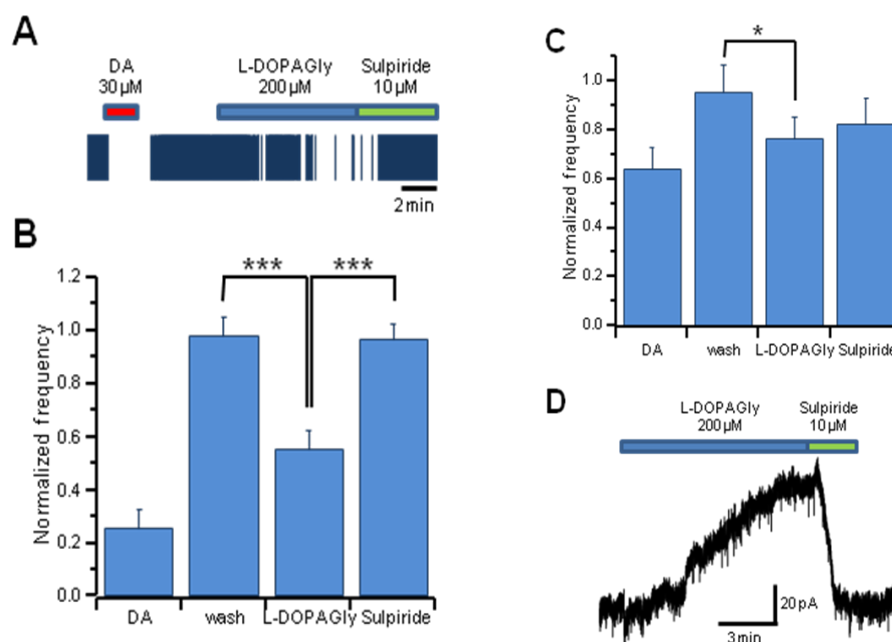
Figure 28 Acute effects of Gly-N-C-DOPA (L-DOPA Gly) on SNpc DA neurons. (A) Raster plot of the spontaneous firing recorded with MEA form a single SNpc DA neuron. DA (30 μM) robustly inhibited firing and, after complete washout of the DA effect, L-DOPA Gly (200 μM) caused a similar slow-onset inhibition of firing. Application of Sulpiride (10 μM) completely reversed L-DOPA Gly-mediated firing inhibition to control value. (B) Group data showing mean firing frequencies, normalized to control value, in 17 SNpc DA neurons during application of DA, washout, L-DOPA Gly and Sulpiride. Note that firing frequency returned to control values both after DA washout and in the presence of Sulpiride. (C) Group data showing mean firing frequencies, normalized to control value, during application of DA, washout, L-DOPA Gly and Sulpiride, in 16 SNpc DA neurons poorly sensitive to DA. Similarly to DA, also L-DOPA Gly exerted only a limited inhibition of firing. Sulpiride effect was minimal. (D) Voltage clamp recording (Vh= -60 mV) from a single SNpc DA neuron showing that L-DOPA Gly activated an outward current that was completely blocked by Sulpiride.

In voltage clamp experiments, the application of L-DOPA Gly activated a slowly developing outward current of about 60 pA in 1 out of 3 DAergic neurons tested (Figure 28 D). This current was completely blocked by the D2 receptor antagonist Sulpiride. In the remaining 2 neurons L-DOPA Gly was without effect (not shown).

These data suggest that L-DOPA Gly displays a DA-like effects in a subpopulation of DAergic neurons, because, similarly to dopamine, L-DOPA Gly-induced firing inhibition and outward current is mediated by D2 receptors. However, the D2 receptor activation could be due to either DA produced by intracellular decarboxylation of L-DOPA Gly or to its direct interaction with D2 receptors in the extracellular environment. Future experiments will address the possible mechanisms underlying L-DOPA Gly-mediated activation of D2 receptors, its ability to enter dopaminergic neurons and to be metabolized into DA.

In a large set of population (53 out of 62) of SNpc neurons inhibited by DA, the protected form of another L-DOPA peptidomimetic, L-DOPA Val Ome **64** (200 μM), caused marked firing inhibition (Figure 29 A,B). However,   differently from L-DOPA Gly, this cellular response seemed to be unspecific, as it was not reversed by Sulpiride. This result was confirmed by patch-clamp recordings. In the example trace of Figure 29 C, L-DOPA ValOme caused an outward current that was insensitive to Sulpiride. By contrast, it was completely blocked by the K_{ATP} channel blocker Tolbutamide (100 μM). These data suggest that L-DOPA Val Ome **64** causes firing inhibition though a mechanism other than D2 receptor stimulation, possibly involving a drop in intracellular ATP content, which causes K_{ATP} channel opening, or a direct action on K_{ATP} channels in SNpc DAergic neurons.

In 9 out of the 62 SNpc DAergic neurons L-DOPA ValOme **64** (200 μM) that cause firing inhibition (< 15%), although they responded to DA with 85.78 ± 6.49% firing inhibition.
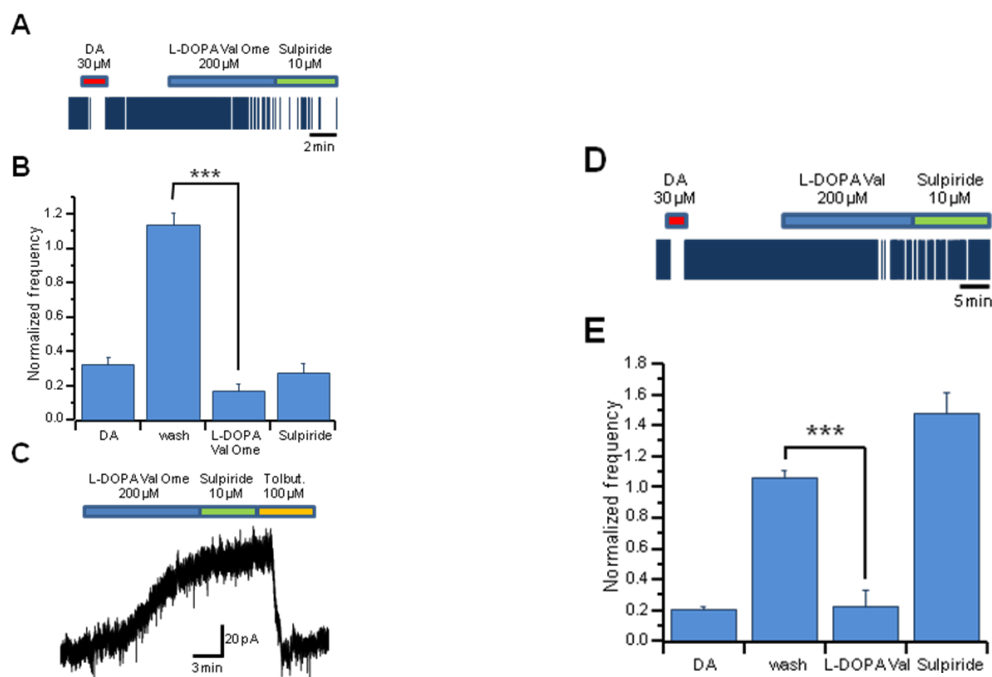
Figure 29. Acute effect of protected and deprotected L-DOPA Val on rat SNpc DAergic neurons. (A) Raster plot of the spontaneous firing recorded with MEA. DA (30 μM) strongly inhibited firing and, after complete washout, L-DOPA ValOme (200 μM) caused a slow-onset inhibition of firing. However, application of Sulpiride (10 μM) did not reverse L-DOPAValOme effect. (B) Group data showing mean firing frequencies in the presence of DA, washout, L-DOPA ValOme and Supliride, in 53 SNpc DA neurons. (C) Patch clamp recording of membrane current (Vh=- 60 mV) of a single SNpc DA neuron. Application of L-DOPA ValOme (200 μM) activated an outward current that was insensitive to Sulpiride and fully blocked by Tolbutamide (100 μM). (D) Raster plot of the spontaneous firing recorded with MEA. DA (30 μM) strongly inhibited firing and, after complete washout, the deprotected form of L-DOPA Val (200 μM) caused a slow-onset inhibition of firing, which was reversed by Sulpiride (10 μM). (E) Group data showing mean firing frequencies in the presence of DA, washout, deprotected L-DOPA Val and Sulpiride, in 12 SNpc DA neurons.

We then recorded 15 neurons inhibited by DA, and in 12 of these neurons application of the deprotected form of L-DOPA Val **74** (200 μM) caused a pronounced (P = 0.000001) firing inhibition. Differently from what previously observed with the protected form, firing inhibition induced by deprotected L-DOPA Val **74** was completely reversed by the D2 receptor antagonist Sulpiride (10 μM; Figure 29 D, E). The 3 out of 15 DAergic neurons, that were insensitive to deprotected L-DOPA Val **74**(200 μM; < 15%) displayed an inhibition by DA of 84.34 ± 0.79%.

1.2.8. CONCLUSIONS

A large panel of L-DOPA peptidomimetics have been prepared in a selective way, using IBX and supported IBX-amide as primary oxidants. The reaction was further extended to a complete eco-friendly approach, using a Tyrosinase-mediated oxidative functionalization.

In this context a new biocatalyst Tyro/MWCNT was investigated in term of preparation, efficiency, stability and reusability. The activity of MWCNT/Tyr was found to be comparable to native Tyr and greater than previously reported Tyr/E-250 catalyst, confirming the benign role of carbon nanotubes in the enzyme immobilization process. MWCNT/Tyr was a stable catalyst for at least six recycle experiments. Under these experimental conditions, two families of L-DOPA peptidomimetics were obtained, differing in the nature of the connection between the L-DOPA moiety and the appropriate *a*-amino acid residue, that is O–C versus N–C bonds. The regiochemistry of the addition between nucleophilic *a*-amino acid and electrophilic DOPA-quinone intermediate followed a Michael-like 1-4 selectivity. We first investigated the anti-oxidant activity of L-DOPA peptidomimetics with the higher effect in DPPH assay, confirming the "in vitro" radical scavenging capacity. Compounds containing residues of glycine showed an antioxidant activity higher than L-DOPA, as a reference. It is interesting to note that a different behavior was observed during the analysis of the antioxidant activity by the comet assay in L5178Y (TK$^{+/\#}$) mouse lymphoma cells, in which case valine derivatives were the most active compounds. These data further confirmed the difference in the evaluation of the anti-oxidant activity between spectroscopic procedures and cellular models.The antioxidant properties of L-DOPA peptidomimetics in L5178Y (TK$^{+/\#}$) mouse lymphoma model were probably related to ROS scavenging mechanism rather than possible modulatory effect on the induced cellular DNA repair, since the time lapse between treatment with H_2O_2 and processing of cells for comet assay was approximately 10 min, a time

clearly insufficient for DNA repair events to take place. The comparison of comet assay data between valine and glycine derivatives suggests a benign role of longer alkyl side chain substituent in the antioxidant activity. Investigation of this class of molecules proceded with evaluation of the dopamine-like activit. We have found that the deprotected forms of L-DOPA peptidomimetics (L-DOPAGly and L-DOPA Val) displayed DA-like effects in the majority of SNpc DA neurons. Indeed, DA, L-DOPA Gly and L-DOPA Val caused a strong inhibition of firing activity. Moreover, L-DOPA Gly and L-DOPA Val activated a D2 receptor-mediated outward current that was blocked by the selective D2 receptor antagonist Sulpiride. However, in a subpopulation of SNpc DA neurons poorly sensitive to DA, L-DOPA Gly and L-DOPA Val exerted mild effects. The reason of this discrepancy among SNpc DA neurons remains unknown and will be further studied in the near future.

1.3. MATHERIALS AND METHODS

1.3.1 Materials

All solvents and reagents used were of analytical grade and were purchased from Aldrich ChemicalCo. Silica gel 60 F254 plates and silica gel 60 were furnished from Merck. IBX was prepared in laboratory as described in the literature. Supported IBX-amide, 2,2-diphenyil-picrylhydrazyl (DPPH), sodium sulfate anhydrous (Na_2SO_4), Boc-Tyrosine-OMe, and protected amino acids were purchased from Sigma-Aldrich.

1.3.2 General procedure for preparation of L-Dopa peptidomimetics

BTO 0.1 mmol was dissolved in 1.5 mL of the appropriate solvent, then 1.0 mmol of amino acid and 0.3 mmol of IBX were added. The reaction mixture was stirred at 45°C for 72h. The reaction was monitored by thin layer chromatography (TLC, n-hexane/EtOAc = 2.0:1.0). After the disappearance of substrate, the reaction mixture was treated with 2 mL of H_2O and 2.0 eq. of $Na_2S_2O_4$ stirring for 15 min. Then was added 2 mL of saturated solution of $NaHCO_3$ and stirring for 30 min. The mixture was extracted several time with AcOEt and separated from H_2O. The organic layer were collected dried with Na_2SO_4 and concentrated under reduced pressure. The crude product was purified by flash-chromatography. 1H and 13C NMR spectra were recorded on a

Bruker (400 MHz) spectrometer. Mass spectra were recorded on a VG 70/250S spectrometer with an electron beam of 70 eV. Spectroscopic data are reported below.

N-Boc-Gly-N-Boc-DOPA-OMe(46) Oil ^{1}H NMR (400 MHz, CDCl$_3$): δ_H (ppm) = 1.28-1.44 (18H, d, 6×CH3), 2.97-3-00 (2H, m, CH$_2$), 3.74 (3H, s, OCH$_3$), 3.94 (2H, s, CH$_2$) 4.62-5.14 (1H, m, CH) , 7.24 (1H, s,CH), 7.42 (1H, s, CH). ^{13}C NMR (100 MHz, CDCl$_3$): δH (ppm) = 28.08 (3×CH$_3$), 28.70 (3×CH$_3$), 32.47 (CH$_2$), 42.89 (CH$_2$) 52.47 (OCH$_3$), 55.79 (CH), 79.53 (-Cº), 80.48 (-Cº), 113.58 (CH), 117.31 (CH), 119.31 (C$_{ar}$), 141.44 (C$_{ar}$), 144.76 (C$_{ar}$), 146.56 (C$_{ar}$), 155.80 (C=O), 158.32 (C=O), 171.90 (C=O), 172.64 (C=O). MS (EI): *m/z* 485; Elemental Analysis calcd: C, 54.54; H, 6.66; N, 5.78; O, 33.02 Elemental Analysis found: C, 54.51; H, 6.62; N, 5.73; O, 33.01.
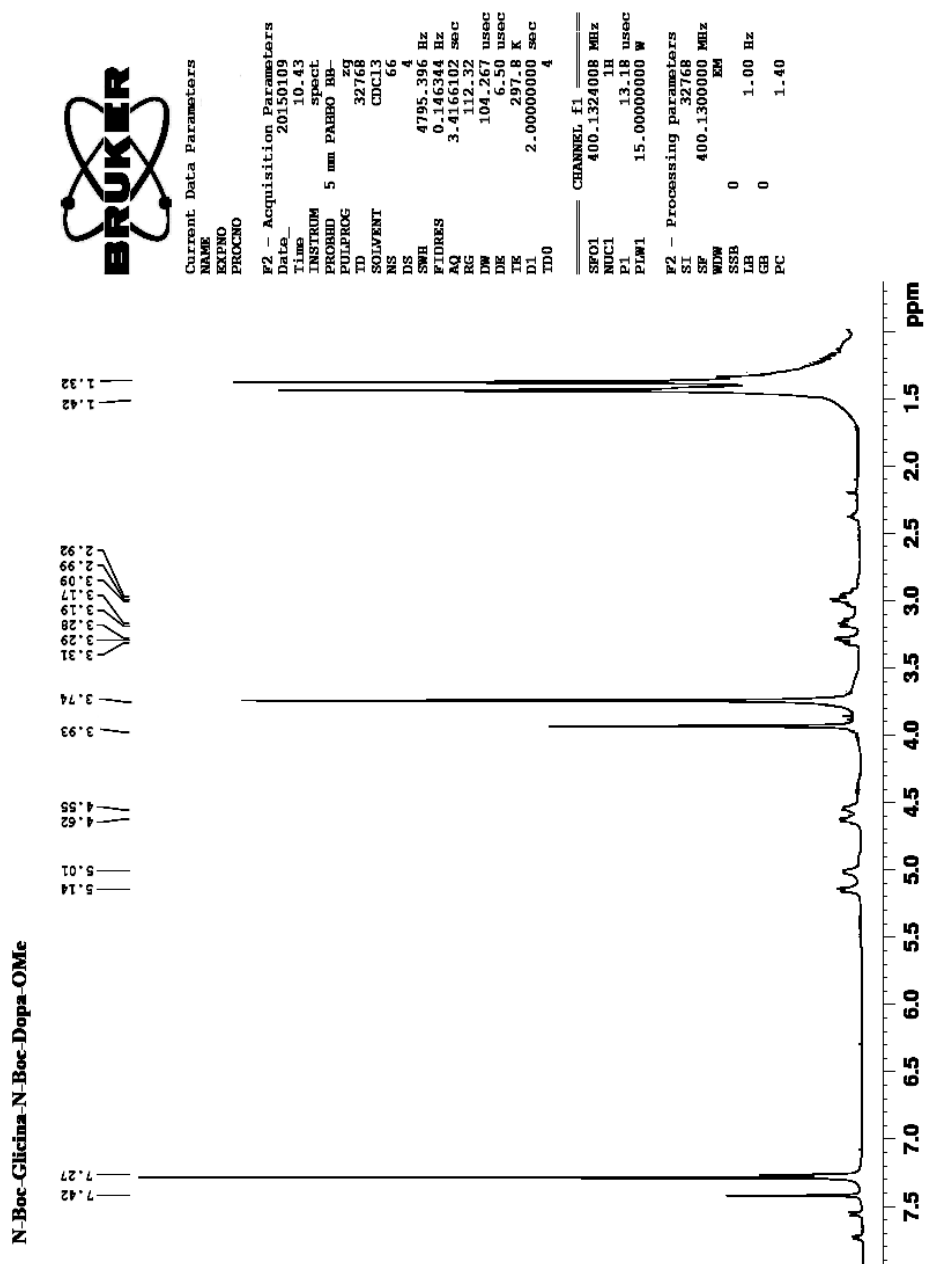
N-Boc-Ala-N-Boc-DOPA-OMe (48) Oil ^{1}H NMR (400 MHz, CDCl$_3$): δ_H (ppm) = 1.28-1.44 (18H, d, 6×CH$_3$), 1.50 (3H, s, CH$_3$), 2.96-3.03 (2H, m, CH$_2$), 3.74 (3H, s, OCH$_3$), 4.12-4.14 (1H, m, CH), 4.62-5.14 (1H, m, CH), 7.24 (1H, s, CH), 7.42 (1H, s, CH) ^{13}C NMR (100 MHz, CDCl$_3$): δH (ppm) = 17.20 (CH$_3$) 28.08 (3×CH$_3$), 28.70 (3×CH$_3$), 32.47 (CH$_2$), 52.47 (OCH$_3$), 53.21 (CH) 55.79 (CH), 79.53 (-C°), 80.48 (-C°), 113.58 (CH), 117.31 (CH), 119.31 (C$_{ar}$), 141.44 (C$_{ar}$), 144.76 (C$_{ar}$), 146.56 (C$_{ar}$), 155.80 (C=O), 158.32 (C=O), 171.90 (C=O), 172.64 (C=O). MS (EI): *m/z* 499; Elemental Analysis calcd: C, 55.41; H, 6.87; N, 5.62; O, 32.09 Elemental Analysis found: C, C, 55.40; H, 6.85; N, 5.61; O, 32.07.

N-Boc-Alanina-N-Boc-Dopa-OMe
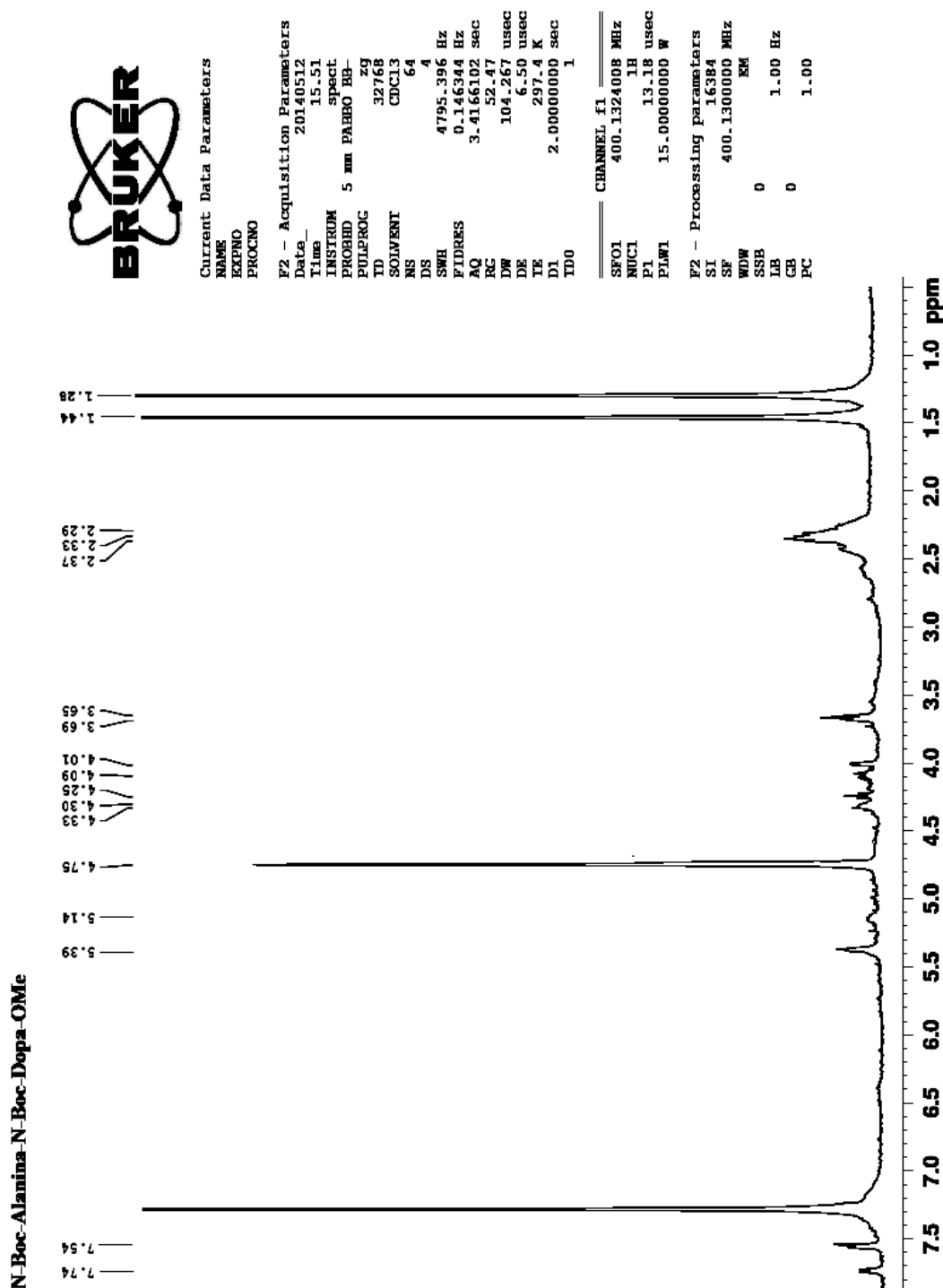
N-Boc-Val-N-Boc-DOPA-OMe(49) Oil ^{1}H NMR (400 MHz, CDCl$_3$): δ_H (ppm) = 0.89-0.98 (6H, d,2×CH$_3$) J=4, 1.07-1.30 (18H, d, 6xCH$_3$), 2.14-2.20 (1H, m, CH), 2.96-3-03 (2H, m, CH$_2$), 3.74 (3H, s, OCH$_3$), 4.52-5.14 (1H, m, CH) 7.49 (1H, s, CH) ^{13}C NMR (100 MHz, CDCl$_3$): δH (ppm) = 18.90 (2xCH$_3$) 28.08 (3×CH$_3$), 28.70 (3×CH$_3$), 30.41(CH), 32.47 (CH$_2$), 52.47 (OCH$_3$), 55.79 (CH), 62.71 (CH), 79.53 (-C°), 80.48 (-C°), 113.58 (CH), 117.31 (CH), 119.31 (C$_{ar}$), 141.44 (C$_{ar}$), 144.76 (C$_{ar}$), 146.56 (C$_{ar}$), 155.80 (C=O), 158.32 (C=O), 171.90 (C=O), 172.64 (C=O). MS (EI): *m/z* 527; Elemental Analysis calcd: C, 57.02; H, 7.27; N, 5.32; O, 30.38 Elemental Analysis found: C, 57.00; H, 7.23; N, 5.29; O, 30.35.
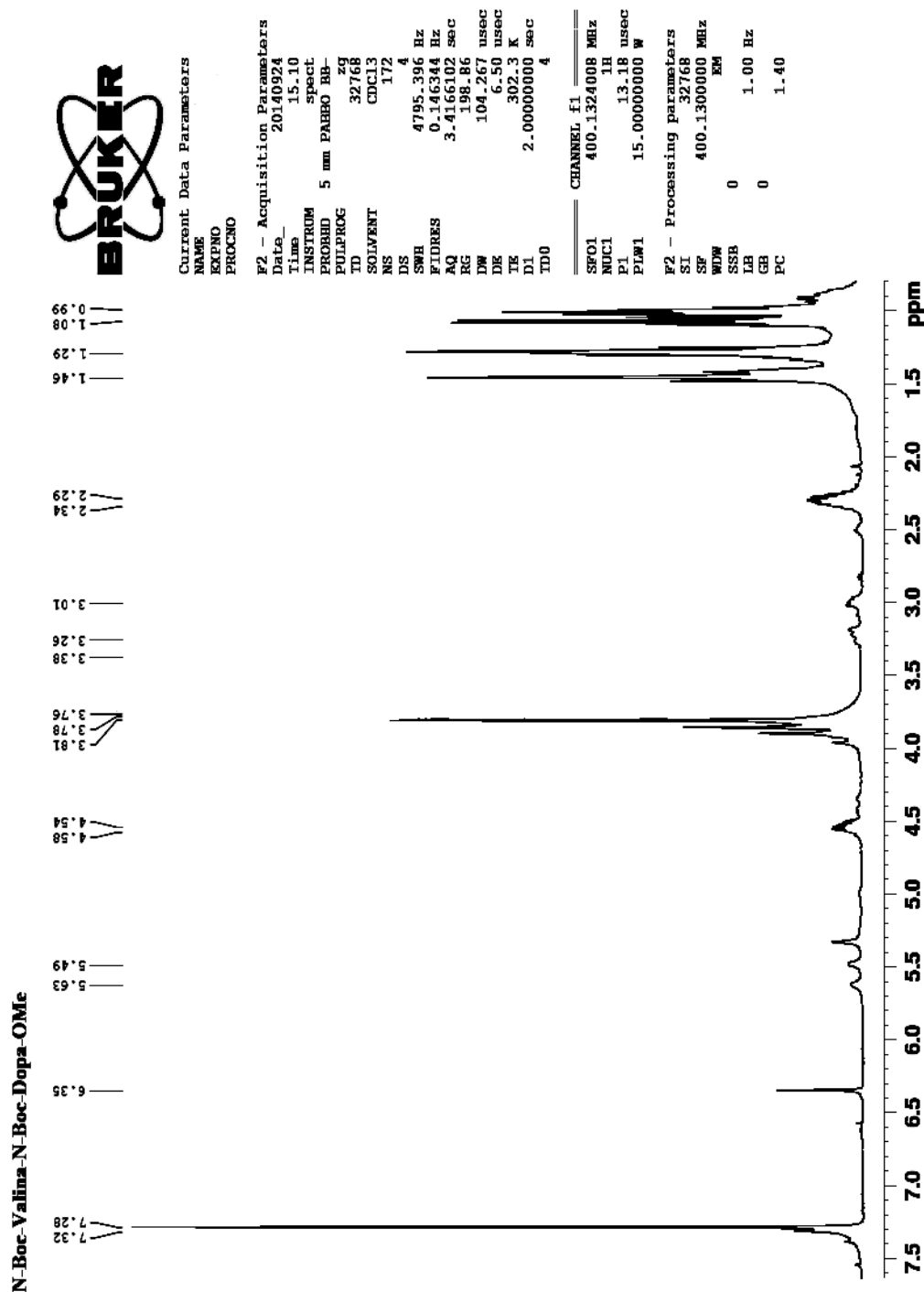
N-Boc-Leu-N-Boc-DOPA-OMe (50) Oil ^{1}H NMR (400 MHz, CDCl$_3$): δ_H (ppm) = 0.88-0.96 (6H, d,2×CH3) J=4, 1.28-1.44 (18H, d, 6xCH$_3$), J=4, 1.60-1.71 (2H, m, CH$_2$), 2.10-2.21 (2H, m, 2xCH), 2.96-3.03 (2H, m, CH$_2$), 3.74 (3H, s, OCH$_3$), 4.52-5.14 (1H, m, CH), 7.49 (1H, s, CH) ^{13}C NMR (100 MHz, CDCl$_3$): δH (ppm) = 22.92 (2xCH$_3$), 24.83 (CH), 28.08 (3×CH$_3$), 28.70 (3×CH$_3$), 30.41(CH), 32.47 (CH$_2$), 40.57 (CH$_2$) 52.47 (OCH$_3$), 55.79 (CH), , 79.53 (-C°), 80.48 (-C°), 113.58 (CH), 117.31 (CH), 119.31 (C$_{ar}$), 141.44 (C$_{ar}$), 144.76 (C$_{ar}$), 146.56 (C$_{ar}$), 155.80 (C=O), 158.32 (C=O), 171.90 (C=O), 172.64 (C=O). MS (EI): *m/z* 541*;* Elemental Analysis calcd: C, 57.76; H, 7.46; N, 5.18; O, 29.60 Elemental Analysis found: C, 57.80; H, 7.41; N, 5.18; O, 29.62.

N-Boc-Phe-N-Boc-DOPA-OMe (51), Oil ^{1}H NMR (400 MHz, CDCl₃): δ_H (ppm) = 1.42-1.50 (18H, d, 6xCH₃), 2.92-3-10 (2H, m, CH₂), 3.74 (3H, s, OCH₃), 4.53-5.14 (1H, m, CH), 6.51 (2H, d, CH₂), 6.71 (1H, s, CH), 6.79 (2H, d, CH₂), 7.20 (1H,s, CH), 7.28(1H, t, CH), ^{13}C NMR (100 MHz, CDCl₃): δH (ppm) = 28.08 (3×CH₃), 28.70 (3×CH₃), 32.47 (CH₂), 36.77 (CH₂), 52.47 (OCH₃), 55.79 (CH),55.82 (CH) 79.53 (-Cº), 80.48 (-Cº), 113.58 (CH), 117.31 (CH), 119.31 (C$_{ar}$), 125.01 (C$_{ar}$), 127.21 (C$_{ar}$), 129.41 (C$_{ar}$) 141.44 (C$_{ar}$), 144.76 (C$_{ar}$), 146.56 (C$_{ar}$), 155.80 (C=O), 158.32 (C=O), 171.90 (C=O), 172.64 (C=O). MS (EI): *m/z* 575; Elemental Analysis calcd: C, 60.62; H, 6.67; N, 4.88; O, 27.84 Elemental Analysis found: C, 60.59; H, 6.61; N, 4.89; O, 27.82.
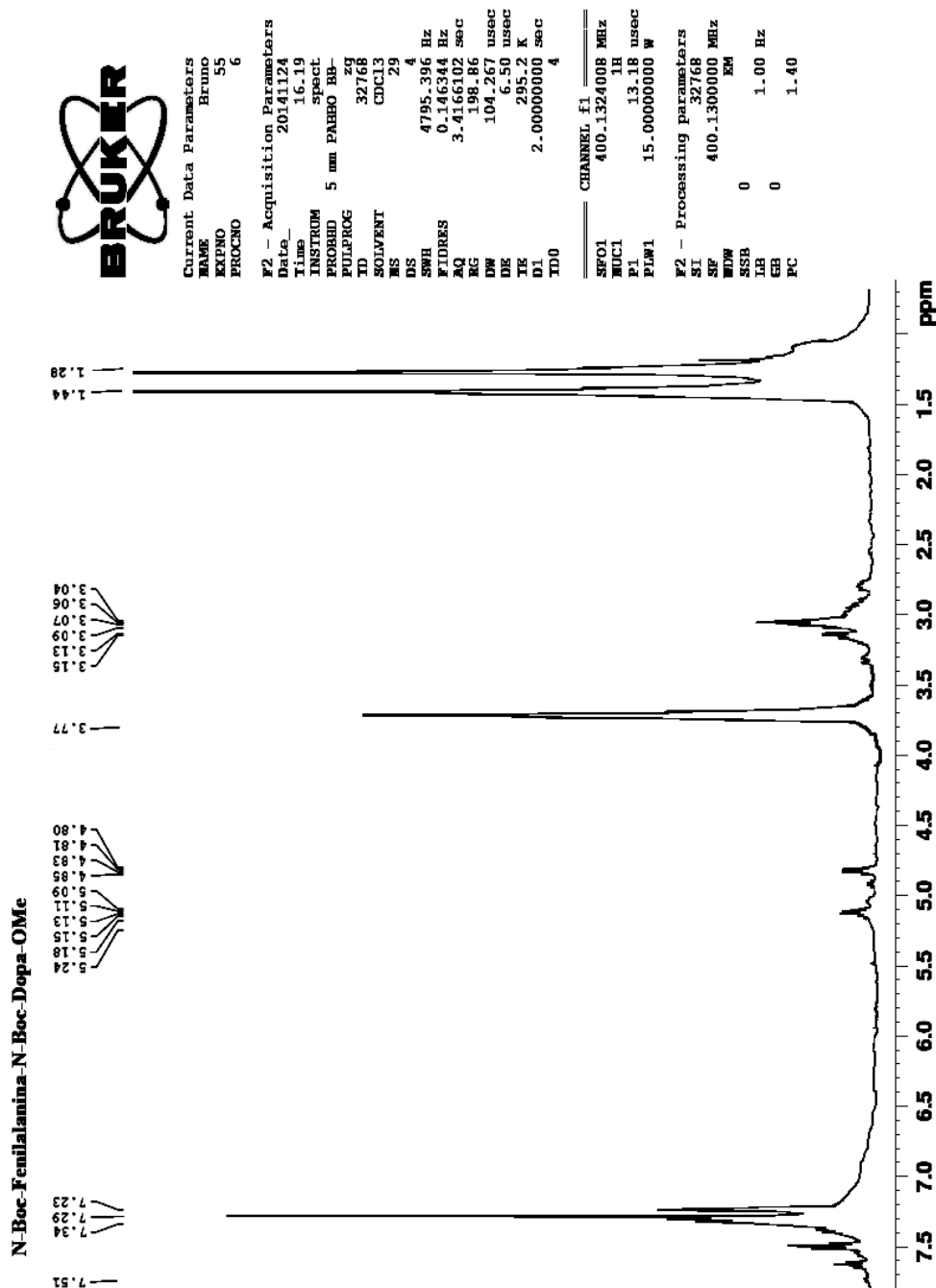
N-Boc-Pro-N-Boc-DOPA-OMe (52), Oil ^{1}H NMR (400 MHz, CDCl$_3$): δ_H (ppm) = 1.38-1.40 (18H, d, 6×CH$_3$), 1.60 (2H, m, CH$_2$), 1.85 (2H, m, CH$_2$), 3.35 (2H, m, CH$_2$), 3.60 (2H, m, CH$_2$), 3.73 (3H, s, OCH$_3$), 4.31-4.50 (1H, m, CH), 6.45 (1H, s, CH), 6.90 (1H, s, CH) ^{13}C NMR (100 MHz, CDCl$_3$): δ_H (ppm) = 24.07 (CH$_2$), 28.02 (CH$_2$), 28.08 (3×CH$_3$), 28.70 (3×CH$_3$), 32.47 (CH$_2$), 52.47 (OCH$_3$), 50.41 (CH), 55.79 (CH), 79.53 (-C^o), 80.48 (-C^o), 113.58 (CH), 117.31 (CH), 119.31 (C$_{ar}$), 141.44 (C$_{ar}$), 144.76 (C$_{ar}$), 146.56 (C$_{ar}$), 155.80 (C=O), 158.32 (C=O), 171.90 (C=O), 172.64 (C=O). MS (EI): *m/z* 525*;* Elemental Analysis calcd: C, 57.24; H, 6.92; N, 5.34; O, 30.50 Elemental Analysis found: C, 57.21; H, 6.94; N, 5.33; O, 30.51.
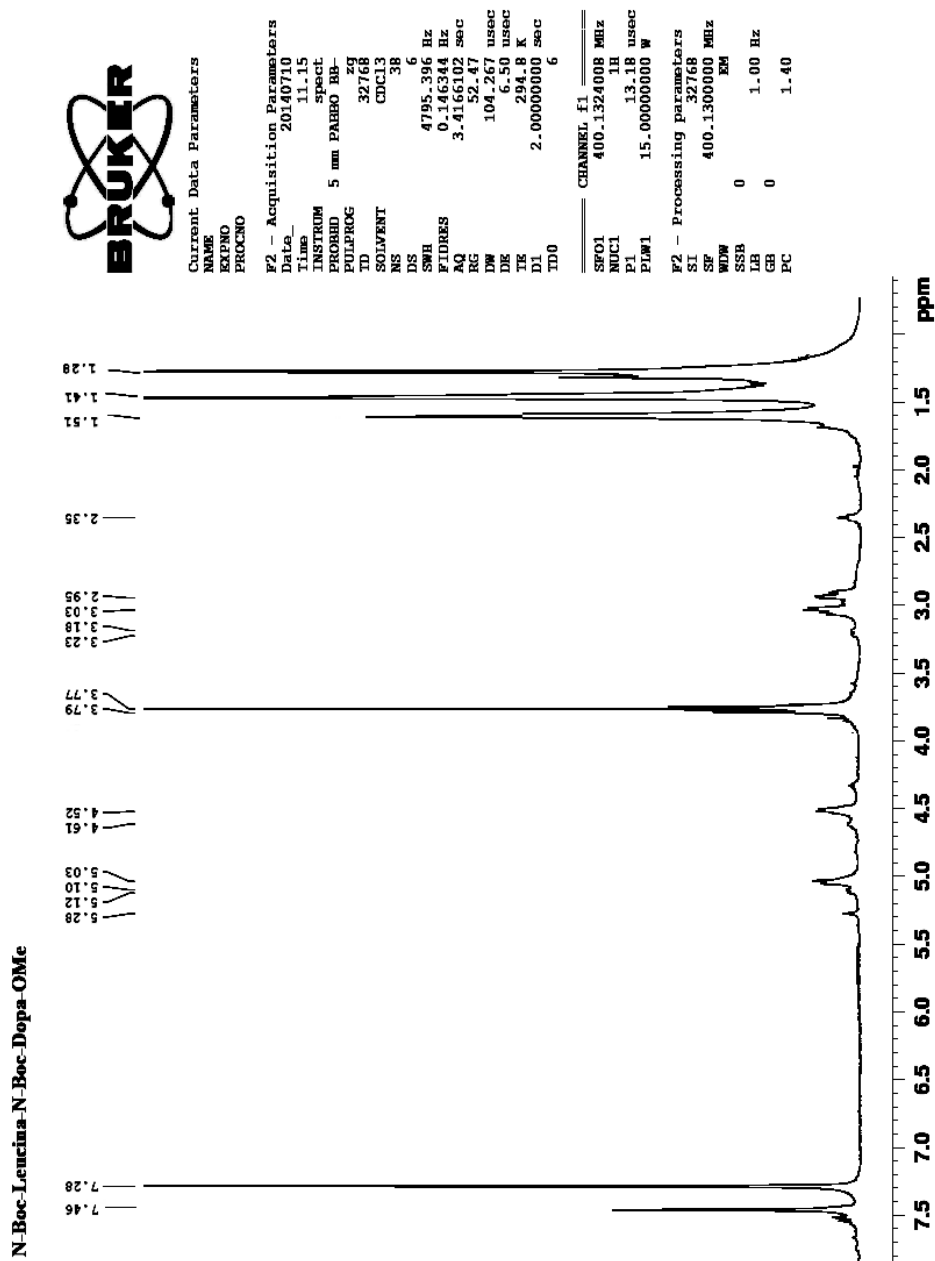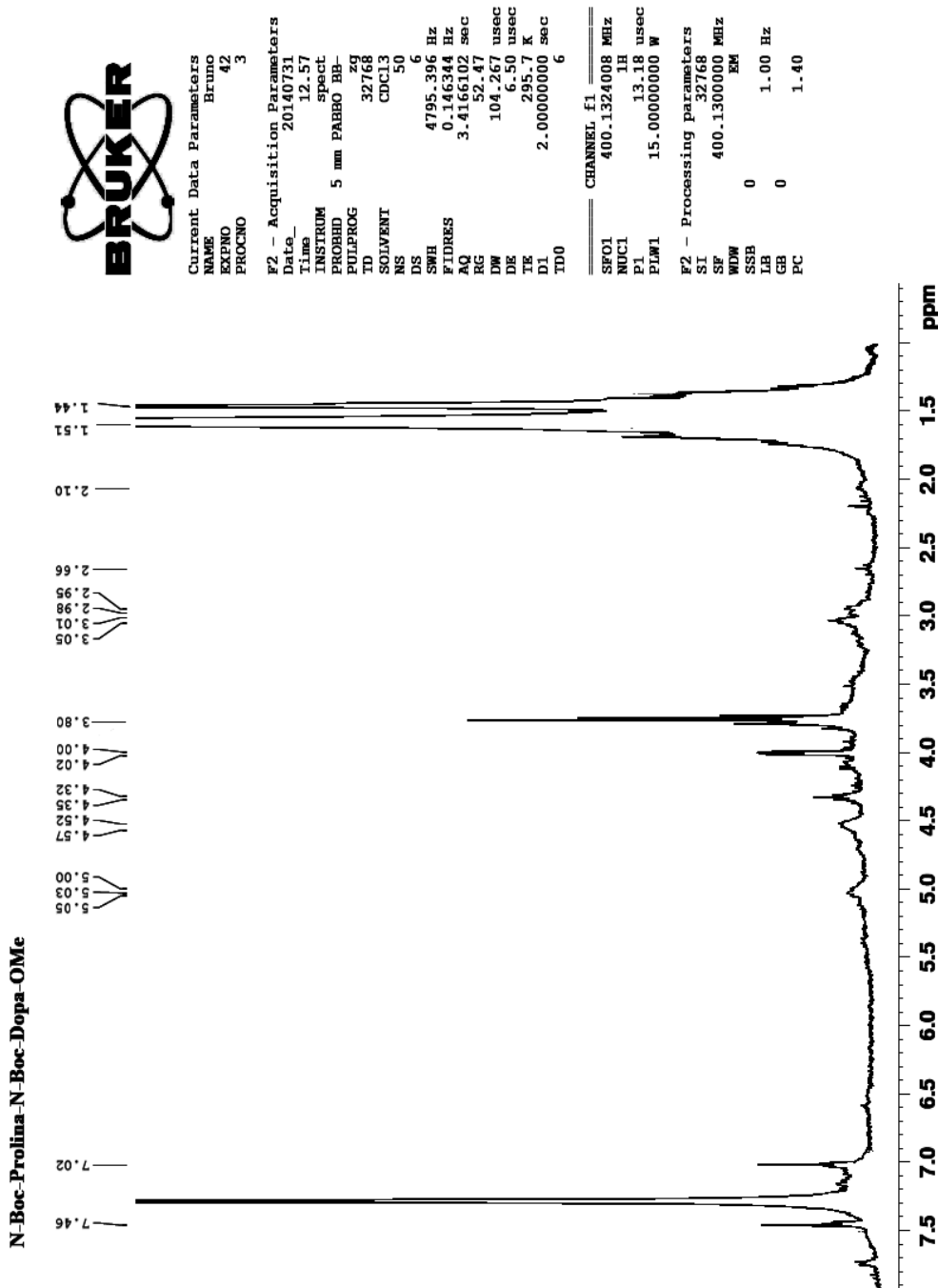
N-Boc-Trp-N-Boc-DOPA-OMe (52) Oil ^{1}H NMR (400 MHz, CDCl$_3$): δ_H (ppm) = 1.42-1.50(18H, d, 6×CH$_3$) J=4, 2.92-3-09 (2H, m, CH$_2$), 3.67 (3H, s, OCH$_3$), 4.58-5.20 (1H, m, CH), 6.71 (1H, s, CH), 7.18 (2H, d, 2xCH) 7.46 (1H, s, CH) J=4, 7.38 (2H, t, 2xCH). ^{13}C NMR (100 MHz, CDCl$_3$): δH (ppm) = 28.08 (3×CH$_3$), 28.40 (CH$_2$) 28.70 (3×CH$_3$), 32.47 (CH$_2$), 52.47 (OCH$_3$), , 55.79 (CH), 59.41 (CH), 79.53 (-C^o), 80.48 (-C^o), 113.58 (CH), 117.31 (CH), 109.74 (C$_{ar}$), 111.14 (C$_{ar}$), 118.80 (C$_{ar}$), 119.31 (C$_{ar}$), 119.84 (C$_{ar}$), 121.10 (C$_{ar}$), 123.00 (C$_{ar}$), 127.44 (C$_{ar}$), 136.59 (C$_{ar}$), 141.44 (C$_{ar}$), 144.76 (C$_{ar}$), 146.56 (C$_{ar}$), 155.80 (C=O), 158.32 (C=O), 171.90 (C=O), 172.64 (C=O). MS (EI): *m/z* 614; Elemental Analysis calcd: C, 60.67; H, 6.41; N, 6.85; O, 26.07 Elemental Analysis found: C, 60.68; H, 6.38; N, 6.81; O, 26.17.

N-Boc-Triptofamo-N-Boc-Dopa-OMe
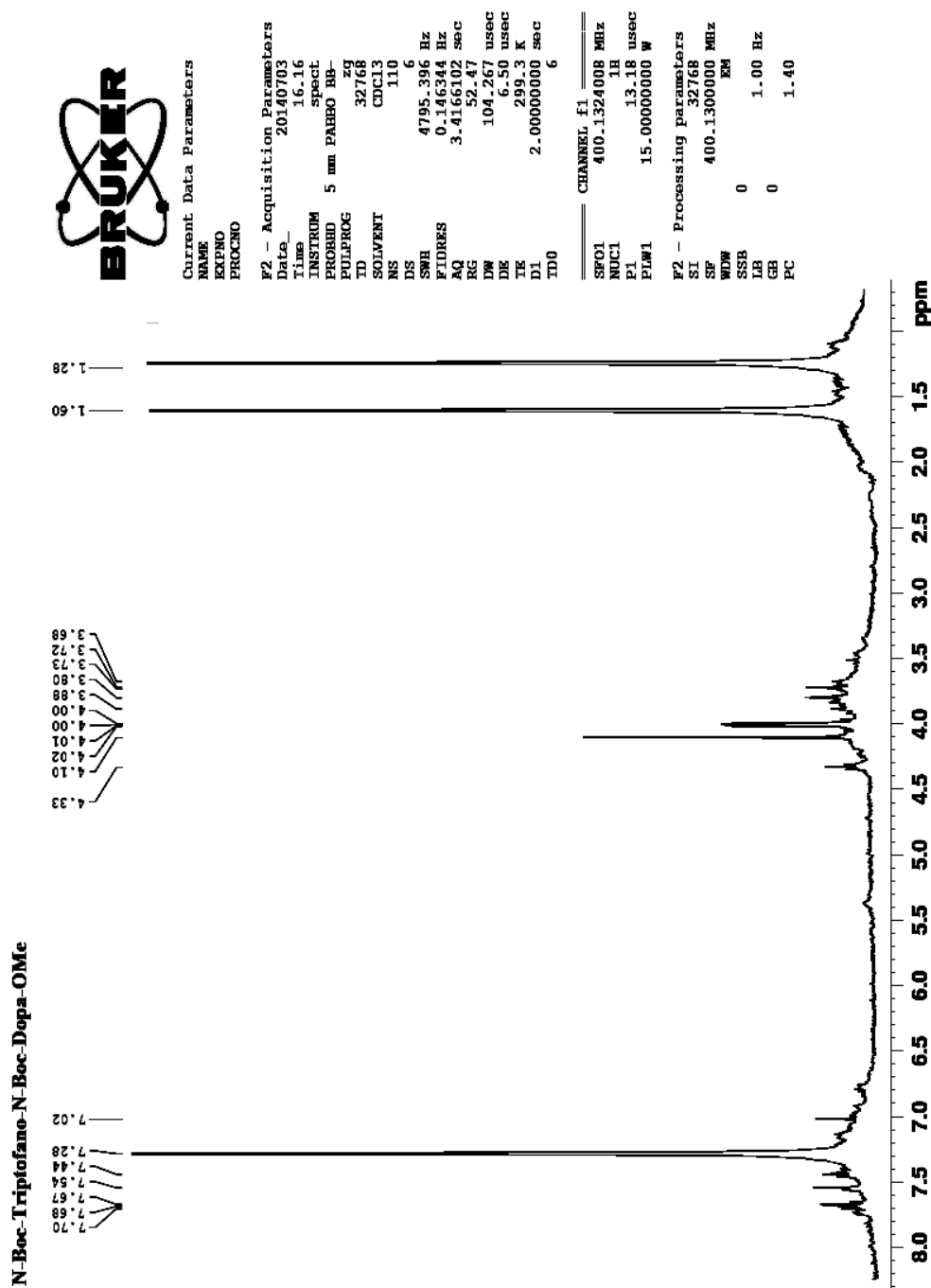
N-Boc-Met-N-Boc-DOPA-OMe (53) Oil ^{1}H NMR (400 MHz, CDCl$_3$): δ_H (ppm) = 1.28-1.46 (18H, d, 6×CH$_3$) J=4, 2.00-2.14 (2H, m, CH$_2$), 2.06 (3H, s, S-CH$_3$), 2.12-2.16 (2H, m,CH$_2$), 2.91-2.94 (2H, t, CH$_2$), 3.77 (3H, s, OCH$_3$), 4.54-5.12 (1H, m, CH), 7.04 (1H, s, CH), 7.42 (1H, s, CH) ^{13}C NMR (100 MHz, CDCl$_3$): δH (ppm) = 15.42 (CH$_3$) 28.08 (3×CH$_3$), 28.70 (3×CH$_3$), 29.72 (CH$_2$) 30.91 (CH$_2$) 42.89 (CH$_2$) 52.47 (OCH$_3$), 56.59 (CH), 79.53 (-C°), 80.48 (-C°), 113.58 (CH), 117.31 (CH), 119.31 (C$_{ar}$), 141.44 (C$_{ar}$), 144.76 (C$_{ar}$), 146.56 (C$_{ar}$), 155.80 (C=O), 158.32 (C=O), 171.90 (C=O), 172.64 (C=O). MS (EI): m/z 559; Elemental Analysis calcd: C, 53.75; H, 6.86; N, 5.01; O, 28.64; S, 5.74 Elemental Analysis found: C, 53.71; H, 6.84; N, 5.12; O, 28.70; S, 5.72.

N-Boc-Metionina-N-Boc-Dopa-OMe
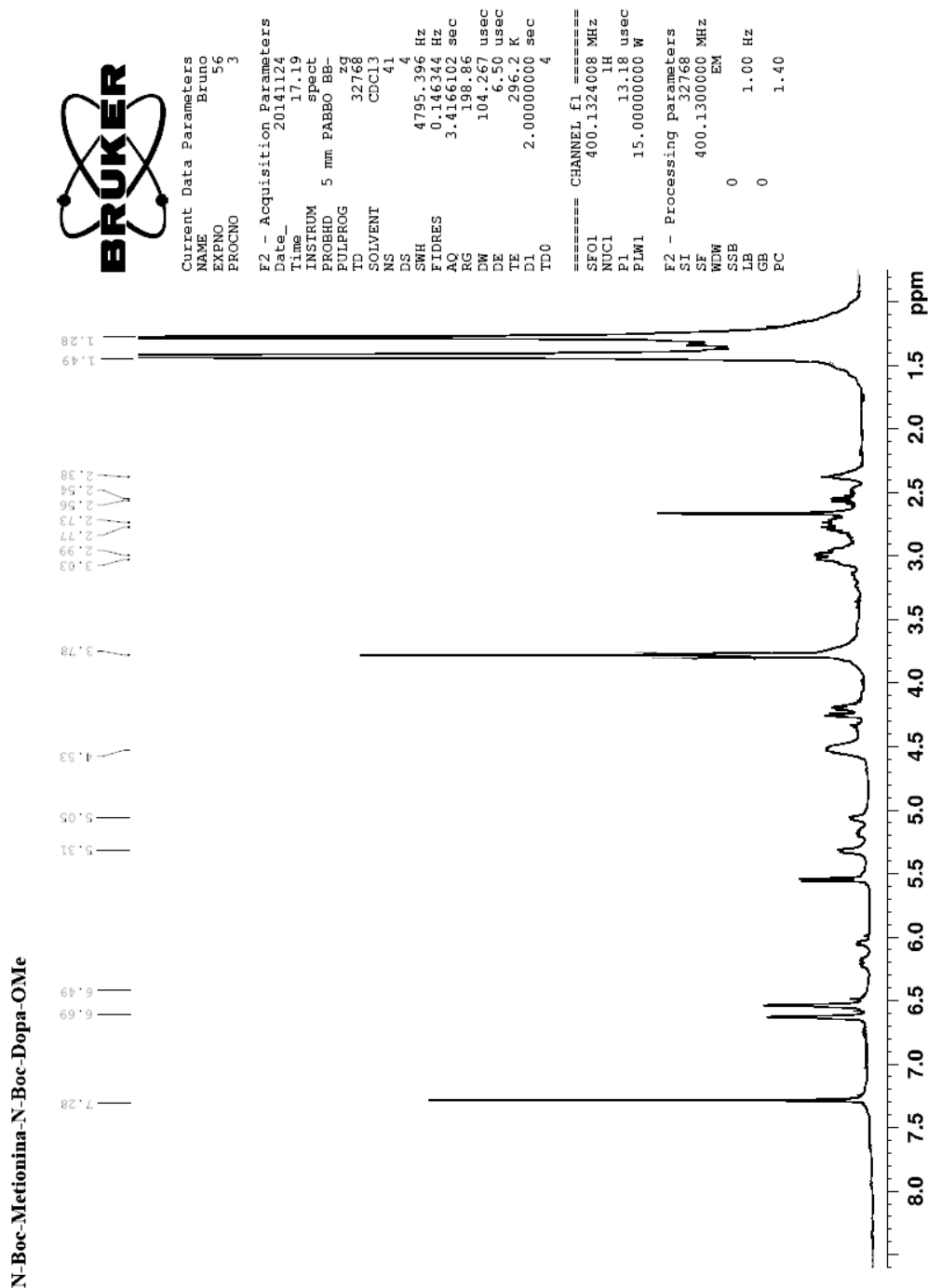
Gly-N-Boc-DOPA-OMe (62) Oil ^{1}H NMR (400 MHz, CDCl$_3$): δ_H (ppm) = 1.44 (9H, s, 3×CH$_3$), 2.90-3.10 (2H, m, CH$_2$), 3.74 (3H, s, OCH$_3$), 3.93 (2H, s, CH$_2$), 4.11 (3H, s, OCH$_3$), 4.62-5.14 (1H, m, CH) J=4, 7.24 (1H, s, CH), 7.42 (1H, s, CH) ^{13}C NMR (100 MHz, CDCl$_3$): δ_H (ppm) = 28.04 (3×CH$_3$), 32.21 (CH$_2$), 42.89 (CH$_2$) 52.47 (OCH$_3$), 52.59 (OCH$_3$), 56.59 (CH), 79.53 (-Cº), 80.48 (-Cº), 113.58 (CH), 117.31 (CH), 119.31 (C$_{ar}$), 141.44 (C$_{ar}$), 144.76 (C$_{ar}$), 146.56 (C$_{ar}$), 155.80 (C=O), 158.32 (C=O), 171.90 (C=O), 172.64 (C=O). MS (EI): *m/z* 399; Elemental Analysis calcd: C, 54.26; H, 6.58; N, 7.03; O, 32.13 Elemental Analysis found: C, 54.25; H, 6.59; N, 7.08; O, 32.13.
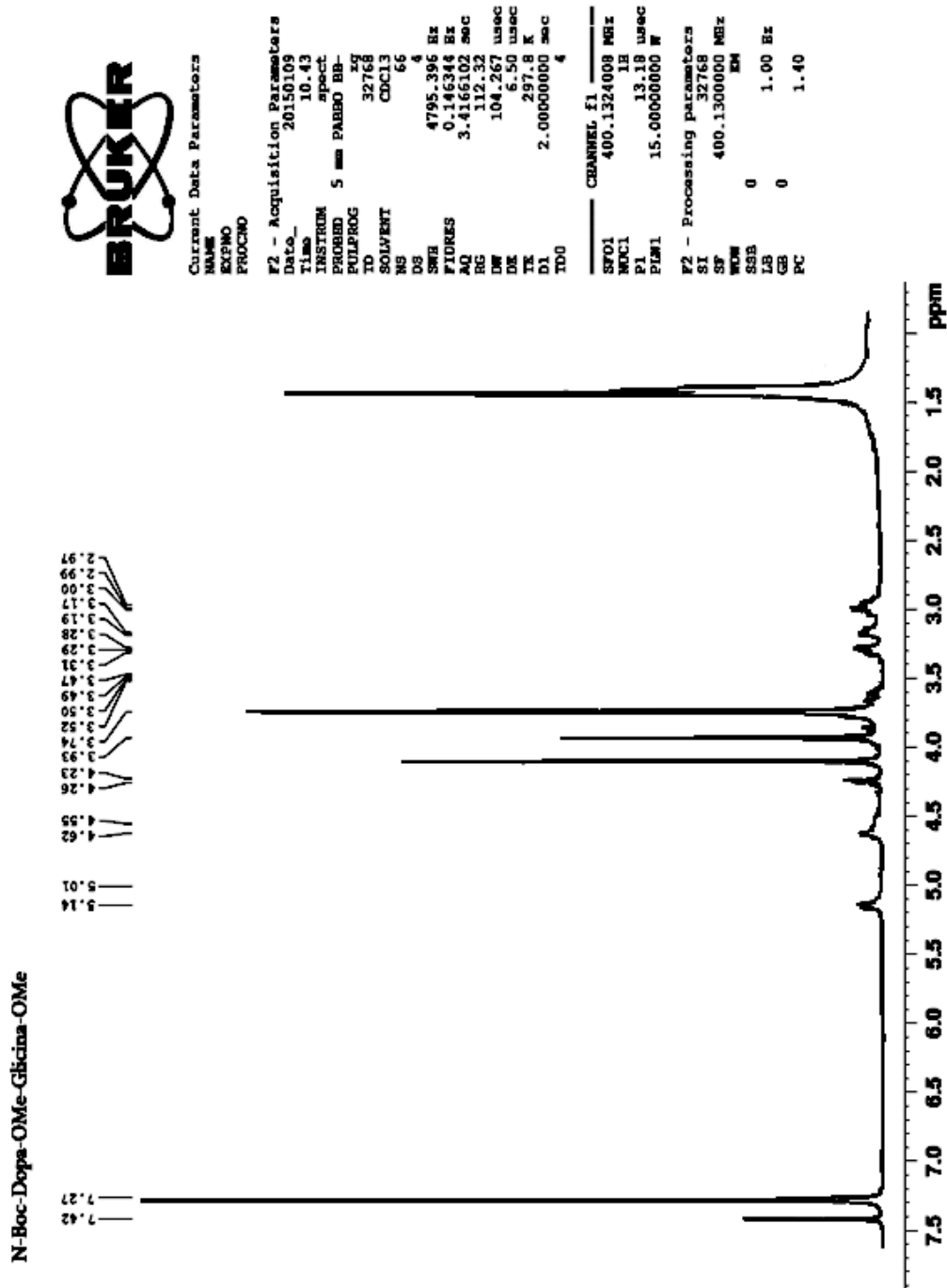
Ala-N-Boc-DOPA-OMe (63) Oil ^{1}H NMR (400 MHz, CDCl$_3$): δ_H (ppm) = 1.44 (9H, s, 3×CH$_3$), 2.29 (3H, s, CH$_3$), 3.65-3.69 (2H, m, CH$_2$), 4.67 (3H, s, OCH$_3$), 4.75 (3H, s, OCH$_3$), 4.79-4.83 (2H, m, CH), 5.19-5.39 (1H, m, CH) , 7.02 (1H, s, CH), 7.54 (1H, s, CH) ^{13}C NMR (100 MHz, CDCl$_3$): δH (ppm) = 18.07 (CH$_3$), 28.04 (3×CH$_3$), 32.21 (CH$_2$), 52.47 (OCH$_3$), 52.59 (OCH$_3$), 55.81 (CH), 56.59 (CH), 79.53 (-C^o), 80.48 (-C^o), 113.58 (CH), 117.31 (CH), 119.31 (C$_{ar}$), 142.34 (C$_{ar}$), 144.76 (C$_{ar}$), 146.56 (C$_{ar}$), 155.80 (C=O), 158.32 (C=O), 171.90 (C=O), 172.64 (C=O). MS (EI): *m/z* 413; Elemental Analysis calcd: C, 55.33; H, 6.84; N, 6.79; O, 31.03 Elemental Analysis found: C, 55.30; H, 6.81; N, 6.76; O, 31.10.

N-Boc-Dopa-OMe-Alanina-OMe
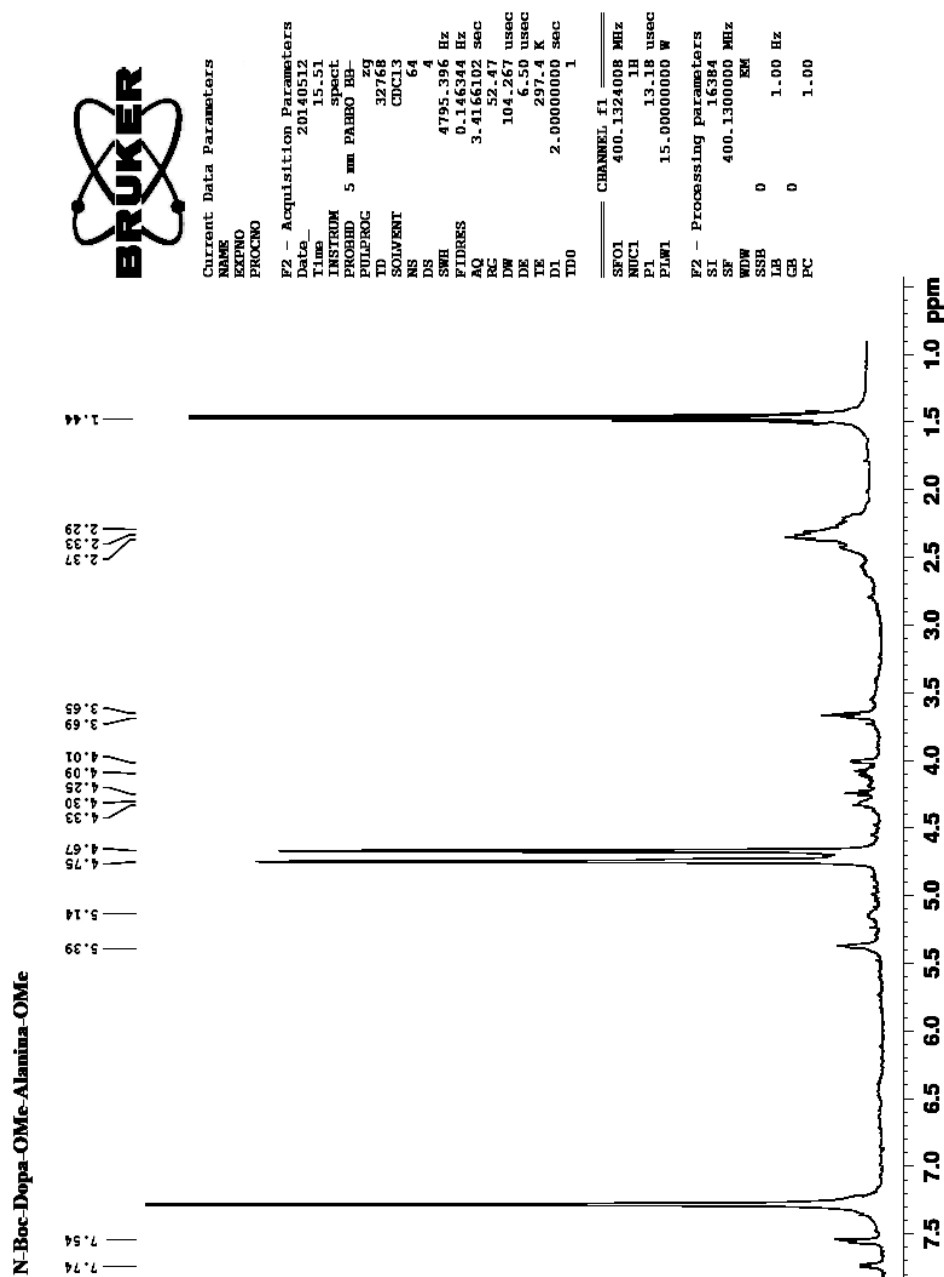
Val-N-Boc-DOPA-OMe (64) Oil ^{1}H NMR (400 MHz, CDCl$_3$): δ_H (ppm) = 0.89 (6H, d, 2×CH$_3$) J=4, 1.32 (9H, s, 3×CH$_3$), 2.90-3.10 (1H, m,CH), 3.74 (3H, s, OCH$_3$), 3.76(3H, s, OCH$_3$), 3.81-3.86 (1H, m, CH) 7.49 (2H, s, 2xCH) ^{13}C NMR (100 MHz, CDCl$_3$): δH (ppm) = 19.25 (2xCH$_3$), 28.04 (3×CH$_3$), 30.63 (CH), 32.21 (CH$_2$), 52.47 (OCH$_3$), 52.59 (OCH$_3$), 55.81 (CH), 74.30 (CH), 79.53 (-C°), 80.48 (-C°), 113.58 (CH), 117.31 (CH), 119.31 (C$_{ar}$), 142.34 (C$_{ar}$), 144.76 (C$_{ar}$), 146.56 (C$_{ar}$), 155.80 (C=O), 158.32 (C=O), 171.90 (C=O), 172.64 (C=O). MS (EI): *m/z* 441; Elemental Analysis calcd: C, 57.26; H, 7.32; N, 6.36; O, 29.06 Elemental Analysis found: C, 57.23; H, 7.31; N, 6.36; O, 29.05.

Leu-N-Boc-DOPA-OMe (65) Oil ^{1}H NMR (400 MHz, CDCl$_3$): δ_H (ppm) = 1.28 (9H, s, 3×CH$_3$), 1.32 (6H, d, 2×CH$_3$) J=4, 2.61-2.64 (1H, m, CH), 2.95-3.03 (2H, m, CH$_2$), 3.77 (3H, s, OCH3), 3.79 (3H, s, OCH$_3$), 4.10 (2H, m, CH$_2$), 4.61-5.03 (1H, m, CH) J=4, 6.49 (1H, s, CH), 6.92 (1H, s, CH) ^{13}C NMR (100 MHz, CDCl$_3$): δH (ppm) = 22.95 (2xCH$_3$), 28.04 (3×CH$_3$), 30.63 (CH), 32.21 (CH$_2$), 40.75 (CH$_2$), 52.47 (OCH$_3$), 52.59 (OCH$_3$), 55.81 (CH), 64.70 (CH), 79.53 (-C°), 80.48 (-C°), 113.58 (CH), 117.31 (CH), 119.31 (C$_{ar}$), 142.34 (C$_{ar}$), 144.76 (C$_{ar}$), 146.56 (C$_{ar}$), 155.80 (C=O), 158.32 (C=O), 171.90 (C=O), 172.64 (C=O). MS (EI): *m/z* 455*;* ElementalAnalysis calcd: C, 58.14; H, 7.54; N, 6.16; O, 28.16 Elemental Analysis found: C, 58.11; H, 7.57; N, 6.10; O, 28.16.

Phe-N-Boc-DOPA-OMe (66) Oil ^{1}H NMR (400 MHz, CDCl$_3$): δH (ppm): 1.44 (9H, s, 3×CH$_3$), 3.04-3.06 (2H, m, CH$_2$), 3.09-3.13 (2H, m, CH$_2$), 3.70 (3H, s, OCH$_3$), 3.77 (3H, s, OCH$_3$), 4.28 (1H, m, CH), 5.24 (1H, m, CH), 6.46 (1H, s, CH), 6.81 (2H, t, 2xCH), 6.94 (2H, d, 2xCH) J=4, 7.24 (1H, s, CH), 7.38 (2H, t, 2xCH) J=8 ^{13}C NMR (100 MHz, CDCl$_3$): δH (ppm) = 28.04 (3×CH$_3$), 32.21 (CH$_2$), 36.95 (CH$_2$), 42.89 (CH$_2$) 52.47 (OCH$_3$), 52.59 (OCH$_3$), 56.59 (CH), 69.69 (CH), 79.53 (-C°), 80.48 (-C°), 113.58 (CH), 117.31 (CH), 119.31 (C$_{ar}$), 124.92 (C$_{ar}$), 127.62 (C$_{ar}$), 129.57 (C$_{ar}$), 144.76 (C$_{ar}$), 141.44 (C$_{ar}$), 144.76 (C$_{ar}$), 146.56 (C$_{ar}$), 155.80 (C=O), 158.32 (C=O), 171.90 (C=O), 172.64 (C=O). MS (EI): *m/z* 489; Elemental Analysis calcd: C, 61.46; H, 6.60; N, 5.73; O, 26.20. Elemental Analysis found: C, 61.46; H, 6.61; N, 5.73; O, 26.27.
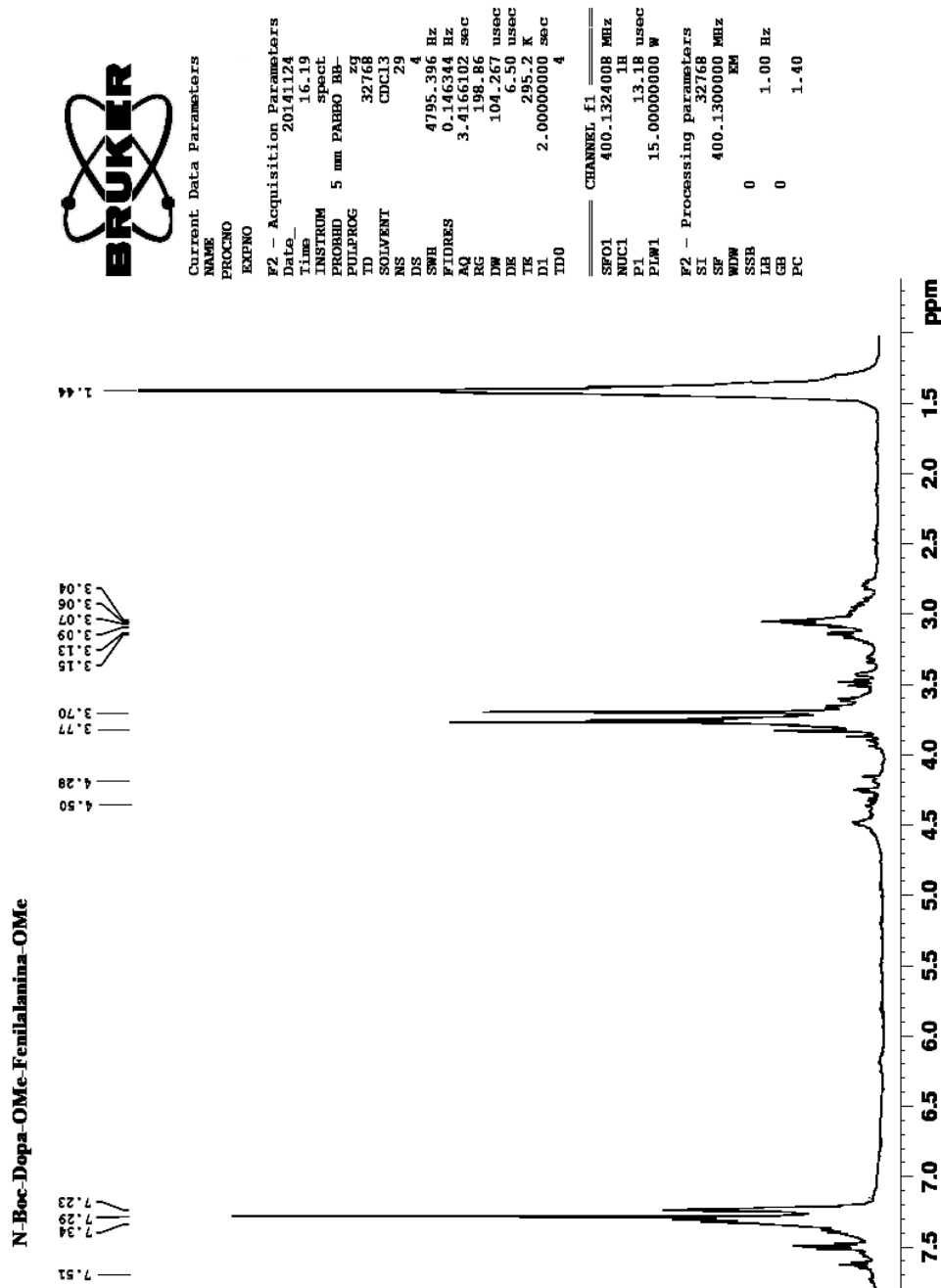
Pro-N-Boc-DOPA-OMe (67) Oil ^{1}H NMR (400 MHz, CDCl$_3$): δH (ppm): 1.44 (9H, 6, 3×CH$_3$), 1.60 (2H, m, CH$_2$), 1.85 (2H, m, CH$_2$), 3.35 (2H, m, CH$_2$), 3.60 (2H, m, CH$_2$), 3.70 (3H, s, OCH$_3$), 3.77 (3H, s, OCH$_3$), 4.31-5.10 (1H, m, CH), 6.45 (1H, s, CH), 6.90 (1H, s, CH) ^{13}C NMR (100 MHz, CDCl$_3$): δH (ppm) =27.56 (CH$_2$), 28.04 (3×CH$_3$), 29.81 (CH$_2$) 32.28 (CH$_2$) 42.89 (CH$_2$) 52.47 (OCH$_3$), 52.59 (OCH$_3$), 56.59 (CH), 74.64 (CH), 79.53 (-C°), 80.48 (-C°), 113.58 (CH), 117.31 (CH), 119.31 (C$_{ar}$), 141.44 (C$_{ar}$), 144.76 (C$_{ar}$), 146.56 (C$_{ar}$), 155.80 (C=O), 158.32 (C=O), 171.90 (C=O), 172.64 (C=O). MS (EI): *m/z* 439*;* Elemental Analysis calcd: C, 57.52; H, 6.90; N, 6.39; O, 29.19 Elemental Analysis found: C, 57.50; H, 6.86; N, 6.36; O, 29.16.
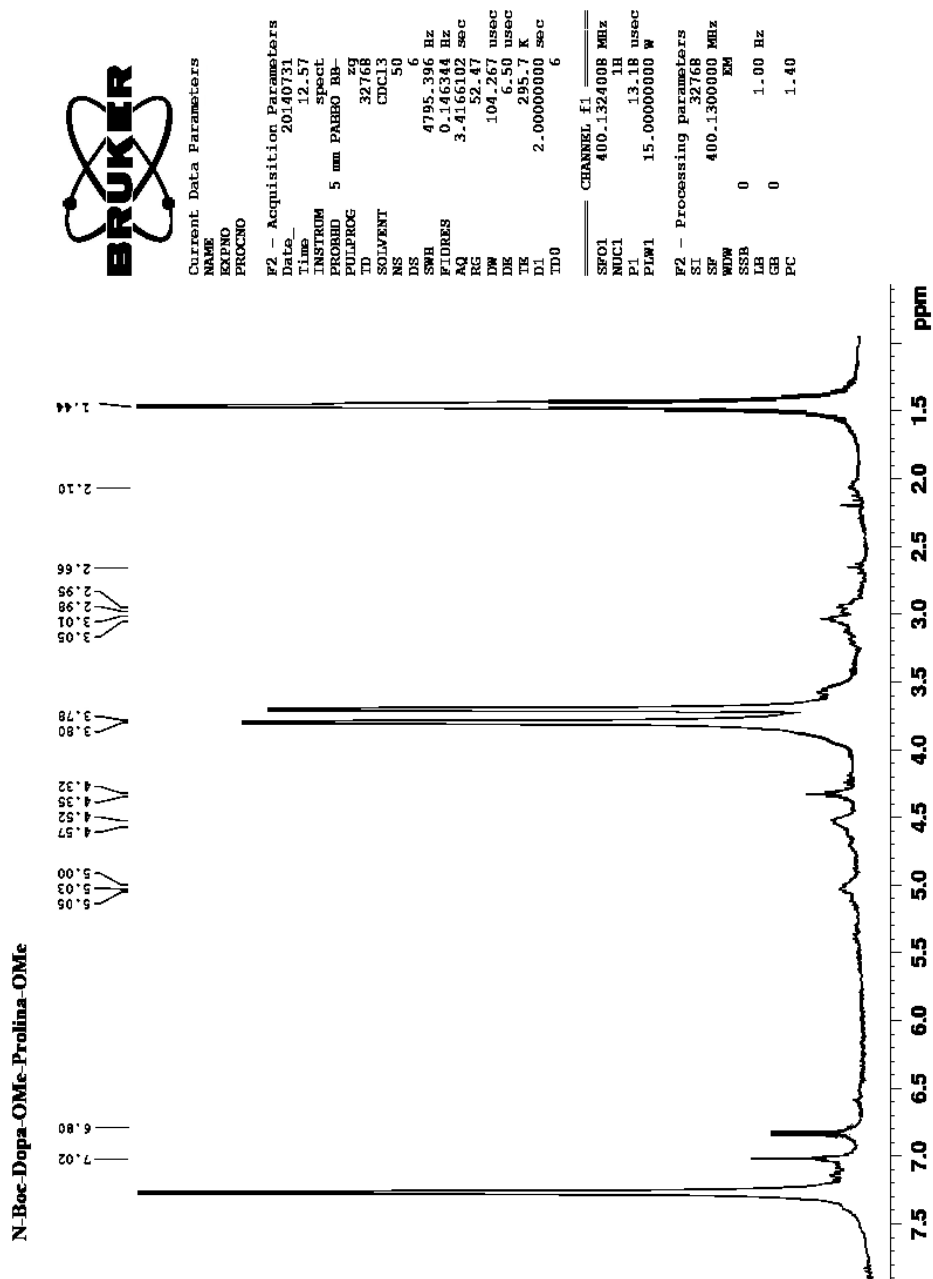
Trp-N-Boc-DOPA-OMe (68) Oil ^{1}H NMR (400 MHz, CDCl$_3$): δH (ppm): 1.44 (9H, s, 3×CH$_3$), 3.68-3.73 (2H, m, CH$_2$) , 3.88-4.00 (2H, m, CH$_2$), 4.10 (3H, s, OCH$_3$), 4.15(3H, s, OCH$_3$), 4.28-5.14 (1H, m, CH), 5.06 (1H, s, CH) , 6.71 (1H, s, CH), 7.18 (2H, d, 2xCH) 7.46 (1H, s, CH) *J*=4, 7.38 (2H, t, 2xCH) ^{13}C NMR (100 MHz, CDCl$_3$): δH (ppm) =, 28.04 (3×CH$_3$), 30.67 (CH$_2$), 52.47 (OCH$_3$), 52.59 (OCH$_3$), 56.59 (CH), 70.70 (CH), 79.53 (-Cº), 80.48 (-Cº), 109.39 (C$_{ar}$), 111.21 (C$_{ar}$), 113.58 (CH), 117.31 (CH), 118.48 (C$_{ar}$)119.31 (C$_{ar}$), 123.55 (C$_{ar}$), 127.66 (C$_{ar}$), 136.39 (C$_{ar}$), 142.34 (C$_{ar}$), 144.76 (C$_{ar}$), 146.56 (C$_{ar}$), 155.80 (C=O), 158.32 (C=O), 171.90 (C=O), 172.64 (C=O). MS (EI): *m/z* 527; Elemental Analysis calcd: C, 61.47; H, 6.30; N, 7.96; O, 24.26 Elemental Analysis found: C, 61.41; H, 6.33; N, 7.92; O, 24.29.
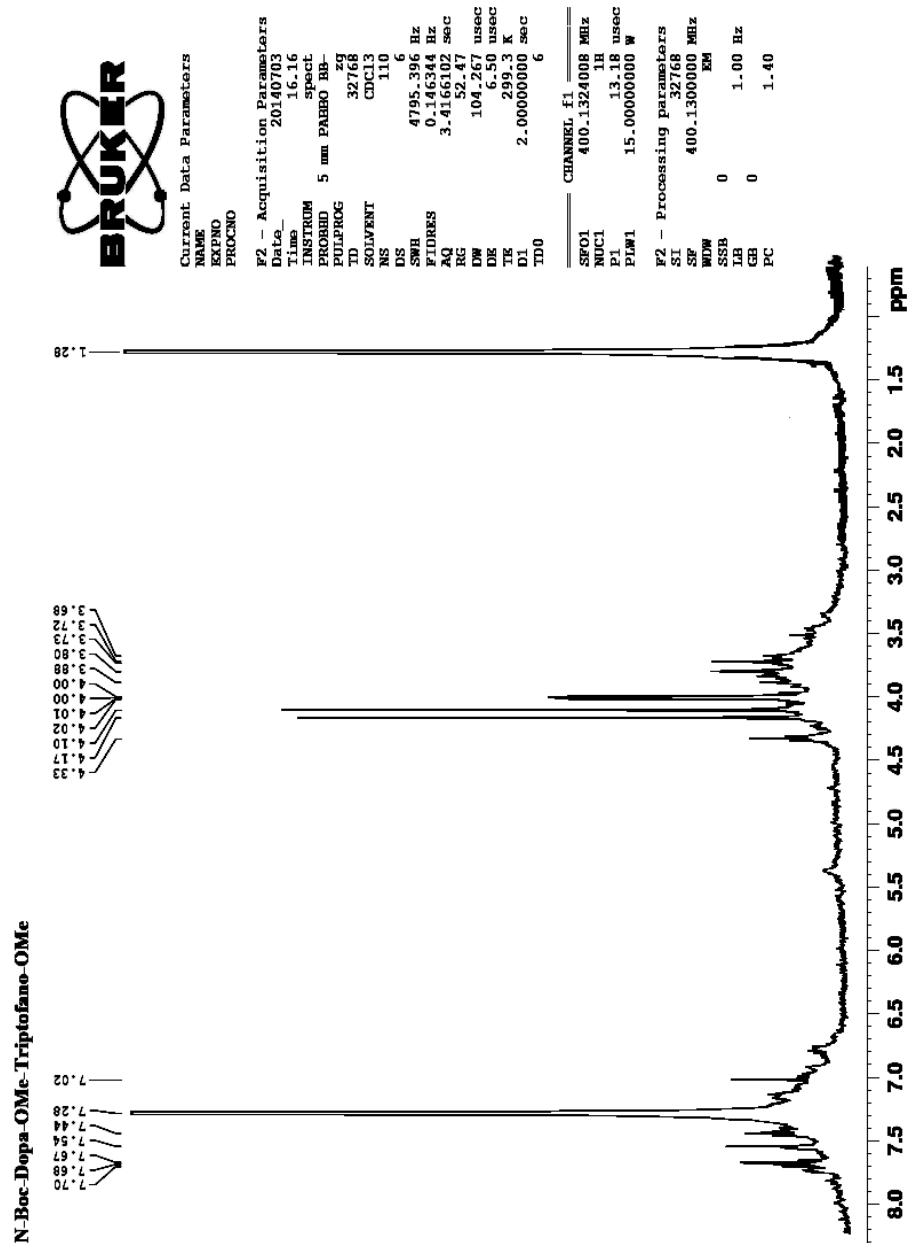
Met-N-Boc-DOPA-OMe (69) Oil ^{1}H NMR (400 MHz, CDCl$_3$): δH (ppm): 1.44 (9H, s, 3×CH$_3$), 2.38-2.40 (2H, m, CH$_2$) J=8, 2.72 (3H, s, S-CH$_3$), 2.73- 2.77 (2H, m, CH$_2$), 2.99-3.03 (2H, m, CH$_2$), 3.74 (3H, s, OCH$_3$), 3.78 (3H, s, OCH$_3$), 4.53-5.05 (1H, m, CH), 6.49 (1H, s, CH), 6.72 (1H, s, CH) ^{13}C NMR (100 MHz, CDCl$_3$): δH (ppm) = 15.43 (CH$_3$), 28.04 (3×CH$_3$), 31.68 (CH$_2$), 32.10 (CH$_2$), 32.21 (CH$_2$), 52.47 (OCH$_3$), 52.59 (OCH$_3$), 56.59 (CH), 66.46 (CH$_2$), 79.53 (-C°), 80.48 (-C°), 113.58 (CH), 117.31 (CH), 119.31 (C$_{ar}$), 141.44 (C$_{ar}$), 144.76 (C$_{ar}$), 146.56 (C$_{ar}$), 155.80 (C=O), 158.32 (C=O), 171.90 (C=O), 172.64 (C=O). MS (EI): *m/z* 473; Elemental Analysis calcd: C, 53.37; H, 6.83; N, 5.93; O, 27.09; S, 6.79 Elemental Analysis found: C, 53.32; H, 6.80; N, 5.98; O, 27.08; S, 6.77.
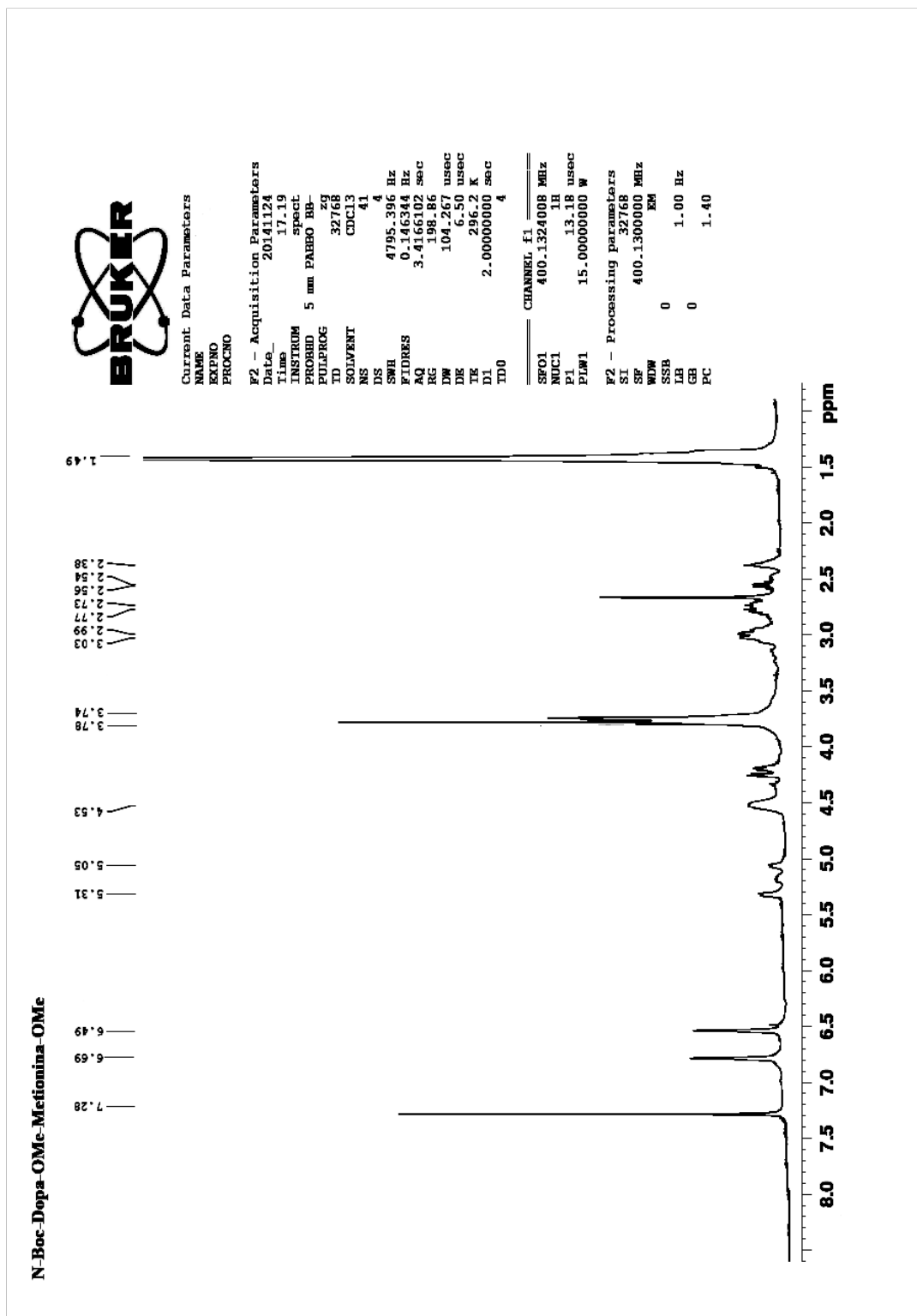
N-Boc-DOPA-OMe-Boc-DOPA-OMe (70) Oil ^{1}H NMR (400 MHz, CDCl$_3$): δ_H (ppm) = 1.28-1.44 (18H, d, 6×CH$_3$) J=4, 2.91-3-05 (2H, m, CH$_2$), 3.74 0(3H, s, OCH$_3$), 4.52-5.04 (1H, m, CH) , 5.75 (1H,s,CH), 7.46 (1H, s, CH). ^{13}C NMR (100 MHz, CDCl$_3$): δH (ppm) = 28.08 (3×CH$_3$), 32.47 (CH$_2$) 52.47 (OCH$_3$), 55.79 (CH), 79.53 (-C°), 113.58 (CH), 119.11 (C$_{ar}$), 119.31 (C$_{ar}$), 141.44 (C$_{ar}$), 144.76 (C$_{ar}$), 146.56 (C$_{ar}$), 155.80 (C=O), 171.90 (C=O),MS (EI): *m/z* 621; Elemental Analysis calcd: C, 58.06; H, 6.50; N, 4.51; O, 30.93 Elemental Analysis found: C, 58.10; H, 6.53; N, 4.50; O, 30.93.

1.3.3 Test systems and culture conditions

L5178Y TK$^{+/-}$ clone (3.7.2C) mouse lymphoma cells were obtained from ATCC (CRL-9518™). Generation time, plating efficiency and absence of mycoplasma were checked at regular intervals. Stocks of the L5178Y cells are stored in liquid nitrogen and subcultures prepared from the frozen stocks for experimental use. Cells were grown in RPMI 1640 supplemented with 10% heat-inactivated horse serum, 2mM L-glutamine and antibiotics (100 IU/mL penicillin and 100 IU/mL streptomycin) and incubated at 37°C in a 5% carbon dioxide atmosphere and 100% nominal humidity. Chinese hamster ovary (CHO) cells were obtained from Prof. A.T. Natarajan (State University of Leiden, The Netherland). This cell line derives from the CHO isolated from an explant of the ovary of the Chinese hamster (Cricetulus griseus, 2n = 22). The CHO cell line is particularly useful for this kind of studies because of its stable karyotype (modal number is 21 chromosomes), short cell cycle (12–14 h) and its high plating efficiency. Stocks of CHO cells are stored in liquid nitrogen and subcultures are prepared from these stocks for experimental use. Cultures were grown as monolayer cultures in Ham's F-10 medium (Gibco BRL) supplemented with 15% foetal bovine serum, 4mM L-glutamine and antibiotics (50 IU/mL penicillin and 50 IU/mL streptomycin). All incubations were at 37 °C in a 5% carbon dioxide atmosphere and 100% nominal humidity.

1.3.4 Chromosomal aberration assays

Approximately 24 hours before treatment exponentially growing cells were detached by trypsin action and an appropriate number of 25 cm^2 plastic cell culture flasks containing 5 mL complete culture medium was individually inoculated with 3.0×10^5 cells. Test compound treatments of CHO cells were performed in the absence of a metabolic activation system for 24 hours (approximately 1.5 cell cycle). Colcemid at 0.27 mM was added during the last 3 hours of culture to accumulate cells in metaphase. Hypotonic shock was induced by 1% trisodium citrate solution for 10 minutes. Cell suspension was fixed in a mixture of methanol and glacial acetic acid (v/v 3:1) followed by three washes. Cytogenetic preparations for analyses of chromosomal aberrations and mitotic indices were stained with an aqueous solution of Giemsa (3%). For each experimental point 100 metaphases were scored for chromosomal aberrations and were classified according to the description of Savage. The mitotic index was expressed in percentage based on the number of metaphases present after a total of 1000 cells scored (interphases and metaphases). Solvent-treated cells served as negative control.

1.3.5 Comet assay

Cultures of mouse lymphoma cells at a concentration of 1×10^6 cells/mL were treated for 30 minutes at 37°C in 5% carbon dioxide atmosphere and 100% nominal humidity, with each synthesized compound at a single dose-level, which was the highest concentration analyzed for scoring of chromosomal aberrations. In additional culture without any treatment which served as control was also included. At the end of treatment 10 µl of each cell suspension was added to 65 µl of 0.7% (w/v) low melting point agarose (Bio-Rad Lab.) and sandwiched between a lower layer of 1% (w/v) normal-melting agarose (Bio-Rad Lab.). For untreated cultured and culture treated compound, two sets of three slides each, were prepared. An aliquot of 50 µl of H_2O_2 (0.25 µM) was added to one set, while PBS was added to the parallel set. The slides were kept at +4°C for 5 minutes and then immersed in lysing solution (2.5 M NaCl, 100 mM Na_2EDTA, 10 mM Tris, pH 10) containing 10% DMSO and 1% Triton x 100 (ICN Biomedicals Inc.) at 4°C overnight. Slides were then randomly placed in a horizontal gel electrophoresis apparatus with fresh alkaline electrophoresis buffer (300 mM NaOH, 1 mM Na_2EDTA, pH>13) and incubated for 25 min at 4°C to allow for DNA unwinding and expression of alkali-labile sites. Electrophoresis was at 4°C for 15 minutes at 30 V (1 V/cm) and 300 mA. After electrophoresis, slides were immersed in 0.3 M sodium acetate in ethanol for 30 min. Slides were then dehydrated in an alcohol series (2 min at 70, 85, and 100%) and air-dried. Slides stained with 20 µg/ml ethidium bromide in the presence of antifade immediately before analysis, were examined at 40X magnification using an automated image analysis system (Comet Assay III; Perceptive Instruments, UK) connected to a fluorescence microscope (Zeiss Axioskop 2). DNA damage was quantified from the tail moment values. A number of 50 cells from each slide (150 cells in total) were analyzed per experimental point.

1.3.6. Extraction of tyrosinase

Mushroom tyrosinase was extracted and purified from *A. bisporus* using two procedures with slight modifications. In the first extraction procedure, 2.5 Kg of fresh mushroom were frozen at -20°C at least one day and then lyophilized. The extraction medium was centrifuged at 6000 rpm for 20 min and the solution obtained was first subjected to ammonium sulphate [$(NH_4)SO_4$] precipitation (35-70%) and then dialyzed against water. In the second extraction procedure, the sporocarps was cleaned to remove earthly residues and then washed with 20mM ascorbic acid maintained at 4°C. After day they had been dried, the sporocarps are sliced and frozen at -20°C at least 1 day before extraction.

0.5 Kg of frozen sporocarp was homogenized twice in 0,6 L of acetone at -20°C in a blender for 1 min. The obtained solid pulp was filtered through a Buchner funnel and homogenized with 0.5 L of 30% v/v acetone in water for 2-3 min. The mixture was centrifuged at 6000 rpm for 20 min. To the supernatant, 1.5 volumes of acetone at -20°C were added dropwise under vigorous stirring. The mixture was allowed to settle at 4°C for 2-3 h; most of the supernatant fluid was decanted and discarded, the remainder was centrifuged and the precipitate was dissolved in water and subjected to precipitation with calcium acetate 1% of saturation. The turbid mixture was frozen at -20°C. Samples obtained from several days were stored frozen at this stage. They were then thawed, mixed and centrifuged. Ammonium sulphate powder [$(NH_4)SO_4$] was added to the collected supernatant to make a 35% saturated solution. The resulting solution was allowed to stand for 30 min at 4°C and centrifuged at 6000 rpm for 20 min. $(NH_4)SO_4$ was added to supernatant to make a 70% saturated solution. The solution was allowed to stand for 2 h at 4°C and centrifuged. The precipitate was dissolved in a minimal volume of cold water and then dialyzed against water and concentrated by means of Vivaflow $^®$ 50 equipped with polyethersulfone (PES) membrane (1000 MWCO). The resulting enzyme solution was lyophilized and stored at -20°C.

1.3.6.1 Determination of protein concentration

Protein concentration was determined spectrophoteometrically at 595 nm according to the Bradford method using bovine serum albumin (BSA) as a standard.

1.3.6.2 Activity assay

Tyrosinase assay was performed by the dopachrome method. Briefly, 1.0 mL of 2.5 mM of L-Tyr solution in water was mixed with 1.9 mL of Na-phosphate buffer 0.1 M, pH 7.0 and incubated at 25°C for 10 min. Then, an appropriate amount of free or immobilized enzyme in 100.0 ml of Na-phosphate buffer was added to the mixture and the initial rate was immediately measured as linear increase in optical density at 475 nm, due to dopachrome production. One unit of enzyme activity was defined as the increase in absorbance of 0.001 per minute at pH 7.0, 25°C in a 3.0 mL reaction mixture containing 0.83 mM of L-Tyr and 67 mM of Na-phosphate buffer pH 7.0. To evaluate the contaminant laccase in enzyme preparation, the laccase activity was determined spectrophotometrically using 2,2' azino-bis(3-ethylbenzthiazoline-6-sulphonic acid) (ABTS) as the substrate (27). The assay mixture contained 0.5 mM ABTS, Na-phosphate buffer 0.1 M, pH 7.0 and the enzyme was incubated at 25°C. The oxidation was followed by an absorbance increase at 415

nm for 1 min. One activity unit was defined as the amount of enzyme that oxidised 1mmol ABTS/min

1.3.7 MWCNTs oxidation

Despite the less surface area in respect to Single Walled Carbon Nanotubes (SWCNTs), the studies are conducted on Multi Walled Carbon Nanotubes (MWCNTs) as a support for immobilization because of the lower production costs (and the higher commercial availability) and the better dispersibility in aqueous solutions. In the literature both MWCNTs and functionalized MWCNTs were reported to be suitable supports for protein immobilization processes.[278] The driving force which was responsible for a successful physical adsorption on non-functionalized MWCNTs was the interaction between the enzyme's hydrophobic regions and the surface of the Carbon Nanotubes. This strategy affords the preservation of the native structural and functional properties of the nanotubes. MWCNTs show a very low dispersibility in aqueous solutions (also after prolonged ultrasonication treatments Figure 61), and this leads to the minimization of the available surface for protein immobilization.
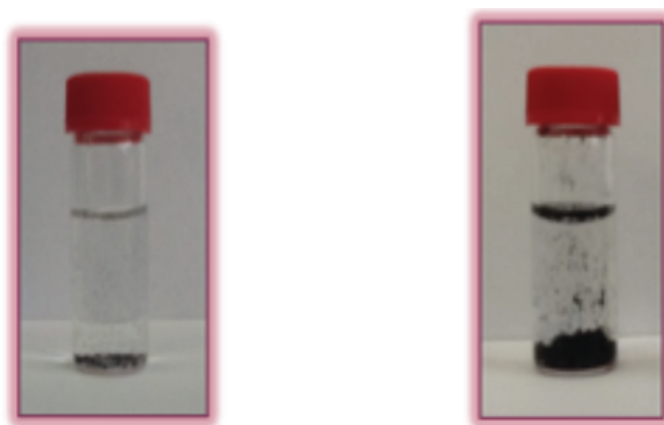
Figure 39: left: MWCNTs in distilled water; right: MWCNTs after 4 h of sonication in distilled water.

Basically, MWCNTs oxidation introduces charged functional groups introduction on the nanotubes's surface and a significant increase of solubility in water solutions. Oxidized MWCNTs (ox-MWCNTs) were prepared following as previously reported in the literature, [279] by treatment with a 3:1 mixture of concentrated sulphuric and nitric acids in a ultrasonication bath for a prolonged time at room temperature.
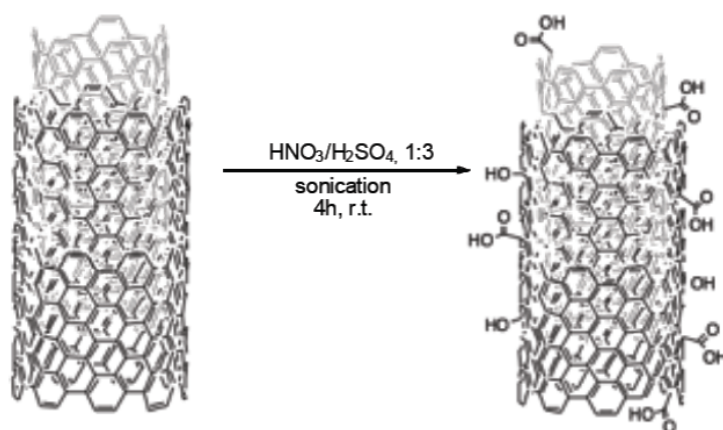
Figure 40. Oxidation of MWCNT using Sulpho-Nitric Mixture.

The acid solution containing ox-MWCNTs was centrifuged to discard the acid supernatant and nanotubes are subjected to several cycles of sonication and centrifugation until a neutral pH of the solution was obtained. The functionalization process also leads to the purification of the nanotubes. The oxidation furnished water soluble nanotubes (Figure 62) thanks to the introduction of charged carboxylic and hydroxyls functional groups on the surface.

Figure 41 MWCNTs after 4 h of sonication in a solfonitric mixture.

The solubilisation of nanotubes in water was verified by UV-VIS spectroscopy. Briefly, ox-MWCNTs are sonicated in milliQ water in order to obtain a solution of known concentration and their maximum absorbance was measured (500 nm). The observed linear relationship between absorbance *versus* ox-MWCNTs solution concentration and the absence of flocculation or precipitation phenomena (also after weeks of storage) suggested a high value of solubility.

1.3.8. PDDA deposition on ox-MWCNTs

Ox-MWCNTs were successively treated with a positively charged polyelectrolyte by the layer by layer technique, which basically allows the homogeneous coating of a given support by means of the alternating deposition of polyelectrolytes of opposite charge. Commercial poly(diallyldimethylammonium chloride) (PDDA) was chosen as a polycation ,[280,281] and the coating was carried out according to procedures known in the literature;[282] briefly, ox-MWCNTs were sonicated in the presence of an appropriate amount of polyelectrolyte in a 0.5 M NaCl solution, the suspension was then subjected to orbital shaking and finally centrifuged. This treatment affords the deposition of the polyelectrolyte film on the negatively charged surface of the ox-MWCNTs (Scheme 63).

a

Poly(diallyldimethylammonium chloride)
(PDDA)

b

ox-MWCNTs   ox-MWCNTs/PDDA
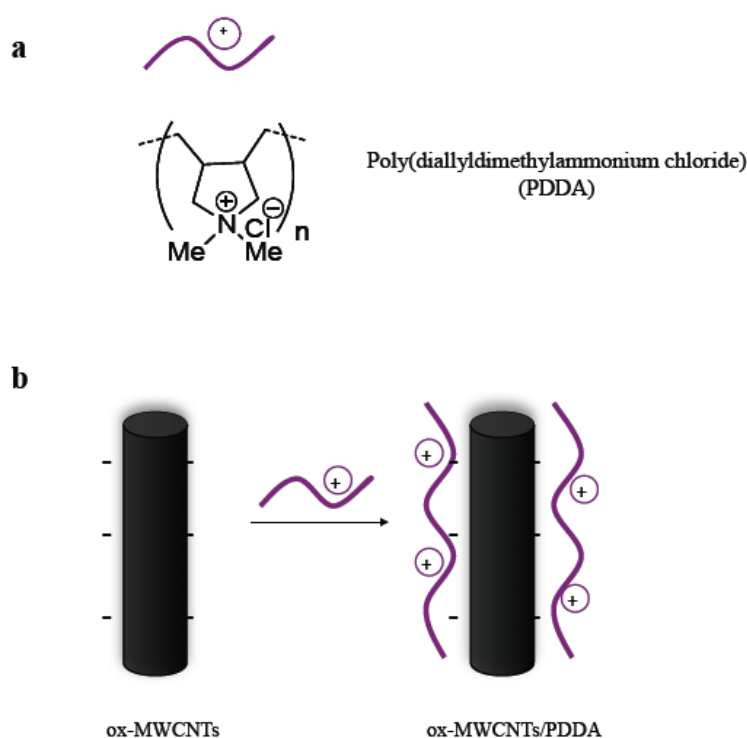
Figure 42. PDDA structure (a) and schematic deposition on ox-MWCNTs (b)

The possibility to obtain a positively charged surface is of crucial importance since tyrosinase globally has a negative charge at its operative pH. The evaluation of the amount of PDDA adsorbed on carbon nanotubes is very important, since partially modified MWCNTs aggregate through electrostatic attraction and precipitate.[84] The presence of a low polyelectrolyte concentration may also lead to bridge flocculation because the high molecular weight PDDA (200000-350000 g/mol) could adsorb as a single polymer on multiple carbon nanotubes.[281] In this regard Ziółkowska *et al.* recently reported a method for the determination of the PDDA concentration in aqueous solution based on the classical Bradford method. PDDA is infact able to stabilize the anionic form of the

Coomassie Brilliant Blue (CBB) dye, thus forming a complex that can be detected at 595 nm. The method involves the construction of a calibration curve by measuring absorbance values of PDDA-CBB complexes using a PDDA stock solution of known concentration.

We did not detect any residual PDDA after the first washing cycle and the amount of immobilized PDDA per mg of ox-MWCNTs was found to be 0.573 ± 0.094 mg, corresponding to an immobilization yield of $30 \pm 6\%$; the immobilization yield was defined as:

$$\text{Immobilization Yield} = (\text{mi PDDA}/\text{m0 PDDA}) * 100$$

$$\text{mi PDDA} = \text{polyelectrolyte contained in the wastewaters}$$

$$\text{m0 PDDA} = \text{polyelectrolyte initially added}$$

These results are in accordance with those reported by Iamsamai et al.,[86] which found 0.48 mg of PDDA per mg of carbon nanotubes to be the minimum quantity to afford a complete coverage of the nanotube's surface.

1.3.9 Electrostatic adsorption and chemical crosslinking

A bio-nanocatalyst was prepared modifying literature procedures which exploited the cross-linking ability of glutaraldheyde (GA), a compound that reacts with the protein lysine ε-amino groups under mild conditions. The extensive cross-linking of enzyme molecules [283] must be prevented and in this regard Broun [284] proposed an inert lysine rich protein to be used as a spacer, e.g. Bovine Serum Albumin (BSA). GA is able to improve the tyrosinase immobilization yield, preserving its shape11 and preventing its release.[285] The use of GA or the system BSA/GA to build tyrosinase biosensors based on carbon nanotubes is fairly widespread. [286, 287] Being both tyrosinase and BSA negatively charged at pH 7.0, our strategy consisted in the simultaneous adsorption of the two proteins on the ox-MWCNT/PDDA in PBS 0.1M pH 7.0, with the subsequent generation of a multi protein-layer *via* cross-linking with GA (Scheme 64). Proteins reticulation occurs because of the formation of Shiff bases between the reactive aldheyde groups and the Lysine's amino groups.

Proteins adsorption was afforded by means of orbital shaking (150 rpm, 40 min, r.t.) and the chemical cross-linking was subsequently performed (150rpm, 30 min, r.t. and then overnight at 4°C).Both of the systems exhibit similar performances, notwithstanding the BSA containing system permits to afford higher loading and immobilization yield values (70%), as well as higher activity

values. This result confirms the positive effects of the combined use of BSA and GA to tyrosinase immobilization.

1.3.10 Nuclear Magnetic Resonance (NMR) analysis

Nuclear magnetic resonance spectroscopy (NMR) analyses were made using a Bruker 200 MHz and Bruker 400 MHz instrument. NMR is a technique that exploits the magnetic properties of certain atominc nuclei to determine physical and chemical properties of atoms or the molecules in which they are contained. (Burton, S.G. *TRENDS* in Biotechnol 2003, 21(12), 543-549.) It relies on the phenomenon of nuclear magnetic resonance and can provide detailed information about the structure, dynamics, reaction state, and chemical environment of molecules. The NMR phenomenon is based on the fact that nuclei of atoms have magnetic properties that can be utilized to yield chemical information. The nuclei of many elemental isotopes have a characteristic spin (I). Some nuclei have integral spins (e.g. 2H, 14N; I=1), some have fractional spins (e.g. 1H, 13C, 15N, 19F, 31P; I= ½), and a few have no spin, I=0 (e.g. 12C,16O,32S).

In this case of study, the spectra of nuclear magnetic resonance of the proton (1H) and carbon (13C) were made with a spectrophotometer Varian 400 MHz using deuterated chloroform (CDCl3) as solvent. The values of "chemical shift" (chemical shifts) are expressed in parts per million (ppm).

1.3.11 General procedure of synthesis of Dopa peptidomimetics in homogeneous conditions

In all reaction we used the same procedure. In a 25 ml flask 20 mg of BTO (0,068 mmoli) were dissolved in mixture of EtOH/buffer phosphate pH 7 (7:3 ratio). To the solution were added 0,68 mmoli of different protected amino acid and Tyrosinase (600 UA), after this step we saw a colour change from colorless solution to yellow (typical characteristic of quinone compounds). The mixture of reaction was stirred for 24 h at 25°C under O_2 atmosphere. The reaction was monitored at regular intervals of time in Thin Layer Chromatography (TLC; Silica Gel 60 F254 Merck) in the mixture hexane / ethyl acetate (2:1) as eluent mixture. TLC were analyzed with iodine vapor and with $KMnO_4$ in order to make clearer the qualitative analysis of the reaction products. Following the absence of the limiting reagent (BTO) were added 2 equivalents of the reducing agent: sodium dithionite ($Na_2S_2O_4$). After 30 minutes, the mixture of reaction was transferred into a separating funnel and it was subjected to extraction in H_2O /AcOEt x3. Organic phases were were collected, washed with brine, anhydrified with sodium sulfate, filtered and concentrated under reduced pressure.

1.3.12 General procedure of synthesis of Dopa peptidomimetics in heterogeneous synthesis

In all reaction we used the same procedure, except for the condition in which we used Val-OMe or N-Boc-Val-OH as amino acid for the oxidative functionalization of the substrate. In these case we used higher amount of catalyst (MWCNT/Tyro). In a 25 ml flask 20 mg of BTO (0,05 mmoli) were dissolved in mixture of EtOH/buffer phosphate pH 7 (7:3 ratio). To the solution were added 0,50 mmoli of different protected amino acid and MWCNT/Tyro (600 UA), after this step we saw a colour change from colorless solution to yellow (typical characteristic of quinone compounds). The mixture of reaction was stirred for 24 h at 25°C under O_2 atmosphere. The reaction was monitored at regular intervals of time in Thin Layer Chromatography (TLC; Silica Gel 60 F254 Merck) in the mixture hexane / ethyl acetate (2:1) as eluent mixture. TLC were analyzed with iodine vapor and with $KMnO_4$ in order to make clearer the qualitative analysis of the reaction products. Following the absence of the limiting reagent (BTO) were added 2 equivalents of the reducing agent: sodium dithionite ($Na_2S_2O_4$). After 30 minutes, the mixture of reaction was transferred into a separating funnel and it was subjected to extraction in H_2O /AcOEt x3. Organic phases were were collected, washed with brine, anhydrified with sodium sulfate, filtered and concentrated under reduced pressure.

CHAPTER II

THE ROLE OF POLYPHENOLS IN ANTIVIRAL THERAPY

2.1. INTRODUCTION

2.1.0 Introduction to polyphenols

Almost all the people assume food every day, but many of them ignore the effects of food on health. The relationship between food and human health is not novel. About 2500 years ago, Hippocrates, universal recognized as father of modern medicine, conceptualized the use of appropriate foods for health and their therapeutic benefits.[1] In 1989, Dr. Stephen de Felice coined the term nutraceuticals, that derived from a fusion of the words "nutrition" and "pharmaceutical", as a food or a food product that provides medical benefits, including the prevention and treatment of diseases.[2] Currently, fruits and vegetables receive considerable interest because plant foods contain many bioactive compounds, such as vitamins and minerals. These physiologically active compounds, simply referred as phytochemicals (from the Greek word *phyto*, meaning plant), which provide benefits for humans, they protect plants from disease and damage and contribute to the plant's color aroma and flavor.[3] Epidemiological studies have consistently shown that a high dietary intake of fruits and vegetables, as well as whole grains, is strongly associated with reduced risk of developing chronic diseases, such as cancer and cardiovascular disease, which are the two major causes of death in most industrialized countries.[4] The exact classification of phytochemicals could have not been performed so far, because of the wide variety of them. In recent years phytochemicals are classified as primary or secondary constituents, depending on their role in plant metabolism. Primary constituents include the common sugars, amino acids, proteins, purines and pyrimidines of nucleic acids and chlorophylls. Secondary constituents are the remaining plant substances such as alkaloids, terpenes, flavonoids, lignans, plant steroids, curcumines, saponins, phenols. Was referred that phenols are the most numerous and structurally diverse plant phytoconstituents, 8000 phenolic derivatives have been reported and they are widely dispersed throughout the plant kingdom.[5,6] These natural compounds are found in fruits, nuts and vegetables as well as beverages, including green tea and red wine.[7] Phenols possess an aromatic ring with one or more hydroxyl groups. They are a class of chemical compounds that include phenols with high and low molecular weight. Despite this structural diversity, this group are often referred to as "polyphenols" and generally are categorized as phenolic acids, flavonoids, stilbenes, coumarins and tannins. They are secondary metabolites which are derived from pentose phosphate, shikimate, and phenylpropanoid pathways

in plants. Natural polyphenols play important roles in plant physiology. For example, they protect against herbivores, microbes or viruses. In addition, they act as signaling compounds to attract pollinating or seed dispersing animals; they protect the plant from ultraviolet radiations and oxidative substances.[8,9]

2.1.1 Biological activities of polyphenols

Along with many other secondary compounds of plant origin, polyphenols are of great importance to humans and this concept it is a very old heritage, furthermore in ancient times secondary metabolites were used as poisons and hallucinogens but they actually have a pharmacological. They learned to use plants in folk medicine and today we have bearing medicinal herbs that are used as drugs in medicine.[10] The healthy related properties of polyphenols are believed are due to their antioxidant activity as scavengers of free radicals.[11,12] In chemistry, a radical is an atom, molecule, or ion that has unpaired valence electrons. Inside the cells, the primary target of radicals are proteins, lipids, DNA and RNA, where these unpaired electrons produce oxidative damage of DNA, proteins and lipids

This damage they accumulate with age and contributes to degeneration of somatic cells and to the pathogenesis of several diseases. Many researchers have shown that lipid peroxides and reactive oxygen species are involved in a wide range of illness including cancer, atherosclerosis, heart disease and kidney damage and also in neurodegenerative disorders.[13,14] Antioxidants limit this damage by acting directly on reactive oxygen species or by stimulating endogenous protective systems. Polyphenols can accept an electron to form relatively stable phenoxyl radicals thereby decrease the oxidative stress in cellular compartments.[15] Polyphenols with catecholic moiety (aromatic rings with two vicinal hydroxyl group) have enhanced radical scavenger activity than those with a simple phenolic group (aromatic ring with a single hydroxyl group)[16,17]. For this reason, natural phenols are definitively recognized as substances for innovative therapeutic strategies. Polyphenols, in the cell, are subject to oxidative metabolism by cytochrome p-450 dependent enzymes that catalyze many hydroxylation reactions; this family plays an important role in biosynthesis of phenolic compounds.[18,19] These metabolic pathways produce highly oxidized phenols by insertion of oxygen atoms on the most activated positions of the molecule, that are the benzyl and aryl positions. This products, comprising benzoquinones, hydroquinones, cathecols and quinone methide derivatives, are capable to modify the value intracellular redox potential or to

irreversibly bind proteins and nucleic acids, thus tuning the biological activity of the parent compound.[20] In fact, these derivatives (with cathecolic, pyrogallolic moiety) are characterized by peculiar antitumoral, antioxidant and antiviral activities and show different chemical properties toward nucleophilic and electrophilic active sites in the cell. This behavior is dependent on the specific value of the redox potential in the cell. These antioxidant compounds are difficult to isolate due to the low concentration of these metabolites in nature, and the difficulty to recover them from mammalian cells or fluids. Among them, require novel procedures for their synthesis in order to afford adequate amounts of compounds for biological assays. On the other hand, only few attentions has been devoted to develop novel oxidative procedures for the synthesis of highly oxidized polyphenols characterized by higher biological activity.[21]

Viral infections are difficult to fight for several reasons. To begin, viruses are made up of only a few structural components which they share with cells and furthermore diseases caused by viral infections are causative agents for several fatal epidemics which have a social impact related to unexpected illnesses and deaths. Recent emergence of newer pandemics for example H1N1 influenza, Ebola, and Zika virus are also a major threat to public health.[22,23] All these emerging viruses have more or less RNA genomes and as a result are capable of rapid mutation and resistance to the clinically available antiviral drugs. The increase of resistance form poses major challenges in clinical management of these viral infections.[24] Viral particles are equipped with powerful tools to aid their invasion into cells and shrewd plans for the corruption of the cellular metabolism. The great similarity between the building blocks of viruses and those of biological cells renders the development of antiviral drugs most difficult, because many antiviral drugs may be more dangerous to the patient than to the pathogen. Further difficulty to fighting viral infections is the high mutability of the genomes, which can lead to new more aggressive forms of viruses and then some pharmacological resistance to traditional antiviral drugs. These issues have led researchers to design new antiviral drugs. In this context polyphenols have been described to possess promising antiviral activity, especially flavonoids are the most studied polyphenols for their properties.[21] Flavonoids appeared to have played a major role in the successful medical treatments in the ancient times, and their use was persevered up to now. Some flavonoids work on the intracellular replication of viruses, whereas others inhibit the infectious properties of the viruses.[25] For example, some flavonoids work on the intracellular replication of viruses, whereas others inhibit the infectious properties of the viruses. Among these natural products, baicalin is a flavonoid obtained from *Scutellaria baicalensis* which is one of the seven plants constituting *Sho-saiko-to* (SST), that is a traditional Chinese and Japanese herbal supplement, believed to enhance liver health, [26] and in

recent years was discovered that this medicinal drug plays a role in HIV replication, especially in peripheral blood mononuclear cells (PBMC).[27] Many natural products can block various stages of the replication cycle of the virus. The discovery and development of flavonoids as anti-HIV agents has expanded in the past two decades. Most of these studies focused on the inhibitory activity of reverse transcriptase, or RNA-directed DNA polymerase.[28,29]

Currently has been identified that polyphenols play an important role like antiviral agents because these compounds are able to monitoring intracellular redox.[21] The antiviral activity of polyphenols is connected to their antioxidant property, this evidence was reported also by Sokmen and coworkers that discovered a polyphenolic extract from the medicinal plant "*Geranium sanguineum*" which characterized by strong anti-influenza activity possess antioxidant and radical scavenging properties.[30] Based on these observations, some authors some authors work for understanding the relationship between viral infection and intracellular redox.[21]

2.1.2 Intracellular redox

A large number of viruses cause an oxidative stress, could play an important role in modulating the activity of several signaling pathways. Many findings have demonstrated that an alteration of the intracellular redox characterizes several viral infections and the progression of viral-induced diseases.[31] Nonetheless, in certain cases, there is reasonable evidence that intracellular oxidative stress is essential for the first phase of virus replication.[30] Moreover, an alteration of intracellular redox state has been described as a characteristic of viral infections that can be caused by several factors, among which the decrease in antioxidant defenses,[31,32] such as intracellular glutathione[33,34] and the increase in reactive oxygen species (ROS) production.[35,36] Furthermore according to researchers, ROS and reactive nitrogen species (RNS) contribute to the development of influenza virus.[37,38] Physiological levels of ROS play a key role in mediating cell signaling, while high levels of ROS can lead to oxidative damage to cellular components and activate several cell death pathways.[39] Antioxidant are synthesized in vivo and others derived from the diet,[40] these radical scavenger activities form part of an ''antioxidant defense network" is not to remove all ROS, but to control their levels so as to allow useful functions whilst minimizing oxidative damage.[41] For this reason, antioxidants represent an interesting class of molecules that have been proposed for the antiviral treatment. In the event of a decrease of endogenous defence against free radical, it would be reasonable to increase radical scavenger activity of the cell using exogenous compounds derived from the diet. Natural antioxidants present in fruit and vegetables, including polyphenols, are currently considered to be beneficial for viral infections.[42] To control ROS attack, the cells is

equipped with a safeguard system which includes enzymes such as superoxide dismutase, catalase, glutathione peroxidase, and glutathione reductase; and some endogenous molecules: high molecular-weight antioxidants such as albumin, ceruloplasmin, and ferritin; and an array of low molecular weight antioxidants such as ascorbic acid, α-tocopherol, β-carotene, glutathione (GSH), and uric acid. Inside the cells a right levels of reactive species and antioxidants is essential because when ROS overcome the antioxidants, occurs oxidative stress that is dangerous for the cell survival.

2.1.3 Influenza A Virus

Influenza, commonly known as the "flu", is an acute viral infection that affects the upper respiratory tract and sometimes infects the lungs, and which is transmitted from person to person.

Influenza comes from the Latin word influentia, meaning "influence of the stars". In ancient times people didn't know that flu is caused by a viral infection but they thought that the stars influenced the spread of influenza. The name of this illness in fact, reflects that belief. In the early 1930s Richard Shope isolated influenza virus from infected pigs and from humans. This revolutionary discovery has proved that a virus, not a bacterium, as widely believed, caused influenza.[54] Influenza viruses continue to represent a severe threat worldwide that have substantial economic impact due to the costs of prevention and treatment, work absenteeism, physician visits and excess hospitalizations.[47]

These annual epidemics are estimated to result about 3 to 5 million cases of severe illness and about 250000 to 500000 deaths.[55]

Influenza viruses belonging to the Orthomyxoviridae family, are enveloped viruses and are characterized by a segmented single-stranded RNA genome. There are four types of influenza viruses: A, B, C and D. Human influenza A and B viruses cause seasonal epidemics of disease almost every winter. Influenza type C infections generally cause a mild respiratory illness and are not thought to cause epidemics. Influenza D viruses primarily affect cattle and are not known to infect or cause illness in people. Influenza A viruses are divided into subtypes based on two proteins on the surface of the virus: the hemagglutinin (HA) and the neuraminidase (N). There are 18 different hemagglutinin subtypes and 11 different neuraminidase subtypes. (H1 through H18 and N1 through N11 respectively).[56] A characteristic that distinguishes the influenza A viruses from influenza B and C, is their capability of infecting a wide variety of avian species, humans, and several mammals, including swine, horses, cats and dogs.[57]

The genomes of influenza viruses are changeable due to point mutations and recombination events that contribute to the evolution of new variants and strains with epidemic or pandemic potential, as the recent global pandemic caused by the origin swine influenza A/H1N1 virus in 2009, a viral subtype that has led to 18000 deaths. Influenza viruses cause annual epidemics and occasional pandemics that have claimed the lives of millions. The emergence of new strains will continue to pose challenges to public health and the scientific communities.[58] Influenza A viruses have a complex structure and possess a lipid membrane (envelope) derived from the host cell. Inside this envelope there are eight segments of single-stranded negative sense RNA that conventionally, are defined from largest to smallest.[59] Every segment encode for 16 proteins, some of them protein are most important for the virus life-cycle. [60] This gene products are subdivided into early proteins or late proteins in function of the infection phase. Three segments encode proteins that form the virus polymerase complex: basic polymerase 2 (PB2) which controls the recognition of host-cell RNA; basic polymerase 1 (PB1), which catalyses nucleotide addition (and which also encodes a small proapoptotic mitochondrial protein that is translated in a different reading frame PB1-F2); and the acid protein (PA), which might possess a transcriptase protease activity.[59] This three polymerases associated with the nucleoprotein (NP) form helical ribonucleoprotein capsids (vRNPs). After infection, the vRNPS are transported to the host cell nucleus, where they undergo transcription and replication.[61] Haemagglutinin and neuraminidase are the two major viral envelope glycoproteins, there are late gene products. The matrix (M1), transmembrane (M2) and second non-structural (NS2) proteins are also transcribed by late genes.[57]

The life cycle of influenza A viruses is similar irrespective of strain   shown in **fig. 2**.[58] The replication of virus starts by a binding between sialic acid galactose link to a cell surface glycoprotein or glycolipid and haemagglutinin on the virus. The virion is taken up in an endocytic vesicle, where acidification activates cellular proteases that cleave haemagglutinin, leading to the release of a fusion peptide and a conformational change that bring viral and endosomal membranes together. Acidification also produces a flow of protons through the M2 ion channel into the interior of the virion, causing the RNPs to dissociate from the M1 matrix and be released into the cytoplasm. After that, they are transported to the nucleus, where a viral polymerase complex performs transcription and replication. The resulting mRNAs move to the cytoplasm and are translated, producing new RNP protein components that are transported back to the nucleus to associate with nascent genome segments. The exit of new RNPs from the nucleus is aided by the viral NS2 (nuclear export protein, NEP). Meanwhile, nascent HA, NA and M2 molecules pass through the Golgi apparatus and undergo glycosylation before moving to the cell membrane. Virion

assembly occurs as RNPs and M1 proteins associate with cytoplasmic tails of HA and NA. Successful release of new virus particles requires that NA cleave sialic acid from galactose on the cell surface or on adjacent virions to prevent HA binding.[62]
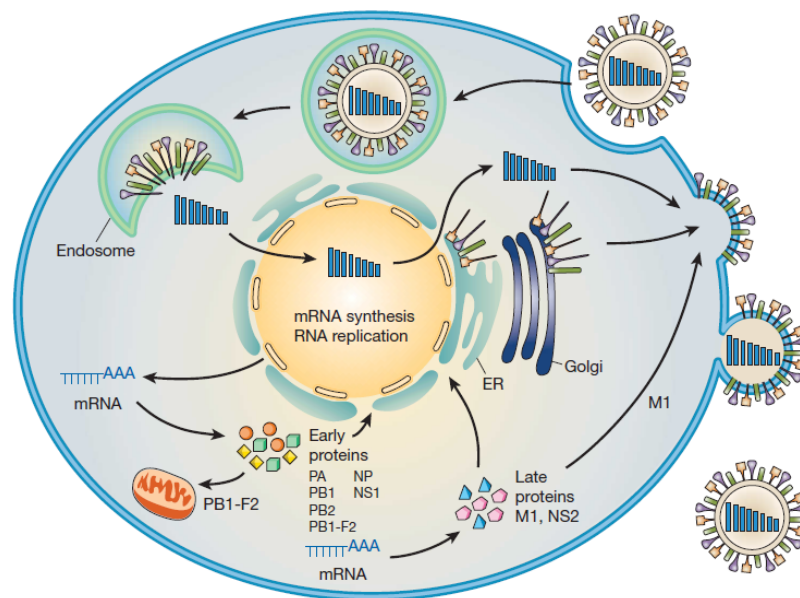
Figure 43 : Schematic representation of the influenza A virus replication cycle.[58]

2.1.4 Current therapies against influenza viruses

Currently, two options are available to fight influenza: vaccination and antiviral drug. For treating and prevent influenza is given a vaccination with an inactivated trivalent influenza vaccine containing two influenza A variants and one influenza B variant. During any influenza season, antigenic drift in the virus may occur after formulation of the year's vaccine has taken place, rendering the vaccine less protective, and outbreaks can more easily occur among high risk populations. In the course of a pandemic, vaccine supplies would be inadequate. Vaccine production by current methods cannot be carried out with the speed required to halt the progress of a new strain of influenza virus; therefore, it is likely that vaccine would not be available for the first wave of spread of virus.[63] Antiviral agents thus form an important part of a rational approach to epidemic influenza and are critical to planning for a pandemic. Due to limitations of this preventive vaccine form, the use of antiviral drugs is essential. There are two major classes of anti-influenza drugs that include the adamantanes, which target the M2 protein and neuraminidase inhibitors. [64]

2.1.5 Influenza virus and oxidative stress

The traditional antiviral strategies, analyzed above, have been developed against influenza virus to intercede with specific events in the replication cycle. Unfortunately, the emergence of strains resistant to antiviral agents, underlines the need for drugs that act on new molecular targets, for that purpose the new drugs should provide an effective protection against all influenza viruses.[73]

The new antiviral strategy must be valid whatever the origin of the virus. Some research show that intracellular signaling pathways are activated during influenza virus infection and play a role in the progression of virus life cycle. Among these several pathways, including phosphatidylinositol 3-kinase (PI3K)/Akt, protein kinase C (PKC) and mitogen activated protein kinase (MAPK), are involved in viral RNP translocation from the nucleus to the cytoplasm. [74] In this context, the entry of influenza virus triggers intracellular cascades finely regulated by small changes of intracellular redox state, they can contribute to inhibit influenza virus replication.[47] Oxidative stress has been described as a characteristic of viral infections, for this reason antioxidants represent interesting molecules that have been proposed for the treatment of influenza. In addition, various plant products have been accredited with anti-influenza virus activity. It would be reasonable to increase antioxidant capacity of the cell using exogenous compounds derived from the diet, thus enhancing cell defenses against the free radical formation. Natural antioxidants present in fruit and vegetables, including vitamins C and E, carotenoids and polyphenols, are currently considered to be beneficial. [64] Among polyphenols, resveratrol is a stilbene-like phytoalexin present in more than 72 plant species, among which grape skin and other fruits, with high antioxidant activity.[75] It plays a relevant role in several diseases including viral infections. Resveratrol can inhibit replication of influenza A virus without significant toxicity. Another class of polyphenols are flavonoid especially catechins, like epigallocatechin gallate (EGCG) and epicatechin gallate (ECG) were the most active catechins against different influenza subtypes.[76] Hydroxytyrosol, one of the major phenolic compounds present in olive fruits and in the oil mill wastewaters, [77] exerts various bioactivities including antiviral activities specially against human immunodeficiency virus in an effort to evaluate the possibility that hydroxytyrosol might be a useful agent against other viruses Yamada et al. reported that this compound inhibits different influenza A viruses.[78] These compounds (shown in **Fig. 5**) they share catecholic and pyrogallolic moieties are associated with an increased activity against influenza A viruses.[47]
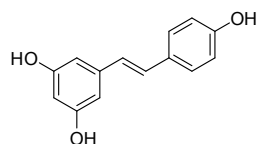
Resveratrol
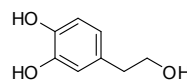
Hydroxytyrosol
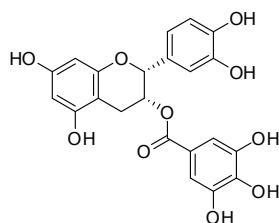
(-) Epicatechin gallate
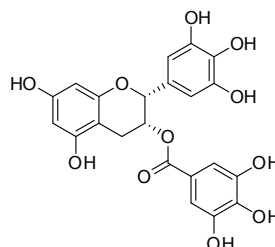
(-) Epigallocatechin gallate

Figure 44. Most active anti-influenza compounds.

2.1.6. Coumarins

Coumarins are a heterogeneous group of phenolic substances found throughout the plant kingdom. [79,80,81] The prototypical compound is coumarin itself which could be considered like the resulting fusion of benzene and 2-pyrone ring shown in **fig. 6**. Their name derives from *Coumarouna odorata*, a leguminosa of South America from which coumarin was extracted for the first time in 1820.[82]
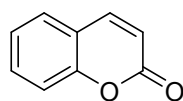
Coumarin
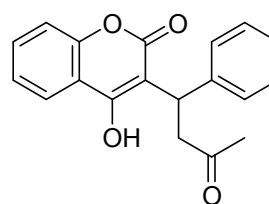
Warfarin

Figure 45, Coumarin and warfarin structure.

Coumarins are found at high level in some essential oils, but they are also found in fruits, green tea and other food such as chicory.[83] More than 300 coumarins have been identified from natural sources, there are four main coumarin sub-types: the simple coumarins, furanocoumarins, pyranocoumarins and the pyrone-substituted coumarins The simple coumarins are hydroxylated and alkylated derivatives of the parent compound, coumarin, along with their glycosides. Coumarins are oxygenated at C-7 and less frequently at C-5,C-6 and C-8. The oxygenation patterns mentioned

above are typical for benzenoid rings of C6-C3 units derived from shikimic acid pathway.[84] The interest in the field of coumarins started at the beginning of 1900 when it was discovered by any chance, Warfarin, that is the most widely used anticoagulant in the world (Figure 45).

The story of Warfarin leads us from a mysterious hemorrhagic disease of cattle to the development of a rat poison which became one of the most commonly prescribed drugs in history.[85]

Beyond that, the commercial interests of coumarins comprises a wide range of applications, such as a fixative and enhancing agent in perfumes and is added to toilet soap and detergents, toothpaste, tobacco products and some alcoholic beverages.[86]

2.1.6.1. Biosynthesis of coumarins in plants

Coumarin biosynthesis pathway has been largely outlined during the '60s and '70s, with the help of tracer feeding experiments.[87]. Coumarins are especially abundant in *Umbelliferae* and *Rutaceae* families where it is demonstrated the existence of this compound.[88] Other tracer experiments conducted with *Lavandula officinalis*, a plant that produces coumarin such as 7-hydroxylated coumarins, revealed that in the latter instance para-hydroxylation preceded the ortho-hydroxylation required for lactonization.[89] This indicated that umbelliferon is derived from cis-p-coumaric acid, whereas coumarin originates from 2,4-dihydroxy-cis-cinnamic acid, and may imply different enzymes for the orthohydroxylation and lactonization of coumarin versus umbelliferone.[90] The conversion of cinnamic acid to cis-p-coumaric acid is catalyzed by cinnamate 4-hydroxylase, a cytochrome P450 monooxygenase from the CYP73A family.[91] This enzyme constitutes the P450 enzyme most studied to date and sets the stage for several branch pathways, such as the lignification,[92] or flavonoid biosynthesis.[93] Following the pertaining literature, cis-p-coumaric acid is ortho-hydroxylated to 2,4-dihydroxy-cis-cinnamic acid. The formation of esculetin was examined in *Cichorium intybus*.[94] These studies revealed that umbelliferone was an efficient precursor; additionally in this step is important the *ortho*-hydroxylation in position 6 of umbelliferone, probably by the action of a P450 monooxygenase. Similar to esculetin, daphnetin in *Daphne mezereum*, was shown to be derived from umbelliferone.

The recent detection of coumarin and hydroxylated coumarins in *Arabidopsis thaliana* have opened the way for new approaches. In this context Munoz and coworkers have identified in *Arabidopsis thaliana* which not only cytochrome p450 enzymes catalyze the reaction from umbelliferon to esculetin, but minimally also other enzymes play a role in this reaction, for example, polyphenol oxidase (PPO) family such as tyrosinase.[95]

2.1.6.2. Coumarin as radical scavenger

Food and Drug Administration in 1952 banned coumarins from the market but since then a lot has changed.[96] Over the last 50 years coumarin compounds have been widely used as anti-coagulant, anti-microbial and anti-inflammatory agents supported by different clinical studies. Currently have diverse biological properties and various effects on the different cellular systems.[97]

Coumarins have important effects in plant biochemistry and physiology, acting as antioxidants, enzyme inhibitors and precursors of toxic substances. In addition, these compounds are involved in the actions of plant growth hormones and growth regulators, the control of respiration, photosynthesis, as well as defense against infection.[98]

A broad array of medicinal applications of coumarins has been investigated, and several recent reviews summarize advances in these fields, especially concerning their antioxidant properties.[99] In this context, they are analyzed the hydroxycoumarins that are typical phenolic compounds, therefore, act as potent metal chelators and free radical scavengers. Recently there has been a great intent in searching for the compounds with antioxidant activity.[100]

There are many methods to evaluate antioxidant activity of potential antioxidants.[102]One of the widely used detection procedures, which facilitates analysis of various antioxidants, is based on 2,2'-diphenyl-1-picrylhydrazyl radical (DPPH) bleaching.[103] DPPH is characterized as a stable free radical by virtue of the delocalization of the spare electron, as would be the case with most other free radicals. The delocalization also gives rise to the deep violet color, characterized by an absorption band in ethanol solution centered at about 520 nm. For each antioxidant concentration tested, the kinetic of the reaction was analyzed calculating the rate of DPPH remaining at the steady state and the values transferred onto a software that using a nonlinear regression curve. Antiradical activity was defined as the amount of antioxidant necessary to decrease the initial DPPH concentration by 50%. This value is called EC_{50} (defined as the concentration of substrate that causes 50% loss of DPPH activity). The lower is the value of EC_{50}, the higher the antioxidant activity. Which is currently used in the interpretation of experimental data from the method.[104]

Some authors as Rehanova and coworkers evaluated the antioxidant activity of coumarins with DPPH test.[100] In this assay the authors for comparing the results of DPPH radical scavenging activity use as a controls three compound which have a known antioxidant activity such as ascorbic acid, trolox and catechin shown in figure 46.
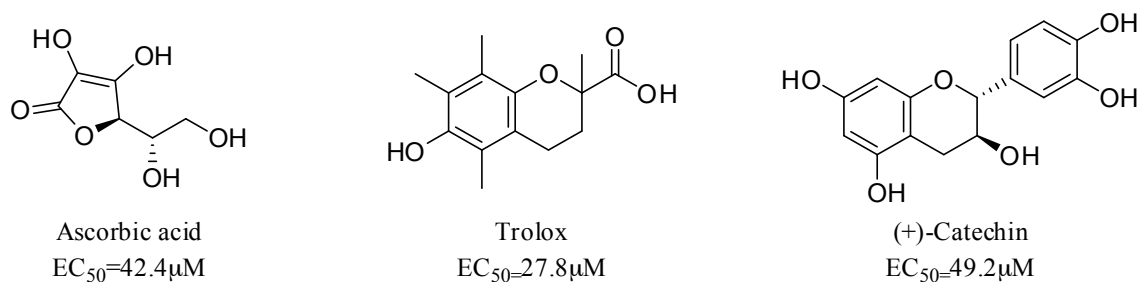
Figure 46. Controls for DPPH assay.

With DPPH assay was demonstrated by the authors that monohydroxycoumarins such as 4-hydroxycoumarin and hymecromone did not show significant antioxidant activity; results of EC_{50} and related compound are shown in **Fig.47** (**1-2**). On the other hand, 7,8-dihydroxy-4-methylcoumarin (**3**) possess excellent radical scavenging activity.[96]
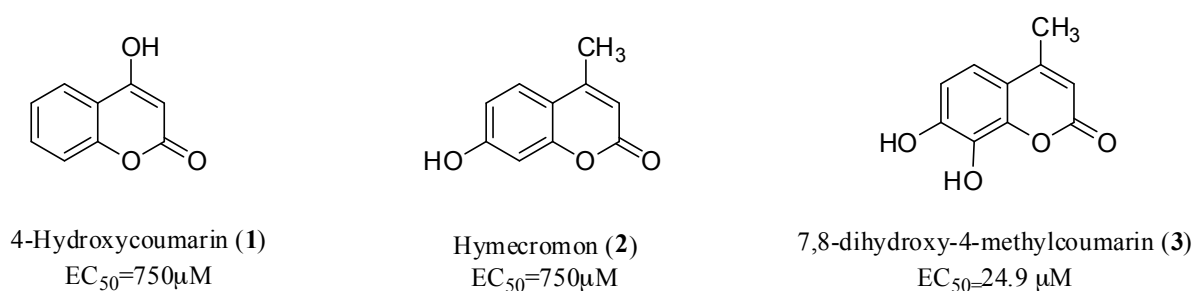
Figure 47. Some of coumarins tested for radical scavenging activity and results of DPPH assay expressed with EC_{50} parameter.

Their EC_{50} values are comparable with that of trolox and two times lower than that of (+)-catechin. These results confirmed the importance of the *ortho*-position of hydroxyl groups to each other reach maximal radical scavenging activity. The DPPH scavenging activity of some coumarins in another study conducted in 2015, is comparable with the analysis conducted by Rehakova et al., it was found that our results are in good agreement with those of the authors mentioned above. This finding is in accordance with our results since coumarins without hydroxyl groups were ineffective or they exhibited very low antioxidant activity.[105] Data showed that the antioxidant activity was present only with the catechol function. Based on these researches, the new anti-influenza A drugs with a relationship between radical scavenger activities related at antiviral therapy has been focused on the synthesis of new antiviral compound with enhanced antioxidant activity and that possess catecholic and pyrogalolic pharmacophores.

2.1.6.3. Bioactivity of hydroxycoumarins

Coumarins are a large class of phenolic secondary metabolites found in plants, bacteria, and fungi characterized by condensed benzene and α-pyrone rings (2H-1-benzopyran-2-one)[106]. Coumarins show several pharmacological activities such as anticoagulant[107], antineurodegenerative[108], anticancer[109] and antimicrobial activities[110]. Coumarins are also active against a large panel of viruses, including human immunodeficiency virus type 1 (HIV-1)[111], hepatitis C virus (HCV)[112], bovine viral diarrhoea virus(BVDV)[113] and herpes simplex virus[114]

Coumarins are quite similar to well recognized antioxidants flavonoids and have been studied extensively for their antioxidant properties.[115] The polyphenolic derivatives with the catechol (ortho-diphenol, 1,2-dihydroxybenzene) pharmacophore (esculetin and 4-methyl esculetin) being the most efficient compounds in the decrease of lipid peroxidation[116] , in the protection of human cells from hydrogen peroxide-induced oxidative damage[117], and in the radical scavenging activity of DPPH and galvinoxyl radicals[118] The antioxidant activity of catechols is associated to their high capacity of transferring single-electron and hydrogen-atom to reactive radicals[119], as well as to binding pro-oxidant species[120]

2.1.6.4 Antioxidant activity of catechol and pyrogallol derivatives

In the last years several examples of that natural and synthetic antioxidant compounds bearing the catechol moiety, active against different DNA and RNA viruses[121], including the influenza A virus[122] ,were reported. In particular, resveratrol analogues inhibited influenza A replication by impairing vRNP traffic, partially restoring the virus-induced GSH depletion[123]. In a similar way, the reduced form of tocopherylquinones (analogues of vitamin E) are active against influenza A virus by regulation of the internal redox potential of the cells[124]. Only one example of inhibition of influenza A virus by coumarins is reported, in which case oligomeric spirodienone–sesquiterpene derivatives from *Toddalia asiatica*, deprived of free hydroxyl moieties, were analyzed[125]

Novel pyrogallol compounds isolated from E. cava, PPB, displayed different degrees of potency in its radical scavenging and protective effects against H_2O_2-induced damage in Vero cells moreover the high antioxidant activity of natural compounds containing the pyrogallol moiety is largely reviewed[126]

2.1.7. Other viruses related to ROS:

2.1.7.1 Poliovirus

Poliovirus, the causative agent of poliomyelitis (commonly known as polio), is a human enterovirus and member of the family of *Picornaviridae*.[127]

Poliovirus is composed of an RNA genome and a protein capsid. The genome is a single-stranded positive-sense RNA genome that is about 7500 nucleotides long.[128] The viral particle is about 30 nm in diameter with icosahedral symmetry. Because of its short genome and its simple composition—only RNA and a nonenveloped icosahedral protein coat that encapsulates it, poliovirus is widely regarded as the simplest significant virus.[129]

Poliovirus was first isolated in 1909 by Karl Landsteiner and Erwin Popper.[130] In 1981, the poliovirus genome was published by two different teams of researchers: by Vincent Racaniello and David Baltimore at MIT[131] and by Naomi Kitamura and Eckard Wimmer at Stony Brook University. [132] Poliovirus is one of the most well-characterized viruses, and has become a useful model system for understanding the biology of RNA viruses. Poliovirus infects human cells by binding to an immunoglobulin-like receptor, CD155, (also known as the poliovirus receptor (PVR))[133,134] on the cell surface.[135] Interaction of poliovirus and CD155 facilitates an irreversible conformational change of the viral particle necessary for viral entry.[136,137] Attached to the host cell membrane, entry of the viral nucleic acid was thought to occur one of two ways: via the formation of a pore in the plasma membrane through which the RNA is then "injected" into the host cell cytoplasm, or that the virus is taken up by receptor-mediated endocytosis.[138] Recent experimental evidence supports the latter hypothesis and suggests that poliovirus binds to CD155 and is taken up by endocytosis. Immediately after internalization of the particle, the viral RNA is released.[139]

Poliovirus is a positive-stranded RNA virus. Thus, the genome enclosed within the viral particle can be used as messenger RNA and immediately translated by the host cell. On entry, the virus hijacks the cell's translation machinery, causing inhibition of cellular protein synthesis in favor of virus–specific protein production.[140] Unlike the host cell's mRNAs, the 5' end of poliovirus RNA is extremely long—over 700 nucleotides—and highly structured. This region of the viral genome is called internal ribosome entry site (IRES), and it directs translation of the viral RNA. Genetic mutations in this region prevent viral protein production.[141,142,143] The first IRES to be discovered was found in poliovirus RNA.[144]

Poliovirus mRNA is translated as one long polypeptide. This polypeptide is then autocleaved by internal proteases into about 10 individual viral proteins. Not all cleavages occur with the same

efficiency. Therefore, the amounts of proteins produced by the polypeptide cleavage vary: for example, smaller amounts of 3D^{pol} are produced than those of capsid proteins, VP1-4.[145,146]

For the infecting (+) RNA to be replicated, multiple copies of (−) RNA must be transcribed and then used as templates for (+) RNA synthesis. Replicative intermediates (RIs) which are an association of RNA molecules consisting of a template RNA and several growing RNAs of varying length, are seen in both the replication complexes for (−) RNAs and (+) RNAs. The primer for both (+) and (−) strand synthesis is the small protein VPg, which is uridylylated at the hydroxyl group of a tyrosine residue by the poliovirus RNA polymerase at a cis-acting replication element located in a stem-loop in the virus genome. Some of the (+) RNA molecules are used as templates for further (−) RNA synthesis, some function as mRNA, and some are destined to be the genomes of progeny virions.[25] In the assembly of new virus particles (i.e. the packaging of progeny genome into a procapsid which can survive outside the host cell), including, respectively:[147]

- Five copies each of VP0, VP3, and VP1 which its N termini and VP4 form interior surface of capsid, assemble into a 'pentamer' and 12 pentamers form a procapsid. (The outer surface of capsid is consisting of VP1, VP2, VP3; C termini of VP1 and VP3 form the canyons which around each of the vertices; around this time, the 60 copies of VP0 are cleaved into VP4 and VP2.)
- Each procapsid acquires a copy of the virus genome, with VPg still attached at the 5' end.

Fully assembled poliovirus leaves the confines of its host cell by lysis[148]4 to 6 hours following initiation of infection in cultured mammalian cells.[149] The mechanism of viral release from the cell is unclear,[3] but each dying cell can release up to 10,000 polio virions.[150]

Drake demonstrated that poliovirus is able to undergo multiplicity reactivation.[151] That is, when polioviruses were irradiated with UV light and allowed to undergo multiple infections of host cells, viable progeny could be formed even at UV doses that inactivated the virus in single infections.

2.1.7.2 Echoviruses

The first isolation of echoviruses occurred from the faeces of asymptomatic children early in the 1950s, just after cell culturing had been developed. The *echo–* part of the name was originally an acronym for "enteric cytopathic human orphan" virus: *Orphan virus* means a virus that is not associated with any known disease. Even though Echoviruses have since been identified with various diseases, the original name is still used.[152] Echovirus is highly infectious, and its primary target is children. The echovirus is among the leading causes of acute febrile illness in infants and young children, and is the most common cause of aseptic meningitis. Infection of an infant with this

virus following birth may cause severe systemic diseases, and is associated with high <u>infant mortality</u> rates. The echovirus can mimic symptoms caused by other common bacterial and viral infections.An echovirus measures 24-30 nanometres (nm), and is similar to other viruses, since it has a naked protein capsid, which makes up 75% of the virus particle that encloses a dense central core of single-stranded RNA. This RNA has a length of approximately 7.5 kilobase (kb), contains an RNA replicase, viral-coded proteins, and a single polyprotein that is responsible for the formation of structural proteins and other proteins necessary for cellular replication. The structural proteins determine host range and play a very important role in delivering the RNA genome into the cytoplasm of new host cells.

Some viral replication of an echovirus occurs in the nasopharynx after infection and then spreads to regional lymph nodes. However, most viral particles are swallowed and they reach the lower gut tract, where the virus is presumed to bind to specific receptors. The virus then spreads to the lower intestinal tract, replicating but not causing any major cellular effects along the way. Next, the virus spreads to many secondary sites in the body such as the central nervous system, liver, spleen, bone marrow, heart and finally the lungs. Additional replication of the virus will occur, causing symptoms 4 to 6 days after infection. The most deadly part however is delayed when symptoms of a central nervous system disease start to appear. Enteroviruses are capable of infecting any cell in the body. These viruses are highly infectious. They can spread through the air to other hosts 1–3 weeks after infection and can spread through feces to other hosts eight weeks after infection.[152]

2.1.7.3. Herpes simplex virus

Herpes simplex virus 1 and 2 (HSV-1 and HSV-2), also known as human herpesvirus 1 and 2 (HHV-1 and HHV-2), are two members of the herpesvirus family, Herpesviridae, that infect humans.[153] Both HSV-1 (which produces most cold sores) and HSV-2 (which produces most genital herpes) are ubiquitous and contagious. They can be spread when an infected person is producing and shedding the virus.

In simple terms, herpes simplex 1 is most commonly known as a "cold sore," while herpes simplex 2 is the one known by the public as "herpes," or "genital herpes." Herpes simplex 1 is known to infect about 95% of the human populace, and is treated less seriously than herpes simplex 2, even though both are incurable.

Symptoms of herpes simplex virus infection include watery blisters in the skin or mucous membranes of the mouth, lips, nose or genitals.[153] Lesions heal with a scab characteristic of herpetic

disease. Sometimes, the viruses cause very mild or atypical symptoms during outbreaks. However, they can also cause more troublesome forms of herpes simplex. As neurotropic and neuroinvasive viruses, HSV-1 and -2 persist in the body by becoming *latent* and hiding from the immune system in the cell bodies of neurons. After the initial or *primary* infection, some infected people experience sporadic episodes of viral *reactivation* or *outbreaks*. In an outbreak, the virus in a nerve cell becomes active and is transported via the neuron's axon to the skin, where virus replication and shedding occur and cause new sores.[154] It is one of the most common sexually transmitted infectionsEntry of HSV into a host cell involves several glycoproteins on the surface of the enveloped virus binding to their transmembrane receptors on the cell surface. Many of these receptors are then pulled inwards by the cell, which is thought to open a ring of three gHgL heterodimers stabilizing a compact conformation of the gB glycoprotein, so that it springs out and punctures the cell membrane.[155] The envelope covering the virus particle then fuses with the cell membrane, creating a pore through which the contents of the viral envelope enters the host cell.

The sequential stages of HSV entry are analogous to those of other viruses. At first, complementary receptors on the virus and the cell surface bring the viral and cell membranes into proximity. Interactions of these molecules then form a stable entry pore through which the viral envelope contents are introduced to the host cell. The virus can also be endocytosed after binding to the receptors, and the fusion could occur at the endosome. In electron micrographs the outer leaflets of the viral and cellular lipid bilayers have been seen merged together;[156] this *hemifusion* may be on the usual path to entry or it may usually be an arrested state more likely to be captured than a transient entry mechanism.

In the case of a herpes virus, initial interactions occur when two viral envelope glycoprotein called glycoprotein C (gC) and glycoprotein B (gB) bind to a cell surface particle called heparan sulfate. Next, the major receptor binding protein, glycoprotein D (gD), binds specifically to at least one of three known entry receptors.[157] These cell receptors include herpesvirus entry mediator (HVEM), nectin-1 and 3-O sulfated heparan sulfate. The nectin receptors usually produce cell-cell adhesion, so provide a strong point of attachment for the virus to the host cell.[155] These interactions bring the membrane surfaces into mutual proximity and allow for other glycoproteins embedded in the viral envelope to interact with other cell surface molecules. Once bound to the HVEM, gD changes its conformation and interacts with viral glycoproteins H (gH) and L (gL), which form a complex. The interaction of these membrane proteins may result in a hemifusion state. gB interaction with the gH/gL complex creates an entry pore for the viral capsid.[156] gB interacts with glycosaminoglycans on the surface of the host cell.

2.1.7.4. Coxsackievirus

Coxsackievirus is a virus that belongs to a family of nonenveloped, linear, positive-sense single-stranded RNA viruses, *Picornaviridae* and the genus *Enterovirus*, which also includes poliovirus and echovirus. Enteroviruses are among the most common and important human pathogens, and ordinarily its members are transmitted by the fecal-oral route. Coxsackieviruses share many characteristics with poliovirus. With control of poliovirus infections in much of the world, more attention has been focused on understanding the nonpolio enteroviruses such as coxsackievirus.The coxsackieviruses were discovered in 1948–49 by Dr. Gilbert Dalldorf, a scientist working at the New York State Department of Health in Albany, New York. Dalldorf, in collaboration with Grace Sickles,[157,158] had been searching for a cure for poliomyelitis. Earlier work Dalldorf had done in monkeys suggested that fluid collected from a nonpolio virus preparation could protect against the crippling effects of polio. Using newborn mice as a vehicle, Dalldorf attempted to isolate such protective viruses from the feces of polio patients. In carrying out these experiments, he discovered viruses that often mimicked mild or nonparalytic polio. The virus family he discovered was eventually given the name Coxsackie, from Coxsackie, New York, a small town on the Hudson River where Dalldorf had obtained the first fecal specimens.[6] Dalldorf also collaborated with Gifford on many early papers.[159,160,161,162]

The coxsackieviruses subsequently were found to cause a variety of infections, including epidemic pleurodynia (Bornholm disease), and were subdivided into groups A and B based on their pathology in newborn mice. (Coxsackie A virus causes paralysis and death of the mice, with extensive skeletal muscle necrosis; Coxsackie B causes less severe infection in the mice, but with damage to more organ systems, such as heart, brain, liver, pancreas, and skeletal muscles.)

The use of suckling mice was not Dalldorf's idea, but was brought to his attention in a paper written by Danish scientists Orskov and Andersen in 1947, who were using such mice to study a mouse virus. The discovery of the coxsackieviruses stimulated many virologists to use this system, and ultimately resulted in the isolation of a large number of so-called "enteric" viruses from the gastrointestinal tract that were unrelated to poliovirus, and some of which were oncogenic (cancer-causing).

The discovery of the coxsackieviruses yielded further evidence that viruses can sometimes interfere with each other's growth and replication within a host animal. Other researchers found this interference can be mediated by a substance produced by the host animal, a protein now known as

interferon. Interferon has since become prominent in the treatment of a variety of cancers and infectious diseases.

In 2007, an outbreak of coxsackievirus occurred in eastern China. It has been reported that 22 children died. More than 800 people were affected, with 200 children hospitalized.[163]

Cavatak, a wild-type Coxsackievirus A21, is being used in human clinical trials as an oncolytic virus.

2.1.7.5. Adenovirus

Adenoviruses represent the largest nonenveloped viruses. They are able to be transported through the endosome (i.e., envelope fusion is not necessary). The virion also has a unique "spike" or fiber associated with each penton base of the capsid (see picture below) that aids in attachment to the host cell via the receptor on the surface of the host cell. (See Replication Section below for discussion of diverse receptors.)

In 2010, scientists announced that they had solved the structure of the human adenovirus at the atomic level, making the largest high-resolution model ever. The virus is composed of around 1 million amino acid residues and weighs around 150 MDa.

Adenoviruses possess a linear dsDNA genome and are able to replicate in the nucleus of vertebrate cells using the host's replication machinery.

Entry of adenoviruses into the host cell involves two sets of interactions between the virus and the host cell. Most of the action occurs at the vertices. Entry into the host cell is initiated by the knob domain of the fiber protein binding to the cell receptor. The two currently established receptors are: CD46 for the group B human adenovirus serotypes and the coxsackievirus adenovirus receptor (CAR) for all other serotypes. There are some reports suggesting MHC molecules and sialic acid residues functioning in this capacity as well. This is followed by a secondary interaction, where a motif in the penton base protein interacts with an integrin molecule. It is the co-receptor interaction that stimulates entry of the adenovirus. This co-receptor molecule is αv integrin. Binding to αv integrin results in endocytosis of the virus particle via clathrin-coated pits. Attachment to αv integrin stimulates cell signaling and thus induces actin polymerization resulting in entry of the virion into the host cell within an endosome.[164]

Once the virus has successfully gained entry into the host cell, the endosome acidifies, which alters virus topology by causing capsid components to disband. These changes, as well as the toxic nature of the pentons, destroy the endosome, resulting in the movement of the virion into the cytoplasm.

With the help of cellular microtubules, the virus is transported to the nuclear pore complex, whereby the adenovirus particle disassembles. Viral DNA is subsequently released, which can enter the nucleus via the nuclear pore.After this the DNA associates with histone molecules. Thus, viral gene expression can occur and new virus particles can be generated.

The adenovirus life cycle is separated by the DNA replication process into two phases: an early and a late phase. In both phases, a primary transcript that is alternatively spliced to generate monocistronic mRNAs compatible with the host's ribosome is generated, allowing for the products to be translated.

The early genes are responsible for expressing mainly non-structural, regulatory proteins. The goal of these proteins is threefold: to alter the expression of host proteins that are necessary for DNA synthesis; to activate other virus genes (such as the virus-encoded DNA polymerase); and to avoid premature death of the infected cell by the host-immune defenses (blockage of apoptosis, blockage of interferon activity, and blockage of MHC class I translocation and expression).

Some adenoviruses under specialized conditions can transform cells using their early gene products. E1A (binds Retinoblastoma tumor suppressor protein) has been found to immortalize primary cells *in vitro* allowing E1B (binds p53 tumor suppressor) to assist and stably transform the cells. Nevertheless, they are reliant upon each other to successfully transform the host cell and form tumors.

DNA replication separates the early and late phases. Once the early genes have liberated adequate virus proteins, replication machinery, and replication substrates, replication of the adenovirus genome can occur. A terminal protein that is covalently bound to the 5' end of the adenovirus genome acts as a primer for replication. The viral DNA polymerase then uses a strand displacement mechanism, as opposed to the conventional Okazaki fragments used in mammalian DNA replication, to replicate the genome.

The late phase of the adenovirus lifecycle is focused on producing sufficient quantities of structural protein to pack all the genetic material produced by DNA replication. Once the viral components have successfully been replicated, the virus is assembled into its protein shells and released from the cell as a result of virally induced cell lysis.[165]

2.1.7.6 Cytomegalovirus

Cytomegalovirus (CMV) is a genus of viruses in the order Herpesvirales, in the family Herpesviridae, in the subfamily Betaherpesvirinae. Humans and monkeys serve as natural hosts.

There are currently eight species in this genus including the type species, human cytomegalovirus (HCMV, human herpesvirus 5, HHV-5), which is the species that infects humans. Diseases associated with HHV-5 include glandular fever, and pneumonia.[166] In the medical literature, most mentions of CMV without further specification refer implicitly to human CMV. Human CMV is the most studied of all cytomegaloviruses.[167]

Within *Herpesviridae*, CMV belongs to the *Betaherpesvirinae* subfamily, which also includes the genera *Muromegalovirus* and *Roseolovirus (HHV-6 and HHV-7)*.[168] It is related to other herpesviruses within the subfamilies of *Alphaherpesvirinae* that includes herpes simplex viruses (HSV)-1 and -2 and varicella-zoster virus (VZV), and the *Gammaherpesvirinae* subfamily that includes Epstein–Barr virus.[167]

All herpesviruses share a characteristic ability to remain latent within the body over long periods. Although they may be found throughout the body, CMV infections are frequently associated with the salivary glands in humans and other mammals.[166] Other CMV viruses are found in several mammal species, but species isolated from animals differ from HCMV in terms of genomic structure, and have not been reported to cause human disease. Viral replication is nuclear, and is lysogenic. Entry into the host cell is achieved by attachment of the viral glycoproteins to host receptors, which mediates endocytosis. Replication follows the dsDNA bidirectional replication model. DNA templated transcription, with some alternative splicing mechanism is the method of transcription. Translation takes place by leaky scanning. The virus exits the host cell by nuclear egress, and budding. Human and monkeys serve as the natural host. Transmission routes are contact, urine, and saliva.[169]

2.2. RESULTS AND DISCUSSIONS

2.2.1 Synthesis of hydroxytyrosol and dihydrocaffeoyl catechols.

Catechol derivatives show different biological properties, including inhibition of hypoxia inducible factor-prolylhydroxylase-2 (HPH),[170] antiepileptogenic,[171] pulmonary fibrosis,[172] anticancer, [173-175] antimicrobial,[176] and anti- Parkinson activities.[177] Moreover, they are active against a large panel of viruses, including rhinovirus,[178] HIV-1 integrase,[179,180] HIV-1 reverse tran-scriptase,[181] and coronavirus. [182] The biological activity of catechols is associated to their capacity of transferring single-electron and/or hydrogen-atom to reactive free radicals,[183-185] as well as, to coordinate pro-oxidant metal ions.[186] The antioxidant activity of catechols can be oriented toward specific cellular compartments by controlling the chemical and physical properties of the substituents on the aromatic ring.[187] For example, the limited accessibility of highly hydrophilic catechols to specific intracellular targets has been improved by the synthesis of lipophilic derivatives possessing long carbon alkyl side chains.[188-190] In the case of bioacitive hydroxytyrosol and dihydrocaffeic acid derivatives,[191-192] which are characterized by the concomitant presence of alcoholic and ortho-diphenol groups,[193-194] the side-chain functionalization requires expensive and tedious protection/deprotection sequences. Dihydrocaffeoyl catechols showed antiviral activity against Influenza A virus, an infection that continue to represent a severe threat word- wide.[195,196] Derivatives characterized by antioxidant activity and longer carbon alkyl side-chains were more effective, suggesting the possibility of novel inhibition mechanisms based on both redox and lipophilic properties.[197,198] The efficacy of tyrosinase in the synthesis of simple catechol derivatives was successively increased by immobilization on multi-walled carbonanotubes (MWCNTs), using the Layer-by-Layer (LbL) procedure. Here we describe the use of MWCNT/Tyr for the synthesis of lipophilic hydroxytyrosol and dihydrocaffeoyl catechols, and their antiviral activity against a large panel of DNA and RNA viruses, including Poliovirus type 1, Echovirus type 9, Herpes simplex virus type 1 (HSV-1) and type 2 (HSV-2), Coxsackie virus type B3 (Cox B3), Adenovirus type 2 and type 5, and Cytomegalovirus (CMV). The mechanism of action of the most active dihydrocaffeoyl derivative was investigated in detail against a model of HSV-1 infection. The MWCNT/Tyr was prepared as described in chapter I. Briefly, mushroom Tyr from Agaricus bisporus and BSA (BSA/Tyr ratio 3:1) were immobilized on oxidized MWCNTs,[199] by deposition of a layer of PDDA (MWCNTs-PDDA/ Tyr ratio of 5:1) in sodium phosphate buffer (PBS; 0.1 M, pH 7) at room temperature. The excess

PDDA was removed by centrifugation/re-dispersion cycles since residual PDDA in the solution can precipitate upon mixing with enzyme.198 The ester derivatives of commercially available 3(4-hydroxyphenyl)propanoic acid 1 and tyrosol 2 (4-hy- droxyphenylethyl alcohol) were used as selected substrates. In particular, the ester derivatives 75a–d (Scheme 18) were prepared by reaction of 75 with an excess of the appropriate alcohol in the presence of trimethylchlorosilane (TMCS) at 25 °C . The esterification of 76 to yield compounds 76 a–d (Scheme 19) was carried-out using lipase from Candida antarctica to avoid the formation of mixture of isomers, due to competition between alcoholic and phenol groups 203 The oxidation of compounds 75 and 75a–d (0.05mmol) was performed with MWCNT/Tyr (240 U) and native Tyrosinase in CH2Cl2/buffer (Na phosphate 0.1 M pH 7, CH2Cl2/buffer ratio 1.0:0.1) at 25°C under O2 atmosphere for 24 h (Scheme 18, Table 8)

75,77: R= H
75a,77a R= CH$_3$
75b,77b R= CH$_2$CH$_3$
75c,77c R= CH$_2$CH$_2$CH$_3$
75d,77d R= CH$_2$(CH$_2$)$_2$CH$_3$
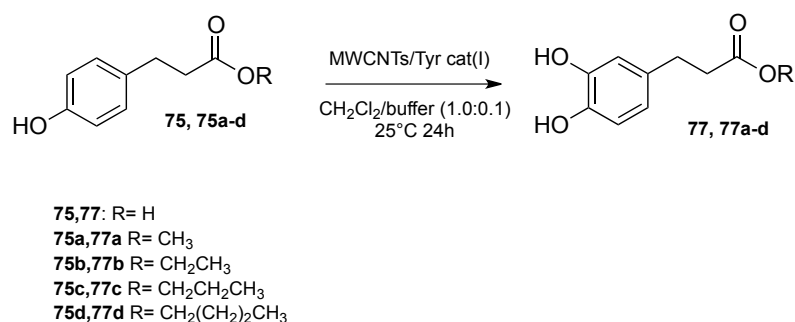
Scheme18. Oxidation of compounds **75** and **75a-d** with MWCNT/Tyr

The use of CH2Cl2 as reaction solvent was necessary to increase the solubility of hydrophobic substrates, in accordance with improved stability and selectivity (with limited formation of ortho-benzoquinones and polymeric side-products). [204]

76a-d

76 a,78a R= COCH$_3$
76b,78b R= COCH$_2$CH$_3$
76c,78c R= COCH$_2$CH$_2$CH$_3$
76d,78d R= COCH$_2$(CH$_2$)$_2$CH$_3$
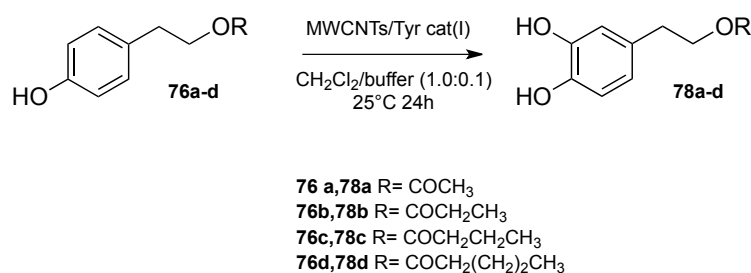
Scheme19. Oxidation of compounds **76 a-d** with MWCNT/Ty

MWCNT/Tyr selectively afforded catechol derivatives **77** and **77a–d** in quantitative conversion of substrate and yield of product (Table 8). In these reactions, MWCNT/Tyr showed a reactivity similar to Tyr (Table 8, entry 3 versus entries 1 and 2, and entry 6 versus entries 4 and 5). In a similar way, the oxidation of tyrosol esters **76a–d** afforded the corresponding lipophilic catechols **78a–d** (Scheme 19) in quantitative conversion of substrate and yield of product (Table 8, entries 10–14).

Table 8. Synthesis of hydroxytyrosol and dihydrocaffeoyl catechol derivatives 77, 77a–d and 78a–d[a]

Entry	Substrate	Catalyst	Product	Conversion(%)	Yield(%)
1	**75**	Tyr	**77**	98	98
3	**75**	MWCNT/Tyr	**77**	98	98
4	**75a**	Tyr	**77a**	98	98
6	**75a**	MWCNT/Tyr	**77a**	98	98
7	**75b**	MWCNT/Tyr	**77b**	98	98
8	**75c**	MWCNT/Tyr	**77c**	98	98
9	**75d**	MWCNT/Tyr	**77d**	98	98
11	**76a**	MWCNT/Tyr	**78a**	98	98
12	**76b**	MWCNT/Tyr	**78b**	98	98
13	**76c**	MWCNT/Tyr	**78c**	98	98
14	**76d**	MWCNT/Tyr	**78d**	98	98

[a]The oxidation was performed on 0.05 mmol of substrate with the appropriate catalyst (240 units) in CH2Cl2/buffer (Na phosphate 0.1 M pH 7, CH$_2$Cl$_2$/buffer ratio 1.0:0.1) at 25 °C under O$_2$ atmosphere for 24 h. b In this case an higher amount of immobilized enzyme (600 units) was required to obtain a quantitative yield of desired product.

With the aim to define the recyclability of the catalyst, MWCNT/Tyr was recovered by centrifugation, washed, and reused with fresh substrate.

Table 9. Recycling experiments for catalyst MWCNT/Tyr.

Entry	Run	MWCTN/Tyr (yield %)
1	1	98
2	2	98
3	3	98
4	4	97
5	5	95
6	6	91

[a]Reusability is expressed as the yield in % of catechol **3** obtained by oxidation of **75** with MWCTN/Tyr. [b] The oxidation of **75** (0.05 mmol) was performed in the presence of the appropriate catalyst (240 units) in CH_2Cl_2/buffer (Na phosphate 0.1 M pH 7, CH_2Cl_2/ buffer ratio 1.0:0.1) at 25 °C under O_2 atmosphere for 24 h.

As shown in Table 9, MWCNT/Tyr was used for at least six cycles with only a slight decrease of efficiency to give **77** (Table 9, entry 1 vs entry 6). MWCNT/Tyr results stable and reusable .

2.2.2 Antiviral activity of hydroxytyrosol and dihydrocaffeoyl catechols.

The antiviral activity of lipophilic catechol derivatives 77, 77 a–d, and 78a–d was evaluated against several DNA and RNA viruses (Polio 1, Echo 9, HSV-1, HSV-2, Cox B3, Adeno 2, Adeno 5 and CMV). Cell monolayers were infected at multiplicity of infection (MOI) 0.1 and treated with different concentrations (ranging from 25 to 200 lg/mL) of each compound. The values of CD_{50} (concentration which inhibited cells growth by 50% when compared with control culture) and ID_{50} (concentration which inhibited virus plaque formation and virus-induced cytopathogenicity by 50%) of catechol derivatives are shown in Tables 10 and 11, respectively. Derivatives 77b, 77d, 78a and 78b were characterized by selective antiviral activity. In particular, compounds 77b and 78a demonstrated the highest level of activity against HSV-1 (DNA virus), with ID_{50} values of 15 and 20 lg/mL, respectively.

Moreover, the same compounds showed slight activity against HSV-2 (60 and 40 lg/mL, respectively) and Cox B3 (RNA virus; 20 and 50 lg/mL, respectively). With regard to 4b, a modest activity against HSV-1 was observed, probably due to toxic effect on cell monolayer, as suggested

Table 10. Antiviral activity of cathecol derivatives 77, 77a-d and 78a-d. against different DNA and RNA viruses.

Compound	$ID_{50}(\mu g/mL)^{a, \ddagger}$							
	Polio 1	CoxB3	ECHO9	HSV-1	HSV-2	Adeno 2	Adeno 5	CMV
77	>200	>200	>200	>200	ND	>200	>200	>200
77a	>100	>100	>100	>100	>100	>100	>100	100
77b	>75	20	>75	15	60	>40	>40	40
77c	>200	>200	>200	>200	ND	>200	>200	ND
77d	>200	100	>200	>200	>200	>200	>200	25
78a	>100	50	>100	20	40	>50	>50	>50
78b	>40	>40	>40	20	40	>40	>40	>40
78c	>100	>100	>100	>100	100	>100	>100	>100
78d	>25	>25	>25	25	ND	>25	>25	>25

[a]Values are mean ± 0·5 SD (maximal SD estimated) for three separate assays. ‡ID_{50}, concentration which inhibited virus plaque formation and virus-induced cytopathogenicity by 50%.

by the low value of CD_{50} (40 lg/mL). Finally, 77b and 77d were effective against CMV (DNA virus), 3d being the most active compound with an ID_{50} value of 25 lg/mL. Since 78b was effective against several RNA or DNA viruses, especially in the case of herpetic viruses (HSV-1, HSV-2 and CMV),its mechanism of action was investigated in more detail using a model of HSV-1 infection. In particular, compound 77b was added at different times on VERO cells infected with 0.1 MOI of HSV-1, to determine the inhibition of the virus yield during specific periods in the virus life-cycle. The results clearly demonstrate that 77b interferes with an early step of the viral replicative cycle. Indeed, the viral replication was blocked during the first hour of infection.

Table 11. Cytotoxicity of cathecol derivatives **77,77a-d** and **78a-d**.

Compound	$CD_{50}(\mu g/mL)^{*,\dagger}$		
	VERO	HEp2	HFF1
77	>200	>200	>200
77a	100	100	100
77b	75	40	40
77c	>200	>200	ND
77d	200	200	100
78a	100	50	50
78b	40	40	40
78c	100	100	100
78d	25	25	25

*Values are mean $\pm$ 0·5 SD (maximal SD estimated) for three separate assays. †CD_{50}, concentration which inhibited cells growth by 50% when compared with control culture.

Otherwise, no reduction was observed when 77b was added after 2 h. Moreover, a slight reduction of virus yield was observed during the adsorption period (Fig. 48). As 77b exerted its activity through the inhibition of the early events in HSV-1 replication, we set up some experiments in order to deepen its mechanism of action. First, the effect of the com- pound was studied during the viral adsorption period by means of the infective center assay. Results obtained from this experiment demonstrated that 3b did not significantly inhibit adsorption of HSV-1 at concentrations higher than 5 times the ID_{50} (Fig. 49). Furthermore, it was important to establish if any virucidal effect.
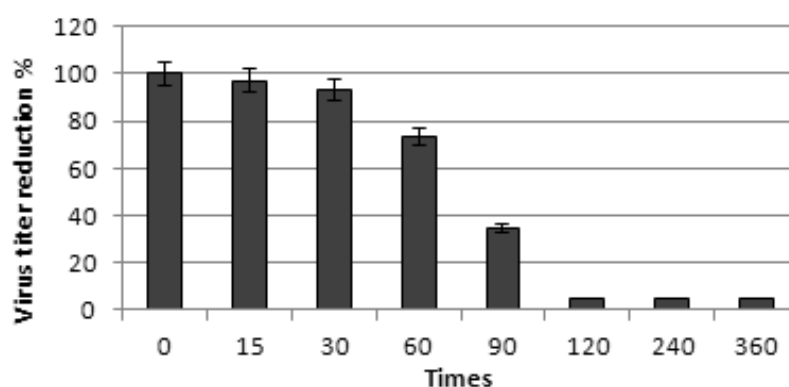
Figure 48. Effect of addition of compound (5 x ID_{50}) at various times during the replicative cycle of HSV-1. Time 0 = post 2h adsorption period at 4° C. The concentrations used are ratios with respect to the ID_{50} (e.g. 5x the ID_{50} is 5 times the ID_{50} of the compound). Each value represents the mean $\pm$ S.E.M. of three separate assays.

or protective actions for Vero cells was produced. Our results demonstrated that 3b was not virucidal for HSV-1 and did not exerted any protective action for the cells, thus suggesting that the reduction in the virus yield, immediately after the adsorption period, could be related to the interference of the compound with penetration, un-coating and/or another early step of HSV-1 replication.
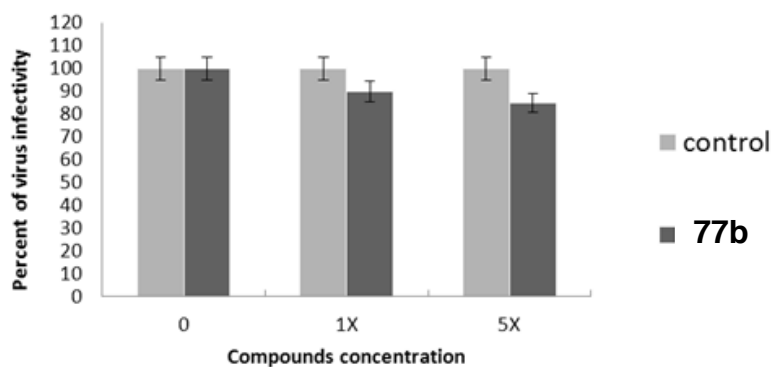
Figure 49. Effect of compound **77b** (1_X, 5_X ID_{50}) on the adsorption of HSV-1. Infective center assay data were plotted as percentage of virus infectivity relative to the no-drug control. The concentrations used are ratios with respect to the ID_{50}.

2.2.3 Synthesis of polyphenolic coumarin derivatives

The relationships between the antioxidant properties of hydroxy-coumarins and the intestinal anti-inflammatory effects has been reported as a consequence of their ability to inhibit the myeloperoxidase activity and to preserve the glutathione (GSH) content[208]. As previously described antioxidants represent interesting compounds for the treatment of influenza[209,210] increasing the oxidative stress and decreasing the antioxidant defenses by depletion of intracellular GSH[211] or by production of reactive oxygen species (ROS)[212]. In order to evaluate a possible effect of polyphenolic coumarins against influenza A we choose a panel of simple coumarins for the synthesis of new cathecol and pyrogallol (1,2,3-trihydroxy benzene) derivatives. Pyrogallol-like coumarin derivatives showed promising anticancer activity but any in depth analysis about anti-influenza activity was investigated[213] As shown before IBX and Supported IBX perform the ortho-hydroxylation of phenol to catechols, and also the over oxidation to pyrogallols, with a selectivity similar to natural polyphenol oxidases, as a consequence of the concerted intramolecular oxygen transfer to substrate[214] Umbelliferone (7-hydroxy coumarin) (**79**), 4-hydroxy umbelliferone (4,7-dihydroxy coumarin) (**81**), 4-methyl umbelliferone (4-methyl-7-hydroxy coumarin) (**83**), 4-methyl-5,7-dihydroxy coumarin (**85**),6-hydroxy coumarin (**87**), 4 trifluoromethyl-7-nitrocoumarin (**89**), 6,7-dihydroxy coumarin (**91**), 6 methoxy,7,8-dihydroxy coumarin (**93**), and derivatives **95-99** (showed in figure)-were selected as substrates for the oxidation with IBX. Every reaction was set-up in different conditions as shown in Tables 12-20 with the aim to obtain acceptable quantity of products to test against Influenza A virus. The appropriate coumarin was dissolved/suspended in the selected solvent and than IBX or supported-IBX were added to the reaction mixture. After detection with TLC (AcOEt/Hex 1:1), the work up was performed by addition of $Na_2S_2O_4$ and water. The organic layer was washed with $NaHCO_3$ to remove the excess of IBX. Chromatographic purification on silica column was then performed.
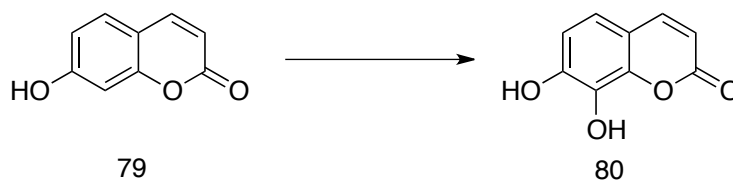
Scheme 20. Oxidation of 7-hydroxy coumarin **(79)**

Table 12. Different conditions for the oxidation of 7-hydroxy coumarin **(79)**

Enry	Catalyst (eq)	Reaction time	Reaction temperature	Reaction solvent	Yield (%)
1	(1eq to 3eq)IBX	7 days	rt to 45°C	CHCl$_3$/MeOH	5
2	(1eq)IBX	2h	r.t.	DMSO	47
3	(1eq)IBX	12 h	rt	DMSO	45

81 → 82
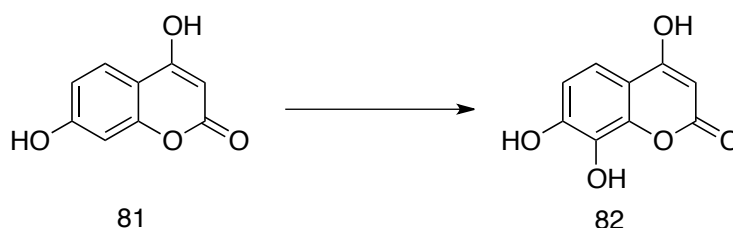
Scheme 21. Oxidation of 4,7-dihydroxy coumarin) **(81)**

Table 13. Different conditions for the oxidation of 4,7-dihydroxy coumarin) **(81)**

Entry	Catalyst (eq)	Reaction time	Reaction temperature	Reaction solvent	Yield (%)
1	(1eq to 3eq)IBX	7 days	rt to 45°C	CHCl$_3$/MeOH	10
2	(1eq)IBX	2h	r.t.	DMSO	45
3	(1eq)IBX	24h	r.t.	DMSO	43
4	(1eq)IBX	2 days	r.t.	DMSO	40
5	(1eq)IBX	3 days	r.t.	DMSO	39
6	(1eq)IBX	7 days	r.t.	DMSO	42
7	(1eq)IBX	7 days	45	DMSO	47

Compounds were oxidized with IBX (from 1.0 equivalent) in chloroform/methanol (3:1 v/v) at different temperature,(Table 12 and 13). Irrespective from the reaction time (from 2h to 7 days) we did not observed the formation of desired products; even for higher temperature and large excess of the oxidant. Better results were obtained performing the reaction in DMSO. The work up of the reactions was performed by addition of ethyl acetate (EtOAc) and a saturated solution of NaHCO$_3$. Under these experimental conditions compounds **79** and **81** were oxidized to afford the corresponding catechol derivatives **80** and **82** in variable yields. The best experimental conditions

were room temperature for 2 h. The best experimental conditions for the synthesis of both compoundswere room temperature for 2 h infact longer reaction time and higher amount of IBX (2.0 equivalents) did not increased the yield of desired products. The oxidation with IBX showed a high regio-selectivity, affording only one of the two possible catechol isomers. This selectivity it is in accordance with the distribution of the electronic density the coumarin ring depending on the initial position (that is C7 versus C6) of the hydroxy group.[169,170,171] Catechols **80** and **82** were unambiguously characterized by Nuclear Magnetic Resonance analysis (NMR), and their data were in accordance with analyses previously reported.

Scheme 22. Oxidation of 4-methyl-7-hydroxy coumarin **(83)**

Table 14. Different conditions for the oxidation of 4-methyl-7-hydroxy coumarin) **(83)**

Enry	Catalyst (eq)	Reaction time	Reaction temperature	Reaction solvent	Yield (%)
1	(1eq)IBX	2h	r.t.	DMSO	74
2	(1eq)IBX	12 h	rt	DMSO	75
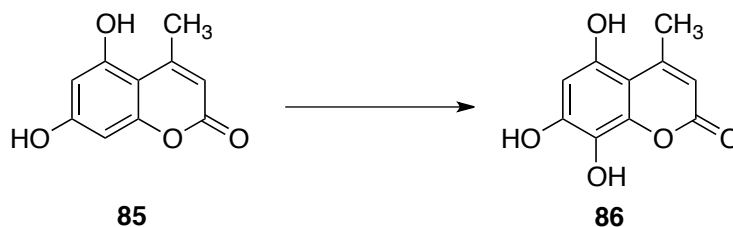
Scheme 23. Oxidation of 4-methyl-5,7-dihydroxy coumarin **(85)**

Table 15. Different conditions for the oxidation of 4-methyl-5,7-dihydroxy coumarin (**85**)

Entry	Catalyst (eq)	Reaction time	Reaction temperature	Reaction solvent	Yield (%)
1	1(eq) IBX	24h	r.t.	CHCl$_3$/MeOH	15
2	(2eq)IBX	24h	r.t.	DMSO	23
3	(1eq)IBX	24h	r.t.	DMSO	15
4	(1eq)IBX	7 day	r.t.	DMSO	18
5	1(eq) IBX	2h	45°	DMSO	25
6	1(eq) IBX	24h	45°	DMSO	22

87　　**88**
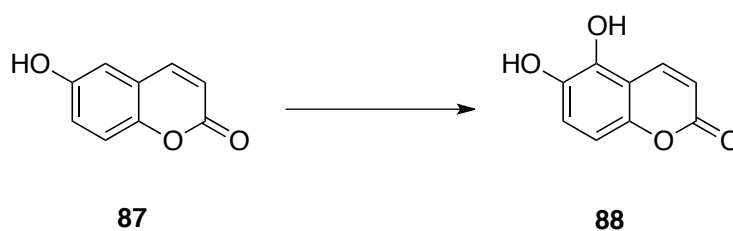
Scheme 24. Oxidation of 6-hydroxy coumarin (**87**)

Table 16. Different conditions for the oxidation of 6-hydroxy coumarin (**87**)

Entry	Catalyst (eq)	Reaction time	Reaction temperature	Reaction solvent	Yield (%)
1	(1eq)IBX	24h	r.t.	CHCl$_3$/MeOH	0
2	(1eq)IBX	2h	r.t.	DMSO	64%

89　　**90**
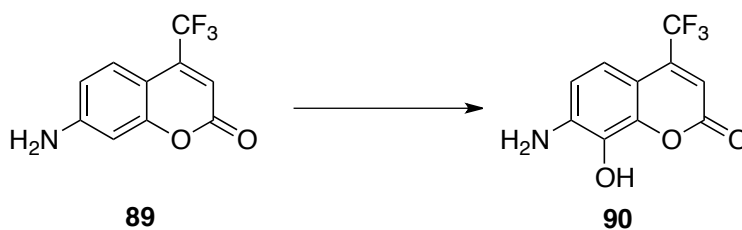
Scheme 25. Oxidation of 4 trifluoromethyl-7-nitrocoumarin (**89**)

Table 17. Different conditions for the oxidation of 4 trifluoromethyl-7-nitrocoumarin (**89**

Entry	Catalyst (eq)	Reaction time	Reaction temperature	Reaction solvent	Yield (%)
1	(1eq)IBX	24h	r.t.	CHCl3/MeOH	10
2	(1eq)IBX	2h	r.t.	DMSO	20%
3	(1eq)IBX	24h	r.t.	DMSO	15%
4	(1eq)IBX	7 day	r.t.	DMSO	0
5	(2eq)IBX	2h	r.t.	DMSO	19%
6	(1eq) IBX	24h	r.t	DMSO	22%

The synthesis of non-natural coumarin derivatives containing the pyrogallol pharmacophore are of pivotal importance for the development of compounds having a radical scavenging activity higher than that of the corresponding catechol derivatives. The high antioxidant activity of pyrogallol natural compounds is reviewed,[188,189] in addition, pyrogallol-like coumarin derivatives showed promising anticancer activity.[190] According to the general procedure, we used IBX for the oxidation of esculetin **91** and fraxetin **92**, bearing the catechol moiety (**Scheme 26 and 27**).

Compounds **93** and **94** were oxidized with IBX (1.0 equivalents) in DMSO for 24 h at 45 °C to afford desired pyrogallol derivatives **93** and **94** in acceptable yields, as evaluated by in-situ NMR analysis (**Table 18 and 19**). Unfortunately, the high polarity of products rendered the isolation of compounds from DMSO very difficult to be achieved. Better results were obtained using solvents with a lower affinity for the products, such as the chloroform/methanol mixture. In this latter cases, pyrogallol derivatives **93 and 94** were obtained in 50% and 68% yields, respectively**.**

91 **92**
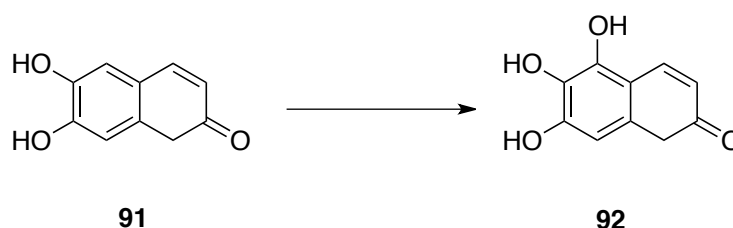
Scheme 26. Oxidation of 6,7-dihydroxy coumarin (**91**)

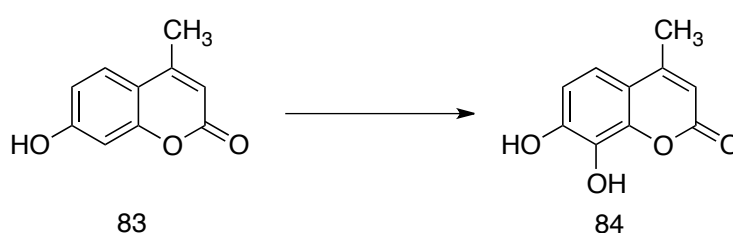**Table 18.** Different conditions for the oxidation of 6,7-dihydroxy coumarin (**91**)

Numero prove	Catalyst (eq)	Reaction time	Reaction temperature	Solvent	Yield (%)
1	(2eq)IBX	24h	r.t.	CHCl3/MeOH	50
3	(2eq)IBX	2h	r.t.	DMSO	58%

93   **94**
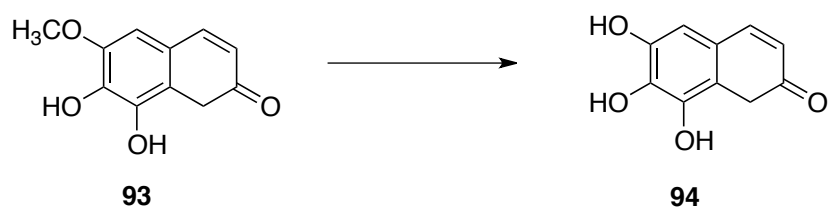
Scheme 27. Oxidation of 6 methoxy,7,8-dihydroxy coumarin (**93**)

Table 19. Different conditions for the oxidation of 6 methoxy,7,8-dihydroxy coumarin (**93**)

Entry	Catalyst (eq)	Reaction time	Reaction temperature	Reaction solvent	Yield (%)
2	(1eq)IBX	24h	45°	DMSO	75
4	(1eq)IBX	24h	r.t.	CHCl3/MeOH	68

95   **96**   **97**   **98**

99
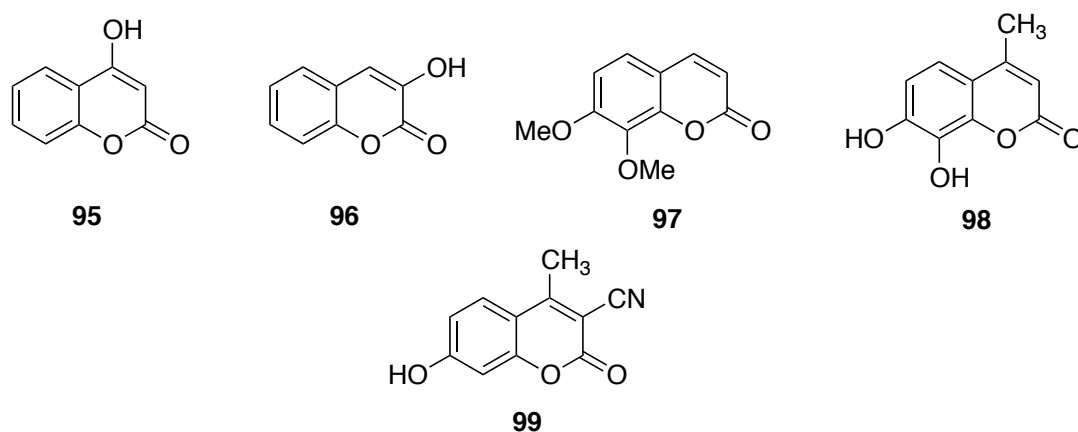
Figure 50. Coumarin derivatives **95**, **96**, **97**, **98**, **99.**

Coumarin derivatives **95-99** were not reactive under optimal experimental conditions. In view of possible technological applications, we analyzed the oxidation of coumarins under heterogeneous conditions. The use of supported reagents reduce the waste of the process, opening the possibility to obtain highly pure products. We decided to use two heterogeneous catalysts:

- commercially available IBX supported on polystyrene (PSS-IBX) [172] (**Figure 51 a**)

- novel IBX supported on Multi Walled Carbon Nanotubes (MWCNTs) catalysts.

-

IBX was immobilized on two different types of MWCNTs, namely MWCNTs-COOH and MWCNTs-OH. They differ for the prevalence of acidic COOH of phenolic OH on their surface.

A   **B**   **C**
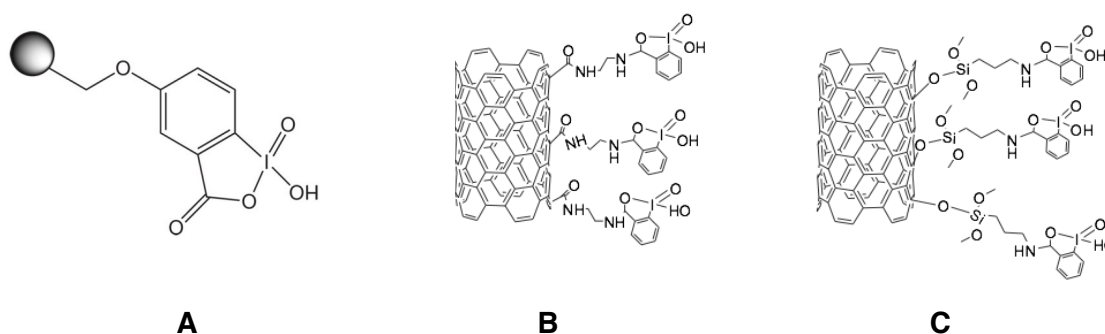
Figure 51 Schematic representation of IBX supported on a) polystyrene b)MWCNT-COOH c) MWCNT-OH.

To load IBX on MWCNTs-COOH we used ethylenediamine as a linker. In the case of MWCNTs-OH we used a propylamine linker (Figure 51 b and c) (details about catalysts preparation are described in Material and methods). The use of these two amines favors the possibility to increase the distance between IBX and the MWCNTs surface, increasing the freedom of the active species. Catalysts PSS-IBX and CNT-IBX were used for the oxidation of 6-hydroxycumarin **87** under optimal conditions. Unfortunately, the reactions performed in DMSO were not operative. Only catalyst PSS-IBX showed an appreciable reactivity in water at 80°C to afford the desired catechol **88** in 43 % yield.

2.2.3 Anti-viral activity of polyphenolic coumarin derivatives

The polyphenolic coumarin derivatives **79-94** were evaluated for the influenza A/PR8/H1N1 virus inhibition at the Department of Public Health and Infectious diseases of the University La Sapienza in Rome, and at the San Raffaele Pisana Scientific Institute for Research (Rome). Influenza A is an enveloped virus, belonging to the *Orthomyxoviridae* family and characterized by a segmented single-stranded RNA genome. Within the envelope,

Compound	IC$_{50}$ (µg/ml)
89	47.9
90	47.8
92	91.5
94	69.6

the eight viral RNA segments, associated with the nucleoprotein (NP) and the viral RNA-dependent RNA polymerase (RdRp) complex, form helical ribonucleoprotein capsids (vRNP$_S$). After uncoating, the vRNP$_S$ are released in the cytosol and transported to the host-cell nucleus, where they undergo transcription and replication. In a late phase of the replication cycle, vRNP complexes are exported into the cytosol to be assembled with the other structural proteins and packaged into progeny virions. Several antiviral compounds have been developed against influenza virus. However, the efficacy of these antiviral compounds is often limited by toxicity and the almost inevitable selection of drug-resistant viral mutants. Influenza A viruses are highly sensitive to changes in the intracellular redox state, and their activation is induced by the oxidative stress. Moreover, the administration of compounds able to restore the redox state in the cell has been demonstrated to inhibit the replication of DNA or RNA virus. This approach could give important advantages, including the broad-spectrum efficacy, the antigenic properties, and the reduced probability to select drug-resistant viral strains. On the basis of this evidence, in a first set of experiments the cytotoxicity of the coumarin analogues (**79-94**) was evaluated on A549 cell monolayers. Briefly, cells were plated at concentration of 2x10^5/ml and after 24 h were treated with various concentrations (range 10-120 µg/ml) of each compound and incubated for the following 24 hours. Microscopical examination, Trypan blue exclusion and cell proliferation assay demonstrated that the compounds did not exert any toxic effect on the cells at all the concentrations tested (data not shown). Next, to evaluate a potential antiviral activity of coumarin derivatives, cells were infected with influenza A/PR8/H1N1 virus and, after viral challenge, were treated with different concentrations (ranging from 30 to 120 µg/ml) of each compound. Twenty-four hours post infection (p.i.), viral particles released in the supernatant of infected cells, were measured by means of hemagglutinating units (HAU). As shown in Figure 52 compounds **89, 90, 92** and **94** were able to
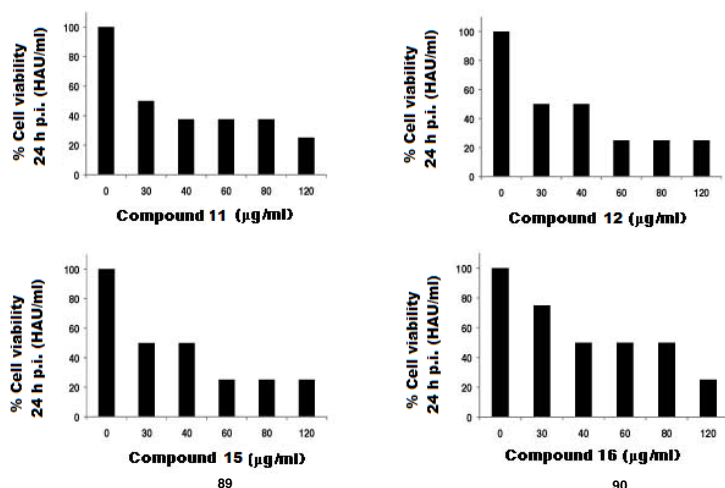
inhibit viral replication compared to un-treated infected cells. In particular, the inhibition was more than 50% and the antiviral activity was dose-dependent.

79   81   80   82   92   94

Figure 52. Dose activity relationship for compounds **89,90,92** and **94**. (IC$_{50}$) is the required Inhibitory Concentration that reduces virus yield by 50%

Cell morphology and viability were unaffected by treatment with these compounds until theconcentration of 30 µg/mL, while at higher doses (60 and 120 µg/ml) an alteration of cell monolayer was detectable, thus indicating an antiviral effect of the compounds at these relatively concentrations (**Figure 52**). Notable that an important reduction (about 50%) was observed by treating infected cells with unnatural compounds **89** and **90** probably related to their toxicity. No effect was observed by treating A549 with the other compounds. Interestingly, the highest inhibition of viral replication was showed by pyrogallolic coumarin derivatives (**92** and **94**). This activity was higher than that observed for the corresponding catechol (**91** and **93**) and all the phenolic derivatives. Note that the highest inhibitory activity of **92** and **94** against influenza A virus is related to their lower value of the redox potential with respect to catechol and phenol derivatives

This property is associated to an increased antioxidant activity (as shown in Figure 53). These data highlight the role of the antioxidant activity on the general mechanism of inhibition of the influenza A virus.[215,216,217]
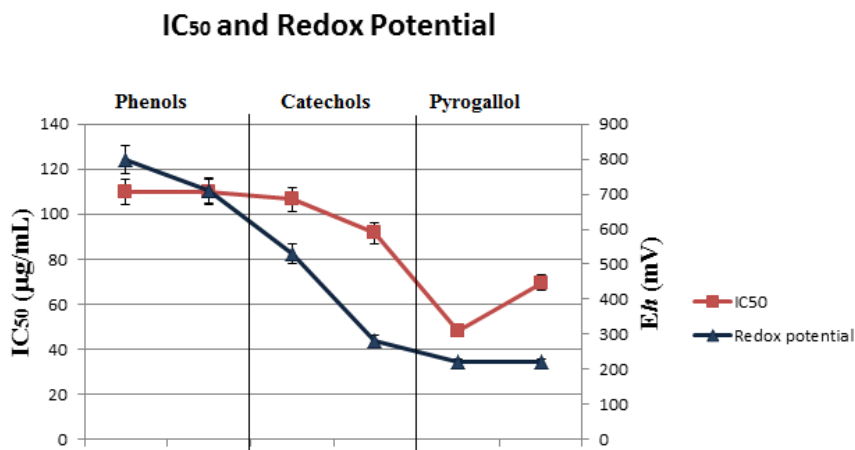
Figure 53. Relationship between redox potential of Coumarin derivatives and IC_{50} (Inhibitory Concentration that reduces virus yield by 50%).

2.3. CONCLUSIONS

In order to evaluate a possible effect of dihydroxytyrosol, dihydrocaffeic and coumarin derivatives against a large panel of DNA and RNA viruses, including Poliovirus type 1, Echovirus type 9, Herpes simplex virus type 1 (HSV-1) and type 2 (HSV-2), Coxsackie virus type B3 (Cox B3), Adenovirus type 2 and type 5, and Cytomegalovirus (CMV)virus, we synthesized a large panel of molecules bearing cathecol and pyrogallol (1,2,3-trihydroxy benzene) moieties on different position of the aromatic ring. About coumarins, the reactions were deep investigated both in homogeneous and heterogeneous conditions using as oxidation agent IBX and new supported IBX catalysts. DMSO and $CHCl_3$/ MeOH were found to be the best solvents for the reactions. In this experimental condition high quantity of new cathecol and pyrogallol coumarins were prepared. Preliminary results on influenza virus demonstrate an important activity of pyrogallol derivatives , suggesting a strict relationship between redox potential and anti-viral activity.

Concerning Dihydroxytyrosol and dihydrocaffeic derivatives, they were synthesized in heterogeneous conditions, using the catalyst MWCNTs/Tyr previously prepared and well characterized in first chapter. MWCNTs/Tyr affords the derivatives in question in quantitative conversion of substrate and yield. Among lipophilic catechols, compounds **77b, 77d, 78a** and **78b** were active against HSV-1, HSV-2, Cox B3 and CMV. In the case of the inhibition of HSV-1 and

HSV-2 viruses, the highest antiviral activity prevailed in derivatives characterized by a low/medium long alkyl side-chain. The mechanism of action of compound **77b** was studied in detail using a model of HSV-1 infection. Data showed that the inhibition of virus replication was effective in earlier stages of the replication cycle, probably related to penetration, un-coating and/or another early step of HSV-1 replication.

2.4 MATERIAL AND METHODS

2.4.1 Materials

All reagents were purchased from Sigma-Aldrich as substrates. Homogeneous IBX and IBX polystyrene were commercially supplied from Sigma-Aldrich. Multi-Walled Carbon Nanotubes, -COOH functionalized and Multi-Walled Carbon Nanotubes,-OH functionalized were purchased from

IoLiTec. Laccase from *Trametes versicolor* and Mushroom Tyrosinase were either purchased from Sigma Aldrich. ^{1}H NMR and ^{13}C NMR spectra were recorded on a Bruker (400 MHz) spectrometer using $CDCl_3$, CD_3OD, $(CD_3)_2SO$ and D_2O as solvents. Chemical shifts (δ) are expressed in parts per million (ppm). Coupling constants J are expressed in Hertz (Hz). Spin multiplicities are given as s (singlet) b (broad), d (doublet), dd (doublet of doublets) and m (multiplet).

2.4.2 Preparation of Dihydroxytyrosol and dihydrocaffeic derivatives

MWCNT/Tyr (240 U) was added to a solution of the appropriate substrate (0.05 mmol) in CH_2Cl_2 (2.5 mL) in PBS (275 lL), and the mixture was stirred at 25 °C under O_2. After 24 h, the catalyst was recovered by centrifugation and the organic fraction was con- centrated and treated with a solution of sodium dithionite in THF and H_2O [1:1 (v/v)]. The mixture was stirred at 25 °C for 5 min to allow the complete reduction of benzoquinones to catechols and extracted twice with ethyl acetate (EtOAc; 2.0 mL 2). The col- lected organic extracts were dried over anhydrous sodium sulfate, filtered and concentrated under vacuum to yield catechol deriva- tives 3, 3a–d and 4a–d. All experiments were conducted in tripli- cate. The structure of catechol derivatives was characterized without further purification by comparison with data previously reported in the literature.

3,4-Dihydroxyphenyl)propanoic acid (77) Oil; ^{1}H NMR (400 MHz, CDCl3): dH (ppm) = 2.64 (2H, m, CH2), 2.81 (2H, m, CH2), 6.76–6.94 (3H, m, Ph-H); ^{13}C NMR (50 MHz,CDCl3): dC (ppm) = 30.44 (CH2), 35.81 (CH2),115.36 (2 CH), 119.46 (CH), 132.33 (C), 145.10 (C), 145.93 (C), 174.98 (CO); MS (EI): m/z 398; elemental analysis: calcd C, 59.34; H, 5.53; O, 35.13, found C, 59.30; H, 5.53; O, 35.04.

3-(3,4-Dihydroxyphenyl)propanoic acid methyl ester (77a) Oil; ^{1}H NMR (400 MHz, CDCl3): dH (ppm) = 2.56 (2H, m, CH2), 3.57 (3H, s, OCH3), 6.8–7.1 (3H, m, Ph-H); ^{13}C NMR (50MHz,

CDCl3): dC (ppm) = 30.68 (CH2), 35.68 (CH2), 51.60 (CH3), 115.90 (CH), 116.20 (CH), 120.30 (CH), 133.30 (C), 144.20 (C), 145.70 (C), 173.65 (CO); MS (EI): m/z 340; elemental analysis: calcd C, 61.22; H, 6.16; O, 32.62, found C, 61.20; H, 6.16; O, 32.68.

3(3,4-Dihydroxyphenyl)propanoic acid ethyl ester (77b) Oil; ^{1}H NMR(400 MHz, CDCl3) dH (ppm) = 1.18 (3H, m, CH3), 2.48 (2H, m, CH2), 2.72 (2H, m, CH2), 4.05 (2H, m, OCH2), 6.65–6.71 (3H, m, Ph-H); ^{13}C NMR (50 MHz, CDCl3): dC (ppm) = 16.10 (CH3), 36.07 (CH2), 60.10 (CH2), 117.00 (2 CH), 120.30 (CH), 133.30 (C), 144.20 (C), 145.70 (C), 172.10 (CO); MS (EI): m/z 354; elemental analysis: calcd C, 62.85; H, 6.71; O, 30.44, found C,62.81; H, 6.71; O, 30.37.

3-(3,4-Dihydroxyphenyl)propanoic acid propyl ester (77c) Oil; ^{1}H NMR(400 MHz, CDCl3): dH (ppm) = 1.20–1.35 (5H, m, CH2+CH3), 2.55 (2H, m, CH2), 2.82 (2H, m, CH2), 4.15 (2H, m, OCH2), 6.40–6.80 (3H, m, Ph-H); ^{13}C NMR (50 MHz, CDCl3): dC (ppm) = 10.35 (CH3), 22.03 (CH2), 30.68 (CH2), 35.95 (CH2), 65.79 (CH2), 115.90 (CH), 116.20 (CH), 120.30 (CH), 132.51 (C), 114.20(C), 145.60 (C), 172.15 (CO); MS (EI): m/z 368; elemental analysis: calcd C, 64.27; H, 7.19; O, 28.54, found C, 64.38; H, 7.18; O, 28.44.

3-(3,4-Dihydroxyphenyl)propanoic acid butyl ester (77d) Oil; ^{1}H NMR(400 MHz, CDCl3): dH (ppm) = 0.90 (3H, m, CH3), 1.20 (2H, m, CH2), 2.50 (2H, m, CH2), 2.80 (2H, m, CH2), 3.50 (2H, m, CH2), 4.10 (2H, m, OCH2), 6.50–7.80 (3H, m, Ph-H);^{13}C NMR (50 MHz, CDCl3): dC (ppm) = 16.10 (CH3), 19.13 (CH2), 30.10 (2 CH2), 36.34 (CH2), 64.10 (CH2), 115.45 (2 CH), 129.10 (CH), 129.50 (C), 137 (C), 143.10 (C), 173.20 (CO); MS (EI): m/z 382; ele- mental analysis: calcd C, 65.53; H, 7.61; O, 26.86, found C, 65.45; H, 7.61; O, 26.75.

Hydroxytyrosol acetate (78a) Oil; ^{1}H NMR(400 MHz, CDCl3): dH (ppm) = 2.13 (3H, s, CH3), 2.75 (2H, m, OCH2), 4.17 (2H, m, CH2), 6.68–6.74 (3H, m, Ph-H); ^{13}C NMR (50 MHz, CDCl3): dC (ppm) = 20.97 (CH3), 34.36 (CH2), 65.36 (CH2), 115.24 (2 CH), 115.77 (CH), 130.19 (C), 142.64 (C), 143.99 (C), 171.69 (CO); MS (EI): m/z 340; elemental analysis: calcd C, 61.22; H, 6.16; O, 32.62, found C, 61.18; H, 6.15; O, 32.54.

Hydroxytyrosol propionate (78b) Oil; ^{1}H NMR(400 MHz, CDCl3): dH (ppm) = 1.08 (3H, m, CH3), 2.28 (2H, m, CH2), 2.78 (2H, m, CH2), 4.20 (2H, m, OCH2), 6.58– 6.76 (3H, m, Ph-H); ^{13}C NMR (50 MHz, CDCl3): dC (ppm) = 15.10 (CH3), 27.45 (CH2), 38.00 (CH2), 65.95 (CH2), 117.00 (2 CH), 124.10 (CH), 131.10 (C), 145.10 (C), 147.0 (C), 175.0 (CO); MS (EI): m/z 354; elemental analysis: calcd C, 62.85; H, 6.71; O, 30.44, found C, 62.81; H, 6.71; O, 30.49.

Hydroxytyrosol butyrate (78c) Oil; ^{1}H NMR(400 MHz, CDCl3): dH (ppm) = 0.88 (3H, m, CH3), 1.58 (2H, m, CH2), 2.25 (2H, m, CH2), 2.78 (2H, m, CH2), 4.21 (2H, m, OCH2), 6.58–6.76 (3H, m, Ph-H); ^{13}C NMR (50 MHz, CDCl3): dC (ppm) = 13.68 (CH3), 18.72 (CH2), 35.35 (CH2), 36.82 (CH2), 66.20 (CH2), 116.98 (2 CH), 121.60 (CH), 130.30 (C), 144.24 (C), 144.45 (C), 173.22 (CO); MS (EI): m/z 368; elemental analysis: calcd C, 64.27; H, 7.19; O, 28.54, found C, 64.23; H, 7.19; O, 28.48.

Hydroxytyrosol pentanoate (78d) Oil; ^{1}H NMR(400 MHz, CDCl3): dH (ppm) = 0.95 (3H, m, CH3), 1.64 (2H, m, CH2), 2.24 (2H, m, CH2), 2.75 (2H, m, CH2), 4.24 (2H, m, OCH2), 6.64–6.75 (3H, m, Ph-H); ^{13}C NMR (50 MHz, CDCl3): dC (ppm) = 13.68 (CH3), 18.72 (CH2), 35.35 (CH2), 36.82 (CH2), 66.20 (CH2), 116.14 (2 CH), 121.70 (CH), 130.30 (C), 144.45 (C), 174.22 (CO). MS (EI): m/z 382; elemental analysis: calcd C, 65.53; H, 7.61; O, 26.86, found C, 65.53; H, 7.69; O, 26.66.

2.4.3 Preparation of coumarins in homogeneous conditions

A solution of substrate (1.0 mmol), DMSO (1.0 mL) and IBX (1 equiv) was stirred at room temperature for 2 hours. During the reaction, different chromatic changes were observed for every substrate (orange, purple, brown). The reaction was monitored by thin layer chromatography (TLC). After the disappearance of the substrate, the reaction mixture was treated with water (1.0 ml) and an excess of sodium dithionite ($Na_2S_2O_4$) and the solution was left under stirring until it became yellow. Ethyl acetate (10 mL) was added and the two phases were separated. The aqueous phase was further extracted with ethyl acetate (2x10 mL). The combined organic layers were treated with a saturated solution of $NaHCO_3$ (10 mL), to remove *o*-iodooxybenzoic acid (IBX), and a saturated solution of NaCl (10 mL). Then it was dried over Na_2SO_4 and concentrated under reduced pressure to afford the desired product.

7,8-dihydroxy-2H-chromen-2-one (80).. Orange solid (26 mg; yield: 34%). ^{1}H NMR (400 MHz, (CD3)2SO) δ 7.9 (d, *J*=8 Hz, 1H); 7.02 (d, *J*=8 Hz, 1H), 6.80-6.78 (b, 1H); 6.22-6.17 (b, 1H). ^{13}C

(100 MHz, (CD$_3$)$_2$SO) δ 161.79, 150.19, 145.54, 132.60, 128.96, 119.27, 112.51, 111.73, 102.6. Ms (ESI): m/z [M+H]$^+$ 179,14.

4,7,8-trihydroxy-2H-chromen-2-one (82). Orange solid (7 mg; yield: 34%). ^{1}H NMR (400 MHz, (CD$_3$)$_2$SO) δ 6.68 (d, *J*=12 Hz, 1H); 6.42 (d, *J*=8 Hz, 1H); 6.33 (s,1H). ^{13}C (100 MHz, (CD$_3$)$_2$SO) δ 166.1, 162.4, 148.3, 144.8, 135.9, 122.8, 114-0, 111.4, 91.1, Ms (ESI): m/z [M+H]$^+$ 195,14

7,8-dihydroxy-4-methyl-2H-chromen-2-one (84). Brown solid (18 mg; yield (51%). ^{1}H NMR (400 MHz, (CD$_3$)$_2$SO) δ 7.09 (d, J=9 Hz,1H); 6.48 (d, J=9 Hz,1H); 5.64 (d, J=10 Hz,1H); 2.1 (s, 3H). ^{13}C (100 MHz, (CD$_3$)$_2$SO) δ 154.4, 149.9, 140.9, 137.4, 133.3, 124.4, 112.5, 110.6, 102.6, 14.5. Ms (ESI): m/z [M+H]$^+$ 193,17

5,7,8-trihydroxy-4-methyl-2H-chromen-2-one (86). Red solid (7 mg; yield: 22%). ^{1}H NMR (400 MHz, (CD3)2SO) δ 10.31 (s, 1H); 6.26 (s, 1H); 5.85 (s, 1H); 2.0 (s, 3H). ^{13}C (100 MHz, (CD3)2SO) δ 161.52, 160.81, 150.43, 148.75, 145.77, 129.75, 109.8, 102.86, 94.62, 29.47. Ms (ESI): m/z [M+H]$^+$ 209,17

5,6-dihydroxy-2H-chromen-2-one (88). Orange solid (115 mg; yield 48%). ^{1}H NMR (400 MHz, (CD$_3$)$_2$SO) δ 9.76 (s, 1H); 8.11 (d, *J*=12 Hz, 1H); 7.03-7.02 (b, 1H); 6.68 (d, *J*=12 Hz, 1H); 6.3 (d, *J*= 12 Hz, 1H). ^{13}C (100 MHz, (CD$_3$)$_2$SO) δ 160.77,147.55,142.24,141.35,139.74,119.47,114.19,109.45,106.19. Ms (ESI): m/z [M+H]$^+$ 179,14.

7-amino-8-hydroxy-4-(trifluoromethyl)-2H-chromen-2-one (90). Orange solid (31 mg; yield 34%). ^{1}H NMR (400 MHz, (CD$_3$)$_2$SO) δ 7.93 (d, J=8 Hz, 1 H); 7.37-7.35 (b, 1H); 6.71-6.67 (b,1H); 6.53 (s,2H). ^{13}C (100 MHz, (CD$_3$)$_2$SO) δ 159.9, 154.6, 141.2, 135.9, 129.6, 121.1, 118.3, 112.7, 107.9, 60.2 Ms (ESI): m/z [M+H]$^+$ 246,15.

5,6,7-trihydroxy-2H-chromen-2-one (92).Orange solid (1,8 mg; yield 15%). ^{1}H NMR (400 MHz, (CD$_3$)$_2$SO) δ 7.12 (d, J=9.6 Hz, 1H); 6.98 (s, 1H); 6.09 (d, J=9.6 Hz, 1H). ^{13}C (100 MHz, (CD$_3$OD). δ 160.10, 149.73, 1   49.65, 141.61, 134.50, 111.96, 11.21, 102.21 Ms (ESI): m/z [M+H]$^+$ 195,14.

6,7,8-trihydroxy-2H-chromen-2-one (94). Orange solid (8.4 mg; 68%). ^{1}H NMR (400 MHz, (CD$_3$)$_2$SO) δ 7.9 (d, J=8); 6.76 (d, J=12 Hz, 1H); 6.39 (s, 1H). ^{13}C (100 MHz, (CD$_2$)$_3$SO) δ 161.02, 145.78, 145.54, 139.80, 133.30, 112.27, 110.68, 100.70 Ms (ESI): m/z [M+H]$^+$ 195,14.

2.4.4 Preparation of IBX supported on MWCNTs,-COOH functionalized
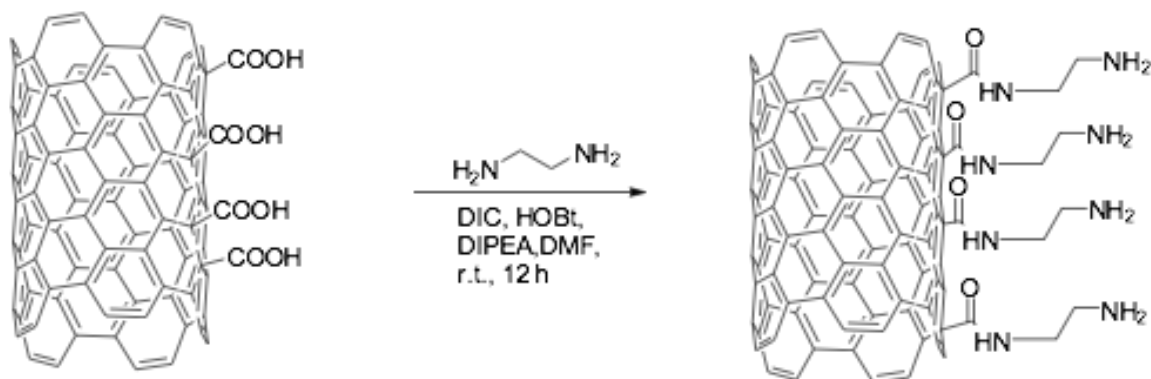
Figure 53. preparation of MWCNTs-NH$_2$.

MWCNTs,-COOH functionalized (5%) (100 mg) were suspended in 125 mL of DMF (0.8 mg/mL). DIC (126 mg, 1 eq), HOBt (136 mg, 1eq) and DIPEA (348 μL, 2eq) were added and the reaction mixture was stirred for 15 minutes at room temperature. Then 60 mg (1 eq) of ethylenediamine was added to the solution, and the mixture was stirred for 12 h at 30°C (Figure 53) . The resulting solution was washed with DMF (5x) centrifuged at 4000 rpm for 20 minutes. The supernatant was removed to afford the ethylenediamine functionalized MWCNTs.
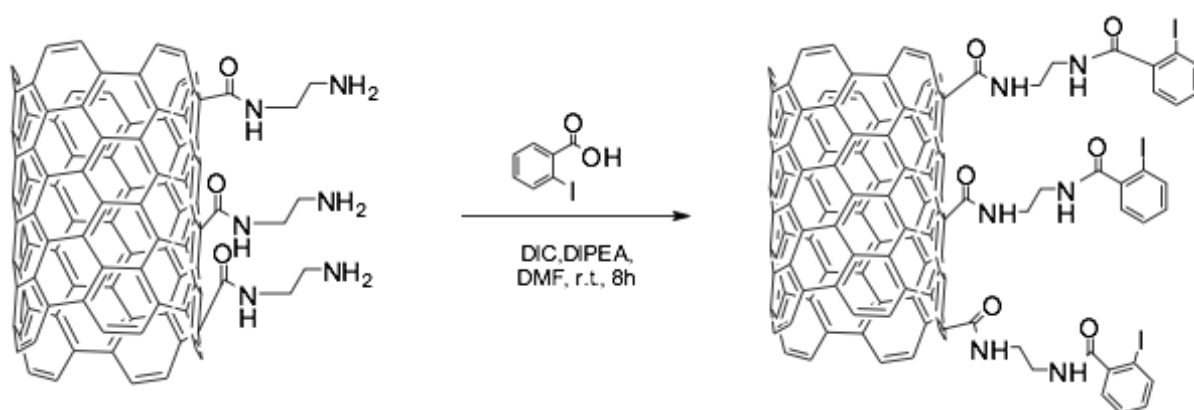
Figure 54. MWCNTs-NH$_2$-IBA

MWCNTs-NH$_2$ (100 mg) were suspended in 125 mL of DMF. DIC (378 mg, 3eq), and DIPEA (1,05 mL, 6eq) were added at the solution. Thereafter, IBA (792 mg, 3 eq) was added to the solution, and the mixture was stirred for 8 h at 30 °C (Figure 54). The resulting solution was washed with DMF (5x), centrifuged at 4000 rpm for 20 minutes and then the supernatant was removed. After that the solution was washed with H$_2$O (3x), centrifuged at 4000 rpm for 20 minutes, the supernatant was removed to afford MWCNTs-NH$_2$-IBA and dried in a freeze dryer.
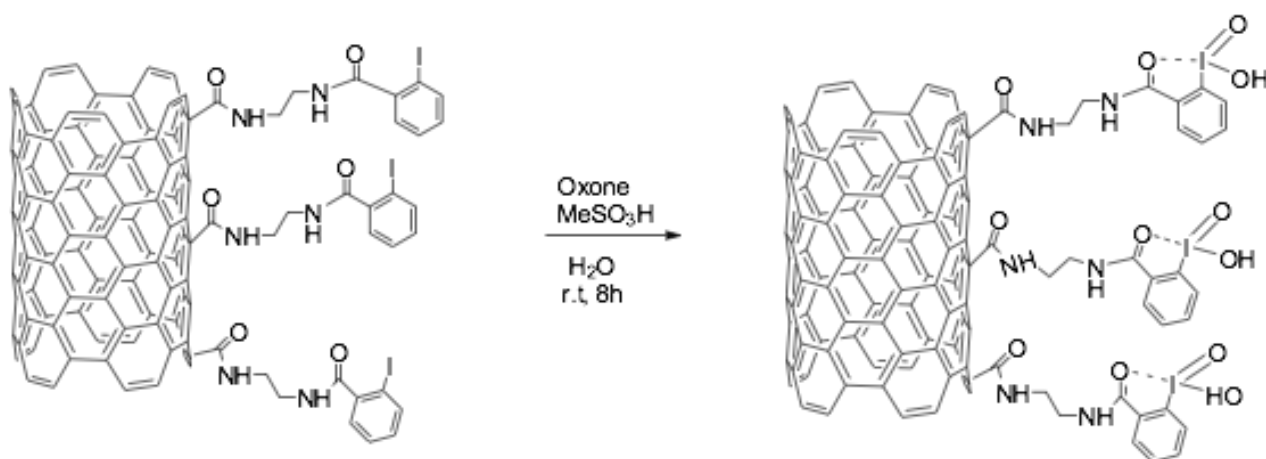
Figure 55. Oxidation of IBA to IBX

MWCNTs-IBA (100 mg) were suspended in H$_2$O (160 mL). Oxone (738 mg, 1,2 eq) and methane sulfonic acid (MeSO$_3$H) (85 µL, 1,2 equiv) were added and the reaction mixture was stirred for 8h at room temperature. The resulting solution was washed with DMF (5x) centrifuged at 4000 rpm for 20 minutes. After that the solution was washed with H2O (3x), centrifuged at 4000 rpm for 20 minutes, the supernatant was removed. Thereafter, the resulting MWCNTs-NH$_2$-IBX was dried in a freeze dryer.[173]

2.4.5 Preparation of IBX supported on MWCNTs,-OH functionalized
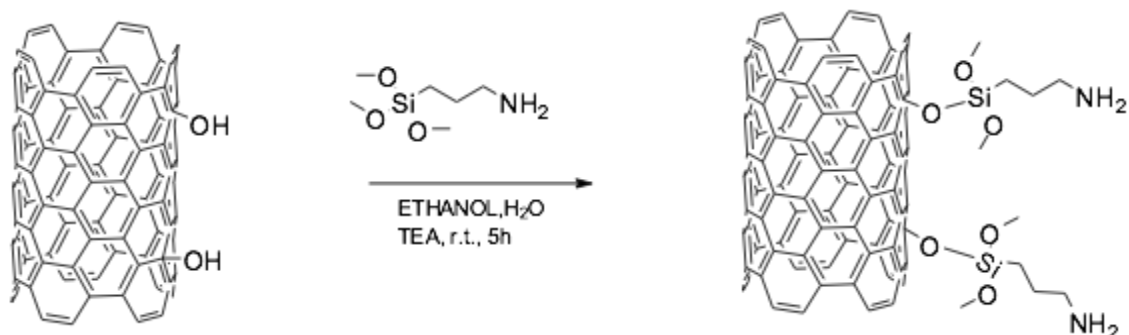
Figure 56. Introduction of APTMS linker

MWCNTs-OH (100 mg) were dispersed in 25 mL of ethanol by ultrasonication for 20 minutes. Then a solution of distilled water (300 μL), (3-Aminopropyl)trimethoxysilane APTMS (300 μL) and 100μL of TEA in ethanol (5mL). Was added to the suspension dropwise. The mixture was stirred at 900 rpm for 5 h. The final product was washed with ethanol and acetone three times respectively and dried in a vacuum desiccator overnight.

For the introduction of IBA and activation of IBA to IBX with oxone see step II and step III of Figure 53/54

2.4.6 Viruses and cells

Poliovirus type 1 (Sabin strain) (VR-1562), Human echovirus type 9 (VR-1050), Herpes simplex type 1 (HSV-1: VR-260), Herpes simplex type 2 (HSV-2: VR-734) and Coxsackie type B3 (Cox B3: VR-1034), were propagated in African green monkey kid- ney cells (Vero: CCL-81). Adenovirus type 2 (VR-1080) and Adenovirus type 5 (VR-1523) were propagated in Human Epithelial type 2 cells (HEp2: CCL-23). Cytomegalovirus (CMV: VR-538) was propagated in Human Foreskin Fibroblast Cell (HFF- 1: SCRC-1041). Viruses and cells were purchased from the American Type Culture Collection (ATCC). Cell lines were kept at 37 °C in a humidified atmosphere with 5% CO_2 and grown in Dulbecco's modified Eagle's Minimum Essential medium (DMEM) supplemented with 10% heat inactivated fetal calf serum (FCS), 2 mM L-glutamine, 0.1% sodium bicarbonate, 200 lg mL^{-1} of streptomycin and 200 units mL^{-1} of penicillin G. Working stocks of all viruses were prepared as cellular lysates using DMEM with 2% heat inactivated FCS (maintenance medium).

2.4.7 Biological assays

The compounds were initially dissolved in dimethyl sulfoxide (DMSO) and further diluted in maintenance medium before use to achieve the final concentration needed. The final dilution of test compounds contained a maximum concentration of 0.01% DMSO, which was not toxic to our cell lines. Acyclovir was used as the reference compounds.

2.4.8 Cell viability

The cytotoxicity of the test compounds was evaluated by measuring their effect on cell morphology and growth. Cell monolayers were prepared in 24-well tissue culture plates and exposed to various concentrations (lg/mL) of the compounds. Plates were checked by light microscopy after 24, 48, 72 and 96h. Cytotoxicity was scored as morphological alterations (e.g., round- ing up, shrinking, and detachment). Cell growth was determined by the 3-(4,5-dimethylthiazol-2-yl)-2,5-diphenyl tetrazolium bro- mide (MTT) method.[205] The cells were seeded at 1 10^4/mL (100 lL/well) in 96- well tissue culture plates such that cell replica- tion remained logarithmic all along the 4-day incubation period. The 50% cytotoxic dose (CD_{50}) was expressed as the highest con- centration of the compound that resulted in 50% inhibition of cell growth.

2.4.9 Antiviral activity

The assay of the antiviral activity against all the viruses tested was carried out by the 50% plaque reduction assay or by 50% virus-induced cytopathogenicity, as previously described.[206-207] The compound concentration required to inhibit virus plaque for- mation or virus-induced cytopathogenicity by 50% is expressed as the 50% effective concentration (ID_{50}) and calculated by dose–response curves and linear regression.

2.4.10 Effect of addition time

Monolayers of cells were grown to confluence in 24-well plates and inoculated with viruses at a MOI (multiplicity of infection) of 0.1. The plates were incubated for 2 h at 4 °C to ensure syn- chronous replication of the viruses, with or without compound R3 for the adsorption period. Then,

the inoculum was removed and fresh medium, with or without the compound, was added at various times after the adsorption period. The plates were incu- bated at 37 °C for 12 h, then cultures were frozen and virus yield was determined by plaque assay.

2.4.11 Inhibition of virus adsorption

Infective center assay was used to study the effect of compound 3b on the virus adsorption step. A VERO cell suspension (10^6 cells/mL) was cooled to 4 °C for at least 1h. HSV-1 (10^6 PFU/mL), incubated for 60 min at 37 °C with different concen- trations of test compound, was cooled to 4 °C, and subsequently added to the cell suspension. Cells were incubated with the virus- drug mixtures for 120 min at 4 °C to prevent the virus entering the cells. After the adsorption period, un-adsorbed virus and free com- pound were removed by washing three times with cold DMEM. The cells were then diluted serially and plaque assayed for cell-as- sociated viral activity.

2.4.12 Inhibition of virus adsorption Cell culture pre-treatment

Pre-treatment of cultures was performed by exposing the cell monolayers to different concentrations of the test compound in maintenance medium for 1 and 2 days at 37 °C. After treatment the cell monolayers were washed thoroughly with PBS and infected with HSV-1 at a MOI of 0.1 to allow viral cytopathic activity. The cell monolayers grown in maintenance medium without the test compounds were used as control. Virus titration was per- formed as described above.

2.4.13 Virucidal activity

To test possible virucidal activity, equal volumes (0.5 mL) of viral suspension (containing 10^6 PFU/ mL) and DMEM containing compound 3b (5 the ID_{50}) were mixed and incubated for 1 h at 37 °C. Infectivity was determined by plaque assay after dilution of the virus below the inhibitory concentration.

CHAPTER III: Prebiotic chemistry. Role of the silica gardens mediated in synthesis of biomolecules from formamide

3.1 INTRODUCTION

The origin of life is one of the most studied topics in science.[1-4] Probably, it occurred on Earth between 3.8 and 4.1billion years ago. [5] Prebiotic chemistry focus on the chemical processes that occurred on the erly Erth before the appearance of the life.[6-8] It is generally recognized that RNA is the most relevant molecule for the origin of life (RNA world),[9] since its specific catalytic and storage information properties.[10,11] The classic Miller–Urey experiment demonstrated that amino acids can be synthesized from a primitive atmosphere under conditions comparable to that existing on the early Earth. Various sources of energy have been proposed for these transformations, including electric discharges, redox processes and radiation. Other approaches (such as "metabolism-first" hypotheses) highlight the role of catalysis to provide biomolecules.[12] These processes are not confined to early Earth, since complex molecules are continuosly found in the Solar System and in the interstellar space, suggesting the generality of the phenomenum.[13,14,15,16] Molecules can be transferred from space to planets by meteorites, asteroids or cosmic dusts, a way that in principle is available for simple micro-organisms (the "panspermia" hypothesis).[17-19] The panspermia hypothesis therefore answers questions of where, not how, life came to be. It only postulates that life may have originated outside of the Earth. Nonetheless, Earth remains the only place in the Universe known to harbour life,[20,21] and fossils evidence from the Earth supplies most studies of abiogenesis. The age of the Earth is about 4.54 billion years;[22,23,24] the earliest undisputed evidence of life on Earth dates from at least 3.5 billion years ago,[25,26,27] possibly as early as the Eoarchean Era, when the crust started to solidify following the earlier molten Hadean Eon. Microbial mat fossils have been found in 3.48 billion-year-old sandstone in Western Australia.[28,29,30] Other early physical evidence of biogenic substances includes graphite [31] and possibly stromatolites [31]discovered in 3.7 billion-year-old metasedimentary rocks in southwestern Greenland, as well as "remains of biotic life" found in 4.1 billion-year-old rocks in Western Australia.[32,33] According to a scientist who commented on the study, "If life arose relatively quickly on Earth … then it could be common in the universe".

3.1.1 Formammide

Formamide (chemical formula: NH_2CHO) is the simplest natural amide. This compound contains all the elements required for the synthesis of biomolecules, including hydrogen, carbon, oxygen and nitrogen (with the only exception of phosphorus and sulfur). In recent years, the prebiotic chemistry of formamide has provided a unique and simple synthetic framework for the formation of components of nucleic acids (purine and pyrimidine nucleobases, nucleosides and nucleotides), amino acids, sugars, amino sugars and carboxylic acids, including important intermediates for cellular metabolism (Figure) [34]. The formamide is a ubiquitous molecule in the universe, was detected in comets [35], as in the case of the comet C / 1995 O1 (Hale-Bopp) [36], in the solid phase in granules around the young stellar object W33A and generally in the interstellar space. Furthermore, recent studies suggest the presence of formamide on some moons of the solar system, including Titan and Europe, where it has been postulated the presence of liquid formamide (pure or partially mixed with water) below the frozen surface.[37] Several experimental and theoretical studies have been conducted to determine how the formamide can be originated in space. [38] This molecule can be synthesized from mixtures of methane and nitrogen under proton radiation (solar wind and cosmic ray radiation)[39] or from frozen hydrogen cyanide (HCN), water and ammonia (NH3) by irradiation with ultraviolet rays[40]. The formamide can also be synthesized in terrestrial conditions from mixtures of low molecular weight compounds such as NH3, formic acid (HCOOH), carbon monoxide and alcohols. [41]
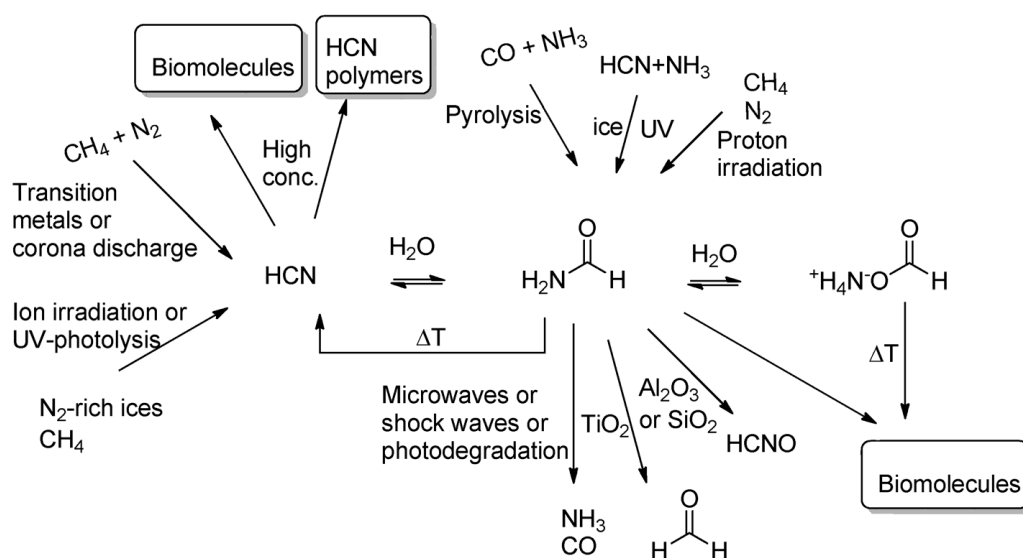
Figure 57. Formation, degradation and evolution of formamide in terrestrial conditions.

Among these routes of synthesis, probably the one that has most significant in terms of chemical terrestrial prebiotic, is the formation of formamide for HCN hydrolysis, a molecule present in significant concentration on the primitive Earth. The HCN in aqueous solution can result in two processes: the polymerization in biomolecules or hydrolysis to formamide. The hydrolysis predominates in dilute solutions, while the polymerization takes place at higher concentrations [42]. The estimated concentration of HCN in the ocean primitive was too low to give rise to polymerization reactions, thus favoring the formation of the formamide [42,43]

An interesting property that characterizes the formamide, as a precursor prebiotic, is linked to the possibility of a partial thermal degradation to generate a group of low molecular weight compounds which turn out to be, in turn, useful intermediates for the prebiotic synthesis of biomolecules, thus increasing the number and variety of possible ways of transformation [44]. Formamide decomposes thermally into NH3 and CO or HCN and H2O. The formation of HCN is usually favored in the presence of suitable catalysts, while in their absence predominates the formation NH3 and CO[45]. Furthermore, in the moment in which the formamide is in the presence of suitable metal oxides (such as titanium dioxide) can degrade to form (HCOH) formaldehyde, the precursor prebiotic currently most studied for the origin of the sugars. The synthetic potential of formamide is also incremented by particular physical conditions, such as by the action of microwave or high pressures [46].Due to its high dielectric constant, the formamide is also a good solvent for both the polar organic compounds and inorganic, the latter play an important role in the synthesis of prebiotics processes by acting as catalysts[47]. Finally, the formamide (and its other derivatives, such as N-methyl formamide, and the 'N, N-dimethyl formamide) may have played an important role in the phenomenon of the subdivision of the first cell, since it has been shown that these compounds catalyze the formation of micelles of ionic surfactants able to mimic a cell membrane[48] .
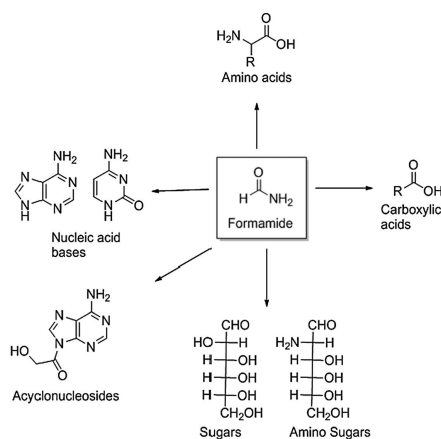
Figure 58. Synthesis of prebiotic molecules starting from formamide.

3.1.2. Synthesis of nucleobases from Formamide

Nucleobases and nucleobase derivatives can be easily synthesized from formamide under a large variety of experimental conditions.[,44] Thermal, photochemical or redox conditions can be applied in these reactions to yield the desired products in high yield[49-56] (Scheme 59)
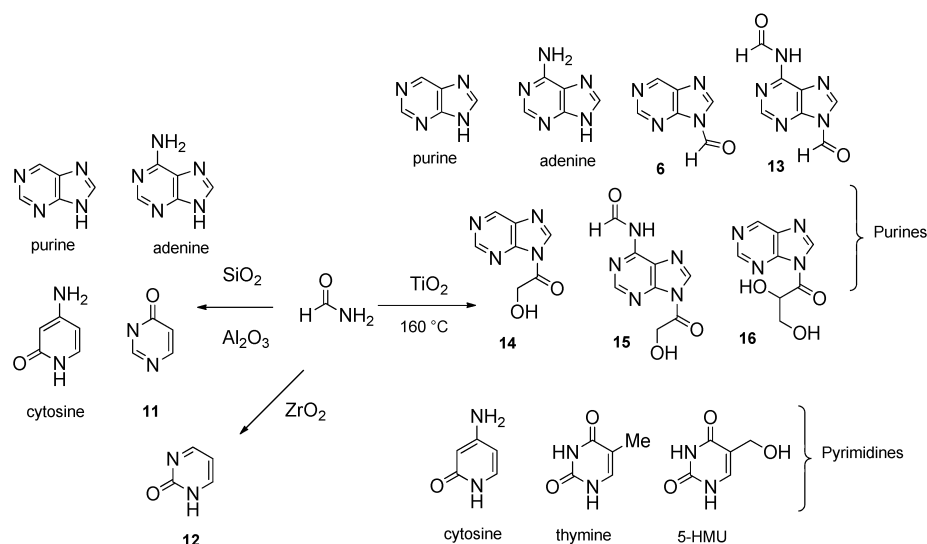
Figure 59. Role of different catalyst in the synthesis of prebiotic molecules starting from formamide.

With regard to the reaction mechanisms, for the adenine it was hypothesized the occurrence of condensation reaction which proceeds via the initial formation of a dimer of formamide, which subsequently reacts with HCN (formed by the decomposition of the same formamide), giving rise to an intermediate type polidiidro-pyrimidine (compound A Figure 60) variously substituted. From the subsequent reaction of this intermediate with NH3 (always generated by the decomposition of formamide) is obtained adenine (compound B figure 60). The mechanism of formation of guanine is similar to that of adenine[57].
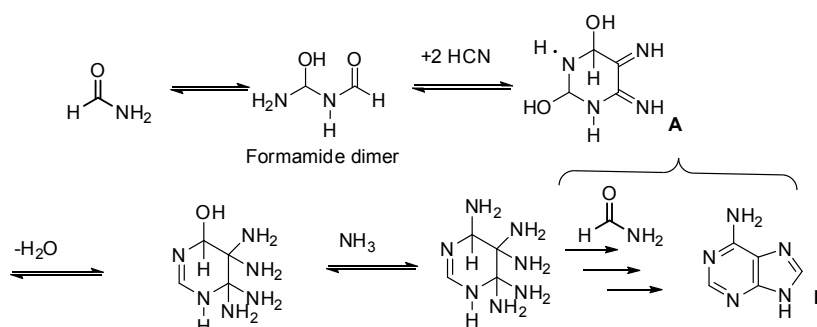
Figure 60. Mechanism of formation for purine ring.

The mechanism of formation of the pyrimidine nucleobases (cytosine, thymine and uracil) is only partially similar to that of purines, anticipating a different selectivity for the two families of components of nucleic acids [58]. For example, in the formation of cytosine (Compound C figure 61), the intermediate poliidro-pyrimidine A needs a redox reaction for the reduction of enamine groups to corresponding amine groups. This step, absent in the case of purines, it is necessary for the formation of the double bond C (5) -C (6) characteristic of the pyrimidine bases (Figure 61).
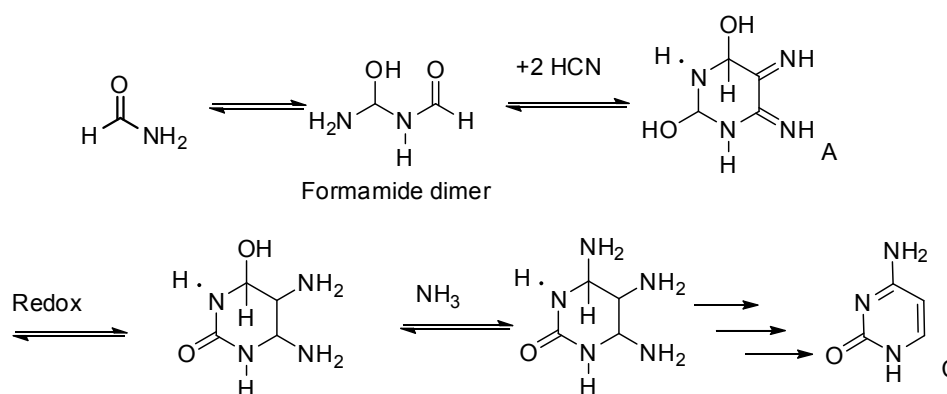
Figure 61. Mechanism of formation of pirimidine ring.

3.1.3. Prebiotic synthesis of sugars, nucleosides and acids.

The thermal condensation of formamide in the presence of titanium dioxide (one of the most abundant metal oxides on the primitive Earth) leads to the formation of acyclo-nucleosides, in which the nucleo base is linked to sugar in the side-chain.[59] Derivatives of this type have been hypothesized as possible components of the first molecules of nucleic acids (pre-RNA and pre-DNA molecules). A fundamental role in the formation of these derivatives is played by formaldehyde (produced by the degradation of formamide) through a process known as the "formose" reaction. In this reaction, the formaldehyde is activated by reaction with a with a base to afford a carbanion that further reacts by a mechanism similar to aldol condensation[60] (Scheme 27 and 28).
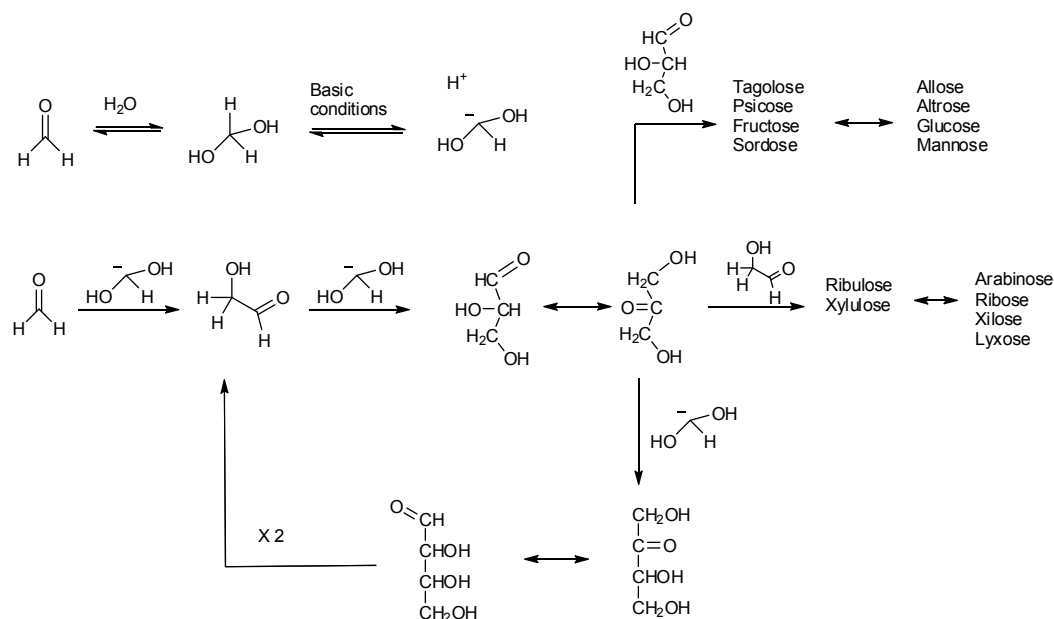
Scheme 27. Pathway proposed for the synthesis of linear sugars.

Carboxylic acids intermediates of the citric acid cycle (cycle of Krebs) and glyoxylic acid can be also synthesized from formamide in the presence of titanium dioxide, sulfur copper minerals or zirconia.[61-62].

.
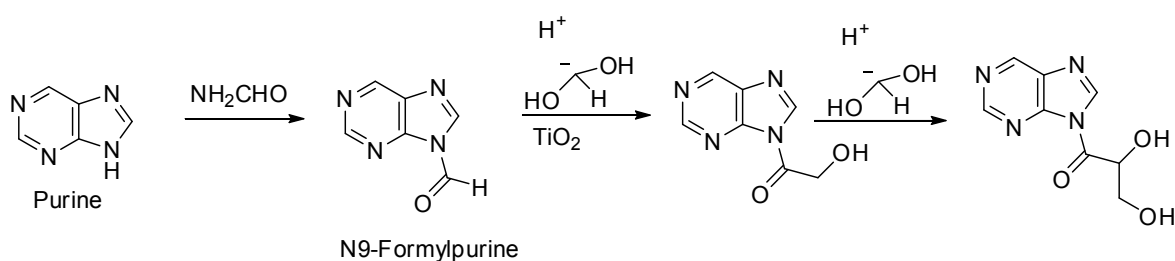
Scheme 28. Acyl-Purine synthesized from NH_2CHO,

3.1.4. Catalysts: silicates and phosphates.

Silicates and phosphates catalyze the synthesis of nucleobases from NH_2CHO. As an example, the thermal condensation of NH_2CHO in the presence of silicates with different magnesium and iron content, such as fayalite ($FeSiO_4$), olivine ($MgFeSiO_4$) and forsterite ($MgSiO_4$), afforded cytosine, uracil, 4(3H)-pyrimidinone and 5,6-dihydrouracil , in addition to the simple purine and urea. The

reaction showed the highest efficiency when performed in the presence of cosmic-dust analogues (CDAs).[63] CDAs are "fluffy" grains of amorphous silicates with variable proportions of silicium and carbonaceous matrices, prepared by laser ablation techniques [64] and repro- ducing the chemical composition and morphology of the silicate dusts present in large amounts in space environments. [65] As a general trend, the yield of nucleic acid bases increased by increasing the amount of iron in the elemental composition of the mineral in the following order of reactivity: fayalite > olivine > forsterite, suggesting the possibility of a redox step as a crucial process for the formation of the pyrimidine scaffold. These data show that CDAs are favorable microenvironments mainly for the synthesis of pyrimidines, which are not easily obtained under terrestrial conditions. [66,67] CDAs analogues of silicates are also efficient catalysts for the synthesis of simple organic compounds, such as hydrocarbons, amine and nitrile derivatives, through Fisher–Tropsch- and Haber–Bosch- like condensations at high temperature. [68] In addition, silicates such as alkali feldspar [(Na, K)AlSi$_3$O$_8$] and clinopyroxene [(Ca, Mg, Fe)SiO$_3$], present in rocks of the Earth's crust as well as on other planets of the Solar system, are characterized by chiral crystal surfaces.[69]

Such natural chiral environments may provide stereoselective functions and resolution of racemic mixtures in prebiotic processes.[70]

Meteorites were also investigated as catalysts in NH_2CHO prebiotic chemistry.[71] Under thermal conditions they catalyzed the condensation of NH_2CHO to nucleobases in addition to carboxylic acids, amino acids and sugar precursors. These results suggested that NH_2CHO condensation reactions in the parent bodies of carbonaceous meteorites could give rise to organic compounds engaged in both genetic and metabolic apparatuses, introducing on the scene two key compo- nents of primitive life. The meteorite minerals had little or no effect in promoting hydrolysis of RNA (see Section 8.2.1) at 80 1C over a pH range from 4.2 to 9.3, the highest stability being observed in the neutral pH range, with a half-life of 5 h.[71]

Minerals can in principle perform at the same time as catalysts and reactants. This is the case of mineral phosphates. Most of the phosphorus in the early Earth would have been in the form of insoluble minerals. On the other hand, chemical and physical conditions exist generating reactive phosphorus from these insoluble materials. As an example, lightning discharges in model prebiotic atmospheres reduce ortho- phosphates to reactive phosphites.[72]

Soluble inorganic phosphates [73] and phosphonic acids [74] were used for the phosphorylation of nucleosides in water to yield mixtures of nucleotide derivatives. The efficiency of this reaction increased in the presence of condensing agents containing activated multiple bonds (cyanamide and urea). A selection of relevant reference is in ref. [75]. Further discussion on this topic is in Section 5. Reviews on phosphorylation, condensation or polymerization of biomolecules with (poly)phosphates poten- tially produced by volcanic activity have been reported.[76,77,78] Simple inorganic phosphates (Na_3PO_4, $Na_4P_2O_7$ and $Na_5P_3O_9$) and mineral phosphates like hureaulite [$Mn^{2+}(PO_3OH)_2(PO_4)_2$- $(H_2O)_4$], libethenite [$Cu^{2+}_2(PO_4)(OH)$], turquoise [$Cu^{2+}Al_6$-$(PO_4)_4(OH)_8(H_2O)_4$], childrenite [$Mn^{2+}(AlPO_4(OH)_2H_2O$], vivianite [$Fe^{2+}_3(PO_4)_2(H_2O)_8$] and vauxite [$Fe^{2+}Al_2(PO_4)_2$- $(OH)_2(H_2O)_6$] catalyzed the thermal condensation of NH_2CHO to yield a large panel of nucleic acid precursors, including purine, adenine, hypoxanthine, cytosine, uracil, 5,6-dihydrouracil. N-formyl glycine and low molecular weight compounds such as urea, parabanic acid and carbodiimide (Scheme 13).[79]

Carbodiimide is one of the most powerful condensing agents in organic chemistry for the formation of amide or ester bonds.[81] In the formation of peptide bonds this compound acts by initial addition of an amino acid on its carbon atom with high electrophile character. This process generates a good leaving group that can be eliminated as an urea molecule during the formation of the new bond between the two amino acid residues.[82] Dehydration of urea yields back carbodiimide.[83] The presence of both urea and carbodiimide among the products of condensation of formamide suggests the existence of a carbodiimide–urea organocatalytic cycle, explaining the presence of N-formylglycine in the reaction mixture. In fact glycine, once formed in the presence of carbodiimide and of an excess of formamide, can be easily formylated by a reaction mimicking the formation of a dipeptide. In principle, the carbodiimide generated by degradation of formamide can catalyze the formation of both peptides and oligonucleotides, the mechanism of formation of the ester bond being similar to that of the amide bond.

3.1.5. Silica Gardens

The easiest way to produce chemical gardens is to place crystals of suitable metal salts into a beaker and pour alkaline silica sol on them (or, conversely, submerge the salt crystals into a large volume of the sol). This will induce the self-assembly of forms as those displayed in Fig. 11.1B. Indeed, almost any metal salt can be used to grow such structures, provided that it contains cations that will precipitate upon reaction with hydroxide and/or silicate anions (which is essentially true for all multivalent cations). Typical cations employed for this purpose include Co^{2+}, $Fe^{2+/3+}$, Cu^{2+}, Ni^{2+}, Zn^{2+}, Mn^{2+}, Al^{3+}, and Ca^{2+}, in salts with counterions such as Cl, NO_3, or SO_4^2 [84]. The silica sol needed to prepare chemical gardens can readily be obtained by diluting commercial water glass ($6.25 M "SiO_2"_{(aq)}$). In fact, the concentration of the sol (and with it, the pH) is the only crucial parameter for the morphological evolution, and an opti- mum structuring effect is generally observed for a certain range of silica con- centrations, which may vary depending on the type of metal salt. For instance, in the case of cobalt chloride, well-developed silica gardens have been generated with 1:4 and 1:8 dilutions (v/v) of water glass, whereas toward both lower and higher silica content, either the structures became more and more ill-defined or growth did not occur at all [85].The choice of the cation determines the color of the resulting precipitates , whereas corresponding morphologies do not show any systematic differences. Usually, silica gardens consist of hollow tubes that may extend over several decimeters in length, while their diameter is limited to a few millimeters and their walls are only some tens of microns in width[86]. These tubes grow more or less vertically from the immersed metal salt crystal, by a mechanism involving forced (osmosis) and free con- vection (buoyancy) as well as chemical reaction (precipitation), as illustrated schematically in Figure 62. [87]: upon addition of silica solution to solid metal salt (Panel 1), a film of hydrated metal silicate is immediately formed over the surface of the crystals
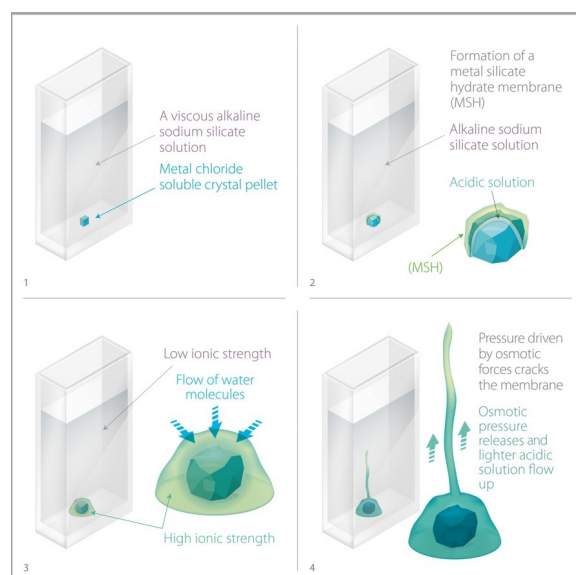
Figure 62. Sketch depicting the formation of silica gardens in a classical setup, where sodium silicate solution is added to random crystals or pellets of solid metal salt (1). Growth of vertical tubes occurs by the following successive events: initial dissolution of metal salt and precipitation of a metal silicate membrane (2), inflow of water through the membrane caused by osmosis (3), rupture of the membrane and ejection of con- centrated metal salt solution, which rises vertically due to buoyancy and becomes solid- ified into a tube by instant precipitation of metal hydroxide and silica (4).

(Figure 62 panel 2). Then, osmosis causes water to flow through this barrier and dissolve the enclosed solid salt (Figure 62 panel 3). This increases the internal pressure and leads to swelling of the flexible membrane, until a critical stage is reached and rupture occurs. At this point, the outer layer breaks, and a jet of con- centrated metal salt solution is ejected into the surrounding medium (Figure 62 panel 4). Owing to buoyancy, the lighter acidic salt solution ascends vertically into the heavier alkaline silica sol and becomes rapidly solidified due to simultaneous precipitation of metal hydroxide and/or silicate at the interface between the chemically distinct environments. In this way, a wall is generated around the initially liquid jet, producing the observed capillary-like tubules. Corresponding work was not only focused on exploring other oxyanions like aluminates, oxalate, or phosphates[88,89] but also included distinct inorganic species such as hexacyanoferrates, which were reacted with Fe^{3+} to give Prussian blue-type precipitates[90]. Recently, the concept of chemical gar- dens was even extended to organic–inorganic composite systems based on polyoxometalates and polyaromatic cations[91]. Procedures applied for the preparation of these modified materials are generally similar to those described earlier for their siliceous counterparts, with greater or lesser modifications as detailed in the respective literature. A first step toward an improved reproducibility of the experiments is to use pressed metal salt pellets, rather than irregular crystals[91]. This will affect morphogenesis for two reasons. On the one hand, the rate of salt dissolution is lower for

pellets than for random microcrystals, so that the kinetics of membrane precipitation will change. On the other hand, commercially available crystals often contain significant amounts of air enclosed in voids, which become released upon dissolution and may form a gas bubble that sometimes guides tube formation. This effect can be excluded in experiments with pressed pellets, especially if the tablets have been further degassed in vacuum prior to use. To prepare the pellets, a predefined mass of metal salt is ground in either an agate mortar or an electric mill for periods of at least one minute (ideally in steps of 20 s to avoid over- heating). For this purpose, salts with the highest possible amount of hydration water should be employed, in order to minimize uncontrolled uptake of the partially strongly hygroscopic substances during grinding. Finally, the homogenized powder is pressed into a tablet with uniform dimensions by means of custom-designed pellet makers at controlled pressures of typically a few bars. [92]

3.1.6. Liquid injection method

Instead of using solid crystals, the metal salt can also be introduced into the silica sol by injecting concentrated solutions. This technique was developed by Steinbock and coworkers[93] to gain a better control over the formation of the tubular structures. In a typical experiment (Figure 63 A), a glass nozzle (inner diameter, 1 mm) is inserted vertically at the bottom of a glass cylinder containing ca. 1 M silica solution. The metal solution (e.g., $CuSO_4$, c ¼ 0.1–0.5 M) is injected through the nozzle using a peristaltic (or syringe) pump at rates ranging from 1 to 20 mL/h. It is important to fill the nozzle and the tubing between the pump and the nozzle first with metal salt solution, before adding the silica sol to the glass cylinder. Otherwise, uncon- trolled precipitation at the outlet may cause clogging of the nozzle; however, any solid deposits in the nozzle are usually removed once the injection is started. In analogy to the classical preparation method, liquid injection leads to the formation of a continuous buoyant jet of solution[56], which is progressively mineralized to yield capillaries of several hundreds of microns in width (independent of the actual nozzle diameter). As a main advantage of this technique, growth occurs in a highly controlled manner under these conditions and affords well-defined tubules with reproducible dimensions, while avoiding random processes like branching or intergrowth.
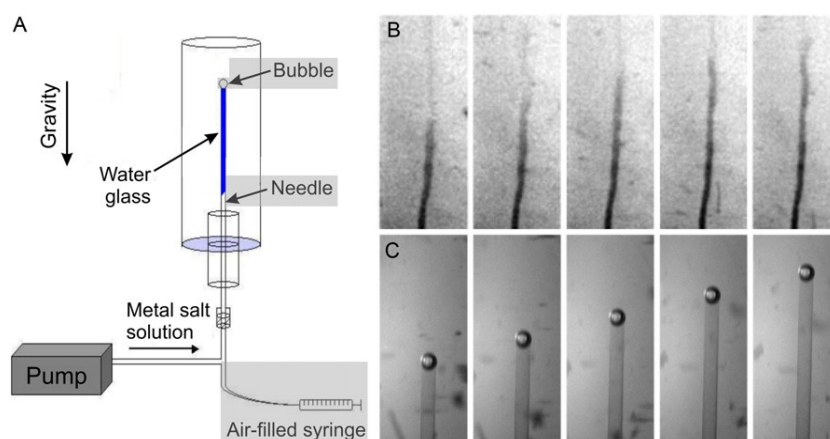
Figure 63. Growth of silica gardens by means of liquid injection. (A) Schematic drawing of the experimental setup. Gray-shaded parts are modifications required for the controlled introduction of a structure-guiding air bubble. (B) Time-lapse series of pictures showing the formation of a tubular structure by injection of 0.25 M cupric sulfate solution into 1 M sodium silicate sol(C) Image sequence illustrating how a manually generated air bubble directs vertical growth of a perfectly straight tube upon injection of 0.5 M CuSO4 into 1 M silicate solution (field of view, 7.3 3.0 mm^2).

Even greater control can be gained via a templating approach, in which an ad hoc generated gas bubble directs the flow of the metal salt solution and thus determines the shape of the emerging tubes[94]. To that end, a needle is inserted into the nozzle and connected to an air-filled syringe (Figure 63 A). Salt solution and air are injected at the same time using T-shaped tubing, whereby the tip of the needle should slightly protrude from the top of the nozzle. While injecting the metal salt solution, air bubbles (typical volumes of 0.1–1 mL) are generated manually at regular intervals, until one of them gets pinned to the forming tube. The bubble then rises vertically in the silica sol, due to buoyancy, and guides the metal salt jet to give perfectly straight hol- low tubules (Figure 56 C). The tube diameter scales in a linear fashion with the size of the bubble and hence can be tuned rather precisely within a range of 100–600 mm[95]. Further parameters able to affect the size and shape of the tube include the concentrations of both the metal salt solution and the silica sol: while increasing amounts of metal ions may favor budded patterns over straight tubules, higher silica contents in the sol can yield intricate twisted ribbonlike forms. Finally, it is worth mentioning that regular silica garden tubes can also be produced in a reversed setup, that is, when silica sol is pumped from the top into an excess of metal salt solution. In this case, the tubules grow along the downward stream of the heavier silicate solution and exhibit roughly similar diameters and morphologies.[95]

3.1.5.1. Isolation and characterization of silica gardens

In general, silica garden tubes are very fragile and thus have to be handled with great care. Nonetheless, manipulations are possible with the aid of a thin brush or needle or by using electrostatic forces with, for example, a charged plastic pipette tip.[96] The dry tube walls may then be ground to give a homogeneous powder suitable for bulk analyses by XRD, IR, Raman, NMR, and XPS spectroscopy.[97] Alternatively, in order to examine the microstructure of the walls in their native state, the intact tubes can be broken into manageable pieces, which subsequently are fixed onto SEM stubs for morphological studies or on X-ray diffraction holders for textural analyses. By varying the orientation of the membrane on the stub, the inner and outer surface of the tube walls as well as their cross section can be studied separately by SEM and EDX. In this way, it was found that the tube walls show a gradient in their composition, with silica-rich domains characterizing the outer side of the wall and an excess of metal hydroxide/oxides covering the inner surface. In order to complement this information, the overall content of relevant elements can be independently determined by dissolving the tube wall in acid and measuring the concentrations of the different species with the aid of atomic emission spectroscopy (AES). Finally, the morphology and crystallinity of nano- and micron scale subunits constituting silica garden membranes can be investigated in detail by means of TEM and electron diffraction, after successful transfer of small fragments onto suitable grids. Despite the insight gained into the nature of chemical gardens via ex situ methods, a more promising way to study the formation of these structures is to follow the growth process in situ. Most frequently, this has been achieved by acquiring time-lapse pictures of the emerging structures, using standard photographic equipment. Such experiments should preferably be carried out in flat rectangular cells to improve the quality of the images. On that basis, the morphological evolution of the system can be monitored and quantified by measuring time-dependent tube dimensions. This sheds light on precipitation kinetics and allows distinct growth regimes (e.g., jetting or budding) to be identified Another interesting class of experiments is dedicated to the role of osmotic pressures and membrane rupture events during the formation of silica gardens. For example, the osmotically forced inflow of water from the silica sol into the inner metal salt compartment was investigated by placing a metal silicate-based membrane in between the two solutions and tracing the volume change on the metal salt side. In turn, the circumstances leading to membrane rupture were studied by pumping metal salt solution into silica sol and measuring the pressure at the inlet as a function of time. Both experiments showed that the self-assembly of silica gardens is driven by consecutive cycles of osmotic pressure increase and relief. [97]

3.1.5.2. Tracing dynamic diffusion and precipitation processes in silica gardens

Beyond simple monitoring of the evolution of these fascinating structures, a recurrent main goal has been to track time-dependent variations in chemical conditions during growth and aging of silica gardens in situ. However, a limiting factor in this context is the diameter of the tubes, which usually reaches some hundreds of microns at most [97] Therefore, the inner metal salt compartment cannot be easily accessed, rendering direct analyses of solution chemistry difficult. This problem was solved in a recent study, where a new experimental setup was developed that allows single macroscopic tubes to be obtained in a very reproducible fashion[98] . The method relies on the use of uniform pressed salt pellets and the controlled and slow addition of silica sol to these pellets, as illustrated by Figure 64A
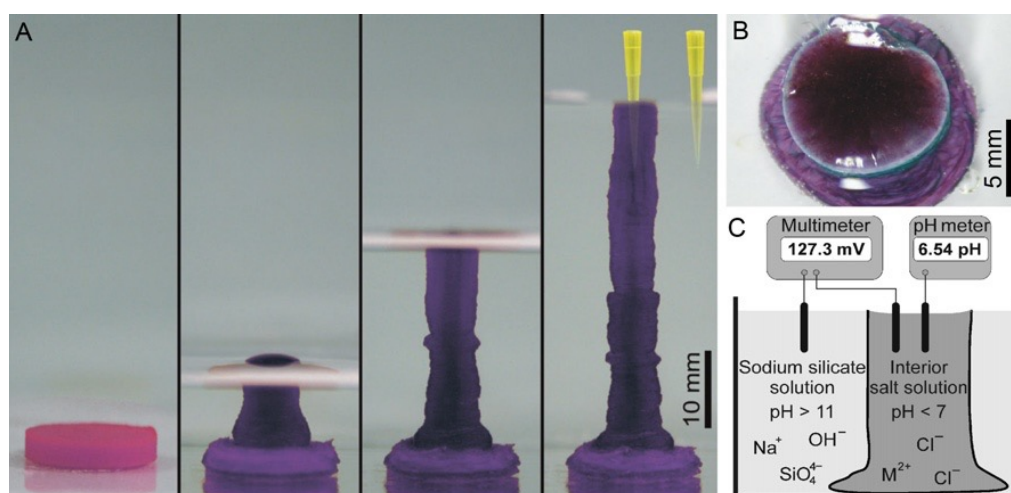
Figure 64. New preparation method for silica gardens. (A) Image sequence showing the formation of a macroscopic tube from a pellet of $CoCl_2$ $6H_2O$ by controlled dosing of silica sol. Pipette tips indicate that samples can easily be drawn from both the inner solu- tion enclosed by the membrane and the outer reservoir surrounding it. (B) Top view of the tube, demonstrating that it has an open end. (C) Schematic representation of the experimental setup used for characterizing the temporal evolution of the macro- scopic silica garden system.

Under suitable conditions, this procedure affords tubes with lengths up to 5 cm and diameters of around 1 cm. Moreover, the tubes have an open end on top rather than being closed (Fig. 57B), so that the solutions on both sides of the membrane can readily be sampled (as indicated by the pipette tips in Figure 64 A).

For the preparation of such large silica garden tubes, ca. 0.5 g of dried metal salt (typically $CoCl_26H_2O$ or CoI_2H_2O) is first ground to a fine powder, which is subsequently transferred to a

hydraulic press and converted to a tablet of about 13 mm in diameter and 2 mm in height by applying a pressure of 3.5 bar for several minutes. The pellet is then fixed at the bottom of a beaker (total volume of 120 mL) by using a piece of double-sided adhesive tape. To initiate growth, 10 mL of silica sol (1:4 dilution of water glass) is added within around 10 s over the rim of the beaker through a needle attached to a syringe. This leads to gradual dissolution of the metal salt pellet, which soon becomes visibly covered by a layer of hydrated silicate. At this point, further silica sol is added, now however by means of an automated dosing device that dispenses the sol at a constant rate of 2 mL/min. In the following, the tube grows continuously, until it has reached its maximum length after about 15 min. Similar structures can be obtained in the same way for other metal salts like $FeCl_2$ or $FeCl_3$, although addition rates have to be adjusted if the cation is changed (generally 1–10 mL/min). It is worth mentioning that after dosing of silica sol has been completed and macroscopic growth essentially ceased, continued inflow of water can cause an overflow of metal salt solution at the open top of the tube, leading to uncontrolled outgrowths along the air–liquid interface. This unwanted process can be avoided by removing small volumes of the inner solution after completed addition, giving uniform vertical tubes as shown in Figure 64 A. The as-formed precipitates are relatively stable and can be iso- lated into dry state without destroying their ultrastructure. For this purpose, the outer silica sol is withdrawn with a syringe, whereas the remaining inner metal salt solution can be carefully sucked out of the tube utilizing a thin needle. After washing with water and ethanol, the dried membranes can be characterized as described in the previous section.

The major advantage of this new synthesis method is that it offers the possibility to monitor ongoing diffusion and precipitation processes by measuring distinct physicochemical parameters as a function of aging time after completed tube preparation (Figure 64 C). For instance, the concentrations of ions dissolved in the inner and outer solution can be determined by drawing aliquots from the two reservoirs and analyzing them by means of AES. As the amount of liquid inside the tube is rather limited (usually about 0.2–0.5 mL), only small volumes (e.g., 10 mL) should be taken, whereas larger samples (100 mL) can be drawn from the outer sol. Subsequently, the samples are diluted with 10 mL water and characterized by AES. This yields precise concentrations for all relevant elements in both compartments at any given time. In essence, these studies have revealed that the development of silica gardens is not at all terminated once macroscopic tube growth is completed and that ion diffusion and precipitation remain active over time frames as long as tens of hours, due to the enormous concentration gradients established during

initial separation of the two compartments. Moreover, the collected concentration data provide clear evidence that the walls of silica gardens cannot be considered semipermeable mem- branes, as commonly believed, but rather combine properties of both diaphragms and membranes, which allow multiple ionic species to diffuse through them with time.

Instead of discontinuous sample drawing as required for AES measurements, the evolution of silica gardens can also be directly followed in situ by introducing suitable sensors into the inner and/or outer solution. Owing to the large diameter of the synthesized tubes and its open end, it is, for example possible to immerse a pH microprobe in the metal salt reservoir and continuously collect data. Again, valuable information can be derived concerning the progress of precipitation and diffusion, in particular because the pH determines the solubility of both metal hydroxides/oxides and silica [98]. Another parameter worth to be investigated in light of the drastic concentration gradients across the tube wall is the elec- trochemical potential difference between the two compartments. Such measurements merely require two platinum stick electrodes, which are sub- merged in the solutions inside and outside the membrane (Figure 64 C). By connecting the electrodes to a conventional multimeter, potentials can directly be recorded in a time-resolved manner. Corresponding data indi- cate that the compartmentalization occurring during the early stages of silica garden formation generates considerable electrochemical potential differ- ences with initial values as high as 100–200 mV [98]. The measured voltage then decreases with time in several steps, which immediately correlate with the progress of ion diffusion and precip- itation. Overall, these findings indicate that silica gardens are complex systems that run through a cascade of dynamic coupled processes before ultimately returning to equilibrium. During this period, significant potential differences are created spontaneously and maintained over hours, which might be promising for the use of silica gardens as self-catalyzed chemical reactors and/or batteries[98]

3.2. RESULTS AND DISCUSSION

The most efficient geological abiotic route to organic compounds results from the aqueous dissolution of olivine, a reaction known as serpentinization[99]. In addition to molecular hydrogen and a reducing environment, serpentinization lead to high-pH alkaline brines that can become easily enriched in silica. Under these chemical conditions, the formation of self-assembled nanocrystalline mineral composites, namely silica/carbonate biomorphs and metal silicate hydrate (MSH) tubular membranes (silica gardens), is unavoidable as previously described. The osmotically driven membranous structures have remarkable catalytic properties that could be operating in the reducing organic-rich chemical pot in which they form. Among one-carbon compounds, formamide (NH_2CHO) has been shown to trigger the formation of complex prebiotic molecules under mineral-driven catalytic conditions, proton irradiation, and laser-induced dielectric breakdown. Here, the study is focused on the MSH membranes as catalysts for the condensation of NH_2CHO, investigating the possible formation of prebiotically relevant compounds, including carboxylic acids, amino acids, and nucleobases. Membranes formed by the reaction of alkaline (pH 12) sodium silicate solutions with selected inorganic salts as $MgSO_4Fe_2(SO_4)_3 \cdot 9H_2O$ $CuCl_2 \cdot 2H_2O$, $ZnCl_2$, $FeCl_2 \cdot 4H_2O$, and $MnCl_2 \cdot 4H_2O$ were studied in terms of catalytic efficiency. As a preliminary approach, we investigated the formation of MSH in the presence of NH_2CHO. MSH formed readily in the presence of up to 40% NH_2CHO from pellets of the selected salts in a sodium silicate solution (SSS) containing 1%, 5%,10% or 40%(v/v) NH_2CHO.

Figure 65.Sodium silicate solution containing 1%, 5%,10% or 40%(v/v) NH_2CHO

On the basis of these data, we designed two sets of experiments able to model the chemical environment in the outer and inner parts (Figure 65)of the tubular structure. In the first experiment, we dipped selected and preformed MSH tubules [$ZnCl_2$, $FeCl_2 \cdot 4H_2O$, $CuCl_2 \cdot 2H2O$,
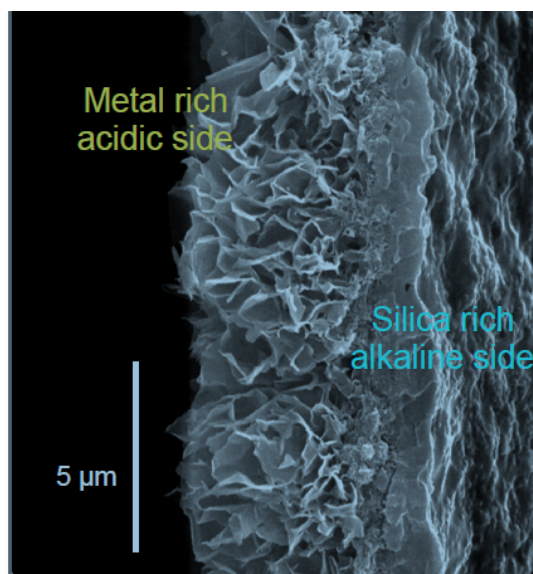
Figure 66. Outer and inner parts of silica garden.

$Fe_2(SO_4)_3 \cdot 9H_2O$, or $MgSO_4$] in an alkaline (pH 12) solution of sodium silicate containing 10% (v/v) NH_2CHO. In two selected cases $FeCl_2$ and $Fe_2(SO_4)_3 \cdot 9H_2O$ the first experiment was repeated in the presence of the membrane in growth by the addition of the pellets of soluble salts directly inside the sodium silicate solution. In the second experiment, we modeled the chemistry of the inner part of the tubular structures by dipping the selected MSH membrane in a water solution and 10% (v/v)NH_2CHO. As a control experiment, we also analyzed the output of an alkaline solution (pH 12) of sodium silicate with NH_2CHO (**101**) (10% v/v) in the absence of MSH membranes.
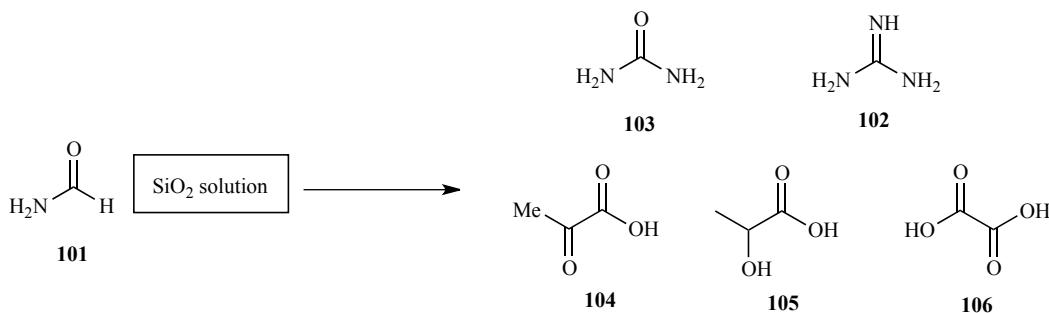
Scheme 29. Products obtained after the Reaction of **101** with SSS at different temperatures

Table21 Products obtained (mg) after the Reaction of NH_2CHO with Sodium Silicate Solution at Different Temperatures[a]

Product/Temperature[b]	25 °C	80°C	120°C
Guanidine 102[b]	traces	traces	traces
Urea 103	1.0×10^{-3}	2.2×10^{-3}	0.5×10^{-3}
Pyruvic ac. 104	1.1×10^{-3}	1.9×10^{-3}	0.3×10^{-3}
Lactic ac. 105	0.7×10^{-3}	1.0×10^{-3}	traces
Glycolic ac. 106	traces	traces	-

[a]NH_2CHO (200 µL) was mixed with the sodium silicate solution (2.0 mL) at the reported temperatures for 24 h. The data are the mean values of three experiments with standard deviations of less than 0.1%.

All of the experiments ran for 24 h at the optimized temperature of 80 °C. The experiments were reproduced three times. The results of the experiments are shown in Table 21 and Scheme 29 . As a general trend, the control reaction at 80 °C afforded a panel of compounds larger than that obtained at 25 and 120 °C. Guanidine (102), urea (103), pyruvic acid (104), lactic acid (105), and glycolic acid (6) were observed in small amounts (Table 21).
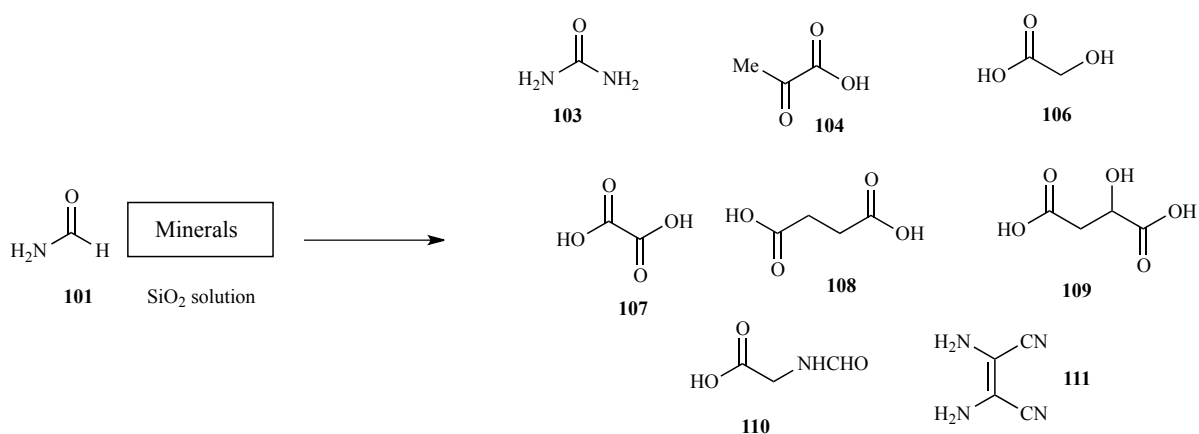
Scheme 30.Products obtained after the Reaction of **101** with SSS at different temperatures in presence of selected

The temperature of 80 °C was selected for the next reactions. In the presence of MSH membranes a larger variety of products was obtained (Tables 22 and 23, respectively). In particular, the experiment modeling the catalytic effect of the outer side of the membrane afforded 102, 103, 104, 105, 106, oxalic acid (107), succinic acid (108), malic acid (109), N-formylglycine (110), and diamino malonitrile (DAMN) (111) (Table 22 and Scheme 30). Similar results were obtained in the

presence of the growing membrane. Interestingly, the chemical environment modeling the inner side of the tubular structures afforded an

Table 22. Products Obtained after the Reaction of NH_2CHO and SSS in the Presence of Selected MSH[a]

Product/MSH[b,c]	ZnCl$_2$	FeCl$_2$	CuCl$_2$	Fe$_2$(SO$_4$)$_3$	MgSO$_4$
Guanidine 102	-	0.90 (0.40)[d]	traces	0.80 (0.90)[d]	traces
Urea 103[c]	2.0 x10-3	0.80 (0.32)	0.90	0.015 (n.d.)[e]	0.01
Pyruvic ac.104	1.9 x10-3	0.83 (0.24)	traces	0.15 (0.05)	-
Lactic ac. 105	0.15	0.63 (0.92)	traces	0.16 (0.11)	-
Glycolic ac. 106	0.11	0.01 (0.12)	-	traces	0.11
Oxalic ac. 107	2.8 x10-3	0.18 (n.d.)	-	0.38 (0.25)	0.12
Succinic ac. 108	-	-	0.16	0.096 (0.01)	0.071
Malic ac. 109	-	-	-	0.02 (0.06)	0.005
N-Formylglycine 110	6.0 x10-3	traces (n.d.)	-	9.0x10-3 (n.d.)	2.3x10-3
DAMN 111	-	0.46 (n.d.)	-	0.13 (0.64)	0.09

[a]NH_2CHO (200 µL) was mixed with SSS (2.0 mL) in the presence of preformed MSH (2.0% w/w) at 80 °C for 24 h.[b]The data are the mean values of three experiments with standard deviations of less than 0.1%.[c]The amount of product is defined as milligrams of compound compared to that of the initial reaction mixture.[d] NH_2CHO (200 µL) was mixed with SSS (2.0 mL) in the presence of selected growing MSH (starting from 2.0% w/w of the corresponding salt's pellet) at 80 °C for 24 h. [e] nd = not determined.
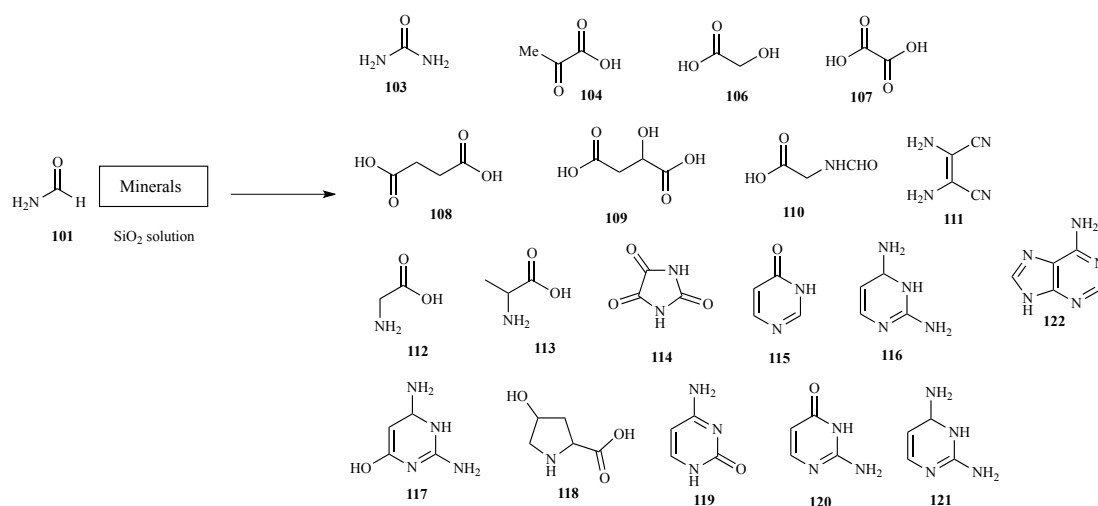
Scheme 31. Products obtained after the Reaction of 101 with distilled water at 80° in presence of selected MSH

Table 23. Products Obtained after the Reaction of NH_2CHO and Distilled Water in the Presence of Specific MSH[a]

Product/MSH[b]	$ZnCl_2$	$FeCl_2$	$CuCl_2$	$MnCl_2$	$Fe_2(SO_4)_3$	$MgSO_4$	CuN_2O_6
Guanidine 2[c]	5.2×10^{-3}	3.4×10^{-3}	1.6	0.1	0.18	0.12	0.67
Urea 3	traces	-	1.7	5.0×10^{-3}	-	traces	-
Pyruvic ac. 4	4.1×10^{-3}	0.01	1.8×10^{-3}	-	0.73	0.7	0.28
Lactic ac. 5	-	-	-	-	0.07	0.05	-
Oxalic ac. 7	traces	-	0.10	-	traces	traces	-
Succinic ac. 8	-	-	-	-	0.21	0.17	0.18
Malic ac. 9	-	-	-	-	0.03	0.03	-
N-Formylgly 10	2.5	0.85	traces	-	1.9	1.8	-
DAMN 11	-	-	-	-	0.02	traces	-
Glycine 12	0.03	0.23	0.76	-	0.57	0.53	-
Alanine 13	traces	traces	traces	-	0.27	0.23	-
Parabanic ac. 14	-	-	0.59	-	-	-	0.9
4(3H)-Pyr 15	-	-	5.6	0.3	traces	traces	0.05
2,4-DAP 16	-	-	0.3	0.02	0.18	0.17	traces
6(OH)-2,4-DAP 17	-	-	0.3	0.06	-	-	traces
2,4-DAP-5COOH 18	-	-	traces	-	traces	traces	0.14
Cytosine 19	-	traces	0.13	-	0.18	0.15	1.2
Isocytosine 20	-	traces	5.0	-	0.11	0.11	1.4
Uracil 21	traces	-	3.8	0.03	0.22	0.23	0.85
Adenine 22	-	-	0.01	-	0.01	0.01	traces

[a]NH_2CHO (200 μL) was mixed with water (2.0 mL) in the presence of selected MSH (2.0% w/w) at 80 °C for 24 h. [b]The data are the mean values of three experiments with standard deviations of less than 0.1%.[c] The amount of product is defined as milligrams of compound compared to that of the initial reaction mixture.

even larger panel of products. In addition to compounds 2−11, the inner environment of the membranes also catalyzed glycine (112), alanine (113), parabanic acid (114), 4(3H)pyrimidinone [4(3H)- Pyr] (115), 2,4-diamino pyrimidine (2,4-DAP) (116), 6-hydroxy- 2,4-diamino pyrimidine [6(OH)-2,4-DAP] (117), 2,4-diamino pyrimidine-5-carboxylic acid (2,4-DAP-5COOH) (118), cytosine (19), isocytosine (120), uracil (121), and adenine (122) (Table   and Figure 2). $MgSO_4$, $Fe_2(SO_4)_3 \cdot 9H_2O$, $CuN_2O_6 \cdot 3H_2O$, and $CuCl_2 \cdot 2H_2O$ were the most active MSH in the synthesis of nucleobases 19, 21, and 22. Amino acids 12 and 13 were also produced in acceptable amounts.

It is interesting to note that the salts of the two metals that form the olivine solid solution, $MgSO_4$ and $Fe_2(SO_4)_3 \cdot 9H_2O$, are the most efficient salts, while $CuCl_2 \cdot 2H_2O$, $ZnCl_2$, $FeCl_2 \cdot 4H_2O$, and

MnCl$_2$·4H$_2$O showed a low reactivity. Carboxylic acids 4−9 were obtained in larger amounts in the outer environment with the exception of only MgSO$_4$ and Fe$_2$(SO$_4$)$_3$· 9H$_2$O. Therefore, this process is selective in terms of mineral properties because different metal silicate hydrated membranes afford different panels of products. Even more interesting is the fact that the panels of compounds formed inside and outside the tubular membrane are specific, as shown in Figure 60. Thus, nucleobases (119, 121, and 122), nucleobase bioisosteres (116 and 120), and nucleobase analogues (121 and 122) are produced only inside the membrane (Figure 67). Amino acids 112 and 113 are also synthesized only inside the membrane. Carboxylic acids 104−109 were obtained in the inner and outer environments.
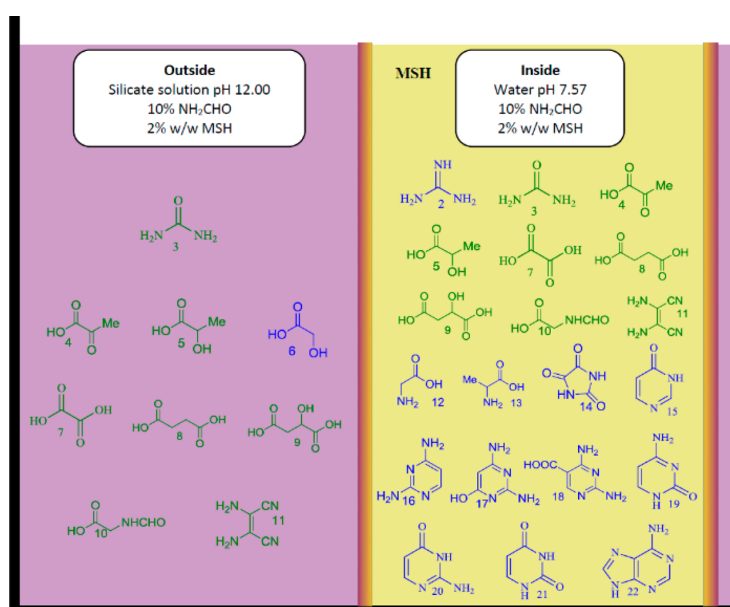
Figure 67. Schematic representation of products obtained with different MSH from NH$_2$CHOoutside (left) and inside (right) of the membranous structure. Color codes: compounds synthesized at both sides of the membrane (green); compounds synthesized only inside the membrane (blue).

The ability of formamide to trigger the synthesis of compounds representative of the major classes of prebiotic precursors in the presence of a number of minerals (including boron-, iron-, sulfur-, zircon-, titanium-, and phosphorus-based minerals, metal oxides of various types, and meteorites) has been previously shown to be particularly efficient under proton irradiation and the simulated impact of an extraterrestrial body. Our results provide the first example of a catalytic process endowed with (a) selective catalysis of the synthesis of biogenic relevant compounds by a textured membrane, (b) intrinsic compartmentalization ability, and (c) a shielding environment against ultraviolet radiation. Interestingly, in the reported experiments, the nucleic acid precursors were

located on the inner side of the membranes. However, we have not found significant differences in either the number or the yield of biochemically relevant compounds when comparing the reactivities of active versus passive metal silicate hydrate membranes. This means that the electron voltage reported in previous silica garden experiments does not play a differential role in the catalysis of prebiotic compounds.

3.3. CONCLUSIONS

The geological niche proposed here for the transition from inorganic to organic geochemistry, a silica-rich, alkaline, aqueous solution in contact with metal-bearing minerals in the presence of NH_2CHO, was highly plausible during the Hadean and Archean times. This niche was settled most likely as early as 4.4 Ga, i.e., almost one billion years earlier than the oldest putative remnants of life on our planet. Therefore, the existence of biological compounds such as carboxylic acids, amino acids, and nucleobases, or their carbon-like derivatives in Hadean zircon crystals or in Archean rocks, is rather plausible. It is worth noting that in these organic geo-niches, silica biomorphs that mimic primitive organisms readily form in the presence of alkaline earth metals.This geological niche is not exclusive to our planet. It should also exist, or have existed, on Earth-like planets, meteorite parent bodies, and comets, as well as in the interstellar dust made of olivine that are or were in contact with enriched regions of NH_2CHO in the universe. These results suggest that the conditions required for the synthesis of the molecular bricks from which life self-assembles, rather than being local and bizarre, seem to be universal and geologically conventional.

3.4. MATERIAL AND METHODS

3.4.1 Materials

Formamide (Fluka, >99%) was used without further purification. Fresh commercial water glass (Sigma-Aldrich, reagent grade, containing about 13.8 wt % Na and 12.5 wt % Si) was used as the silica source and was further diluted 1/4 (v/ v) with Millipore water.

3.4.2 Preparation of Silica Garden

We obtained silica gardens by dipping small pellets of a metal soluble salt into the (diluted) sodium silicate solution containing 2%, 5%, or 10% (v/v) NH_2CHO. Different metal soluble salts were used, namely, $ZnCl_2$, $FeCl_2 \cdot 4H_2O$, $CuCl_2 \cdot 2H_2O$, $Fe_2(SO_4)_3 \cdot 9H_2O$, and $MgSO_4$.

3.4.3 Reaction conditions

To model the chemical environment on the outer side of the tubular structures, NH_2CHO (200 µL) was mixed with the sodium silicate solution (2.0 mL) in the presence of preformed MSH [$ZnCl_2$, $FeCl_2 \cdot 4H_2O$, $CuCl_2 \cdot 2H_2O$, $Fe_2(SO_4)_3 \cdot 9H_2O$, and $MgSO_4$] (2.0% w/w) at 80 °C for 24 h. In two selected cases [$FeCl_2$ and $Fe_2(SO_4)_3 \cdot 9H_2O$], NH_2CHO (200 µL) was mixed with the sodium silicate solution (2.0 mL) in the presence of selected growing MSH (starting from 2.0% w/w of the corresponding salt's pellet) at 80 °C for 24 h. For the inner environment, NH_2CHO (200 µL) was mixed with distilled water (2.0 mL) in the presence of selected MSH (2.0% w/w) at 80 °C for 24 h. The reaction of NH_2CHO (10% v/v) with the sodium silicate solution (pH 12) without MSH membranes was also analyzed under similar experimental conditions.

3.4.4 Derivatization and analysis

The products were analyzed by gas chromatography associated with mass spectrometry (GC-MS) after treatment with N,N- bis-trimethylsilyl trifluoroacetamide in pyridine (620 µL) at 60 °C for 4 h in the presence of betulinol (CAS Registry Number 473-98-3) as the internal standard (0.2 mg). Mass spectrometry was performed by the following program: injection temperature 280 °C, detector temperature 280 °C, gradient 100 °C for 2 min, and 10 °C/min for 60 min. To identify the structure of the products, two strategies were followed. First, the spectra were compared with commercially available electron mass spectrum libraries such as NIST (Fison, Manchester, U.K.). Second, GC-MS analysis was repeated with standard compounds. All products have been recognized with a similarity index (SI) greater than 98% compared to that of the reference standards. The analysis was limited to products of ≥1 ng/mL, and the yield was calculated as micrograms of product per starting formamide.

REFERENCES CHAPTER I

1. Abou-Sleiman, P. M.; Muqit, M. M.; Wood, N. W., Expanding insights of mitochondrial dysfunction in Parkinson's disease. *Nat. Rev. Neurosci.,* **2006**, *7* (3), 207- 219.

2. Schapira, A. H.; Bezard, E.; Brotchie, J.; Calon, F.; Collingridge, G. L.; Ferger, B.; Hengerer, B.; Hirsch, E.; Jenner, P.; Le Novère, N. Novel pharmacological targets for the treatment of Parkinson's disease. *Nat. Rev. Drug Discov.,* **2006**, *5* (10), 845-854.

3. Misra, A.; Ganesh, S.; Shahiwala, A.; Shah, S. P. Drug delivery to the central nervous system: a review. *J. Pharm. Pharm. Sci.,* **2003**, *6* (2), 252-73.

4. Mena, M. A.; Casarejos, M. J.; Solano, R. M.; de Yebenes, J. G. Half a century of L-DOPA. *Curr. Top. Med. Chem.,* **2009**, *9* (10), 880-93.

5. Fox, S. H.; Chuang, R.; Brotchie, J. M. Parkinson's disease- -opportunities for novel therapeutics to reduce the problems of levodopa therapy. *Prog. Brain res.,* **2008**, *172*, 479-94.

6. Hornykiewicz, O. L-DOPA: from a biologically inactive amino acid to a successful therapeutic agent. *Amino acids* **2002**, *23* (1-3), 65-70.

7. Del-Bel, E.; Padovan-Neto, F. E.; Raisman-Vozari, R.; Lazzarini, M. Role of nitric oxide in motor control: implications for Parkinson's disease pathophysiology and treatment. *Curr. pharm. des.,* **2011**, *17* (5), 471-88.

8. Di Stefano, A.; Mosciatti, B.; Mario Cingolani, G.; Giorgioni, G.; Ricciutelli, M.; Cacciatore, I.; Sozio, P.; Claudi, F. Dimeric L-Dopa derivatives as potential prodrugs. *Bioorg. Med. Chem. Lett.,***2001**, *11* (8), 1085- 1088.

9. Umanah, G. K.; Huang, L.; Ding, F. X.; Arshava, B.; Farley, A. R.; Link, A. J.; Naider, F.; Becker, J. M. Identification of residue-to-residue contact between a peptide ligand and its G protein-coupled receptor using periodate-mediated dihydroxyphenylalanine cross-linking and mass spectrometry. *J. Biol. chem.,* **2010**, *285* (50), 39425-36.

10. Nambi, P., & Aiyar, N. G protein-coupled receptors in drug discovery. *Assay and drug development technologies* **2003**, *1*(2), 305-310.

11. Sakakura, A.; Shioya, K.; Katsuzaki, H.; Komiya, T.; Imamura, T.; Aizono, Y.; Imai, K. Isolation, structural elucidation and synthesis of a novel antioxidative pseudo- di-peptide, Hanasanagin, and its biogenetic precursor from the< i> Isaria japonica</i> mushroom. *Tetrahedron* **2009**, *65* (34), 6822-6827.

12. Yu, J.; Wei, W.; Danner, E.; Israelachvili, J. N.; Waite, J. H. Effects of interfacial redox in mussel adhesive protein films on mica. *Adv. mat.,* **2011**, *23* (20), 2362-6.

13. Malakoutikhah, M.; Teixido, M.; Giralt, E. Toward an optimal blood-brain barrier shuttle by synthesis and evaluation of peptide libraries. *J. Med. Chem.,* **2008**, *51* (16), 4881-9.

14. Guazzaroni, M.; Crestini, C.; Saladino, R. Layer-by-Layer coated tyrosinase: An efficient and selective synthesis of catechols. *Bioorg. Med. Chem.,* **2012**, *20* (1), 157-66.

15. Beal MF. Mitochondria take center stage in aging and neurodegeneration *Ann Neurol.* **2005** Oct;58(4):495-505.

16. Jenner P. Oxidative stress in Parkinson's disease. *Ann Neurol.* **2003**;53(Suppl 3):S26–S36. discussion S36-S28

17. Yoritaka A, Hattori N, Uchida K, Tanaka M, Stadtman E, Mizuno Y. Immunohistochemical detection of 4-hydroxynonenal protein adducts in Parkinson disease. *Proc Natl Acad Sci U S A.* **1996**;93:2696–2701

18. Floor E, Wetzel M. Increased protein oxidation in human substantia nigra pars compacta in comparison with basal ganglia and prefrontal cortex measured with an improved dinitrophenylhydrazine assay. *J Neurochem.* **1998**;70:268–275

19. Alam ZI, Jenner A, Daniel SE, Lees AJ, Cairns N, Marsden CD, Jenner P, Halliwell B. Oxidative DNA damage in the Parkinsonian brain: An apparent selective increase in 8-hydroxyguanine levels in substantia nigra. *J Neurochem.* **1997**;69:1196–1203

20. Zhang J, Perry G, Smith MA, Robertson D, Olson SJ, Graham DG, Montine TJ. Parkinson's disease is associated with oxidative damage to cytoplasmic DNA and rna in substantia nigra neurons. *Am J Pathol*. **1999**;154:1423–1429

21. Tais Hitomi Wakamatsu; Murat Dogru; Kazuo Tsubota- Tearful relations: oxidative stress, inflammation and eye diseases Arq. Bras. Oftalmol. vol.71 no.6 supl.0 São Paulo Nov./Dec. 2008

22. Smith DG, Cappai R, Barnham KJ. The redox chemistry of the Alzheimer's disease amyloid beta peptide. *Biochim Biophys Acta*. **2007**;1768:1976–1990

23. Muller FL, Liu Y, Van Remmen H. Complex III releases superoxide to both sides of the inner mitochondrial membrane. *J Biol Chem*. **2004**;279:49064–49073

24. Valko M, Leibfritz D, Moncol J, Cronin MT, Mazur M, Telser J. Free radicals and antioxidants in normal physiological functions and human disease. *Int J Biochem Cell Biol*. **2007**;39:44–84

25. Malkus KA, Tsika E, Ischiropoulos H. Oxidative modifications, mitochondrial dysfunction, and impaired protein degradation in Parkinson's disease: How neurons are lost in the Bermuda triangle. *Mol Neurodegene*. **2009**;4:24

26. Carr AC, McCall MR, Frei B. Oxidation of LDL by myeloperoxidase and reactive nitrogen species : Reaction pathways and antioxidant protection. *Arteriosclerosis, Thrombosis, and Vascular Biology*. **2000**;20:1716–1723.

27. Szabo C, Ischiropoulos H, Radi R. Peroxynitrite: Biochemistry, pathophysiology and development of therapeutics. *Nat Rev Drug Discov*. **2007**;6:662–680

28. Vincent VA, Tilders FJ, Van Dam AM. Production, regulation and role of nitric oxide in glial cells. *Mediators Inflamm*. **1998**;7:239–255

29. Johnson WM, Wilson-Delfosse AL, Mieyal JJ. Dysregulation of glutathione homeostasis in neurodegenerative diseases. Nutrients. **2012**;4:1399–1440.

30. Dumont M, Beal MF. Neuroprotective strategies involving ROS in Alzheimer's disease. *Free Radic Biol Med*. **2011**;51:1014–1026.

31. Yan MH, Wang X, Zhu X. Mitochondrial defects and oxidative stress in Alzheimer disease and Parkinson disease. *Free Radic Biol Med*. **2011**;62:90–101

32. Johnson WM, Wilson-Delfosse AL, Mieyal JJ. Dysregulation of glutathione homeostasis in neurodegenerative diseases. *Nutrients*. **2012**;4:1399–1440.

33. Jenner P, Olanow W. The pathogenesis of cell death in Parkinson's disease. N*eurol*. **2006**;66:S24–S36

34. Uhl GR, Li S, Takahashi N, Itokawa K, Lin Z, Hazama M, Sora I. The VMAT2 gene in mice and humans: Amphetamine responses, locomotion, cardiac arrhythmias, aging, and vulnerability to dopaminergic toxins. FASEB J. **2000;**14:2459–2465

35. Hastings TG. Enzymatic oxidation of dopamine: The role of prostaglandin H synthase. *J Neurochem*. **1995**;64:919–924.

36. Graham D. Pathways for catecholamines in the genesis of neuromelanin and cytotoxic quinones. *Mol Pharmacol*. **1978**;14:633–643

37. Qi Z, Miller GW, Voit EO - PLoS ONE, Computational systems analysis of dopamine metabolism **(2008)**

38. Vera Dias, Eunsung Junn, and M. Maral Mouradian- The Role of Oxidative Stress in Parkinson's Disease *Journal of Parkinson's disease*. **2013**;3(4):461-491. doi:10.3233/JPD-130230

39. Feany M, Pallanck L. Parkin: A multipurpose neuroprotective agent? *Neuron*. **2003**;38:13–16

40. Jiang H, Ren Y, Zhao J, Feng J. Parkin protects human dopaminergic neuroblastoma cells against dopamine-induced apoptosis. *Hum Mol Genet*. **2004**;13:1745–1754

41. Zhou W, Freed CR. DJ-1 up-regulates glutathione synthesis during oxidative stress and inhibits A53T alpha-synuclein toxicity. *J Biol Chem*. **2005**;280:43150–43158.

42. Ishikawa S, Tanaka Y, Takahashi-Niki K, Niki T, Ariga H, Iguchi-Ariga SM. Stimulation of vesicular monoamine transporter 2 activity by DJ-1 in SH-SY5Y cells. *Biochem Biophys Res Commun*

43. Lev N, Barhum Y, Pilosof NS, Ickowicz D, Cohen HY, Melamed E, Offen D. DJ-1 protects against dopamine toxicity: Implications for Parkinson's disease and aging. *J Gerontol A Biol Sci Med Sci*. **2013**;68:215–225

44. Wang X, Petrie TG, Liu Y, Liu J, Fujioka H, Zhu X. Parkinson's disease-associated DJ-1 mutations impair Mitochondrial dynamics and cause mitochondrial dysfunction. *J Neurochem*. **2012**;121:830– 839

45. Irrcher I, Aleyasin H, Seifert EL, Hewitt SJ, Chhabra S, Phillips M, Lutz AK, Rousseaux MW, Bevilacqua L, Jahani-Asl A, Callaghan S, MacLaurin JG, Winklhofer KF, Rizzu P, Rippstein P, Kim RH, Chen CX, Fon EA, Slack RS, Harper ME, McBride HM, Mak TW, Park DS. Loss of the Parkinson's disease-linked gene DJ-1 perturbs mitochondrial dynamics. *Hum Mol Genet*. **2010**;19:3734–3746

46. Saha S, Guillily MD, Ferree A, Lanceta J, Chan D, Ghosh J, Hsu CH, Segal L, Raghavan K, Matsumoto K, Hisamoto N, Kuwahara T, Iwatsubo T, Moore L, Goldstein L, Cookson M, Wolozin B. LRRK2 modulates vulnerability to mitochondrial dysfunction in caenorhabditis elegans. *J Neurosci*. **2009**;29:9210–9218

47. F. Blandini, J. T. Greenamyre, *Drugs Today (Barc)* **1999**, *35*, 473-483] [H. D. Kao, A. Traboulsi, S. Itoh, L. Dittert, A. Hussain, *Pharm Res* **2000**, *17*, 978-984

48. More on dopamine and its drug- *Biochemical Pharmacology, chapter 13*

49. D. G. Standaert, A. B. Young, *Goodman and Gilman's The Pharmacological Basis of Therapeutics***1996**

50. W. Birkmayer, W. Danielcyk, E. Neumayer, P. Riederer, *J Neural Transm* **1973**, *34*, 133-143

51. P. S. Leppert, M. Cortese, J. A. Fix, The Effects of Carbidopa Dose and Time and Route of Administration on Systemic L-Dopa Levels in Rats *Pharm Res* 1988**, *5,* 587-591.**

52. J. G. Nutt, W. R. Woodward, J. L. Anderson, The effect of carbidopa on the pharmacokinetics of intravenously administered levodopa: The mechanism of action in the treatment of parkinsonism *Ann Neurol* **1985**, *18*, 537-543.

53. J. M. Cedarbaum, *Clin Pharmacokinet* **1987**, *13*, 141-178.

54. P. S. Papavasiliou, G. C. Cotzias, S. E. Duby, A. J. Steck, C. Fehling, M. A. Bell, Levodopa in Parkinsonism: Potentiation of Central Effects with a Peripheral Inhibitor *N Engl J Med* 1972**, *286*, 8- 14.**

55. W. Birkmayer, M. Mentasti, Further experimental studies on the catecholamine metabolism in extrapyramidal diseases (Parkinson and chorea syndromes *Arch Psychiatr Nervenkr* 1967**, *210*, 29- 35**

56. N. D. Huebert, M. G. Palfreyman, K. D. Haegele, A comparison of the effects of reversible and irreversible inhibitors of aromatic L-amino acid decarboxylase on the half-life and other pharmacokinetic parameters of oral L-3,4- dihydroxyphenylalanine. *Drug Metab Dispos* **1983**, *11*, 195-200

57. K. Sasahara, T. Nitanai, T. Habara, T. Kojima, Y. Kawahara, T. Morioka, E. Nakajima, Dosage form design for improvement of bioavailability of levodopa IV: Possible causes of low bioavailability of oral levodopa in dogs*J Pharm Sci* **1981**, *70*, 730-733.

58. J. Goole, F. Vanderbist, K. Amighi, Development and evaluation of new multiple-unit levodopa sustained-release floating dosage forms. *Int J Pharm* **2007**, *334*, 35-41

59. J. Cedarbaum, H. Kutt, F. McDowell, *Neurology* **1989**, *39*, 38-44; discussion 59

60. D. MacMahon, D. Sachdev, H. Boddie, C. Ellis, B. Kendal, N. Blackburn, A comparison of the effects of controlled-release levodopa (Madopar CR) with conventional levodopa in late Parkinson's disease. *Journal of Neurology, Neurosurgery & Psychiatry* **1990,** *53*, 220-223

61. J. I. Sage, M. H. Mark, *Clinical neuropharmacology* **1993**, *17*, S1-6.

62. S. Gauthier, D. Amyot, Sustained Release Antiparkinson Agents: Controlled Release Levodopa *The Canadian journal of neurological sciences. Le journal canadien des sciences neurologiques* **1992**, *19*, 153-155

63. S. Kaakkola, H. Teräväinen, S. Ahtila, H. Rita, A. Gordin, *Neurology* **1994**, *44*, 77-77.

64. A.Gordin, S. Kaakkola and H. Teravainen- Clinical advantages of COMT inhibition with entacapone- a review *Journal of neural transmission* 2004, 111, 1343-1363

65. U. Rinne, J. Larsen, Å. Siden, J. Worm-Petersen, *Neurology* **1998**, *51*, 1309-1314.

66. W. Poewe, G. Deuschl, A. Gordin, E. R. Kultalahti, M. Leinonen, *Acta Neurologica Scandinavica* **2002**, *105*, 245-255.

67. D. J. Brooks, H. Sagar, Entacapone is beneficial in both fluctuating and non-fluctuating patients with Parkinson's disease: a randomised, placebo controlled, double blind, six month study *Neurosurgery & Psychiatry* **2003**, *74*, 1071-1079

68. F. Stocchi, O. Rascol, K. Kieburtz, W. Poewe, J. Jankovic, E. Tolosa, P. Barone, A. E. Lang, C. W. Olanow, Initiating levodopa/carbidopa therapy with and without entacapone in early Parkinson disease: The STRIDE-PD study *Annals of neurology* **2010**, *68*, 18-27

69. C. Hartmann, V. Meyer, *Chem. Ber.* **1893**, *26*, 1727-1732.

70. D. B. Dess, J. C. Martin, *J. Org. Chem.* **1983**, *48*, 4155-4156.

71. D. B. Dess, J. C. Martin, *J. Am. Chem. Soc.* **1991**, *113*, 7277-7278.

72. D. Depernet,; B. François, WO 02/057210 A1, PCT/FR02/00189, US 2002/0107416 or C.A.. **2002**, 137, 10912.

73. Y.-D. Shen, H.-Q. Wu, S.-L. Zhang, X.-Z. Bu, L.-K. An, Z.-S. Huang, P.-Q. Liu, L.-Q. Gu, Y.-M.. Li, A. S. C. Chan, *Tetrahedron* **2005**, *61*, 9097-9101.

74. D. Magdziak, A. A. Rodriguez, R. W. Van De Water, T. R. R. Pettus, *Org. Lett.* **2002**, *4*, 285-288.

75. Y.-M.. Li, A. S. C. Chan, *Tetrahedron* **2005**, *61*, 9097-9101.

76. K. C. Nicolaou, P. S. Baran, Y.-L. Zhong, S. Barluenga, K. W. Hunt, R. Kranich, J. A. Vega, *J. Am. Chem. Soc.* **2002**, *124*, 2233-2244.

77. B. Janza, A. Studer, *J. Org. Chem.* **2005**, *70*, 6991-6994

78. Pezzella, L. Lista, A. Napolitano, M. d'Ischia, *Tetrahedron Lett.* **2005**, *46*, 3541-3544.

79. V.V. Zhdankin, P. Stang, Journal of Chemical Reviews 102 (2002) 2523

80. T. Wirth, Angewandte Chemie International Edition 44 (2005) 3656;

81. K.C. Nicolaou, T. Montagnon, P.S. Baran, Y.-L. Zhong, Journal of the American Chemical Society 124 (2002) 2245;

82. dainserire

83. J.D. More, N.S. Finney, Organic Letters 4 (2002) 3001.

84. K. Surendra, N.S. Krishnaveni, M.A. Reddy, Y.V.D. Nageswar, K.R. Rao, Journal of Organic Chemistry 68 (2003) 2058.

85. Z. Liu, Z.-C. Chen, Q.-G. Zheng, Organic Letters 5 (2003) 3321.

86. V.V. Zhdankin, D.N. Litvinov, A.Y. Koposov, T. Luu, M.J. Ferguson, R. McDonald, R.R. Tykwinski, Chemical Communications (2004) 106;

87. V.V. Zhdankin, A.Y. Koposov, B.C. Netzel, N.V. Yashin, B.P. Rempel, M.J. Ferguson, R.R. Tykwinski, Angewandte Chemie International Edition 42 (2003) 2194;

88. V.V.Zhdankin,A.Y.Koposov,D.N.Litvinov,M.J.Ferguson,R.McDonald,T.Luu, R.R.J. Tykwinski, Journal of Organic Chemistry 70 (2005) 6484;

89. A.Y. Koposov, D.N. Litvinov, V.V. Zhdankin, Tetrahedron Letters 45 (2004) 2719;

90. U. Ladziata, A.Y. Koposov, K.Y. Lo, J. Willging, V.N. Nemykin, V.V. Zhdankin, Angewandte Chemie International Edition 44 (2005) 7127;

91. A.Y. Koposov, V.V. Zhdankin, Synthesis (2005) 22;

92. B.V. Meprathu, M.W. Justik, J.D. Protasiewicz, Tetrahedron Letters 46 (2005) 5187;

93. A.P. Thottumkara, T.K. Vinod, Tetrahedron Letters 43 (2002) 569.

94. U. Ladziata, J. Willging, V.V. Zhdankin, Organic Letters 8 (2006) 167.

95. M. Mulbaier, A. Giannis, Angewandte Chemie International Edition 40 (2001) 4393;

96. G. Sorg, A. Mengel, G. Jung, J. Rademann, Angewandte Chemie International Edition 40 (2001) 4395;

97. N.N. Reed, M. Delgado, K. Hereford, B. Clapham, K.D. Janda, Bioorganic and Medicinal Chemistry Letters 12 (2002) 2047;

98. Z.Lei,C.Denecker,S.Jegasothy,D.C.Sherrington,N.K.H.Slater,A.J.Sutherland, Tetrahedron Letters 44 (2003) 1635;

99. Z.Q. Lei, H.C. Ma, Z. Zhang, Y.X. Yang, Reactive and Functional Polymers 66 (2006) 840..

100. W.-J. Chung, D.-K. Kim, Y.-S. Lee, Tetrahedron Letters 44 (2003) 9251;

101. D.-K. Kim, W.-J. Chung, Y.-S. Lee, Synlett (2005) 279;

102. H.-S. Jang, W.-J. Chung, Y.-S. Lee, Tetrahedron Letters 48 (2007) 3731.

103. da inserire

104. Chung, D.-K. Kim, Y.-S. Lee, Synlett (2005) 2175.

105. P . Lecarpentier, S. Crosignani, B. Linclau, Molecular Diversity 9 (2005) 341.

106. Journal of Industrial and Engineering Chemistry 20 (2014) 29–36 Hyung-Seok Jang , Yo-Han Kim, Young-O Kim, Sang-Myung Lee , Jung Won Kim , Woo-Jae Chung, Yoon-Sik Lee .

107. P. Grunwald, *Biocatalysis*, **2009**, Imperial College Press

108. J. J. Straathof, *Applied Biocatalysis*, **2000**, Harwood Acad., 2nd Edition

109. P. Grunwald, *Biocatalysis*, **2009**, Imperial College Press

110. M. Vihinen, E. Torkkila, Accuracy of Protein Flexibility Predictions, *Proteins*, **1994**, 19,141-149

111. R. Sheldon, Enzyme Immobilization: The Quest for Optimum Performance, *Adv. Synth. Catal.*, **2007**, 349, 1289-1307

112. Sheldon RA. Cross-linked enzyme aggregates (CLEAs): stable and recyclable biocatalysts. Biochem Soc. 2007;35 (6):1583_1587

113. Brodelius P, Mosbach K. Immobilization techniques forcells/organelles. In: Mosbach K, editor. Methods in enzymology.London: *Academic Press*; **1987.** p. 173_454.

114. Buchholz K, Klein J. Characterization of immobilizedbiocatalysts. In: Mosbach K, editor. Methods in enzymology.London: Academic Press; 1**987**; p. 3_30.

115. Li S, Hu J, Liu B. Use of chemically modified PMMA microspheres for enzyme immobilization. *Biosystems.* **2004**;77:253

116. Foresti ML, Ferreira ML. Chitosan-immobilized lipases for the catalysis of fatty acid esterifications. *E n z y m e Microb Technol.* **2007**;40:769777

117. Balcao VM, Paiva AL, Malcata FX. Bioreactors with immobilized lipases: state-of-the-art. Enzyme M i c r o b Technol. **1996**;18:392_416.

118. De Lathouder KM, van Benthem DTJ, Wallin SA, Mateo C, Fernandez LF, Guisan JM, Kapteijn F, Moulijn JA. Poliethyleneimine (PEI) functionalized ceramic monolithsas enzyme carriers: preparation   and performance. *J Mol Ca*tal B. **2008;**50:20_27

119. Tischer W, Wedenkind F. Immobilized enzymes: methodsand application. In: Fessner WD, editor.   T o p i c s i n chemistry. Berlin: *Springer Verlag*; **1999.** p. 100_108.,

120. Spahn C, Minteer SD. Enzyme immobilization in biotechnology. *Recent Pat Eng*. **2008**;2:195_200.

121. Khan AA, Alzohairy MA. Recent advances and applications of immobilized enzymes technologies: a review. *Res J Biol Sci.* **2010**;5(8):565_575

122. Boller T, Meier C, Menzler S. Eupergit oxirane acrylic beads: how to make enzymes fit for b i o c a t a l y s i s. *Org Process Res De*v. **2002**;6(4):509_519.

123. Cao L, Langen L, Sheldon RA. Immobilised enzymes: carrier-bound or carrier-free? *Curr Opin   B i o t e c h n o l.* **2003**;14:387_394

124. Pairat I, Thidarat C, Jitchon P, Navadon S, Jittima C. Application of agriculture waste as support for l i p a s e immobilization. *Biocatal Agric Biotechnol*. **2014**;3 (3):77_82.

125. Wu C, Zhou G, Jiang X, Ma J, Zhang H, Song H. Active biocatalysts based on Candida rugosa lipase immobilized in vesicular silica. *Process Biochem*. **2012**;47:953_959.

126. Kim JB, Grate JW, Wang P. Nanostructures for enzyme stabilization. *Chem Eng Sci*. **2006**;61:1017_1026

127. Khan AA, Akhtar S, Hussain Q. Direct immobilization of polyphenol oxidases on celite 545 from a m m o n i u m sulphate fractionated proteins of potato (Solanum tuberosum). *J Mol Catal* B. **2006**;40:58_63

128. Ansari SA, Husain Q. Lactose hydrolysis from milk/whey in batch and continuous processes by concanavalin A-celite 545 immobilized Aspergillus oryzae b-galactosidase. *Food Bioprod Process*. **2012**;90(2):351_359

129. Datta S, Rene CL, Rajaram YRS. Enzyme immobilization: an overview on techniques and support materials. 3 *Biotech*. **2013;**3(1):1_9

130. Brena BM, Batista-Viera F. Immobilization of enzymes. In: Guisan JM, editor. Immobilization of enzymes and cells. *2nd ed. New Jersey (NJ): Humana Press* Inc.; **2006**. p. 123_124

131. Gemenier P. Materials for enzyme engineering. In: Gemeiner P, editor. Enzyme engineering. 1st ed. N e w Y o r k (NY): Ellis Horwood; **1992**. p. 13_119

132. Gorecka E, Jastrzebska M. Immobilization techniques and biopolymer carriers. *Biotechnol Food Sci***. 2011**;75:65_8

133. Lee CH, Lin TS, Mou CY. Mesoporous materials for encapsulating enzymes. *Nano*. **2009**;4:165_179

134. Guisan JM. Immobilization of enzymes as the 21st centurybegins. In: Guisan JM, editor. I m m o b i l i z a t i o n ofenzymes and cells. *2nd ed. New Jersey (NJ): HumanaPress* Inc.; **2006**. p. 1_13.

135. Guowei Z, Cuicui W, Xiaojie J, Jingyun M, Huayong Z,Hongbin S. Active biocatalysts based on C a n d i d a rugosa lipase immobilized in vesicular silica. *Process Biochem*. **2012**;47:953_959

136. Asuri P, Karajanagi SS, Sellitto E, Kim DY, Kane RS,Dordick JS. Water-soluble carbon nanotube- e n z y m e conjugatesas functional biocatalytic formulations. *Biotechnol Bioeng*. **2006;**95(5):804_81

137. Kim J, Jia H, Wang P. Challenges in biocatalysis forenzyme-based biofuel cells. *Biotechnol Adv*. **200**6;24:296_308

138. Asuri P, Karajanagi SS, Sellitto E, Kim DY, Kane RS,Dordick JS. Water-soluble carbon nanotube- e n z y m e conjugates as functional biocatalytic formulations. *BiotechnolBioeng*. **2006**;95(5):804_811.

139. Saifuddin N, Raziah AZ, Junizah AR. Carbon nanotubes: a review on structure and their interaction with proteins. *J Chem*. **2013**; 2013:676815,

140. Wang L, Wei L, Chen Y, Jiang R. Specific and reversible immobilization of NADH oxidase on functionalized carbon nanotubes. *J Biotechnol*. **2010**;150(1):57_63

141. Verma ML, Naebe M, Barrow CJ, Puri M. Enzyme immobilisation on amino-functionalised multi- walled carbon nanotubes: structural and biocatalytic characterisation.*PLOS One*. **2013**;8:1_9

142. Chiou SH, Wu WT. Immobilization of Candida rugosa lipase on chitosan with activation of the h y d r o x y l groups.*Biomaterials**. 2004**;25:197_204

143. Costa SA, Azevedo HS, Reis RL. Enzyme immobilization in biodegradable polymers for biomedical applications. In: Reis RL, Rom_an JS, editors. Biodegradable systems in tissue engineering and regenerative medicine. *London:CRC Press LLC*; **2005**. p. 109_112

144. Brena BM, Batista-Viera F. Immobilization of enzymes. In: Guisan JM, editor.Immobilization of enzymes and cells. 2nd ed. New Jersey (NJ): *Humana Press Inc*.; **2006.** p. 123_124

145. Chiou SH, Wu WT. Immobilization of Candida rugosa lipase on chitosan with activation of the h y d r o x y l groups. *Biomaterials*. **2004;**25:197_204

146. Nur Royhaila Mohamad An overview of technologies for immobilization of enzymes and surface a n a l y s i s techniques for immobilized enzymes *Biotechnology & Biotechnological Equipment*, **2015** Vol. 29, No. 2, 205_220

147. Flickinger MC, Drew SW. Fermentation, biocatalysis and bioseparation. In: Flickinger MC, editor. Encyclopedia of bioprocess technology. *Vol. 1. 1st ed. New York (NY): Wiley*; **1999.**

148. Jegannathan KR, Abang S, Poncelet D, Chan ES, Ravindra P. Production of biodiesel using immobilized lipase _ a critical review. *Crit Rev Biotechnol*. **2008**;28:253_264.

149. Kumar N. Studies of glucose oxidase immobilized carbon nanotube-polyaniline composites [MSc t h e s i s]. Patiala (India): *Thapar University*; July 2009

150. Gupta M, Mattiason B. Determination of coupling yields and handling of labile proteins in i m m o b i l i z a t i o n technology. In: Taylor RF, editors. Protein immobilization. Fundamentals and applications. New York (NY): Marcel Dekker; **199**2. p. 161_179.

151. End N, Schoning KE. Immobilisation of biocatalyst in industrial research and production. Top *Curr C h e m .* **2004**;242:273_317

152. Tosa T, Mori T, Fuse N, Chibata I. Studies on continuous enzyme reactions. I. Screening of carriers f o r preparation of water-insoluble aminoacylase. *Enzymologia*. **1966**;31: 214_224.

153. Cao L. Carrier-bound immobilized enzymes: principles, application and design. Weinheim: Wiley- VCH; 2005

154. Hanefield U, Gardossi L, Magner E. Understanding enzyme immobilisation. *Chem Soc Rev*. **2008**;38:453_468

155. Bahulekar R, Ayyangar NR, Ponrathnam S. Polyethyleneimine in immobilization of biocatalysts. *E n z y m e Microb Technol*. **1991;**13:858_868

156. Datta S, Rene CL, Rajaram YRS. Enzyme immobilization: an overview on techniques and support materials. 3 *Biotech*. **2013**;3(1):1_9

157. Costa SA, Azevedo HS, Reis RL. Enzyme immobilization in biodegradable polymers for biomedical applications. In: Reis RL, Rom_an JS, editors

158. Nelson DL, Cox MM. Principles of biochemistry. 4th ed. New York (NY)

159. W. H. Freeman and Co.; 2005. Roy I, Gupta MN. Bioaffinity immobilization. In: Guisan JM, editor. Immobilization of enzymes and cells. 2nd ed. New Jersey (NY): Humana Press Inc.; **2006**. p. 189_192

160. Sardar M, Roy I, Gupta MN. Simultaneous purification and immobilization of Aspergillus niger xylanase on the reversibly soluble polymer Eudragit(TM) L-100. *Enzyme Microb Technol*. **2000**;27:672_679

161. William Putzbach and Niina J. Ronkainen Immobilization Techniques in the Fabrication of Nanomaterial-Based Electrochemical Biosensors: A Review *Sensors* **2013**, *13*(4), 4811-4840; doi:10.3390/s130404811

162. Huang L, Cheng ZM. Immobilization of lipase on chemically modified bimodal ceramic foams for o l i v e o i l hydrolysis. Chem Eng J. 2008;144:103_109;

163. Chronopoulou L, Kamel G, Sparago C, Bordi F, Lupi S. Structure-activity relationships of Candida rugosa lipase immobilised on polylactic acid nanoparticles. Soft Matter. 2011;7:2653_2662

164. Subramanian A, Kennel SJ, Oden PI, Jacobson KB, Woodward J, Doktycz MJ. Comparison of techniques for enzyme immobilisation on silicon supports _ effect of cross-linker chain length on enzyme a c t i v i t y . *E n z y m e Microb Technol*. 1999;24(1):26_34.

165. Chiang C-J, Hsiau L-T, Lee W-C. Immobilization of cellassociated enzymes by entrapment in polymethacrylamide beads. *Biotechnol Technol*. **2004**;11(2):121_125.

166. Klotzbach TL, Watt MM, Ansari Y, Minteer SD. Improving the microenvironment for enzyme immobilization at electrodes by hydrophobically modifying chitosan and Nafion polymers. *J Memb S c i .* **2008**;311:81_88.

167. Aehle W. Enzymes in industry. 3rd ed. Weinheim: Wiley-VCH; **2007.**

168. Costa SA, Azevedo HS, Reis RL. Enzyme immobilization in biodegradable polymers for biomedical applications. In: Reis RL, Rom_an JS, editors. Biodegradable systems in tissue engineering and regenerative medicine. London: *CRC Press LLC*; **2005**. p. 109_112.

169. Won K, Kim S, Kim KJ, Park HW, Moon SJ. Optimization of lipase entrapment in Ca-alginate gel beads. *Process Biochem*. **2005;**40:2149_2154

170. Shen Q, Yang R, Hua X, Ye F, Zhang W, Zhao W. Gelatin-templated biomimetic calcification for b- galactosidase immobilization. *Process Biochem*. **201**1;46:1565_1571

171. Khan AA, Akhtar S, Hussain Q. Direct immobilization of polyphenol oxidases on celite 545 from ammonium sulphate fractionated proteins of potato (Solanum tuberosum). *J Mol Catal B*. **2006**;40:58_63.

172. Keeling-Tucker T, Brennan JD. Fluorescent probes as reporters on the local structure and dynamics in sol-gel derived nanocomposite materials. *Chem Mater*. **2001**;13:3331_3350.

173. Gill I. Bio-doped nanocomposite polymers: sol-gel bioencapsulates. *Chem Mater*. **2001**;13:3404_3421.

174. Jin W, Brennan JD. Properties and applications of proteins encapsulated within sol-gel derived materials. *Anal Chim Acta*. **2002**;461:1_36.

175. Tsai HC, Doong R. Preparation and characterization of urease-encapsulated biosensors in poly(vinyl alcohol)-modified silica sol-gel materials. *Biosens Bioelectron*. **2007;**23:66_73.

176. Guisan JM. Immobilization of enzymes as the 21st century begins. In: Guisan JM, editor. Immobilization of enzymes and cells. 2nd ed. New Jersey (NJ): *Humana Press* Inc.; **2006**. p. 1_13.

177. Lopez A, Lazaro N, Marques AM. The interphase technique: a simple method of cell immobilization in gelbeads. *J Microbiol Methods*. **1997**;30:231_234

178. Won K, Kim S, Kim KJ, Park HW, Moon SJ. Optimization of lipase entrapment in Ca-alginate gel beads. *Process Biochem*. **2005;**40:2149_2154

179. Gorecka E, Jastrzebska M. Immobilization techniques and biopolymer carriers. *Biotechnol Food Sci*. **2011**;75:65_86

180. Flickinger MC, Drew SW. Fermentation, biocatalysis and bioseparation. In: Flickinger MC, editor. *Encyclopedia of bioprocess technology*. Vol. 1. 1st ed. New York (NY): Wiley; **1999**;

181. Shi Y, Jin F, Wu Y, Yan F, Yu X, Quan Y. Improvement of immobilized cells through permealilizing and crosslinking. *Chin J Biotechnol*. **1997;**13(1):111_113

182. Honda T, Miyazaki M, Nakamura H, Maeda H. Immobilization of enzymes on microchannel surface through cross-linking polymerization. *AIChE Spring National Meeting*; **2006** Apr 23_27; Orlando, FL

183. Migneault I, Dartiquenave C, Bertrand MJ, Waldron KC. Glutaraldehyde: behaviour in aqueous solution, reaction with proteins, and application to enzyme crosslinking. *Biotechniques*. **2004;**37(5):790_802

184. Hanefield U, Gardossi L, Magner E. Understanding enzyme immobilisation. *Chem Soc Rev*. **2008**;38:453_468

185. Obzturk B. Immobilization of lipase from Candida rugosa on hydrophobic and hydrophilic supports [MSc dissertation]. _Izmir (Turkey): Izmir Institute of Technology; **2001**. p. 40

186. Kim JB, Grate JW, Wang P. Nanostructures for enzyme stabilization. *Chem Eng Sci*. **2006**;61:1017_1026,

187. Datta S, Rene CL, Rajaram YRS. Enzyme immobilization:an overview on techniques and support materials. 3 *Biotech*. **2013;**3(1):1_9. ,

188. Huang L, Cheng ZM. Immobilization of lipase on chemically modified bimodal ceramic foams for olive oil hydrolysis. Chem Eng J. 2008;144:103_109. , Wu L, Yuan X, Sheng J. Immobilization of cellulase in nanofibrous PVA membranes by electrospinning. *J Memb Sci*. **2005**;250:167_173.

189. Sakai S, Liu Y, Yamaguchi T, Watanabe R, Kawabe M, Kawakami K. Immobilization of Pseudomonas cepacia lipase onto electrospun polyacrylonitrile fibers through physical adsorption and application to transesterification in nonaqueous solvent. *Biotechnol Lett*. **2010**;32: 1059_1062.

190. Ren G, Xu X, Liu Q. Electrospun poly(vinyl alcohol)/ glucose oxidasebiocomposite membranes for b i o s e n s o r applications. *React Funct Polym*. **2006**;66:1559_1564

191. Guisan JM. Immobilization of enzymes as the 21st century begins. In: Guisan JM, editor. Immobilization of enzymes and cells. 2nd ed. New Jersey (NJ): Humana Press Inc.; **2006**. p. 1_13.

192. Singh BD. Biotechnology expanding horizonsa-amylase immobilization on the silica nanoparticles for cleaning performance towards starch soils in laundry detergents. *J Mol Catal B*. **2009**;74:1_5

193. Obzturk B. Immobilization of lipase from Candida rugosa on hydrophobic and hydrophilic supports *Institute of Technology*; **2001.** p. 40

194. Dandavate V, Keharia H, Madamwar D. Ethyl isovelarate synthesis using Candida rugosa lipase immobilized on silica nanoparticles prepared in nonionic reverses micelles. *Process Biochem*. **2009**;44:349_352

195. Yilmaz E, Can K, Sezgin M, Yilmaz M. Immobilization of Candida rugosa lipase on glass bead for enantioselective hydrolysis of racemic naproxen methyl ester. *Bioresour Technol*. **2011;**102:499_506

196. Roger A. Sheldon and Sander van Pelt- Enzyme immobilisation in biocatalysis: why, what and how DOI: 10.1039/C3CS60075K (Tutorial Review) Chem. Soc. Rev., **2013,** 42**,** 6223-6235

197. Damnjanovıc J. Covalently immobilized lipase catalyzing high-yielding optimized geranyl butyrate synthesis in a batch and fluidized bed reactor. *J Mol Catal B*. **2012**;75:50_59

198. Ispas C, Sokolov I, Andreescu S. Enzyme-functionalized mesoporous silica for bioanalytical applications. *Anal Bioanal Chem*. **2009**;393:543_554

199. Bing Z, Rui Z, Yazhen W, Congcong L, Jingtao W, Jindun L. Chitosan_halloysite hybrid nanotubes: h o r s e r a d i s h peroxidase immobilization and applications in phenol removal. *Chem Eng J.* **2013**;214:304_309

200. D.F. Reinhold, T. Utne, N.L. Abramson, Process for L-dopa. *United States patent 4716246,***1987**

201. G.M.J. Carvalho, T.L.M. Alves, D.M.G. Freire, L-DOPA production by immobilized tyrosinase, *Appl. Biochem. Biotechnol.*, **2000,** 84, 791–800

202. R. O. de Faria, V. R. Moure The Biotechnological Potential of Mushroom Tyrosinases,*Food Technol. Biotechnol*, **2007**, 45(3), 287-294

203. P. Pialis, B.A. Saville, Production of L-DOPA from tyrosinase immobilized on nylon 6,6: Enzyme stability and scaleup, *Enzyme Microb. Technol.,* **1998**, 22, 261–268

204. S. Halaouli, M. Asther, Fungal tyrosinases: new prospects in molecular characteristics, bioengineering a n d biotechnological applications, *J. Appl. Microbiol.*, **2006**, 100, 219

205. P. Estrada, R. Sanchez-Muniz, Characterization and optimization of immobilized polyphenol oxidase i n low-water organic solvents, *Biotechnol. Appl. Biochem.*, **1991**, 14, 12-20

206. Boshoff, M.H. Burton, Optimization of Catechol Production by Membrane-Immobilized Polyphenol O x i d a s e : A Modeling Approach, *Biotech Bioeng*, **2003**, 83 (1), 1-7

207. J.C. Espin, C. Soler-Rivas, Synthesis of the Antioxidant Hydroxytyrosol Using Tyrosinase as Biocatalys, *J. Agric. Food Chem.*, **2001**, 49(3), 1187–1193

208. R. Kazandjiand, A. M. Klibanov, Regioselective Oxidation of Phenols Catalyzed by Polyphenol O x i d a s e i n Chloroform, *J. Am. Chem. Soc.*, **1985**, 107, 5448-5450

209. H. Frauenfelder, P.W. Fenimore, B.H. McMahon, Hydration, slaving and protein function; *Biophys. Chem.*, **2002**, 98, 35–48

210. C.R. Dawson, W.B. Tarpley, *Ann. N.Y. Acad. Sci.,* **1963**, 100, 937-948

211. S. Tembe, M. Karve, S. Inamdar, S. Haram, J. Melo, S.F. D'Souza, Development 57 of e l e c t r o c h e m i c a l biosensor based on tyrosinase immobilized in composite biopolymeric film, *Anal.* Biochem., **2006**, 349, 72–77

212. M.P. Sammartino, M. Tomassetti, New enzyme sensor for phenol determination in non aqueous and a q u e o u s medium, *Sens. Actuat. B-Chem.*, **1992**, 7, 383–388,

213. J. Li, L.S. Chia, N.K. Goh, S.N. Tan, Silica sol-gel immobilized amperometric biosensor for the determination of phenolic compounds, *Anal. Chim. Acta,* **1998**, 362, 203–211

214. C. Nistor, J. Emneus, L. Gorton, A. Ciucu, Improved stability and altered selectivity of tyrosinase based graphite electrodes for detection of phenolic compounds, *Anal. Chim. Acta,* **1999**, 387 309–326

215. S.G. Lee, S.P. Hong, M.H. Sung, Removal and bioconversion of phenol in wastewater by a thermostable b-tyrosinase, *Enzyme Microb. Technol.,* **1996**, 19, 374–37

216. *Nanotubes, white paper*, CMP Cientifica, January **2003**

217. Ram Bhagat , Nanotechnology and Clean Water: How Safe Is Our Drinking Water

218. M.S. Dresselhaus, G. Dresselhaus, *Graphite fibers and Filaments* ,Springer, Berlin,Heidelberg, **1988**, 392,393,406,407,411

219. S. Niyogi, M.A. Hamon, H. Hu, B. Zhao, P. Bhowmik, Chemistry of Single-Walled Carbon Nanotubes, *Acc. Chem. Res.*, **2002**, 35(12), 1105-1113

220. Jia Choi, PhD and Yong Zhang- Properties and Applications of Single-, Double- and Multi-Walled Carbon Nanotubes

221. J. Lu, J. Han, Carbon Nanotubes and Nanotube-based Nano Devices, *Int. J. High Spee*68 *d Elec. And Sys,*. **1998**, 9, 101-123

222. P. Asuri, S.S. Karajanagi, Water soluble Carbon Nanotube-Enzyme Conjugates as Functional Biocatalytic Formulations, *Biotechnol. Bioeng.,* **2006**, 95(5), 804-811

223. M. Shim, NWS Kam, RJ Chen, Functionalization of carbon nanotubes for biocompatibility and biomolecular recognition, *Nano Lett*, **2002**, 2, 285-288

224. S.S.Asuri, A.A. Vertegel Structure and Function of Enzymes Adsorbed onto Single-Walled Carbon Nanotubes, *Langmuir*, **2004,** 20, 11594-11599

225. K. Matsuura, T. Saito , T. Okazaki , S. Ohshima , M. Yumura , Iijima S. Selectivity of watersoluble proteins in single-walled carbon nanotube dispersions, *Chem Phys Lett,* **2006**, 429, 497–502

226. C.A. Lee,Y.C. Tsai, Preparation of multiwalled carbon nanotube–chitosan–alcohol dehydrogenase nanobiocomposite for amperometric detection of ethanol, *Sensor Actuat. B*, **2009**, 138, 518–523

227. X. Wu, B. Zhao, P.Wu, H. Zhang, H. Cai, Effects of ionic liquids on enzymatic catalysis of the glucose oxidase toward the oxidation of glucose, *J Phys Chem B,* **2009**, 113, 13365–13373

228. S. Bi, H. Zhou,S. Zhang, Multilayers enzyme-coated carbon nanotubes as biolabel for ultrasensitive chemiluminescence immunoassay of cancer biomarker, *Biosens. Bioelectron.,***2009**, 24, 2961–2966

229. W. Huang, S. Taylor , K. Fu, Y. Lin, D. Zhang, T.W. Hanks, Attaching proteins to carbon nanotubes via diimide-activated amidation, *Nano Lett,* **2002**, 2, 311–314.

230. G.B. Broun, Chemically aggregated enzymes, **1976**, *In* K. Mosbach (Ed.), Methods in enzymology, Academic Press, New York, 263-280

231. B.J. Kim, B.K. Kang, Y.Y. Bahk, K.H. Yoo, K.J. Lim, Immobilization of horseradish peroxidase on multiwalled carbon nanotubes and its enzymatic stability, *Curr Appl Phys*, **2009**, 9, 263–265

232. Miles Hacker,William S. Messer II, Kenneth A. Bachm*ann Pharmacology: Principles and Practice. Academic Press, Jun 19, 2009. pp. 216-217*

233. C. G. Wermuth, C. R. Ganellin, P. Lindberg, L. A. Mitscher; Ganellin; Lindberg; Mitscher (1998). "Glossary of terms used in medicinal chemistry (IUPAC Recommendations **1998)**". *Pure and Applied Chemistry* 70 (5): 1129. doi*:*10.1351/pac199870051129

234. Malhotra, B; Gandelman, K; Sachse, R; Wood, N; Michel, M. C. (**2009**). "The design and development of fesoterodine as a prodrug of 5-hydroxymethyl tolterodine (5-HMT), the active metabolite of tolterodine". *Curr Med Chem.* 16 (33): 4481–9. doi*:*10.2174/092986709789712835. PMID 19835561

235. Stella, VJ; Charman, WN; Naringrekar, VH (**1985**). "Prodrugs. Do they have advantages in clinical practice?". Drugs 29 (5): 455–73. doi:10.2165/00003495-198529050-00002. PMID 3891303

236. B.Y. Zeng, R. Pearce, G. MacKenzie, P. Jenner, Chronic high dose L-dopa treatment does not alter the levels of dopamine D-1, D-2 or D-3 receptor in the striatum of normal monkeys: an autoradiographic study *Journal of neural transmission* 2001, *108*, 925-941

237. N. Quinn, D. Parkes, I. Janota, C. Marsden, *Movement Disorders* 19**86**, *1*, 65-68

238. M. Colamartino, M. Santoro, G. Duranti, S. Sabatini, R. Ceci, A. Testa, L. Padua, R. Cozzi, *Neurotox Res* **2014**

239. F. Pinnen, I. Cacciatore, C. Cornacchia, A. Mollica, P. Sozio, L. S. Cerasa, A. Iannitelli, A. Fontana, C. Nasuti, A. Di Stefano, *Amino acids* **2012**, *42*, 261-269.

240. M. Malakoutikhah, M. Teixidó, E. Giralt, Toward an Optimal Blood−Brain Barrier Shuttle by Synthesis and Evaluation of Peptide Libraries *Journal of medicinal chemistry* **2008**, *51*, 4881-4889

241. *S. S. More, R. Vince, Design, synthesis and biological evaluation of glutathione peptidomimetics as components of anti-Parkinson prodrugs* Journal of medicinal chemistry ***2008, 51, 4581-4588***

242. K. Bobrowski, G. L. Hug, D. Pogocki, B. Marciniak, C. Schöneich, *Journal of the American Chemical Society* **2007**, *129*, 9236-9245

243. Mamta Singh, Seema Gupta, Udita Singhal, Rajesh Pandey, S.K. Aggarwal *Evaluation of the Oxidative Stress in Chronic Alcoholics

244. N. Denora, V. Laquintana, A. Lopedota, M. Serra, L. Dazzi, G. Biggio, D. Pal, A. K. Mitra, A. Latrofa, G. Trapani, G. Liso, *Pharm Res* **2007**, *24*, 1309-1324

245. J. Benavides, B. Peny, D. Ruano, J. Vitorica, B. Scatton, *Brain research* **1993**, *604*, 240-250.

246. A.Durand, J. Thenot, G. Bianchetti, P. Morselli, *Drug metabolism reviews* **1992**, *24*, 239-266

247. B.Asproni, A. Pau, M. Bitti, M. Melosu, R. Cerri, L. Dazzi, E. Seu, E. Maciocco, E. Sanna, F. Busonero, *Journal of medicinal chemistry* **2002**, *45*, 4655-4668

248. K. L. Audus, R. T. Borchardt, *Annals of the New York Academy of Sciences* **1987**, *507*, 9-18

249. D. Pal, K. L. Audus, T. J. Siahaan, *Brain research* **1997**, *747*, 103-113

250. L. Dazzi, M. Serra, M. L. Porceddu, A. Sanna, M. F. Chessa, G. Biggio, *Synapse* **1997**, *26*, 351-358

251. J. A. M. Christiaans, H. Timmerman, *European Journal of Pharmaceutical Sciences* **1996**, *4*, 1-22;

252. A.Di Stefano, B. Mosciatti, G. Mario Cingolani, G. Giorgioni, M. Ricciutelli, I. Cacciatore, P. Sozio, F. Claudi, *Bioorganic & medicinal chemistry letters* **2001**, *11*, 1085-1088

253. T.Zhou, R. C. Hider, P. Jenner, B. Campbell, C. J. Hobbs, S. Rose, M. Jairaj, K. A. Tayarani-Binazir, A. Syme, *European journal of medicinal chemistry* **2010**, *45*, 4035-4042

254. M.-F. Otis, L. Levesque, F. Marceau, J. Lacroix, R. Gaudreault, *Inflammopharmacology* **1992**, *1*, 201-212

255. M. C. Recio, J. Andujar, J. L. Rios, Anti-inflammatory agents from plants: progress and potential. *Curr. Med. Chem.*, **2012**, 19, 2088

256. B.D. Welch, A. P. Van Demark, A. Heroux, C. P. Hill, M. S. Kay, *Proceedings of the National Academy of Sciences*, **2007,** 104, 16828-16833

257. L. D. Walensky, A. L. Kung, I. Escher, Activation of apoptosis in vivo by a hydrocarbon-stapled BH3 helix. *Science*, **2004**, 305, 1466-1470

258. *P. M. Abou-Sleiman, M. M. Muqit, N. W. Wood, Expanding insights of mitochondrial dysfunction in Parkinson's disease* Nature Reviews Neuroscience ***2006, 7, 207-219***

259. J. P. Bai, G. L. Amidon, *Pharm Res* **1992**, *9*, 969-978

260. Y.J. Fei, Y. Kanai, S. Nussberger, V. Ganapathy, F. H. Leibach, M. F. Romero, S. K. Singh, W. F. Boron, M. A. Hediger, *Nature*,**1994** Apr 7;368(6471):563-6

261. K. Miyamoto, T. Shiraga, K. Morita, H. Yamamoto, H. Haga, Y. Taketani, I. Tamai, Y. Sai, A. Tsuji, E. Takeda, *Biochim Biophys Acta* **1996,** *1305*, 34-38

262. C.L. Wang, Y.-B. Fan, H.-H. Lu, T.-H. Tsai, M.-C. Tsai, H.-P. Wang, *Journal of biomedical science* **2010**, *17*, 1-8

263. H.P. Wang, J.-S. Lee, M.-C. Tsai, H.-H. Lu, W. Hsu, *Bioorganic & Medicinal Chemistry Letters* **1995**, 5 , 2195-2198

264. J. O'Neill, F. Veitch, T. Wagner-Jauregg, *The Journal of Organic Chemistry* 1956, *21*, 363-364, Niu, J.; Lawrence, D.S. *J.Biol.Chem.* **1997**, 272, 1493-1499

265. S. K. Chowdhury, J. Eshraghi, H. Wolfe, D. Forde, A. G. Hlavac, D. Johnston, *Anal Chem* 1995, *67*, 390-398; S. Ranganathan, N. Tamilarasu, *Tetrahedron letters* **1994,** *35*, 447-450;

266. S. Ranganathan, N. Tamilarasu, *Tetrahedron letters* **1994**, *35*, 447-450

267. J. Ueda, T. Ozawa, M. Miyazaki, Y. Fujiwara, *J Inorg Biochem* **1994,** *55*, 123-130.

268. J. C. Grammer, J. A. Loo, C. G. Edmonds, C. R. Cremo, R. G. Yount, *Biochemistry* **1996,** *35*, 15582- 15592.

269. F. Lazzaro, M. Crucianelli, F. De Angelis, V. Neri, R. Saladino, A novel oxidative side-chain transformation of ï¡-amino acids and peptides by methyltrioxorhenium/H$_2$O$_2$ system" *Tetrahedron Lett.* **2004**, 45, 9237-9240

270. R. Saladino, M. Mezzetti, E. Mincione, A. T. Palamara, P. Savini, S. Marini, synthesis, cytotoxic effect and antiviral activity of 5-bromo-N^4-substituted-1-(ï¢-D-arabinofuranosyl)cytosine and 5- bromo-O4-methyl-1-(ï¢-D-arabinofuranosyl)pyrimidin-2(1H)-one derivatives" Nucleosides & Nucleotides , **1999**, 18(11 & 12), 2499-2510, New York, U.S.A

271. G. Botta, M. Delfino, M. Guazzaroni, C. Crestini, S. Onofri, R.Saladino, Selective Synthesis of DOPA and DOPA Peptides by Native and Immobilized Tyrosinase in Organic Solvent *ChemPlusChem* **2013**, *78*, 325-330

272. M. Guazzaroni, M. Pasqualini, G. Botta, R. Saladino, A Novel Synthesis of Bioactive Catechols by Layer-by- Layer Immobilized Tyrosinase in an Organic Solvent Medium *ChemCatChem* **2012**, 4, 89

273. S. K. Chowdhury, J. Eshraghi, H. Wolfe, D. Forde, A. G. Hlavac and D. Johnston, Anal. Chem., **1995**, 67, 390– 398.

274. S. Ranganathan and N. Tamilarasu, Tetrahedron Lett., **1994**, 35, 447–450.

275. J. Ueda, T. Ozawa, M. Miyazaki and Y. Fujiwara, J. Inorg. Biochem., **1994**, 55, 123–130.

276. J. C. Grammer, J. A. Loo, C. G. Edmonds, C. R. Cremo and R. G. Yount, Biochemistry, **1996**, 35, 15582–15592.

277. F. Lazzaro, M. Crucianelli, F. de Angelis, V. Neri and R. Saladino, Tetrahedron Lett., **2004**, 45, 9237–9240.

278. R. Saladino, M. Mezzetti, E. Mincione, A. T. Palamara, P. Savini and S. Marini, Nucleosides Nucleotides, **1999**,18, 2499–2510.

279. G. Botta, M. Delfino, M. Guazzaroni, C. Crestini, S. Onofri and R. Saladino, ChemPlusChem, **2013**, 78, 325–330.

280. C. Fonseca, M. R. M. Domingues, C. Sim˜oes, F. Amado and P. Domingues, J. Mass Spectrom., **2009**, 44, 681– 693.

281. R. Bernini, M. Barontini, F. Crisante, M. C. Ginnasi and R. Saladino, Tetrahedron Lett., **2009,** 50, 6519–6521.

282. D. Magdziak, A. A. Rodriguez, R. W. van de Water and T. R. Pettus, Org. Lett., **2002**, 4, 285–288.

283. A. Ozanne, L. Pouys´egu, D. Depernet, B. Francois and S. Quideau, Org. Lett., **2003**, 5, 2903–2906.

284. S. Quideau, L. Pouys´egu, D. Deffieux, A. Ozanne, J. Gagnepain, I. Fabre and M. Oxobya, ARKIVOC, **2003**, 6, 106–119.

285. R. Bernini, S. Cacchi, G. Fabrizi and E. Filisti, Org. Lett., **2008**, 10, 3457–3460.

286. R. Bernini, E. Mincione, M. Barontini and F. Crisante, J. Agric. Food Chem., **2008**, 56, 8897–8904.

287. K. Marumo and J. Waite, Biochim. Biophys. Acta. Protein. Struct. Mol. Enzymol., **1986**, 872, 98–103.

288. R. Bernini, E. Mincione, F. Crisante, M. Barontini and G. Fabrizi, Tetrahedron Lett., **2009**, 50, 1307–1310.

289. P. Vlieghe, V. Lisowki, J. Mcertines and M. Khrestchatinsky, Drug Discovery Today, **2010**, 15, 40–56.

290. S. M. Miller, R. J. Simon, S. Ng, R. N. Zucherman, J. M. Kerr and W. H. Moos, Drug Dev. Res., **1995**, 35, 20–32.

291. B. Liu, L. Burdine and J. Thomas Kodadek, J. Am. Chem. Soc., **2006**, 128(47), 15228–15235.

292. L. Burdine, T. G. Gillette, H. J. Lin and T. J. Kodadek, J. Am. Chem. Soc., **2004**, 126, 11442–11443.

293. L. A. Burzio and J. H. Waite, Biochemistry, **2000**, 39, 11147– 11153.

294. S. Jus, I. Stachel, W. Schloegl, M. Pretzler, W. Friess and M. Meyer, et al., Mater. Sci. Eng. C, 2011, 31, 1068–1077.

295. M. L. Mattinen, R. Lantto, E. Selinheimo, K. Kruus and J. Buchert, J. Biotechnol., **2008**, 133, 395.

296. G. Matheis and T. R. Whitaker, J. Food Biochem., 1984, 8, 137.

297. E. Valero, R. Varon and F. Garcıa-Carmona, Arch. Biochem. Biophys., **2003**, 416, 218–226.

298. M. Jimenez, F. Garcia-Carmona, F. Garcia Canovas, J. L. Iborra, J. A. Lozano and F. Martinez, Arch. Biochem. Biophys., **1984**, 235, 438–448.

299. M. Uyanik, T. Mutsuga and K. Ishihara, Molecules, **2012**, 17, 8604–8616.

300. V. Satam, A. Harad, R. Rajule and H. Pati, Tetrahedron, **2010**, 66(39), 7659–7706.

301. S. Quideau, L. Pouys ́egu, D. Deffieux, A. Ozanne,

302. J. Gagnepain, I. Fabre and M. Oxobya, ARKIVOC, **2003**, IV, 106–119.

303. D. E. Fullenkamp, D. G. Barrett, D. R. Miller, J. W. Kurutz and P. B. Messersmith, RSC Adv., 2014, 4, 25127–25134.

304. M. S. Yusubova and V. V. Zhdankin, Mendeleev Commun., 2010, 20, 185–191.

305. T. K. Achar, S. Maitia and P. Mal, RSC Adv., 2014, 4, 12834– 12839.

306. R. A. Floyd, Exp. Biol. Med., 1999, 222, 236–245.

307. P. A. Serra, G. Esposito, P. Enrico, M. A. Mura, R. Migheli, M. R. Delogu, M. Miele, M. S. Desole, G. Grella and E. Miele, Br. J. Pharmacol., 2000, 130, 937–945.

308. M. Reale, M. Pesce, M. Priyadarshini, M. A Kamal and A. Patruno, Curr. Drug Targets: CNS Neurol. Disord., 2012, 11, 430–438.

309. X. Liu, N. Yamada, W. Maruyama and T. Osawa, J. Biol. Chem., 2008, 283, 34887–34895.

310. C. Lipinski, F. Lombardo, B. Dominy, P. Feeney, Cross Ref, CAS, Web of Science® Times Cited, 1997, 3107.

311. S. K. Han, C. Mytilineou and G. Cohen, J. Neurochem., 1996, 66, 501–510

312. A. V. Carrano, J. Occup. Med., 1986, 28, 1112–1116.

313. S. Derochette, T. Franck, A. Mouithys-Mickalad, G. Deby- Dupont, P. Neven and D. Serteyn, Intra- and extracellular antioxidant capacities of the new water-soluble form of curcumin (NDS27) on stimulated neutrophils and HL-60 cells, Chem.-Biol. Interact., 2013, 201, 49–57.

314. N. I. Fedotcheva, R. E. Kazakov, M. N. Kondrashova and N. V. Beloborodova, Toxicol. Lett., 2008, 180, 182–188.

315. M. Dusinsk ́a, Z. Dzupinkov ́a, L. Ws ́olov ́a, V. Harrington and A. R. Collins, Mutagenesis, 2006, 21, 205–211.

316. T. Francka, A. Mouithys-Mickalada, T. Robertc, G. Ghittic, G. Deby-Duponta, P. Nevend and D. Serteyna, Chem.-Biol. Interact., 2013, 206(2), 194–203.

317. M. Guazzaroni, M. Pasqualini, G. Botta, R. Saladino, A Novel Synthesis of Bioactive Catechols by Layer-by-Layer Immobilized Tyrosinase in an Organic Solvent Medium ChemCatChem 2012, 4, 89 – 99.

318. G. Botta, M. Delfino, M. Guazzaroni, C. Crestini, S. Onofri, R.Saladino, Selective Synthesis of DOPA and DOPA Peptides by Native and Immobilized Tyrosinase in Organic Solvent ChemPlusChem 2013, 78, 325-330.

319. E. I. Solomon,U. M Sundaram, Multicopper oxidases and oxygenases, Chem. Rev., 1997, 96(7), 2563- 2606.

320. a. G. Prota, Tyrosinase. In Melanins and Melanogenesis, Jovanovich, H.B., ed., Academic Press, San Diego, 1992, 34-62. b. Gasowska, Kfarski, Interaction of mushroom Tyrosinase with aromatic amines, odiamines and o-aminophenols, Biochim. Biophys. Acta, 2004, 1673, 170-177.

321. a. J. Espìn, Kinetic characterization of the substrate specificity and mechanism of mushroom Tyrosinase, Eur. J. Biochem., 2000, 267, 1270-1279. b. M. Guazzaroni, C. Crestini, R. Saladino, Layer-by-Layer coated tyrosinase: An efficient and selective synthesis of catechols, Bioorg. Med. Chem., 2012, 20(1), 157-66.

322. a. Miller S.M., Simon R.J., Ng S., Zucherman R.N., Kerr J.M., Moos W.H., Drug Dev. Res., 1995, 35, 20-32. b. Vlieghe P., Lisowki V., Mcertines J., Khrestchatinsky M., Drug Discov. Today, 2010, 15, 40-56.

323. a. Bo Liu, Lyle Burdine and Thomas Kodadek, J. Am. Chem. Soc., 2006, 128(47), 15228-15235. b. Burdine L., Gillette T.G., Lin H.J., Kodadek T. J. Am. Chem. Soc., 2004, 126, 11442-11443. c. Burzio L. A., Waite J. H., Biochemistry, 2000, 39, 11147-11153. d. S. Jus, I. Stachel, W. Schloegl, M. Pretzler, W. Friess, M. Meyer, et al. Materials Science and Engineering C, 2011, 31, 1068-1077.

324. a. M. Jimenez, F. Garcia-Carmona, F. Garcia Canovas, J. L. Iborra, J. A. Lozano, F. Martinez, Arc. of Biochem. and Bioph. 1984, 235, 438-448. b. Edelmira Valero, Ramon Varon, Francisco Garcia-Carmona, Arc. of Biochem. and Bioph. 416 (2003) 218–226.

325. C. Lipinski, F. Lombardo, B. Dominy, P. Feeney, CrossRef, CAS, Web of Science® Times Cited 1997, 3107.

326. a) Brena, B.; González-Pombo, P.; Batista-Viera, F. Methods Mol. Biol. 2013, 1051, 15-31. b) Barbosa, O.; Torres, R.; Ortiz, C.; Berenguer Murcia, A.; Rodrigues, R. C.; Fernandez-Lafuente, R. Biomacromolecules 2013, 14, 2433-2462. c) Rodrigues, R. C.; Ortiz, C.; Berenguer-Murcia, A.; Torres, R.; Fernández-Lafuente, R. Chem. Soc.Rev. 2013, 42, 6290-6307. d) Zhou, Z.; Hartmann, M. ibid. 2013, 42, 3894-3912. e) Verma, M. L.; Barrow, C. J.; Puri, M. Appl. Microbiol. Biot. 2013, 97, 23-39. f) Hwang, E. T.; Gu, M. B. Eng.Life Sci. 2013, 13, 49-61. g) Rajkumar, K.; Palla, S.; Paladugu, A.; Reddy, E. R.; Reddy, K. R. Int.Res. J. Pharm. 2013, 4, 36-44.

327. Vered Shuster, Ayelet Fishman- Isolation, cloning and characterization of a tyrosinase with improved activity in organic solvents from Bacillus megaterium. J Mol Microbiol Biotechnol 2009 6;17(4):188-200.

328. S. Naish-Byfield , P.A. Riley - Oxidation of monohydric phenol substrates by tyrosinase. An oximetric study. Biochem J. 1992, 288, 63-7.

329. P. Asuri, S.S. Karajanagi, Water soluble Carbon Nanotube-Enzyme Conjugates as Functional Biocatalytic Formulations, Biotechnol. Bioeng., 2006, 95(5), 804-811

330. G.B. Broun, Chemically aggregated enzymes, 1976, In K. Mosbach (Ed.), Methods in enzymology, Academic Press, New York, 263-28]

331. C. Satish, J.T. Mohapatra, Time dependent behaviour of the cross-linking reaction of α-chymotrypsin with Glutaraldehyde, Biotechnol. Tech., 1994, 8, 13–16.

332. G. Botta, B.M. Bizzarri, A.Garozzo, R.Timpanaro, B. Bisignano, D. Amatore, A.T.Palamara, L.Nencioni, R.Saladino- Carbon nanotubes supported tyrosinase in the synthesis of lipophilic hydroxytyrosol and dihydrocaffeoyl catechols with antiviral activity against DNA and RNA viruses- Bioorganic & Medicinal Chemistry journal homepage: www.elsevier .com

333. Mercuri NB, Calabresi P, Bernardi G. The electrophysiological actions of dopamine and dopaminergic drugs on neurons of the substantia nigra pars compacta and ventral tegmental area. Life Sci. 1992;51(10):711-8. Review. PubMed PMID:1355254.

REFERENCES CHAPTER II

1. M.P. Palthur, S.S.S. Palthur, S.K. Chitta, Nutraceuticals: concept and regulatory scenario Int. J. Pharm. Pharm. Sci, 2010, 2, 14-20

2. H.K. Biesalski, Nutraceuticals: the link between nutrition and medicine. In: K. Kramer, P.P. Hoppe and L. Packer eds. Nutraceuticals in health and disease prevention. New York: Marcel Deckker Inc. pp. 1-26, 2001.

3. E.L. Gibson, J. Wardel, C.J. Watts, Appetite, 1998, 31, 205-228.

4. J.J. Thiele, C. Schroeter, S.N. Hsieh, M. Podda, L. Packer, Curr. Probl. Dermatol. 29 (2001) 26–42.

5. Hahn NI. Is Phytoestrogens Nature's Cure for What Ails Us? A Look at the Research. Journal of the American Dietetic Association, 1998; 98: 974-976.

6. D. Strack, 1997, Phenolic metabolism. In P.M. Dey and J.B. Harborne (eds), Plant Biochemistry. Academic Press, London, pp. 387–416.

7. Manach, C.; Williamson, G.; Morand, C.; Scalbert, A.; Rémésy, C. Bioavailability and bioefficacy of polyphenols in humans. I. Review of 97 bioavailability studies. Am. J. Clin. Nutr., 2005, 81, 230S-242S.

8. T. Swain, Ann. Rev. Plant Physiol., 1977, 28, 479.

9. T.M. Kutchan, Plant Physiol, 2001, 125, 58.

10. P. M. Dey, J. B. Harborne, Plant Biochemistry,1997

11. C.A. Rice-Evans, N.J. Miller, G. Paganga, Free Radic Biol Med, 1996, 20, 933-56.

12. R.L. Prior, G. Cao, Hort Sci, 2000, 35, 588-92.

13. B.N. Ames, M. Shigenga, T.M. Hagen, Proc Natl Acad Sci USA, 1993, 90, 7915-22.

14. B.P. Yu, Free Radic Biol Med, 1996, 21, 651-68.

15. J.P. Kehrer, C.V. Smith, 1994. Free radicals in biology: Sources, reactivities, and roles in the etiology of human diseases. In: Natural antioxidants. 25–62. Frei, B., ed. San Diego, Academic Press.

16. A. Scalbert, G. Williamson, J Nutr, 2000, 130, 2073S–85S.

17. C. Manach, A. Scalbert, C. Morrand, C. Rèmèsy, L. Jimènez, Am. J. Clin. Nutr., 2004, 79, 727-747

18. Gustafson, D. L.; Beall, H. D.; Bolton, E. M.; Ross, D.; Waldren, C. A. Mol. Pharmacol. 1996, 50(4), 728-735.

19. Prescott, A. G.; John, P. Annu. Rev. Plant Physiol. Plant Mol. Biol. 1996, 47, 245-271.

20. Palamara, A.T.; Nencioni, L.; Aquilano, K.; De Chiara, G.; Hernandez, L.; Cozzolino, F.; Ciriolo, M.R.; Garaci, E. J. Infect. Dis., 2005, 191, 1719.

21. R.Saladino, G. Gualandi, Angela Farina, Claudia Crestini, Lucia Nencioni and Anna Teresa Palamara Current Medicinal Chemistry, 2008, 15, 1500-1519

22. Emerging Infectious Diseases: MERS-COV, Avian Influenza Remind us of the Ongoing Challenge, 2016. http:// www.infectioncontroltoday.com

23. D.M. Morens, A.S. Fauci, Emerging infectious diseases in 2012: 20 years after the institute of medicine report, MBio 3 (2012).

24. C.R. Howard, N.F. Fletcher, Emerging virus diseases: can we ever expect the unexpected? Emerg. Microb. Infect. 1 (2012) e46.

25. B. H. Havsteen The biochemistry and medical significance of the flavonoids. Pharmacology & Therapeutics 96 (2002) 67– 202

26. R.J. Nijveldt, E. van Nood, D.E.C. van Hoorn, P.G. Boelens, K. van Norren, P.A.M. van Leeuwen, Flavonoids: a review of probable mechanisms of action and potential applications. Am J Clin Nutr, 2001, 74, 418-425.

27. Ohtake, N.; Nakai, Y.; Yamamoto, M.; Sakakibara, I.; Takeda, S.; Amagaya, S.; Aburada, M. J. Sho-saiko-to, a traditional herbal medicine, regulates gene expression and biological function by way of microRNAs in primary mouse hepatocytes Chromatogr. B Analyt. Technol. Biomed. Life Sci. 2004, 812, 135.

28. Li, B.Q.; Fu, T.; Yan, Y.D.; Baylor, N.W.; Ruscetti, F.W.; Kung, H.F. Cell. Mol. Biol. Res. 1993, 39, 119.

29. Ng TB, Huang B, Fong WP, Yeung HW. Anti-human immunodeficiency virus (anti-HIV) natural products with special emphasis on HIV reverse transcriptase inhibitors. Life Sci 1997;61:933–49.

30. Sokmen, M.; Angelova, M.; Krumova, E.: Protective effect of polyphenol-rich extract on acute lung injury in influenza virus infected mice. Life Sci., 2005, 76, 2981-2993

31. Beck, M.A., Handy, J., Levander, O.A., 2000. The role of oxidative stress in viral infections. Ann. N Y Acad. Sci. 917, 906–912.

32. Palamara, A.T., Perno, C.F., Ciriolo, M.R., Dini, L., Balestra, E., D'Agostini, C., Di Francesco, P., Favalli, C., Rotilio, G., Garaci, E., 1995. Evidence for antiviral activity of glutathione: in vitro inhibition of herpes simplex virus type 1 replication. Antiviral Res. 27 (3), 237–253.

33. Yamada, Y.; Limmon, G.V.; Zheng, D.; Li, N.; Li. L.; Yin, L.; Chow, V.T.; Chen, J.; Engelward, B.P. Major shifts in the spatiotemporal distribution of lung antioxidant enzymes during influenza pneumonia. PLoS One, 2012, 7(2):e31494.

34. Sheridan, P.A.; Zhong, N.; Carlson, B.A.; Perella, C.M.; Hatfield, D.L.; Beck, M.A. Decreased selenoprotein expression alters the immune response during influenza virus infection in mice. J. Nutr., 2007, 137(6), 1466-1471.

35. Sgarbanti, R.; Nencioni, L.; Amatore, D.; Coluccio, P.; Fraternale, A.; Sale, P.; Mammola C.L.; Carpino, G.; Gaudio, E.; Magnani,M.; Ciriolo, M.R.; Garaci, E.; Palamara, A.T. Redox regulation of the influenza hemagglutinin maturation process: a new cellmediated strategy for anti-influenza therapy. Anti.Redox Signal, 2011, 15(3), 593-606

36. Nencioni, L.; Iuvara, A.; Aquilano, K.; Ciriolo, M.R.; Cozzolino, F.; Rotilio, G.; Garaci, E.; Palamara, A.T. Influenza A virus replication is dependent on an antioxidant pathway that involves GSH and Bcl-2. FASEB J., 2003, 17(6), 758-60.

37. Amatore, D.; Sgarbanti, R.; Aquilano, K.; Baldelli, S.; Limongi, D.; Civitelli, L.; Nencioni, L.; Garaci, E.; Ciriolo, M.R.; Palamara, A.T. Influenza virus replication in lung epithelial cells depends on redox-sensitive pathways activated by NOX4-derived ROS. Cell Microbiol., 2014

38. Peterhans, E. Oxidants and antioxidants in viral diseases: disease mechanisms and metabolic regulation. J. Nutr., 1997, 127, S962-546 -Kumar P, Sharma S, Khanna M, Raj HG. Effect of Quercetin on lipid peroxidation and changes in lung morphology in experimental influenza virus infection. Int J Exp Pathol. 2003;84(3):127–133.

39. Akaike, T.; Noguchi, Y.; Ijiri, S.; Setoguchi, K.; Suga, M.; Zheng, Y.M.; Dietzschold, B.; Maeda, H. Pathogenesis of influenza virusinduced pneumonia: involvement of both nitric oxide and oxygen radicals. Proc. Natl. Acad. Sci. U S A, 1996, 93, 2448-53.

40. Van der Vliet, A.; Eiserich, J.P.; Cross, C.E. Nitric oxide: a proinflammatory mediators in lung disease? Respir Res., 2000; 167-72.

41. Dai, D.F.; Chiao, Y.A.; Marcinek, D.J.; Szeto, H.H.; Rabinovitch, P.S. Mitochondrial oxidative stress in aging and healthspan. Longev. Health., 2014, 3:6.

42. B. Halliwell, J.M.C. Gutteridge, Free Radicals in Biology and Medicine, fourth ed., Clarendon Press, Oxford, UK, 2007.

43. J.J. Thiele, C. Schroeter, S.N. Hsieh, M. Podda, L. Packer, Curr. Probl. Dermatol. 29 (2001) 26 42.

44. Rietjens, I.; Boersma, M.; de Haan, L.; Spenkelink, B.; Awad, H.M.; Cnubben, N.H.; van Zanden, J.J.; Woude, Hv.; Alink, G.M.; Koeman, J.H. The pro-oxidant chemistry of the natural antioxidants vitamin C, vitamin E, carotenoids and flavonoids. *Environ. Toxicol. Pharmacol.,* 2001, *11,* 321e33.

45. Meister A, Anderson ME. Glutathione. Annu. Rev. Biochem. 1983;52:711–760.

46. Townsend DM, Tew KD, Tapiero H. The importance of glutathione in human disease. Biomed. Pharmacother. 2003;57:145–155.

47. R. Saladino, M. Barontini, M. Crucianelli, L. Nencioni, R. Sgarbanti and A.T. Palamara Current Advances in Anti-Influenza Therapy Current Medicinal Chemistry, 2010, 17, 2101-2140

48. Nencioni, L.; Sgarbanti, R.; De Chiara, G.; Garaci, E.; Palamara, A.T. Influenza virus and redox mediated cell signaling: a complex network of virus/host interaction. New Microbiol., 2007, 30(4), 367-375.

49. Cai, J.; Chen, Y.; Seth, S.; Furukawa, S.; Compans, R.W.; Jones, D.P. Inhibition of influenza infection by glutathione. *Free Radic. Biol. Med.,* **2003**, *34*, 928–936.

50. Witschi, A; Reddy, S; Stofer, B; Lauterburg, BH (1992). "The systemic availability of oral glutathione". Eur J Clin Pharmacol. 43 (6): 667–9.

51. Palamara, A.T.; Brandi, G.; Rossi, L.; Millo, E.; Benatti, U.; Nencioni, L.; Iuvara, A.; Garaci, E.; Magnani, M. New synthetic glutathione derivatives with increased antiviral activities. Antiv. Chem. Chemother., 2004, 15, 83-91.

52. Sgarbanti, R.; Nencioni, L.; Amatore, D.; Coluccio, P.; Fraternale, A.; Sale, P.; Mammola C.L.; Carpino, G.; Gaudio, E.; Magnani, M.; Ciriolo, M.R.; Garaci, E.; Palamara, A.T. Redox regulation of the influenza hemagglutinin maturation process: a new cellmediated strategy for anti-influenza therapy. Anti.Redox Signal, 2011, 15(3), 593-606.

53. Wilkinson B, Gilbert HF (Jun 2004). "Protein disulfide isomerase". Biochimica et Biophysica Acta. 1699 (1-2): 35–44. doi:10.1016/j.bbapap.2004.02.017

54. Heather L. Van Epps Influenza: exposing the true killer JEM Home » 2006 Archive » 17 April » 203 (4): 803

55. WHO, WHO facts sheet No.211 Influenza (seasonal) March 2014.

56. CDC. Centers for Disease Control and Prevention Influenza (Flu) September 15, 2016

57. Palese, P.; Shaw, M.L. In Virology; Fields, B.N.; Knipe, D.M.; Howley, P.M. Ed.; Lippincott-Raven Publishers: Philadelphia, 2007; Vol. 47, pp. 1647-1689.

58. Gabriele Neumann, Takeshi Noda & Yoshihiro Kawaoka Emergence and pandemic potential of swine-origin H1N1 influenza virus Nature 459, 931-939 (18 June 2009).

59. Martha I. Nelson1 & Edward C. Holmes The evolution of epidemic influenza, Nature Reviews Genetics 8, 196-205 (March 2007).

60. Wu Y., Wu Y., Tefsen B., Shi Y., Gao GF. Bat-derived influenza-like viruses H17N10 and H18N11. Trends Microbiol. 2014 Apr;22(4):183-91.

61. Hale BG1, Randall RE, Ortín J, Jackson D. The multifunctional NS1 protein of influenza A viruses. J Gen Virol. 2008 Oct;89(Pt 10):2359-76.

62. John Beigel , Mike Bray. Current and future antiviral therapy of severe seasonal and avian influenza. "Current and future antiviral therapy of severe seasonal and avian influenza." Antiviral research 78.1 (2008): 91-102.

63. Hayden FG. Pandemic influenza: is an antiviral response realistic? Pediatr Infect Dis J 2004;23:Suppl:S262-S269

64. Sgarbanti R, Amatore D, Celestino I, Marcocci ME, Fraternale A, Ciriolo MR, Magnani M, Saladino R, Garaci E, Palamara AT, Nencioni L. Intracellular redox state as target for anti-influenza therapy: are antioxidants always effective? Curr Top Med Chem. 2014;14(22):2529-41.

65. Pinto LH, Lamb RA. The M2 proton channels of influenza A and B viruses. J Biol Chem. 2006 Apr 7;281(14): 8997-9000. Epub 2005 Dec 30.

66. Leonov H, Astrahan P, Krugliak M, Arkin IT (2011) How do aminoadamantanes block the influenza M2 channel, and how does resistance develop? J Am Chem Soc 133(25):9903–9911.

67. Frederick G. Hayden, M.D. Antiviral Resistance in Influenza Viruses — Implications for Management and Pandemic Response. N Engl J Med 2006; 354:785-788February 23, 2006.

68. Von Itzstein M1, Wu WY, Kok GB, Pegg MS, Dyason JC, Jin B, Van Phan T, Smythe ML, White HF, Oliver SW, et al. Rational design of potent sialidase-based inhibitors of influenza virus replication. Nature. 1993 Jun 3;363(6428):418-23.

69. Anne Moscona, M.D. Neuraminidase Inhibitors for Influenza N Engl J Med 2005; 353:1363-1373September 29, 2005.

70. Whitley RJ, Hayden FG, Reisinger KS, et al. Oral oseltamivir treatment of influenza in children. Pediatr Infect Dis J 2001;20:127-133[Erratum, Pediatr Infect Dis J 2001;20:421.

71. Kiso M, Mitamura K, Sakai-Tagawa Y, et al. Resistant influenza A viruses in children treated with oseltamivir: descriptive study. Lancet 2004;364:759-765.

72. Moscona A. Oseltamivir-resistant influenza? Lancet 2004;364:733-734.

73. De Clercq E. Human viral diseases: what is next for antiviral drug discovery? Curr Opin Virol. 2012 Oct;2(5): 572-9.

74. Nencioni L1, De Chiara G, Sgarbanti R, Amatore D, Aquilano K, Marcocci ME, Serafino A, Torcia M, Cozzolino F, Ciriolo MR, Garaci E, Palamara AT. Bcl-2 expression and p38MAPK activity in cells infected with influenza A virus: impact on virally induced apoptosis and viral replication. J Biol Chem. 2009 Jun 5;284(23):16004-15.

75. Palamara, A.T.; Nencioni, L.; Aquilano, K.; De Chiara, G.; Hernandez, L.; Cozzolino, F.; Ciriolo, M.R.; Garaci, E.: Inhibition of Influenza A virus replication by resveratrol. J. Infect. Dis., 2005, 191, 1719-1729.

76. Nakayama, M.; Suzuki, K.; Toda, M.; Okubo, S.; Hara, Y.; Shimamura, T. Inhibition of the infectivity of influenza virus by tea polyphenols. Antiviral. Res., 1993, 21(4), 289-99.

77. Brenes, M.; Garcia, A.; Gracia, P.; Rios, J.J.; Garrido, A. Phenolic compounds in Spanish oils. J. Agric. Food. Chem., 1999, 47, 3535-3540.

78. Lee-Huang, S.; Huang, P.L.; Zhang, D.; Lee, J.W.; Bao, J.; Sun, Y.; Chang, Y.T.; Zhang, J.Z.H. and Huang, P.L. Discovery of small-molecule HIV-1 fusion and integrase inhibitors oleuropein and hydroxytyrosol: Part II. Integrase inhibition. Biochem. Biophys. Res. Commun., 2007, 354, 879-884.

79. D. Egan, R. O'Kennedy, E. Moran, D. Cox, E. Prosser, R.D. Thornes, Drug Metab Rev, 1990, 22, 503-529.

80. D. Egan, R. O'Kennedy, J Chromatogr B, 1992, 582, 137-143.

81. G. Finn, E. Kenealy, B. Creaven, D. Egan, Cancer Letts, 2002, 183, 61-68.

82. Vogel, A (1820). "Darstellung von Benzoesäure aus der Tonka-Bohne und aus den Meliloten - oder Steinklee - Blumen (Preparation of benzoic acid from tonka beans and from the flowers of melilot or sweet clover)". Annalen der Physik. 64 (2): 161–66.

83. B. Lake, Food Chem Tox, 1999, 37, 423-453.

84. Riveiro ME, De Kimpe N, Moglioni A, Vázquez R, Monczor F, Shayo C, Davio C. Coumarins: old compounds with novel promising therapeutic perspectives. Curr Med Chem. 2010;17(13):1325-38.

85. Douglas Wardrop and David Keeling The story of the discovery of heparin and warfarin British Journal of Haematology Volume 141, Issue 6, Version of Record online: 18 MAR 2008.

86. A.J. Cohen. Food and Cosmetics Toxicology Volume 17, Issue 3, 1979, Pages 277-289

87. Brown SA (1981) Coumarins. In: Stumpf PK, Conn EE (eds) The biochemistry of plants—A comprehensivetreatise, vol 7. Academic Press, New York, pp 269–300.

88. Garcia-Molina MO1, Munoz-Munoz JL, Garcia-Molina F, Rodriguez-Lopez JN, Garcia-Canovas F. Study of umbelliferone hydroxylation to esculetin catalyzed by polyphenol oxidase. Biol Pharm Bull. 2013;36(7):1140-5.

89. Brown SA (1962) Biosynthesis of coumarin and herniarin in lavender. Science 137:977–978

90. F. BourgaudEmail authorA. HehnR. LarbatS. DoerperE. GontierS. KellnerU. Matern, Biosynthesis of coumarins in plants: a major pathway still to be unravelled for cytochrome P450 enzymes. Phytochemistry Reviews June 2006, Volume 5, Issue 2, pp 293–308.

91. Teutsch HG, Hasenfratz MP, Lesot A, Stoltz C, Garnier JM, Jeltsch JM, Durst F, Werckreichhart D (1993) Isolation and Sequence of a Cdna-Encoding the Jerusalem-Artichoke Cinnamate 4-Hydroxylase, a Major Plant Cytochrome-P450 Involved in the General Phenylpropanoid Pathway. Proc Natl Acad Sci USA 90:4102–4106

92. Anterola AM, Lewis NG (2002) Trends in lignin modification: a comprehensive analysis of the effects of genetic manipulations/mutations on lignification and vascular integrity. Phytochemistry 61:221–294

93. Harborne JB (1999) Classes and functions of secondary products from plants. In Walton NJ, Brown DE (eds) Chemicals from plants. Imperial College Press, London, pp 1–25

94. Brown SA (1985) Biosynthesis of 6,7-dihydroxycoumarin in Cichorium intybus. Can J Biochem Cell Biol 63:292–295.

95. Garcia-Molina MO1, Munoz-Munoz JL, Garcia-Molina F, Rodriguez-Lopez JN, Garcia-Canovas F. Study of umbelliferone hydroxylation to esculetin catalyzed by polyphenol oxidase. Biol Pharm Bull. 2013;36(7):1140-5.

96. Naceur, H.; Fischmeister, C.; Puerta, M.; Valerga, P. A rapid access to new coumarinyl chalcone and substituted chromeno[4,3-c]pyrazol-4(1H)-ones and their antibacterial and DPPH radical scavenging activities. Med. Chem. Res. 2011, 20, 522–530.

97. Irena Kostova , Synthetic and Natural Coumarins as Antioxidants Mini Reviews in Medicinal Chemistry, Volume 6, Number 4, April 2006, pp. 365-374(10)

98. Dr. Jignesh Lunagariya et al. Coumarin as a Potential Pharmacophore in Medicinal Chemistry, International Journal for Research in Management and Pharmacy Vol. 3, Issue 1 Jan. February 2014

99. M.A. Soobratteea, V.S. Neergheena, A. Luximon-Rammaa, O.I. Aruomab, , , T. Bahoruna, Phenolics as potential antioxidant therapeutic agents: Mechanism and actions Mutation Research/Fundamental and Molecular Mechanisms of Mutagenesis Volume 579, Issues 1–2, 11 November 2005, Pages 200–213.

100. Rehakova Z1, Koleckar V, Cervenka F, Jahodar L, Saso L, Opletal L, Jun D, Kuca K. DPPH Radical Scavenging Activity of Several Naturally Occurring Coumarins and Their Synthesized Analogs Measured by the SIA Method. Toxicol Mech Methods. 2008;18(5):413-8.

101. Vaya, J.; Aviram, M. Nutritional Antioxidants Mechanisms of Action, Analyses of Activities and Medical Applications Current Medicinal Chemistry - Immunology, Endocrine & Metabolic Agents, Volume 1, Number 1, 1 May 2001, pp. 99-117(19).

102. Vitaly Roginskya, Eduardo A. Lissi. Review of methods to determine chain-breaking antioxidant activity in food. Food Chemistry Volume 92, Issue 2, September 2005, Pages 235–254.

103. Bondet, V., Brand-Williams, W. and Berset, C. 1997. Kinetics and mechanisms of antioxidant activity using the DPPH free radical method, Leben- smittel-Wissenschaft und -Technologie/Food Science and Technology, 30: 609-615.

104. Philip Molyneux, The use of the stable free radical diphenylpicryl- hydrazyl (DPPH) for estimating antioxidant activity Polymer Chemistry), Macrophile Associates, 9 Brewery Lane, Salisbury, Wiltshire, SP1 2LJ, U.K 2003.

105. F. Šeršeň , M. Lácová Antioxidant activity of some coumarins Volume 62, Issue s9 (Jun 2015).

106. R. D. H. Murray, "Naturally occuring plant coumarins," in *Progress in the Chemistry ofOrganicNatural Products*, pp. 2–105, Springer, NewYork, NY,USA, 1997; F. Bourgaud, A. Hehn, R. Larbat et al., "Biosynthesis of coumarins in plants: a major pathway still to be unravelled for cytochrome P450 enzymes," Phytochemistry Reviews, vol. 5, no. 2-3, pp. 293–308, 2006]

107. Gomez-Outes A, Suarez-Gea ML, Calvo-Rojas G (2012) Discovery of anticoagulant drugs: a historical perspective. Curr Drug Discov Technol 9:83–104

108. Anand P, Singh B, Singh N (2012) A review on coumarins as acetylcholinesterase inhibitors for Alzheimer's disease. Bioorg Med Chem 20:1175–1180

109. Kraljević, T.G., Harej, A., Sedić, M., Pavelić, S.K., Stepanić, V., Drenjančević, D., Talapko, J., Raić-Malić, S. Synthesis, in vitro anticancer and antibacterial activities and in silico studies of new 4-substituted 1,2,3-triazole–coumarin hybrids. European Journal of Medicinal Chemistry Volume 124, 29 November 2016, Pages 794-808

110. Golfakhrabadi, F., Shams Ardakani, M.R., Saeidnia, S., Akbarzadeh, T., Yousefbeyk, F., Jamalifar, H., Khanavi, M. In vitro antimicrobial and acetylcholinesterase inhibitory activities of coumarins from Ferulago carduchorum. Medicinal Chemistry Research Volume 25, Issue 8, 1 August 2016, Pages 1623-1629

111. Kouki Matsuda, Shinichiro Hattori, Ryusho Kariya, Yuji Komizu, Eriko Kudo, Hiroki Goto, Manabu Taura, Ryuichi Ueoka, Shinya Kimura, Seiji Okada. Inhibition of HIV-1 entry by the tricyclic coumarin GUT-70 through the modification of membrane fluidity. Biochemical and Biophysical Research Communications 457 (2015) 288e294.; Wan-Gang Gu, Xuan Zhang , Denis Tsz-Ming Ip, Liu-Meng Yang, Yong-Tang Zheng ,David Chi-Cheong Wana. Discovery of a novel HIV-1 integrase inhibitor from natural compounds through structure based virtual screening and cell imaging. FEBS Letters 588 (2014) 3461–3468

112. Daniel B. Nichols, Raquel A. C. Leao, Amartya Basu, Maksim Chudayeu, Paula de F. de Moraes, Tanaji T. Talele, Paulo R. R. Costa, Neerja Kaushik-Basu. Evaluation of Coumarin and Neoflavone Derivatives as HCV NS5B Polymerase Inhibitors. Chem Biol Drug Des 2013; 81: 607–614 .

113. Munjed M. Ibrahim , Mauro Mazzei, Ilenia Delogu, Robert Szabo, Giuseppina Sanna, Roberta Loddo. Activity of bis(7-hydroxycoumarin) Mannich bases against bovine viral diarrhoea virus. Antiviral Research 134 (2016) 153e160).

114. Shokoohinia Y., Sajjad, S.-E., Gholamzadeh S., Fattahi A., Behbahani M. Antiviral and cytotoxic evaluation of coumarins from Prangos ferulacea. Pharmaceutical Biology Volume 52, Issue 12, 1 December 2014, Pages 1543-1549.

115. Pantaleon V., Marakos P., Pouli N., Mikros E., Andreadou I. Interactions of a series of novel spiropyranocoumarin derivatives with reactive oxygen species J. Pharm. Pharmacol. 2003, 55, 1029-1039; b. Rehakova Z., Koleckar V., Cervenka F DPPH radical scavengin activity of several naturally occurring coumarins and their synthesized analogs measured by the SIA method. Toxicol Mech. Method. 2008, 18, 413-418)

116. Martin-Arago S, Benedi J.M., Villar A.M. Effects of the antioxidant 6,7-dihydroxycoumarin esculetin on the glutathione system and lipid peroxidation).

117. Subramaniam S.R., Ellis E.M., Esculetin induced protection of human hepatoma HepG2 cells against hydrogen peroxide is associated with Nrf2-dependent induction of the NAD(P)H:quinone oxidoreductase 1 gene. Toxicol. Appl. Pharm. 2011, 250, 130-136

118. Razo-Hernandez R.S., Pineda-Urbina K., Velazko-Medel M.A. QSAR study of the DPPH center dot radical scavenging activity of coumarin derivatives and xanthine oxidase inhibition by molecular docking. Cent. Eur. J. Chem. 2014, 12, 1067-1080.

119. Srinivrasan K. Crit. Rev. Food Sci. Nutr. 2014,54,352

120. Lemanska K., Van der Woude H., Srymusiak H., Boersma M. G., Gliszczyriska-Swiglo A., Rietjens I. M.C.M., Tyrakowska B. Free Rad. Res. 2004, 38, 639.

121. Botta G., Bizzarri B.M., Garozzo A., Timpanaro R., Bisignano B., Amatore D., Palamara A.T3, Nencioni L., Saladino R. Carbon nanotubes supported tyrosinase in the synthesis of lipophilic hydroxytyrosol and dihydrocaffeoyl catechols with antiviral activity against DNA and RNA viruses. Bioorg Med Chem. 2015, 23(17), 5345-51

122. R. Saladino, M. Barontini, M. Crucianelli, L. Nencioni, R. Sgarbanti, A.T. Palamara. Current Advances in Anti-Influenza Therapy. Curr. Med. Chem., 2010, 17, 2101-2140.

123. Fioravanti, R.; Celestino, I.; Costi, R.; Cuzzucoli Crucitti, G.; Pescatori, L.; Mattiello, L.; Novellino, E.; Checconi, P.; Palamara, A. T.; Nencioni, L.; Di Santo, R.. Effects of polyphenol compounds on influenza A virus replication and definition of their mechanism of action. Bioorg. Med. Chem., 2012, 20, 5046–5052.

124. Saladino, R.; Neri, V.; Farina, A.; Crestini, C.; Nencioni, L.; Palamara, A.T. A Novel and Efficient Synthesis of Tocopheryl Quinones by Homogeneous and Heterogeneous Methyltrioxorhenium/Hydrogen Peroxide Catalytic Systems. Adv. Synth. Catal., 2008, 350, 321-331.

125. Zhong-Hai Tang, Yun-Bao Liu†, Shuang-Gang Ma, Li Li, Yong Li, Jian-Dong Jiang, Jing Qu, and Shi-Shan Yu. Antiinfluenza A activity: Antiviral Spirotriscoumarins A and B: Two Pairs of Oligomeric Coumarin Enantiomers with a Spirodienone–Sesquiterpene Skeleton from Toddalia asiatica Org. Lett., 2016, 18 (19), pp 5146–5149.

126. Olivares-Tenorio, M.-L., Dekker, M., Verkerk, R., van Boekel, M.A.J.S. Health-promoting compounds in cape gooseberry (Physalis peruviana L.): Review from a supply chain perspective. Trends in Food Science and Technology Volume 57, 1 November 2016, Pages 83-92; Ratz-Yko, A. ,Arct, J., Majewski, S., Pytkowska, K. Influence of polyphenols on the physiological processes in the skin. Phytotherapy Research Volume 29, Issue 4, 1 April 2015, Pages 509-51

127. Hogle J (2002). "Poliovirus cell entry: common structural themes in viral cell entry pathways". *Annu Rev Microbiol*. **56**: 677–702. doi:10.1146/annurev.micro.56.012302.160757.

128. Goodsell DS (1998). *The machinery of life*. New York: Copernicus. ISBN 0-387-98273-6.

129. Paul JR (1971). *A History of Poliomyelitis*. (Yale studies in the history of science and medicine). New Haven, Conn: Yale University Press. ISBN 0-300-01324-8.

130. Racaniello and Baltimore; Baltimore, D (1981). "Molecular cloning of poliovirus cDNA and determination of the complete nucleotide sequence of the viral genome". *Proc. Natl. Acad. Sci. U.S.A*. **78** (8): 4887–91. doi:10.1073/pnas.78.8.4887. PMC 320284. PMID 6272282.

131. Kitamura N, Semler B, Rothberg P, et al. (1981). "Primary structure, gene organization and polypeptide expression of poliovirus RNA". *Nature*. **291** (5816): 547–53. doi:10.1038/291547a0. PMID 6264310.

132. De Jesus NH (2007). "Epidemics to eradication: the modern history of poliomyelitis". *Virol. J*. **4** (1): 70. doi:10.1186/1743-422X-4-70. PMC 1947962. PMID 17623069.

133. Mendelsohn Cl; Wimmer E; Racaniello VR (1989). "Cellular receptor for poliovirus: molecular cloning, nucleotide sequence, and expression of a new member of the immunoglobin superfamily". *Cell*. **56** (5): 855–865. doi:10.1016/0092-8674(89)90690-9. PMID 2538245.

134. He Y, Mueller S, Chipman P, et al. (2003). "Complexes of poliovirus serotypes with their common cellular receptor, CD155". *J Virol*. **77** (8): 4827–35. doi:10.1128/JVI.77.8.4827-4835.2003. PMC 152153. PMID 12663789.

135. Dunnebacke TH, Levinthal JD, Williams RC (1 October 1969). "Entry and release of poliovirus as observed by electron microscopy of cultured cells". *J. Virol*. **4** (4): 505–13. PMC 375900. PMID 4309884.

136. Kaplan G, Freistadt MS, Racaniello VR (1 October 1990). "Neutralization of poliovirus by cell receptors expressed in insect cells". *J. Virol*. **64** (10): 4697–702. PMC 247955. PMID 2168959.

137. Gomez Yafal A, Kaplan G, Racaniello VR, Hogle, JM (1993). "Characterization of poliovirus conformational alteration mediated by soluble cell receptors". *Virology*. **197** (1): 501–5. doi:10.1006/viro.1993.1621. PMID 8212594.

138. Mueller S, Wimmer E, Cello J (2005). "Poliovirus and poliomyelitis: a tale of guts, brains, and an accidental event". *Virus Res*. **111** (2): 175–93. doi:10.1016/j.virusres.2005.04.008. PMID 15885840.

139. Brandenburg B, Lee LY, Lakadamyali M, Rust MJ, Zhuang X, Hogle JM (2007). "Imaging poliovirus entry in live cells". *PLOS Biology*. **5** (7): e183. doi:10.1371/journal.pbio.0050183. PMC 1914398. PMID 17622193.

140. Attardi, G. and Smith, J. Virus specific protein and a ribonucleic acid associated with ribosomes in poliovirus infected HeLa cells. Cold Spring Harbor Symp. Quant. Biol. 27: 271–292. 1962

141. Chen CY, Sarnow P (1995). "Initiation of protein synthesis by the eukaryotic translational apparatus on circular RNAs". *Science*. **268** (5209): 415–7. doi:10.1126/science.7536344. PMID 7536344.

142. Pelletier J, Sonenberg N (1988). "Internal initiation of translation of eukaryotic mRNA directed by a sequence derived from poliovirus RNA". *Nature*. **334** (6180): 320–5. doi:10.1038/334320a0. PMID 2839775.

143. Jang SK, Kräusslich HG, Nicklin MJ, Duke GM, Palmenberg AC, Wimmer E (1 August 1988). "A segment of the 5' nontranslated region of encephalomyocarditis virus RNA directs internal entry of ribosomes during in vitro translation". *J. Virol*. **62** (8): 2636–43. PMC 253694. PMID 2839690.

144. Harper, David R. (2012). *Viruses: Biology, Applications, and Control*. The United States of America: Garland Science. p. 57. ISBN 978-0-8153-4150-5.

145. Charles Chan and Roberto Neisa. "Poliomyelitis". Archived February 22, 2007, at the Wayback Machine. Brown University.

146. John Carter; Venetia A. Saunders (2007). *Virology: Principles and Applications*. John Wiley & Sons. p. 164. ISBN 978-0-470-02386-0.

147. John Carter; Venetia A. Saunders (2007). *Virology: Principles and Applications*. John Wiley & Sons. p. 165. ISBN 978-0-470-02386-0.

148. John Carter; Venetia A. Saunders (2007). *Virology: Principles and Applications*. John Wiley & Sons. p. 161, 165. ISBN 978-0-470-02386-0.

149. John Carter; Venetia A. Saunders (2007). *Virology: Principles and Applications*. John Wiley & Sons. p. 166. ISBN 978-0-470-02386-0.

150. Kew O, Sutter R, de Gourville E, Dowdle W, Pallansch M (2005). "Vaccine-derived polioviruses and the endgame strategy for global polio eradication". *Annu Rev Microbiol*. **59**: 587–635. doi:10.1146/annurev.micro. 58.030603.123625. PMID 16153180.

151. Drake E JW (August 1958). "Interference and multiplicity reactivation in polioviruses". *Virology*. **6** (1): 244–64. doi:10.1016/0042-6822(58)90073-4. PMID 13581529.

152. Yin-Murphy M, Almond JW (1996). Baron S, et al., eds. *Picornaviruses.* in: *Baron's Medical Microbiology* (4th ed.). Univ of Texas Medical Branch. ISBN 0-9631172-1-1.   1

153. Ryan KJ, Ray CG (editors) (2004). *Sherris Medical Microbiology* (4th ed.). McGraw Hill. pp. 555–62. ISBN 0-8385-8529-9.

154. "Herpes simplex". DermNet NZ — New Zealand Dermatological Society. 2006-09-16. Retrieved 2006-10-15.

155. Clarke RW (2015). "Forces and Structures of the Herpes Simplex Virus (HSV) Entry Mechanism". *ACS Infectious Diseases*. **1** (9): 403–415. doi:10.1021/acsinfecdis.5b00059.

156. Subramanian RP, Geraghty RJ (2007). "Herpes simplex virus type 1 mediates fusion through a hemifusion intermediate by sequential activity of glycoproteins D, H, L, and B". *Proc. Natl. Acad. Sci. U.S.A*. **104** (8): 2903–8. doi:10.1073/pnas.0608374104. PMC 1815279. PMID 17299053.

157. Akhtar J, Shukla D (2009). "Viral entry mechanisms: Cellular and viral mediators of herpes simplex virus entry". *FEBS Journal*. **276** (24): 7228–7236. doi:10.1111/j.1742-4658.2009.07402.x. PMC 2801626. PMID 19878306

158. Coxsackie NY and the virus named after it posted to Virology Blog 10 AUGUST 2009 by Professor Vincent Racaniello. Accessed via internet August 20, 2012.

159. Dalldorf G, Gifford R (June 1951). "Clinical and epidemiologic observations of Coxsackie-virus infection". *N. Engl. J. Med*. **244** (23): 868–73. doi:10.1056/NEJM195106072442302. PMID 14843332.

160. Dalldorf G, Gifford R (November 1952). "Adaptation of Group B Coxsackie virus to adult mouse pancreas". *J. Exp. Med*. **96** (5): 491–7. doi:10.1084/jem.96.5.491. PMC 2136156. PMID 13000059.

161. Dalldorf G, Gifford R (January 1954). "Susceptibility of gravid mice to Coxsackie virus infection". *J. Exp. Med*. **99** (1): 21–7. doi:10.1084/jem.99.1.21. PMC 2136322PMID 13118060.

162. DALLDORF G, GIFFORD R (February 1955). "Recognition of mouse ectromelia". *Proc. Soc. Exp. Biol. Med*. **88** (2): 290–2. PMID 14357417.

163. "China says it controls viral outbreak in children". *Reuters*. 2007-05-19.

164. Harrison, S. C. (2010). "Virology. Looking inside adenovirus". *Science*. **329** (5995): 1026–1027. Bibcode: 2010Sci...329.1026H. doi:10.1126/science.1194922. PMID 20798308.

165. Wu E, Nemerow GR (2004). "Virus yoga: the role of flexibility in virus host cell recognition". *Trends Microbiol*. **12** (4): 162–168. doi:10.1016/j.tim.2004.02.005. PMID 15051066

166. Mattes FM, McLaughlin JE, Emery VC, Clark DA, Griffiths PD (August 2000). "Histopathological detection of owl's eye inclusions is still specific for cytomegalovirus in the era of human herpesviruses 6 and 7". *J. Clin. Pathol*. **53** (8): 612–4. doi:10.1136/jcp.53.8.612

167. Ryan KJ, Ray CG, eds. (2004). *Sherris Medical Microbiology* (4th ed.). McGraw Hill. pp. 556; 566–9. ISBN 0-8385-8529-9.

168. Koichi Yamanishi; Arvin, Ann M; Gabriella Campadelli-Fiume; Edward Mocarski; Moore, Patrick; Roizman, Bernard; Whitley, Richard (2007). *Human herpesviruses: biology, therapy, and immunoprophylaxis*. Cambridge, UK: Cambridge University Press. ISBN 0-521-82714-0.

169. Yum, S., Doh, H.J., Hong, S., Jeong, S., Kim, D.D., Park, M., Jung, Y. *Eur. J. Pharmacol.* **2013**, 699, 124–131.

170. Coelho, V.R., Vieira ,C.G.,Pereira de Souza, L., Moysés, F., Basso C.,Mausolff Papke, D.,Pires T.R., Siqueira, I.R., Picada, J.N, Pereira, P. *Life Sciences* **2015,** 122,65–71.

171. Zhang, L., Ji, Y., Kang, Z., Li, C., Jiang, W. *Toxicol and Applied Pharmacology* **2015**, 283, 1, 50-56.

172. Hsieh, M.-J.abc, Chien, S.-Y.def, Chou, Y.-E.c, Chen, C.-J.ghi, Chen, J.j, Chen, M.-K.k *Phytomedicine* **2014,** 21, 1746-1752.

173. Ibrahim, A.S., Sobh, M.A., Eid, H.M., Salem, A., Elbelasi, H.H., El-Naggar, M.H., AbdelBar, F.M., Sheashaa, H., Sobh, M.A., Badria, F.A. *Tumour biology : the journal of the International Society for Oncodevelopmental Biology and Medicine* **2014,** 35, 10, 9941-9948.

174. Lee, D.-H.a , Kim, D.-W.b, Jung, C.-H.c, Lee, Y.J.a, Park, D.d *Toxicology and Applied Pharmacology* **2014** 279, 253-265.

175. Zinglé, C., Tritsch, D., Grosdemange-Billiard, C., Rohmer, M. *Bioorganic and Medicinal Chemistry* **2014**, 22, 3713-3719.

176. Zhao, X., Zhai, S., An, M.-S., Wang, Y.-H., Yang, Y.-F., Ge, H.-Q., Liu, J.-H., Pu, X.P., *PLoS ONE* **2013** 8, 10, n° 78220.

177. Park S.H., Song, J.H., Kim,T, Shin, W.S., Park, G.M., Lee,S., Kim,Y.J., Choi, P., Kim, H., Kim,H.S., Kwon, D.H., Choi, H.J., and Ham, J., *Drugs* **2012**, 10(10), 2222-2233.

178. Pawar, R.a, Das, T.b, Mishra, S.a, Nutanb, Pancholi, B.b, Gupta, S.K.b , Bhat, S.V.a *Bio. Med. Chem. Letters* **2014**, 24, 1, 302-307.

179. Gigante, B. , Santos, C., Silva, A.M., Curto, M.J.M., Nascimento, M.S.J., Pinto, E., Pedro, M., Cerqueira, F., Pinto, M.M., Duarte, M.P., Laires, A., Rueff, J., Gonçalves, J., Pegado, M.I., Valdeira, M.L. *Bio. Med. Chem.* **2003**,11,8,1631-1638.

180. Frey, K.M.a, Gray, W.T.a, Spasov, K.A.a, Bollini, M.b, Gallardo-Macias, R.b, Jorgensen, W.L.b , Anderson, K.S.a, *Chem. Bio. Drug Design* **2014**, 83, 5, 541-549.

181. Lee, C.a, Lee, J.M.b, Lee, N.-R.b, Kim, D.-E.a, Jeong, Y.-J.b , Chong, Y.a *Bio.Med. Chem. Lett.s*, **2009,** 19, 16, 4538-4541.

182. Srinivasan, K. *Crit. Rev. Food Sci.Nutr.***2014**, 54, 3, 352-372.

183. Kubra, I.R., Rao, L.J.M. *Crit. Rev. Food Sci.Nutr.,* **2012**, 52, 8, 651-688.

184. Saladino, R., Gualandi, G., Farina, A., Nencioni, L., Palamara, A.T. *Curr. Med. Chem.* **2008,** 15, 15, 1500-1519.

185. Lemańska, K.a, Van Der Woude, H.b, Szymusiak, H.a, Boersma, M.G.b, Gliszczyńska-Swigło, A.a, Rietjens, I.M.C.M.b, Tyrakowska, B., *Fre.Rad. Res.* **2004**, 38, 6, 639-647.

186. Jeong, S.,Park, H., Hong,S.,Yum, S., Kim, W.,Jung, Y., *Eur. J. Pharm.* **2015,** 747, 114–122 .

187. Tabernero, M., Sarriá, B., Largo, C., Martínez-López, S., Madrona, A., Espartero, J.L., Bravo, L., Mateos, R. *Food Func.* **2014** 5, 7, 1556-1563.

188. Sorensen, A. D. M.; Nielsen, N. S.; Yang, Z.; Xu, X.; Jacobsen, C. *Eur. J. Lipid Sci*. Technol. **2012**, 114, 134.

189. Zhong, Y.; Shahidi, F. J. *Agric. Food Chem. 2012*, 60, 4.

190. Aparicio-Soto, M., Sánchez-Fidalgo, S., González-Benjumea, A., Maya, I., Fernández-Bolaños, J.G., Alarcón-de-la-Lastra, C. *J. Agric. Food Chem.* **2015**, 63, 3, 838-846.

191. Georgiev, L., Chochkova, M. , Totseva, I., Seizova, K., Marinova, E., Ivanova, G., Ninova, M., Najdenski, H., Milkova, T. *Med. Chem. Res.* **2013**, 22, 9, 4173-4182.

192. Tofani, D.; Balducci, V.; Gasperi, T.; Incerpi, S.; Gambacorta, A. *J. Agric. Food Chem.* **2010**, 58, 529;

193. Torres de Pinedo, A.; Penalver, P.; Pèrez-Victoria, I.; Rondòn, D.; Morales, *J. C. Food Chem.* **2007**, 105, 657.

194. Bozzini, T.,Botta,G., Delfino, M. , Onofri, S., Saladino, R., Amatore, D., Sgarbanti, R., Nencioni, L., Palamara, A.T., *Bio. Med. Chem.* **2013**, 21 7699–7708.

195. Ramsden, C.A., Riley, P.A., *Bio. Med. Chem.*Volume **2014**, 22, 8, 2388-2395.

196. Ramey, A.M., Reeves, A.B., Sonsthagen, S.A., TeSlaa, J.L., Nashold, S., Donnelly, T., Casler, B., Hall, J.S. *Virol*ogy, **2015**, 482, 79-83.

197. Palamara, A. T.; Brandi, G.; Rossi, L.; Millo, E.; Benatti, U.; Nencioni, L.; Iuvara, A.; Garaci, E.; Magnani, M. *Antiviral Chem. Chemother.* **2004**, 15, 83.

198. Subrizi,F., Crucianelli,M., Grossi,V., Passacantando, M., Pesci, L., Saladino, R., *ACS Catal.* **2014**, 4, 810−822.

199. Asuri, P.; Karajanagi, S.S.; Sellitto, E.; Kim, D.-Y.; Kane, R.S.; Dordick, J.S. *Biotechnol. Bioeng.* **2006**, *95*, 804-811.

200. Manvar D., Pelliccia S., La Regina G., Famiglini V., Coluccia A., Ruggieri A., Anticoli S., Lee J-C., Basu A., Cevik O., Nencioni L., Palamara A.T., Zamperini C., Botta M., Neyts J., Leyssen P., Kaushik-Basu N., Silvestri R., *Eur. J. Med. Chem.* **2014**: 90, 497-506.

201. Civitelli L., Panella S., Marcocci M.E., De Petris A., Garzoli S., Pepi F., Vavala E., Ragno R., Nencioni L., Palamara A.T., Angiolella L., *Phytomedicine* **2014**, 21, 857-865.

202. Saladino R., Neri V., Checconi P., Celestino I., Nencioni L., Palamara A. T., Crucianelli M., *Chemistry Eur. J.* **2013**, 19, 2392-2404.

203. Fioravanti R., Celestino I., Costi R., Cuzzucoli Crucitti G., Pescatori L., Mattiello L., Novellino E., Checconi P., Palamara A. T., Nencioni L., Di Santo R., *Bioorg. Med. Chem.* **2012**, 20, 5046–5052.

204. Sgarbanti R., Nencioni L., Amatore D., Coluccio P., Fraternale A., Sale P., Mammola C. L., Carpino G., Gaudio E., Magnani M., Ciriolo M. R., Garaci E., Palamara A., *Antioxid. Redox Signal* **2011**, 15 (3), 593-606.

205. Palamara A. T., Nencioni L., Aquilano K., De Chiara G., Hernandez L., Cozzolino F., Ciriolo M. R., Garaci E., *J Infect Dis* **2005**: 191, 1719-1729.

206. Cutrí, C. C. C., Garozzo, A., Siracusa, M. A., Sarvá, M. C., Tempera, G., Geremia, E., Pinizzotto M. R., Guerrera, F. *Bio. Med. Chem*., **1998**, 6(12), 2271-2280.

207. Haslam, E. Shikimic, *John Wiley & Sons*, **1993**.

208. Witaicenis A., Noboru Seito L., da Silveira Chagas A., de Almeida Junior L. D., Luchini A. C., Rodrigues-Orsi P., Cestari S. H., Di Stasi L. C. Antioxidant and intestinal anti-inflammatory effects of plant-derived coumarin derivatives. Phytomed. 2014, 21, 240-246

209. Friel, H.; Lederman, H. A nutritional supplement fo The influenza viruses are able to modulate the intracellular redox in order to promote viral replication and pathogenesis

210. Sgarbanti S., Amatore D., Celestino I., Marcocci M. E., Fraternale, A., Ciriolo M.R., Magnani M., Saladino R., Garaci E., Palamara A.T., Nencioni L.

211. Nencioni, L.; Sgarbanti, R.; Amatore, D.; Checconi, P.; Celestino, I.; Limongi. D.; Anticoli, S.; Palamara, A.T.; Garaci, E. Intracellular redox signaling as therapeutic target for novel antiviral strategy. Curr. Pharm. Des., 2011, 17(35), 3898-904)

212. Sgarbanti, R.; Nencioni, L.; Amatore, D.; Coluccio, P.; Fraternale, A.; Sale, P.; Mammola C.L.; Carpino, G.; Gaudio, E.; Magnani, M.; Ciriolo, M.R.; Garaci, E.; Palamara, A.T. Redox regulation of the influenza hemagglutinin maturation process: a new cellmediated strategy for anti-influenza therapy. Anti.Redox Signal, 2011, 15(3), 593-606.

213. Nehad A. Abdel Latif, Rasha Z. Batran, Mohammed A. Khedr, Mohamed M. Abdalla. Influence of polyphenols on the physiological processes in the skin. Phytotherapy Research Volume 29, Issue 4, 1 April 2015, Pages 509-517).

214. Bruno Mattia Bizzarria, Cristina Pieri, Giorgia Botta, Lili Arabuli, Pasquale Mosesso, Serena Cinelli, Angelo Schinoppi and Raffele Saladino. Synthesis and antioxidant activity of DOPA peptidomimetics by a novel IBX mediated aromatic oxidative functionalization.

215. Quansheng Wu and Howard D. Dewald Voltammetry of Coumarins WILEY-VCH Verlag GmbH, D-69469 Weinheim, 2001.

216. S. Steenken One-Electron Redox Potentials of Phenols. Hydroxy- and Aminophenols and Related Compounds of Biologlcal Interest. 1982 American Chemical Society.

217. Koji Furuno, T. Akasako, and N.Sugihara The Contribution of the Pyrogallol Moiety to the Superoxide Radical Scavenging Activity of Flavonoids. Biol. Pharm. Bull. 25(1) 19—23 (2002

REFERENCES CHAPTER III

1. Oparin 1953, p. vi

2. Peretó, Juli (2005). "Controversies on the origin of life" (PDF). *International Microbiology*. Barcelona: Spanish Society for Microbiology. **8** (1): 23–31. ISSN 1139-6709. PMID 15906258. Retrieved 2015-06-01. ^

3. Scharf, Caleb; et al. (18 December 2015). "A Strategy for Origins of Life Research". *Astrobiology (journal)*. **15** (12): 1031–1042. doi:10.1089/ast.2015.1113. PMC 4683543. PMID 26684503. Retrieved 28 November 2016.

4. Warmflash, David; Warmflash, Benjamin (November 2005). "Did Life Come from Another World?". *Scientific American*. Stuttgart: Georg von Holtzbrinck Publishing Group. **293** (5): 64–71. doi:10.1038/scientificamerican1105-64. ISSN 0036-8733.

5. Yarus 2010, p. 47

6. Elizabeth A. Bell. "Potentially biogenic carbon preserved in a 4.1 billion-year-old zircon".

7. Voet & Voet 2004, p. 29

8. Dyson 1999

9. Davies, Paul (1998) "The Fifth Miracle, Search for the origin and meaning of life" (Penguin)

10. Copley, Shelley D.; Smith, Eric; Morowitz, Harold J. (December 2007). "The origin of the RNA world: Co-evolution of genes and metabolism" (PDF). *Bioorganic Chemistry*. Amsterdam, the Netherlands: Elsevier. **35** (6): 430–443.

11. Robertson, Michael P.; Joyce, Gerald F. (May 2012). "The origins of the RNA world". *Cold Spring Harbor Perspectives in Biology*. Cold Spring Harbor, NY: Cold Spring Harbor Laboratory Press. **4** (5): a003608. doi:10.1101/cshperspect.a003608. ISSN 1943-0264. PMC 3331698. PMID 20739415.

12. Cech, Thomas R. (July 2012). "The RNA Worlds in Context". *Cold Spring Harbor Perspectives in Biology*. Cold Spring Harbor, NY: Cold Spring Harbor Laboratory Press. **4** (7): a006742. doi:10.1101/cshperspect.a006742. ISSN 1943-0264. PMC . PMID 21441585.

13. Keller, Markus A.; Turchyn, Alexandra V.; Ralser, Markus (25 March 2014). "Non−enzymatic glycolysis and pentose phosphate pathway−like reactions in a plausible Archean ocean". *Molecular Systems Biology*. Heidelberg, Germany: EMBO Press on behalf of the European Molecular Biology Organization. **10** (725). doi:10.1002/msb.20145228. ISSN 1744-4292. PMC 4023395. PMID 24771084.

14. Ehrenfreund, Pascale; Cami, Jan (December 2010). "Cosmic carbon chemistry: from the interstellar medium to the early Earth.". *Cold Spring Harbor Perspectives in Biology*. Cold Spring Harbor, NY: Cold Spring Harbor Laboratory Press. **2** (12): a002097. doi:10.1101/cshperspect.a002097. ISSN 1943-0264. PMC 2982172. PMID 20554702.

15. Perkins, Sid (8 April 2015). "Organic molecules found circling nearby star". *Science* (News). Washington, D.C.: American Association for the Advancement of Science. ISSN 1095-9203. Retrieved 2015-06-02.

16. King, Anthony (14 April 2015). "Chemicals formed on meteorites may have started life on Earth". *Chemistry World* (News). London: Royal Society of Chemistry. ISSN 1473-7604. Retrieved 2015-04-17.

17. Rampelotto, Pabulo Henrique (26 April 2010). *Panspermia: A Promising Field Of Research* (PDF). Astrobiology Science Conference 2010. Houston, TX: Lunar and Planetary Institute. p. 5224. Bibcode:2010LPICo1538.5224R. Retrieved 2014-12-03. Conference held at League City, TX

18. Loeb, Abraham (October 2014). "The habitable epoch of the early Universe". *International Journal of Astrobiology*. Cambridge, UK: Cambridge University Press. **13** (4): 337–339. arXiv:1312.0613. Bibcode: 2014IJAsB..13..337L. doi:10.1017/S1473550414000196. ISSN 1473-5504.Loeb, Abraham (3 June 2014). "The Habitable Epoch of the Early Universe". arXiv:1312.0613v3[astro-ph.CO].

19. Dreifus, Claudia (2 December 2014). "Much-Discussed Views That Go Way Back". *The New York Times*. New York: The New York Times Company. p. D2. ISSN 0362-4331. Retrieved 2014-12-03.

20. Graham, Robert W. (February 1990). "Extraterrestrial Life in the Universe" (PDF) (NASA Technical Memorandum 102363). Lewis Research Center, Cleveland, Ohio: NASA. Retrieved 2015-06-02.

21. Altermann 2009, p. xvii

22. "Age of the Earth". United States Geological Survey. 9 July 2007. Retrieved 2006-01-10.

23. Dalrymple 2001, pp. 205–221

24. Manhesa, Gérard; Allègre, Claude J.; Dupréa, Bernard; Hamelin, Bruno (May 1980). "Lead isotope study of basic-ultrabasic layered complexes: Speculations about the age of the earth and primitive mantle characteristics". *Earth and Planetary Science Letters*. Amsterdam, the Netherlands: Elsevier. **47** (3): 370–382. Bibcode:1980E&PSL.. 47..370M. doi:10.1016/0012-821X(80)90024-2. ISSN 0012-821X.

25. Schopf, J. William; Kudryavtsev, Anatoliy B.; Czaja, Andrew D.; Tripathi, Abhishek B. (5 October 2007). "Evidence of Archean life: Stromatolites and microfossils". *Precambrian Research*. Amsterdam, the Netherlands: Elsevier. **158** (3–4): 141–155. doi:10.1016/j.precamres.2007.04.009. ISSN 0301-9268.

26. Schopf, J. William (29 June 2006). "Fossil evidence of Archaean life". *Philosophical Transactions of the Royal Society B*. London: Royal Society. **361** (1470): 869–885. doi:10.1098/rstb.2006.1834. ISSN 0962-8436. PMC 1578735. PMID 16754604.

27. Raven & Johnson 2002, p. 68

28. Borenstein, Seth (13 November 2013). "Oldest fossil found: Meet your microbial mom". *Excite*. Yonkers, NY: Mindspark Interactive Network. Associated Press. Retrieved 2015-06-02.

29. Pearlman, Jonathan (13 November 2013). "'Oldest signs of life on Earth found'". *The Daily Telegraph*. London: Telegraph Media Group. Retrieved 2014-12-15.

30. Noffke, Nora; Christian, Daniel; Wacey, David; Hazen, Robert M. (16 November 2013). "Microbially Induced Sedimentary Structures Recording an Ancient Ecosystem in the *ca.* 3.48 Billion-Year-Old Dresser Formation, Pilbara, Western Australia". *Astrobiology*. New Rochelle, NY: Mary Ann Liebert, Inc. **13** (12): 1103–1124. Bibcode:2013AsBio..13.1103N. doi:10.1089/ast.2013.1030.

31. Ohtomo, Yoko; Kakegawa, Takeshi; Ishida, Akizumi; et al. (January 2014). "Evidence for biogenic graphite in early Archaean Isua metasedimentary rocks". *Nature Geoscience*. London: Nature Publishing Group. **7** (1): 25–28. Bibcode:2014NatGe...7...25O. doi:10.1038/ngeo2025. ISSN 1752-0894.

32. Wade, Nicholas (31 August 2016). "World's Oldest Fossils Found in Greenland". *New York Times*. Retrieved 31 August 2016.

33. Borenstein, Seth (19 October 2015). "Hints of life on what was thought to be desolate early Earth". *Excite*. Yonkers, NY: Mindspark Interactive Network. Associated Press. Retrieved 2015-10-20. [21] R. Saladino, C. Crestini, S. Pino, G. Costanzo and E. Di Mauro, *Physics of life reviews* **2012**, *9*, 84-104.

34. R. Stribling and S. L. Miller, *Icarus* **1987**, *72*, 48-52.

35. R. Hudson and M. Moore, *Icarus* **1999**, *140*, 451-461.

36. E. A. McKenna, A. Othoneos, N. Kiratzis and M. Stoukides, *Industrial & engineering chemistry research* **1993**, *32*, 1904-1913.

37. Y. Takano, T. Kaneko, K. Kobayashi, D. Hiroishi, H. Ikeda and K. Marumo, *Earth, planets and space* **2004**, *56*, 669-674.

38. D. E. Woon, International journal of quantum chemistry **2002**, 88, 226-235.

39. T. Koike, T. Kaneko, K. Kobayashi, S. Miyakawa and Y. Takano, *Biological Sciences in Space* **2003**, *17*, 188-189.

40. P. Gerakines, M. Moore and R. Hudson, *Icarus* **2004**, *170*, 202-213.

41. G. Deschamps, Chimie et Industrie **1931**, 589-597.

42. S. Miyakawa, H. J. Cleaves and S. L. Miller, *Origins of Life and Evolution of the Biosphere* **2002**, *32*, 195-208.

43. R. Stribling and S. L. Miller, Origins of Life and Evolution of the Biosphere **1987**, 17, 261-273.

44. V. S. Nguyen, T. M. Orlando, J. Leszczynski and M. T. Nguyen, *The Journal of Physical Chemistry A* **2013**, *117*, 2543-2555.

45. D. J. Drury, Kirk-Othmer Encyclopedia of Chemical Technology **2000**.

46. L. Čechová, P. Jansa, M. Šála, M. Dračínský, A. Holý and Z. Janeba, *Tetrahedron* **2011**, *67*, 866-871.

47. G. Costanzo, R. Saladino, C. Crestini, F. Ciciriello and E. Di Mauro, *BMC evolutionary biology* **2007**, *7*, S1.

48. M. S. Akhter and S. M. Alawi, *Colloids and Surfaces A: Physicochemical and Engineering Aspects* **2003**, *219*, 281-290.

49. *R. Saladino, U. Ciambecchini, C. Crestini, G. Costanzo, R. Negri and E. Di Mauro, ChemBioChem **2003**, 4, 514-521.*

50. *M. Chadha and A. Choughuley, Origins of life **1984**, 14, 469-476.*

51. *R. Saladino, C. Crestini, U. Ciambecchini, F. Ciciriello, G. Costanzo and E. Di Mauro, ChemBioChem **2004**, 5, 1558-1566.*

52. R. Saladino, C. Crestini, V. Neri, J. R. Brucato, L. Colangeli, F. Ciciriello, E. Di Mauro and G. Costanzo, *ChemBioChem* **2005**, *6*, 1368-1374.

53. R. Saladino, C. Crestini, V. Neri, F. Ciciriello, G. Costanzo and E. Di Mauro, *ChemBioChem* **2006**, *7*, 1707-1714.

54. S. Senanayake and H. Idriss, *Proceedings of the National Academy of Sciences of the United States of America* **2006**, *103*, 1194-1198.

55. *H. L. Barks, R. Buckley, G. A. Grieves, E. Di Mauro, N. V. Hud and T. M. Orlando, ChemBioChem **2010**, 11, 1240-1243.*

56. R. Saladino, C. Crestini, C. Cossetti, E. Di Mauro and D. Deamer, *Origins of Life and Evolution of Biospheres* **2011**, *41*, 437-451.

57. J. S. Hudson, J. F. Eberle, R. H. Vachhani, L. C. Rogers, J. H. Wade, R. Krishnamurthy and G. Springsteen, *Angewandte Chemie* **2012**, *124*, 5224-5227.

58. M. W. Powner, B. Gerland and J. D. Sutherland, *Nature* **2009**, *459*, 239-242.

59. A. Cairns-Smith, P. Ingram and G. Walker, *Journal of theoretical biology* **1972**, *35*, 601-604.

60. O. Leslie E, *Critical reviews in biochemistry and molecular biology* **2004**, *39*, 99-123.

61. R. Saladino, V. Neri, C. Crestini, G. Costanzo, M. Graciotti and E. Di Mauro, *Journal of the American Chemical Society* **2008**, *130*, 15512-15518.

62. R. Saladino, V. Neri, C. Crestini, G. Costanzo, M. Graciotti and E. Di Mauro, *Journal of molecular evolution* **2010**, *71*, 100-110.

63. R. Saladino, C. Crestini, V. Neri, J. R. Brucato, L. Colangeli, F. Ciciriello, E. Di Mauro and G. Costanzo, ChemBioChem, 2005, 6, 1368–1374.

64. A. Rotundi, J. R. Brucato, L. Colangeli, G. Ferrini, V. Mennella and E. Palomba, Meteorit. Planet. Sci., 2002, 37, 1623–1635.

65. L. Colangeli, T. Henning, J. R. Brucato, D. Cle` ment, D. Fabian, O. Guillois, F. Huisken, C. Ja¨ ger, E. K. Jessberger, A. Jones, G. Ledoux, G. Manico` , V. Mennella, F. J. Molster, H. Mutschke, V. Pirronello, C. Reynaud, J. Roser, G. Vidali and L. B. F. M. Waters, Astron. Astrophys. Rev., 2003, 11, 97–152.

66. M. A. Septhon, Nat. Prod. Rep., 2002, 19, 292–311.

67. S. Pizzarello, Acc. Chem. Res., 2006, 39, 231–237.

68. H. G. M. Hill and J. A. Nuth, Astrobiology, 2003, 3, 291–304.

69. R. M. Hazen, Chiralcrystal faces of common rock-forming minerals, in Progress in Biological Chirality, ed. G. Palyi, Elsevier, New York, 2004, pp. 137–151.

70. R. M. Hazen and D. A. Sverjensky, Cold Spring Harbor Perspect. Biol., 2010, 2, a002162.

71. R. Saladino, C. Crestini, C. Cossetti, E. Di Mauro and D. Deamer, Origins Life Evol. Biospheres, 2011, 41, 437 451.

72. D. Glindemann, R. M. De Graaf and A. W. Schwartz, Origins Life Evol. Biospheres, 1999, 29, 555–561.

73. A. Beck, R. Lohrmann and L. E. Orgel, Science, 1967, 157, 952.

74. R. M. De Graaf, J. Visscher and A. W. Schwartz, J. Mol. Evol., 1997, 44, 237–241.

75. S. L. Miller and L. E. Orgel, The Origin of Life on the Earth, Prentice-Hall, New York, NY, 1974.

76. Y. Yamagata, H. Watanabe, M. Saitoh and T. Namba, Nature, 1991, 352, 516–519.

77. A. D. Keefe and S. L. Miller, J. Mol. Evol., 1995, 41, 693–702.

78. A. Schwartz, Origins Life Evol. Biospheres, 1997, 27, 505–512.

79. R. Saladino, C. Crestini, V. Neri, F. Ciciriello, G. Costanzo and E. Di Mauro, ChemBioChem, 2006, 7, 1707–1714.

80. Y. Yamagata, Y. Kusano and K. Inomata, Origins Life, 1981, 11, 317–320.

81. J. Hulshof and C. Ponnamperuma, Origins Life Evol. Biospheres, 1976, 7, 197–224.

82. M. Takeishi, M. Tadano and S. Hayama, Makromol. Chem., Rapid Commun., 1982, 3, 871–874.

83. P. E. Gagnoni, J. L. Boivin and J. H. Dickson, Can. J. Chem., 1959, 37, 520–524.

84. Balko¨se et al., 2002; Cartwright, Escribano, Khokhlov, & Sainz-Diaz, 2011; Cartwright, Escribano, & Sainz-Diaz, 2011; Cartwright et al., 2002; Coatman et al., 1980; Collins et al., 1998; Duan, Kitamura, Uechi, Katsuki, & Tanimoto, 2005; Parmar et al., 2009

85. Coatman et al., 1980

86. Cartwright, Escribano, & Sainz-Diaz, 2011; Coatman et al., 1980; Parmar et al., 2009

87. Cartwright et al., 2002; Novella, 2000

88. Coatman et al., 1980; Collins et al., 1999; Collins, Mokaya, & Klinowski, 1999), carbonates (Maselko & Strizhak, 2004

89. Maselko, Geldenhuys, Miller, & Atwood, 2003; Toth, Horvath, Smith, McMahan, & Maselko, 2007

90. Bormashenko, Bormashenko, Stanevsky, & Pogreb, 2006; Coatman et al., 1980

91. Baker et al., 2009; Cartwright, Escribano, & Sainz-Diaz, 2011; Glaab et al., 2012; Maselko et al., 2003; Maselko & Strizhak, 2004

92. Ritchie et al., 2009

93. Thouvenel-Romans & Steinbock, 2003

94. Pagano, 2008; Pagano et al., 2008; Roszol & Steinbock, 2011; Thouvenel-Romans, Pagano, & Steinbock, 2005)

95. Thouvenel-Romans et al., 2005

96. Bansagi, & Steinbock, 2007

97. Balko¨se et al., 2002; Cartwright, Escribano, Khokhlov, et al., 2011; Cartwright, Escribano, & Sainz Diaz, 2011; Collins, Mann, et al., 1999; Collins, Mokaya, & Klinowski, 1999; Pagano, Thouvenel-Romans, & Steinbock, 2007; Parmar et al., 2009).

98. Glaab et al., 2012

99. Sleep, N.H., et al. (2004) Proc. Natl. Acad. Sci. USA 101, 12818−12822